Vessel and cargo motions

A frequency domain method to study combined vessel and cargo responses

A.J. van der Heiden

TU Delft

BIGLIFT
KEY IN HEAVY LIFT

Vessel and cargo motions

A frequency domain method to study combined vessel and cargo responses

by

A.J. van der Heiden

to obtain the degree of Master of Science
at the Delft University of Technology,
to be defended publicly on Friday September 20, 2019 at 10:00 AM.

Student number:	4213580	
Project duration:	November 9, 2018 – September 20, 2019	
Thesis committee:	Dr. Ir. P.R. Wellens,	Delft University of Technology, chairman
	Dr. -Ing. S. Schreier,	Delft University of Technology, supervisor
	Dr. Ir. M.B. Duinkerken,	Delft University of Technology
	Ir. A. Vreeburg,	BigLift Shipping, supervisor
	MSc PhD A. van Deyzen,	Royal HaskoningDHV

An electronic version of this thesis is available at `http://repository.tudelft.nl/`.

TU Delft

BIG LIFT
KEY IN HEAVY LIFT

Contents

List of Figures

List of Tables

Preface

The final project that a student has to fulfill before he can graduate is his master thesis. This report is the result of my master thesis to complete the Master's program Marine technology at Delft University of Technology. The specialisation of my master is ship hydromechenics. The project has been carried out on behalf of BigLift Shipping. At BigLift Shipping I have been a graduation intern at the Engineering department.

Let me start with showing my gratitude for the graduation committee. Dr. Ir. P.R. Wellens, thank you for stepping in as the chair during the last phase of my master project. Ir. M.B. Duinkerken thank you for taking the time to take part of the committee. Dr. Ir. S. Schreier, thank you very much for all the time you spend to help me during my research. Thank you for all the knowledge you shared and the questions that pushed me to think in other directions. Your questions also helped me to go back to the principles of the problem.

I also want to express my appreciation to BigLift Shipping. The Engineering department for providing me with a place to work and all the advice I got. Thank you Anne Vreeburg and Gerardo Rodriguez Conde for your daily supervision. Thank you for all the times you helped me with guidance and valuable feedback.

I would like to thank my family. I will start with my parents, Ben and Carla. Thank you for the endless support and your open arms. Thank you for teaching me to always try my hardest. Maarten, my elder brother, thank you for all your advice.

The next words are reserved for my friends. Thank you all for the welcome distraction from studying. From sailing in the J22 and SB20, Studying in Trondheim and all other activities we did together. Thank you Joren for all the, somewhat longer, coffee talks we had during our study days in Delft. Thank you all for making my study time the amazing time it was.

Finally I would like to thank Lisanne. Thank you for all your love and patience. Thank you for your reassuring words on the moments I got home tired and the moments I was really busy. Even on the moments I wanted to procrastinate writing the thesis or preparing my presentation.

A.J. van der Heiden
Delft, September 2019

Abstract

When lifting operations are performed by a heavy lifting vessel, the motions of the vessel and cargo are predicted by conventional six degrees of freedom calculations. It is assumed that the cargo is attached to the crane top in order to decrease the stability of the vessel and perform accurate calculations. While these conventional calculations can be used to calculate the vessel motions and the motions of the crane top, the cargo motions are not taken into account. In conventional calculations the dynamical aspects of the cargo are not taken into account and the forces due to cargo motions are neglected.

In several recent projects carried out by BigLift Shipping swell waves have presented BigLift Shipping with challenges. Due to these swell waves the vessel and cargo where excited which caused problems during these lifting operations. Therefore BigLift Shipping is intrested in a method to calculate the vessel motions in combination with the cargo motions.

There are two objectives of the research presented in this report. The first objective is to increase knowledge of the dynamical effects of the cargo on the vessel motions and vice versa. The second objective of this research is to investigate if it is possible to reduce the cargo motions during lifting operations by changing variables in a lifting plan or by controlling the cargo with cargo control systems. To fulfill both objectives a tool is created.

The tool that is created is a mathematical model of the vessel and cargo body. In this model the vessel and cargo are modelled as a multi-body system and is based on the frequency domain. A multi-body frequency domain model is able to calculate the responses of both the vessel and cargo motions quickly. For the input of the model the vessel constraints of the vessel and cargo body with each other and the outside world has to be described in a mathematical way. The constraints can be divided over four different modules. The first module of constraints follow from the vessel hydrodynamics. The connection of the cargo to the vessel via the crane cable are described in the second module. The influences of mooring lines on the multi-body system are described in the third module. Lastly the influences of cargo control systems are described in the fourth module. With the different modules the influence of variables of a lifting operation on the vessel and cargo motions can be studied. The output of the tool consists of the vessel RAOs. Together with wave spectra calculations these RAOs can be translated to response spectra and most probable maximum values.

The tool that is created is used to fulfill the two research objectives. First a set of calculations are done to determine the baseline responses of the multi-body system. Different variables of a lifting operation are varied and the influence of the cargo mass, crane cable length, crane top position, vessel draught and vessel metacentric height are studied. This study showed that these variables can have a large influence on the responses and natural frequencies of the multi-body system. Cargo control systems are also implemented in the multi-body model. Calculations that included cargo control systems showed that the increased stiffness of such systems can vary the natural frequencies of the different degrees of freedom in the multi-body model. When damping is applied via cargo control systems the most probable maximum values of the motions can be reduced with maximum of 55.3%.

1
Introduction

BigLift Shipping is a heavy lifting transport company. The company transports heavy cargo all over the world. Most of BigLift's vessels are equipped with two heavy lifting cranes and these cranes are used to lift cargoes on-board and of-board of a vessel. Lately BigLift Shipping experiences problems during lifting operations due to swell waves. When swell waves occur at lifting operations, the cargo hanging in the crane can start to oscillate which can cause an unsafe work environment. BigLift Shipping is interested in the origin of these motions. When the origion of these motions is understood a possible solution can be studied.

In this report a study regarding the influence of heavy cargo hanging in a vessel crane is studied, as well as possible reduction methods are presented. This report is the result of a study carried out at BigLift Shipping with supervision of Delft University of Technology. To start this research first the profile of BigLift Shipping is explained in section 1.1. In section 1.2 the problem statement is worked out followed by the origin of this problem statement in section 1.3. Thereafter the problem statement is elaborated in section 1.4. The objectives are discussed in section 1.5 and the approach of the study is given in section 1.6. Lastly the thesis layout is explained in section 1.7.

1.1. BigLift Shipping

BigLift Shipping is the company where this project is carried out. As explained in the introduction BigLift Shipping transports heavy cargo. In this section the heavy lifting marked and company profile of BigLift Shipping are worked out.

1.1.1. Heavy Lift Market

BigLift Shipping mainly operates in the heavy lifting market. The heavy lifting market is a market in which lifting operations with cargoes between 60 and 60.000 mton are executed for the purpose of transportation. Cargoes lighter than this weight are not considered as heavy lift cargoes and heavier cargoes are not common, although possible with newer vessels. There are a lot of different heavy lift companies around the world. However, since the range of cargo weights in heavy lifting is large, the amount of different specializations is also large. For semi-submersible vessels the lifting capacity is almost equal to the deadweight of the vessel. The largest single hull semi-submersible, the Boka Vanguard, can lift up to 117.000 ton. The largest double hull semi-submersible crane vessel in the world, the Heerema Sleipnir, can lift cargoes up to 18.000 mton and the largest single hull crane vessel, the Zhen Hua 30, can lift op to 12.000 mton. However, these large crane vessels are mainly designed for the lifting operation and are not designed to transport the lifted cargo. While the large heavy lifting crane vessels are not designed to transport the cargo the design can be fully focused on the lifting operation itself. These vessels have methods to increase their stability and reduce the motions of the vessel. Vessels that also need to transport their cargo cannot be optimized in such a way, reducing the lifting capabilities of the vessel.

The heavy lift transport vessels are operating in a complete new market but the largest limitations of the heavy lift transport vessels are the capacity of the on board cranes. Therefore it is common to express the capacity of a heavy lift vessel in the maximum lifting weight of the crane instead of the of the maximum deadweight of the vessel. BigLift competes with Jumbo and SAL Heavy Lift in this market.

1.1.2. Company Profile

BigLift Shipping is a heavy lift transportation company that currently operates with a fleet of 21 heavy lift vessels and 4 heavy transport vessels. The largest heavy lift vessel is the Happy Star with a combined lifting capacity of 2200 mton. The smallest vessel type has a combined lifting capacity of 800 mton. The 4 heavy transport vessels are not equipped with cranes and use the roll on, roll off method. In figure 1.1 three different vessel types are shown.

The company's head office can be divided in two departments. The commercial department and operational department. The head office is located in Amsterdam and BigLift has smaller offices all over the world with local agents. In the head office all the orders and bookings that are inquired worldwide are taken care of. The operational department handles all requirements for a smooth operation from stowage possibilities to loading arrangements and stability calculations.

(a) BigLift's Happy Star, the largest heavy lifting vessel of BigLift Shipping

(b) Biglift's Happy-D type vessel. A vessel with 2 cranes of 400 mton and 1 crane of 120 mton.

(c) BigLift's Happy Buccaneer. BigLifts oldest, still sailing vessel operating in a remote location

Figure 1.1: Three different vessels of BigLift Shipping.

1.2. Problem Statement

BigLift Shipping is a heavy lift shipping company with 21 heavy lift vessels and 4 heavy transport vessels. All the heavy lift vessels are equipped with 2 or more cranes. The lifting capacity of the cranes vary between 400 mton safe working load for the smaller vessels up to 1100 mton safe working load per crane. The cranes on board of the vessel can also operate in tandem lifts increasing the lifting capacity to 800 mton and 2200 mton respectively. The deadweight of the largest vessel is equal to 19.000 mton. This means that the lifting capacity of the largest vessel is equal to 5.5 % of the vessels deadweight in single lift operations. Which is a considerable amount. In tandem lift operations the cargo can have a weight equal to 11 % of the vessels deadweight.

The heavy lift vessels transport the cargoes all over the world. The loading operations also take place all over the world, from the North Sea to the Gulf of Mexico to the far East and Australia. Due to this variation in loading sites the environmental conditions of each loading operation is different. The environmental conditions influence the motions of the vessel and cargo during lifting operation.

In several recent projects carried out by BigLift Shipping swell has presented BigLift with challenges. Although usually BigLift contracts states that the loading / discharge berth shall be "Always Safe" and "Swell Free", in practice BigLift is facing swell affected ports from time to time. Working in swell poses safety issues since the cargo will be set in motion due to the vessel response. This problem from a shipping company is the origin of this study. BigLift is considering swell as the not modifiable cause of the problem. However, since swell waves are an external factor all waves can be researched during this study. Mooring configurations are considered part of the vessel's configuration. Although mooring arrangements are dependent on the loading location the mooring arrangements are mechanically a part of the vessel configurations. Therefore mooring arrangements should not be restricting factors in the research. The parts that can be modified, to some extend, are the vessel and cargo properties. Therefore the influence of waves on and the interaction between vessel and cargo motions must be studied. The results of this study can be used to increase the time in which lifting operations are feasible and safe.

The problem of this study can be described by one problem statement, which is shown below.

Problem statement:
"Determine the influence of vessel motions and cargo motions on each other during lifting operations in waves and develop a method to decrease the motions during these lifting operations in waves"

This problem statement contains several different aspects. These different aspects will be worked out in the following sections.

1.3. Origin of the Problem Statement

In this section the problem statement and the origin are further explained. This is done by splitting the problem in different elements. Firstly the lifting operation process is detailed by explaining the sequence of events in a lifting operation.

1.3.1. Lifting Operations

Lifting operations are executed to lift cargo from shore on board of the vessel or the other way around. Cargoes can also be lifted on or from barges or other vessels next to the heavy lifting vessel. Heavy cargoes are difficult to manage during the lifting operation. The cargoes are vulnerable or voluminous which creates no room for errors. During the lifting operation and slewing of the cranes the stability and draught of the vessel has to be controlled. The stability and draught of the vessel can be controlled by pumping water in and out of the different ballast tanks of the vessel. A lifting operation from shore to ship can be divided in five stages. These stages are listed with a small explanation below.

- **Free flotation:** Free flotation is the condition of the vessel before the lifting operation starts. The vessel and cargo are not yet connected to each other. Thus they do not influence each other yet.
- **Pretension:** During this part of the lifting operation the cargo is connected to the vessel. The mechanical connection via the crane cable couples the two bodies to each other.
- **Free hanging - Above shore:**At this point the cargo is lifted from the ground. While the cargo is hanging above the shore/barge, the outreach of the crane is relative large. The cargo can swing like a pendulum. These swinging motions should be limited to prevent clashes between the cargo and its surrounding objects. The swinging motions of the cargo will also create a load on the vessel which is another reason why the cargo swinging motions must be limited.
- **Free hanging - Above vessel:** When the crane rotates the cargo above deck the outreach of the crane is relative small. Reducing some of the loads on the vessel due to the outreach of the crane. The cargo can still swing like a pendulum which can damage the cranes or cargo holds of the vessel when the cargo is lowered on deck.
- **Put down:** Placing the cargo on deck. The relative motions between the vessel and cargo determine how difficult this stage is. This stage is critical while clashes between the vessel and cargo will damage both the cargo and vessel bodies.

The largest vessel of BigLift Shipping can lift cargoes up to 5.5% of their deadweight with a single lift operation. This percentage goes up to 11 % for tandem lift operations where two cranes are used. Since the distance between the centre of gravity of the vessel and the crane tip is much larger than the metacentric height of the vessel, large loads due to cargo motions can occur. Large motions of the cargo in the crane can also cause a collision between the cargo and the vessel crane's or hold or make it impossible to put down the cargo safely on shore or on the vessel's deck. Therefore the cargo motions must be kept small during lifting operations.

The vessel and cargo bodies are interconnected due to the coupling via the crane cable. Due to this coupling the vessel and cargo motions are coupled to each other. When waves excite the vessel hull, the vessel hull is not the only body that is excited by the waves. The cargo itself has no direct connection with the waves. However indirectly the cargo will also translate by the waves via the connection between the vessel and the cargo. The relation between the cargo and vessel motions must be determined in a mathematical way before the influence of waves can be calculated.

1.3.2. Waves during Lifting Operations

When waves 'hit' the hull of a vessel or other floating object energy is transferred from this wave to the vessel or object. The energy that is transferred will set the vessel into motion.

As stated before BigLift contracts states that the loading / discharge berth shall be "Always Safe" and "Swell Free". However this is not always the case during lifting operations. Most operations take place behind breakwaters which reduces the waves around the vessel during lifting operations. However breakwaters will not nullify all waves. Large waves can move past smaller breakwaters and a residue of the waves will still enter the loading site. At the same time swell waves, waves with a relative large period, also tend to move past breakwaters.

The most common waves during lifting operations are swell waves. Swell waves are waves that find their origin by distant weather systems. The weather at the lifting location do not influence the swell waves themselves. Swell waves often have a long period which also means that they have a long wave length. These waves with a long wave length tend to have a lot of energy in them which can be transferred to vessel motions. Swell waves also tend to move past breakwaters easier than waves generated by local weather, also called sea waves.

Since swell waves tend to occur more often during lifting operations than sea waves the main objective is to investigate the influence of swell waves. However, since a tool is being generated to solve the problem statement the tool is designed in such a way that sea waves can also be investigated with the tool. Sine every port or loading site has its own influence on the wave patterns that occur the influences of the ports, quays and bays on waves is not studied. Basic wave patterns are assumed in the calculations.

When BigLift operates in remote or offshore locations breakwaters are not installed. Here waves will be even larger than the waves in protected areas for the same weather conditions. Thus waves can occur during all lifting operations. These waves will influence the lifting operations and limit the operational window of lifting operations. The influence of waves on both the vessel and cargo motions must be studied before a solution to these motions can be proposed.

The waves at different locations can influence the vessel and cargo motion in such a way that these lifting operations become unsafe and dangerous for both the people performing the lifting operation and the objects used during and located around the lifting operation. When it is unsafe to perform the lifting operation must be stopped until safer work environments occur. These delays are a problem for the project of which the lifting operation is part of but severe delays can also be a problem for upcoming projects while the vessel cannot start these projects before finishing the current project.

1.3.3. Control of Cargo Motions

During lifting operations the cargo can swing like a pendulum. This causes problems in handling the cargo in a safe way. One way to control the cargo motions is by creating fixed connections between the cargo and the vessel. When these connections are made the cargo can not move away from its relative position to the vessel's centre of gravity. However, during lifting operations the cargo must be transferred from one location to another location. This does also mean that it is impossible to create fixed connections between the vessel and cargo while the distance between the cargo and the vessel's centre of gravity does change. Therefore a fixed connection between the vessel and cargo is not possible. However, when one end of the fixed connection is connected to a winch-like machine the connection can be controlled. This could make it possible to move the cargo with the crane as long as the winches are controlled to move along with the crane. These winches are called tugger winches. However, such connections will also transfer forces between the vessel and cargo which can create other dangerous situations.

To reduce the motions in a system the kinetic energy needs to be extracted from the multi-body system. In other dynamical problems dampers are used to reduce the motions of certain bodies. A common used example is the use of shock-absorbers in cars. Shock-absorber transfers kinetic energy of the car into heat. This reduces the motions of the car. An other example is a damper placed between the mooring line and the shore to reduce mooring forces. Such a method can also be used to reduce the forces transferred via the tugger wires.

Connections between the cargo and vessel will always introduce new dynamical relations between the two bodies. These relations will influence the relation between vessel and cargo motions. Therefore these relations and their influence must be studied.

1.4. Elaboration of the problem statement

As stated in section 1.3.1 both the vessel and cargo will be excited by waves. In section 1.3.2 is explained that not all lifting sites will be swell free and section 1.3.3 is explained that there are methods to control the cargo. When these three aspects are combined it is clear that the waves that can be present at almost every location can influence the lifting operations. BigLift is facing problems due to swell more often than in the past. Therefore BigLift is interested in a study to the combination of vessel and cargo motions during lifting operations. In this study the influence of different vessel and cargo variables and cargo control systems will investigated.

The first part of the problem statement states: "*Determine the influence of vessel and cargo motions on each other during lifting operations"*. This parts covers the study with regards to the combined vessel and cargo motions. In this part of the problem statement the vessel and cargo motions are defined as the research subjects. In current or conventional calculations the cargo is seen as a part of the vessel itself and the cargo cannot move independently from the vessel. This makes it possible to do some easy and quick calculations with regards to the vessel motions when cargo is lifted in the cranes but the motions of the cargo and the interaction between the vessel and cargo cannot be calculated. In the conventional calculations the free hanging cargo is accounted for but the dynamical swinging aspects of the cargo is not accounted for. No public research is done with regards to the combined motions of the vessel and the cargo.

During lifting operations the cargo is coupled via the crane cable. First the physical constraints between the vessel and the cargo must be examined. These physical constraints have to be described in a mathematical way in order to calculate the influence of both motions on each other. Third party multi-body dynamic software might solve the coupling between the vessel and the cargo but this software is probably not equipped with tools to solve the hydrodynamic aspects of the physical problem. Therefore it is not useful to use third-party multi-body dynamics software and the constraints will be studied. Subsequently a mathematical tool will be developed to calculate the vessel and cargo motions. The tool created can be used to determine the natural frequencies of the vessel and cargo, but the tool can also be used to determinate the influence of different lifting configurations on the responses of the vessel and cargo.

The second part of the problem statement states "*each other during lifting operations **in waves***". This part states that the waves influence both the vessel and cargo motions. The influence of waves on both the vessel and cargo motions must be examined. Hydrodynamic properties of both the vessel and waves must be added to the mathematical tool. The hydrodynamic properties of the vessel will describe how the vessel and cargo motions are influenced by the water and how the bodies are excited from wave forces. The waves will create excitation forces that will both influence the vessel and cargo bodies. These forces follow from the hull shape and loading properties of the vessel.

While swell waves have the largest influence on loading operations according to BigLift Shipping, the influence of most wave types can be calculated in the same way. Therefore the calculations are created in such a way that the influence of both sea waves and swell waves can be calculated and even waves with an even higher period. Wave spectra calculations can be used to calculate the influence of different types of waves on the motions of the vessel and the cargo. The main focus will be on the swell waves with a period between 12 and 16 seconds. However, in the tool that is created the influence of sea waves can also be calculated.

The last part of the problem statement states: "*and develop a method to decrease the motions during lifting operations in waves*". As in every mechanical system there are excitation frequencies at which the bodies of the vessel and cargo show larger responses. This is called resonance and occurs around the natural frequency of a mechanical system. The motions of the vessel and cargo that occur during lifting operations are dependent on the waves that occur during these lifting operations. When these wave excitate the vessel and cargo around their natural frequency the responses of these bodies on the waves will be large. Different variables of a lifting operation will influence the responses in different ways. Knowledge of this influence can be used to chose lifting configurations that show smaller influences of the waves that occur during lifting operations and reduce the responses of the vessel and cargo motions.

Another method to reduce the motions of the cargo is by introducing cargo control systems. Such systems are briefly explained in section 1.3.3. Besides introducing a stiffer connection between the vessel and cargo bodies damping can be introduced to transfer kinetic energy from the cargo into another kind of energy. In the tool created the constraints from a stiff connection between the vessel and cargo will be added as well as damping. The influence of these two properties will be studied. From this study a method to decrease the responses of the cargo on the waves can be created.

1.5. Objectives

This reason this research is fulfilled can be traced back in three objectives. The first objective of the research is to gain a better understanding of the vessel and cargo interactions. In this chapter it has been described a number of times that there are no public methods to calculate the interaction between vessel and cargo motions. BigLift is sometimes hindered by cargo motions in such severe ways that the loading operations has to be cancelled for a certain amount of time. Once the mutual relationship has been mapped BigLift engineers can use this information to find solutions for these problems during lifting operations. When BigLift can operate in more severe weather conditions the money loss due to delays will decrease.

The second objective is the tool itself. While the understanding of relations between the vessel and cargo is useful for decision making by gut feeling or knowing which variables of a lifting configuration can be changed in order to influence the vessel and cargo motions, the tool itself can be used to calculate the exact influence of such changes. The tool can be used in future projects to determine what the best lifting configuration is for that project.

The third objective is to create a better understanding of the influence of cargo control techniques. Right now some techniques to control the cargo are known. However, public research on the effects is never done. The exact influence of both a stiff connection and applied damping is not known at BigLift Shipping. Even if such studies are done by other companies the results are hidden and not available for public use. Therefore the influence of cargo control systems on both the amplitude of the responses as the form of the responses.

These three objectives can be combined in one thesis objective. This objective is given below: *Develop a tool that can calculate the coupled responses of both the vessel and cargo bodies on waves and use this tool to study the influence of different lifting configurations and cargo control systems on the vessel and cargo responses.*

To fulfill the thesis objective first the interaction between the vessel hull and waves will be determined. The wave forces are the main excitation forces during lifting operations. From these forces the responses of both the vessel and cargo can be calculated. The tool will be made modular that different input variables can be studied at any given time without large alterations of the tool. When the tool is finished the tool can be used for different projects executed by BigLift Shipping to predict vessel and cargo motions during the lifting operations of these projects.

1.6. Approach

Now that it is clear that some lifting operations can not be performed due to waves the approach to investigate the problem and search for solutions can be described.

1.6.1. Multi-Body System

The motions that are studied are motions that occur during lifting operations. When a vessel is in transit the cargo is seafastened and thus integrated with the vessel motions while the lashings keep the cargo in place. During lifting operations the cargo hanging in a crane will act like a pendulum. The cargo can develop motions and through coupling these motions can increase or reduce the vessel motions. Therefore lifting operations require other calculations than normal stability, seakeeping or hydrostatic calculations. In conventional calculations the cargo weight is attached to the crane tip during lifting operations. This will give an accurate solution for simple stability calculations of the vessel. However, the interaction between the vessel and the cargo motions is not taken into account. The coupling of the cargo to the vessel via a crane cable must be modelled in a mathematical way that not only the influence of the cargo weight on the vessel motions is taken into account but also the influence of the motions of both bodies on each other is taken into account.

In this study the vessel and cargo will be seen as two separate bodies which can move independently from each other but are coupled through certain dynamical constraints. Due to these constraints forces are transferred between the two bodies which will influence the responses of both bodies. The dynamical system of the vessel and its cargo are treated as a multi-body system. In multi-body systems the constraints are described via mathematical formulations. All the responses of the different bodies and directions the bodies can move in are calculated at the same time. In this way the cargo and the vessel motions can be calculated as a combined system. From this multibody system all or specific responses of both the vessel and cargo can be extracted and studied.

The lifting operations that are considered can be lifting operations at sea or in a bay where no mooring lines are attached or at a quay where mooring lines are part of the calculations. Therefore the influence of mooring lines will also be studied. The influence of quays, ports and breakwaters on waves and thus wave forces is different for every single location around the world. A study to wave patterns such as refraction and reflection will not be executed. The different wave patterns that can occur are assumed to be input values and thus not part of the study goal.

1.6.2. Frequency Domain

Equations of motion that consists of a time varying aspect that is also harmonic can be solved in the time domain or in the frequency domain. When the equation of motion is solved in the time domain the equation of motion is solved directly for different time steps. E.g. the equation of motion is solved for every 0.1 second. The advantage of the time domain calculations is that the solutions contain the non-linear behaviour in the equation of motions. Mooring lines, tugger lines, low frequency drift forces, viscous damping and forces due to wind and currents can cause these non-linear motions. In section 2.3 the equation for the pendulum motions are described. When the pendulum is excited in the horizontal and vertical direction at the same time non linear behaviour could also occur. This non-linear behaviour results in two, or more, natural frequencies. These natural frequencies follow from the different linear motions that form the non-linear pendulum motion. When the horizontal and vertical direction are considered as the two degrees of freedom two different linear natural frequencies occur. The first natural frequency is related to the natural frequency in the horizontal translation and the second natural frequency is related to the vertical translation. When the X, Y and Z directions are considered as the three different translations of the pendulum three different natural frequencies will form the non-linear motion from the three natural frequencies of the X, Y and Z translations. This combination of translations is called parametric excitation.

The disadvantage of a time domain calculation is that the model becomes complex, the results are statistically hard to interpret and the calculations are time consuming. Since time domain calculations are expensive in computational power and computation time the user must have a great understanding of the physical problem for efficient calculations. Since all these disadvantages are at odds with the goal of this project time domain simulations are not the favourable solution method.

When the equations of motions are linearized in all different aspects the equations can be solved in the frequency domain. Since the forces and excitations are harmonic, which will be further elaborated in section 2.2, only the different mass, damping and stiffness values must be linearized. The advantages of frequency domain calculations are time efficiency, simple frequency calculations instead of time step calculations and easy to interpret results. The calculations and derivations that have to be solved are fairly easy and statistical formulations can be used to interpret the results. The biggest disadvantage of frequency domain calculations is that non-linearity cannot be included in the calculations. All the different non-linear aspects of the equation of motion must be linearized. However, most non-linear aspects do not have a big influence on the model since the non-linear motions are small or the influence is not in a frequency of interest. When the influence of these non-linear aspects are small they could also be neglected. Wind induced motions are expected to be small since low wind speeds are required to allow safe lifting operations. Some non-linear motions will break down before large amplitudes are generated, such as sub-harmonic motions (Journee and Massie)[12] and for other non-linear aspects a linear model is sometimes available such as the Ikeda method [13] for the viscous damping.

1.6.3. Model Layout

To solve the research question a model will be made. This model will be made in the mathematical program Python. Python[7] is a programming language that can be used to solve a series of equations and other orders. Therefore it is particularly suitable to solve the multi-body problem of vessel and cargo motions. In this model different parts need to be taken into account. First all the constrains and coupling terms between the vessel motions and cargo motions must be described in a mathematical way. When all constraints of the multibody system are determined the response of the vessel and cargo due to wave forces can be calculated. These responses can be used to study the influences of different lifting configurations and the influence of cargo control systems. how this is done is described in chapter 3

To create a model that can be used for every single lifting operation the tool will be made modular. This means that the different constraints can be implemented in a flexible way. For example: the mooring lines can be neglected with one single option. While the model is modular different lifting configurations can be solved in rapid succession of each other to calculate the influence of different loading configurations on the combined vessel and cargo motions for all different projects.

1.7. Thesis layout

First the theoretical background will be explained in chapter 2. In this chapter the physics required to solve the problem will be described. First multi-body dynamics will be explained. Multi-body dynamics are used to calculate the responses of both the vessel and cargo at the same time. Thereafter the hydrodynamic properties of both waves and the vessel will be described. As third the physical properties of mooring lines and linearization of spring values are explained. The connection between the vessel and cargo via the crane cable will be described as fourth followed by the influence of damping on multi-body systems. Thereafter the natural frequency calculations and their properties and usefulness will be explained. The influence of non-linearities will be tackled in the last section of the theoretical background.

After the theoretical background the model will be described in chapter 3. First the layout of the model will be explained. Thereafter the input of the vessel hydromechanics are explained. Next the mathematical coupling between the cargo and the vessel via the crane cable is explained. As fourth the mathematical modelling of mooring lines are explained followed by the explanation of the modelling of the cargo control systems. After all these input properties the motion calculations are explained. Thereafter the calculations of significant motions are worked out. After that the verification is explained followed by the validation of the model. Next the mathematical influence of lifting variables are worked out when the sensitivity study is explained.

In chapter 4 the baseline calculations that have been carried out are explained. These baseline calculations are prepared for both the sensitivity of the lifting variables study and the cargo control system influence study. In this chapter first the baseline case is explained. After the case the chosen wave direction is explained. Thereafter the natural frequencies and eigenvectors of the baseline case are calculated and explained. Lastly the behaviour of the baseline case in terms of RAOs and most probable maximum values are worked out.

The influence of the different variables during a lifting operation are studied in chapter 5. In this chapter first the influence of the cargo mass is calculated followed by the crane cable length. As third, fourth and fifth the influence of the Crane top in Z, Y and X direction are studied respectively. Thereafter the influence of the vessel draught is studied followed by the influence of the metacentric height. After all these different variable studies the results are summarized. The influence of mooring lines on the multi-body system are also studied in this chapter

In chapter 6 the influence of cargo control systems are studied. First the influence of tugger wires with a low stiffness value is studied followed by a study of tugger wires with a high stiffness value. Thereafter the influence of low amounts of damping are studied followed by the influence of large damping values. In chapter 7 the study is discussed. Lastly in chapter 8 the conclusion is given.

2
Theoretical Background

In this chapter the theoretical background required to solve the problem is described. Since the multi-body system consist of of two bodies it is important to understand all the dynamics of the system before combining all the different influences. The vessel and the cargo are two different bodies. However, both bodies are influenced by external factors, themselves and each other. All these influences will be described in the sections in this chapter. But first multi-body dynamics must be described to understand how the different theoretical influences can be translated to equations. In section 2.1 multi-body dynamics are explained. Thereafter Section 2.2 the influences of waves and the vessel's hydrodynamic properties are explained. Next the dynamics of a pendulum are explained in section 2.3. The influence of mooring lines and the linearization of spring values are worked out in section 2.4. In section 2.5 the influence of damping on dynamical systems is explained. Thereafter the influence of natural frequencies and resonance is clarified in section 2.6 followed by the explanation of natural frequency calculations of multi-body systems in section 2.7. Lastly the nonlinearities are worked out in section 2.8.

2.1. Multi-Body Dynamics

The problem consists of two different bodies, the vessel and the cargo. Both bodies can move independently but are influenced by each other. To understand how the bodies are influenced first multi-body dynamics must be described. Multi-body dynamics are dependent on the amount of bodies in the system, the degrees of freedom per body and the interaction between the different degrees of freedom in the system. A body is considered to be a rigid or flexible part of a mechanical system. Examples of this are a single arm of a robot, a solid block and the weight of a pendulum. The different bodies in a multi-body system are connected to each other or the world via constraints which restrict the relative motions, velocities or accelerations of the bodies. Examples of these constraints are a spring between two bodies or the ground, water around a vessel or air around a body hanging from a crane. The degree of freedom of a system is the number of independent motions that the system which consists of. In other words it is the number of parameters in which the state of a physical system can be described. For example the position of a single locomotive along a train track has one single degree of freedom since the body can only move alongside the rail track and the position of the body can be described by the distance travelled along the rail track. The position of a rigid body in the open space, such as a vessel in water, will have six degrees of freedom. The six degrees of freedom contain three translations and three rotations. These six degrees of freedom will be further described in section 2.2. In multi-body dynamics it is important to determine if the translations and rotations of the different bodies are truly independent. A train consisting out of a train with a wagon consist out of two different bodies but those bodies have a solid connection between them which causes the bodies to be dependent on each other. The locomotive cannot move without moving the wagon in the same direction with the same distance. This system consisting out of two different bodies does only have one single degree of freedom. Lastly the interaction between the different degrees of freedom is important. These interactions are often coupled to the constraints between two bodies or a body and the world. A spring connected between two bodies will transmit a force to the two bodies when the relative distance between the two bodies changes. The different constraints in multi-body dynamics can be translated in an algebraic equation that defines the relative translation or rotation, and their time derivatives, between the different degrees of freedom of a body, the different bodies or a body and the world. For example, the force that a spring transfers to a body can simply be calculated by multiplying the spring stiffness with the relative extension of the spring. The equations that describe the different constraints can be combined in one big system. When all the constraints that occur in a system are combined in a mathematical model the interactions between the bodies and the world can be calculated. In multi-body dynamics is the dynamic behavior a result from the equilibrium of applied forces and change of momentum. The applied forces in the system consist of external forces but also of forces resulting from the stiffness and damping in the system. Since the motions of both bodies and all degrees of freedom can be

calculated at the same time with multi-body dynamics, multi-body dynamics is a good method to calculate the interaction between vessel and cargo motions.

Since multibody dynamics is essentially a combination of different mathematical equations the general laws of nature do apply on multi-body systems in the same way as in single body dynamics. Therefore the laws of motion described by Newton in "Principia Mathematica Philosophiae Naturalis" can be used. The second law, which explains how the velocity of an object changes when it is subjected to an external force is the most important one for this study and shown in equation 2.1. This equation can be extended with damping and spring terms to develop an equation of motion of a mass-spring-damper system as shown in equation 2.2. In this equation M contains the mass component of a body, B contains the damping component applied to a body and C stands for the stiffness that is applied to the body. x, $\dot{x}$ and $\ddot{x}$ represent the displacement, velocity and acceleration of the body respectively. Lastly the external forces acting on the body are given by F. The equation of motion that describes a mass-spring-damper system is important because the essentials of this equation are the same as the essentials of multi-body dynamics. When the Mass, Damping and Stiffness components of the single body calculation are changed in matrices and the displacement, velocity, acceleration and force components are changed in vectors the multi-body equation is formed.

Since the frequency domain is used all properties in the equation are linear. Due to the linearity the superposition principle can be used. *The superposition principle states that for linear systems, the net response caused by two or more inputs, is the sum of the inputs each would have caused on its own*[40]. In other words, all different influences on the multi-body systems can be calculated separately and added together to solve the combined influence on the multi-body system. This is useful since it makes it possible to calculate all different constraints separately. When all constraints are known and translated to a mathematical relation all these mathematical relations can be combined to solve the responses of the multi-body system.

In equation 2.2 different aspects such as hydrodynamic spring terms and pendulum spring terms, can be combined as long as the different systems can be linearized. This makes the equation of motion very useful to calculate the influence of different lifting configurations and cargo control systems. Every part of the multi-body system, such as hydrodynamics of the vessel, cargo pendulum and cargo control systems can be calculated separately and simply added to the combined system or removed as long as the different degrees of freedom are used in the same order in each and every individual system.

$$m \cdot a = F \tag{2.1}$$

$$M \cdot \ddot{x} + B \cdot \dot{x} + C \cdot x = F \tag{2.2}$$

The ship and cargo system contains two bodies. Both bodies exist out of three translations and three rotations thus the combined system will contain out of a twelve degree of freedom system as long as all degrees of freedom are independent from each other. Since there are no rigid connections between the vessel and the cargo all degrees of freedom in the system are independent. The crane cable is considered a spring, which will be further elaborated in section 2.3. Although this spring is very stiff the vessel and the cargo can have an independent translation. In this twelve degree of freedom system the first six degrees of freedom will describe the motions of the vessel and the last six degrees of freedom will describe the motions of the cargo in the crane. The twelve degree of freedom system will result in 12 by 12 matrices and vectors with a length of 12 components in the equation of motion. Since the first six degrees of freedom contain the translations and rotations of the vessel and the last six degrees of freedom contain the cargo translations and rotations the matrices can be divided in four quadrants as shown in figure 2.1. The top left quadrant shows the influence of the vessel on itself. The top right quadrant shows the influence of vessel motions on the cargo swing motions. The bottom left quadrant represents the influence of cargo motions on the vessel motions and the influence of cargo motions on itself are shown in the bottom right quadrant.

Throughout the report the numbers coupled to the different degrees of freedom will stay constant. The corresponding numbers for each degree of freedom are explained below. In section 2.2 the degrees of freedom and their directions will be further elaborated.

- x_1 = Vessel Surge
- x_2 = Vessel Sway
- x_3 = Vessel Heave
- x_4 = Vessel Roll
- x_5 = Vessel Pitch
- x_6 = Vessel Yaw
- x_7 = Cargo Surge
- x_8 = Cargo Sway
- x_9 = Cargo Heave
- x_{10} = Cargo Roll
- x_{11} = Cargo Pitch
- x_{12} = Cargo Yaw

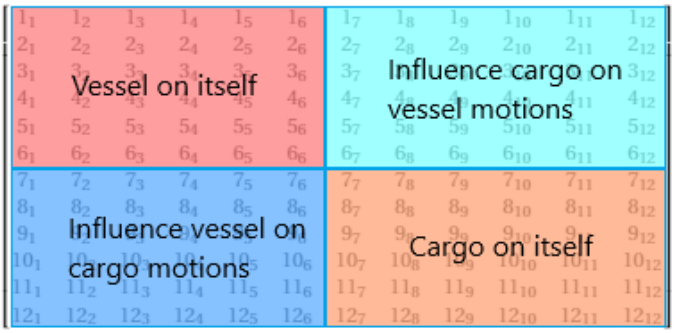

Figure 2.1: Matrix quadrant visualization

2.2. Hydrodynamic Background

Two important hydrodynamic aspects in this multi-body system are vessel motions and ocean waves. The vessel motions are important since the vessel motions are part of the multi-body system. Ocean wave theories are important because the theory explains how waves are formed and how the excitation force applied to a vessel forms from this theory.

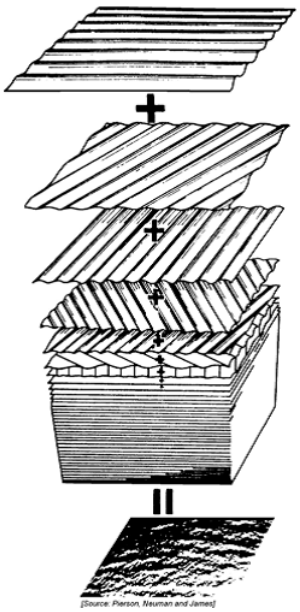

Figure 2.2: Illustration that a sum of many simple regular waves makes an irregular sea[12][32]

In ocean wave theory it is assumed that an irregular sea consists out of many simple, regular harmonic waves as proven by St. Denis and Pierson [32]. Each wave has its own amplitude, frequency, direction of propagation and phase angle. The summation of the different regular waves is illustrated in figure 2.2. Due to linearization the response of the vessel in a specific sea state can be calculated with the superposition principle by calculating the response of the vessel for each individual regular wave and combining these responses. A regular wave can be described with the equation given in equation 2.3. In this equation ζ stands for the water surface elevation at any given time and location. ζ_a is the amplitude of the water surface elevation. The wave frequency is given by ω and the time is given by t. The wave number is given by k and x represents the position of the wave along the x-axis. An illustration of a regular wave is given in figure 2.3

$$\zeta(x,t) = \zeta_a \cdot sin(\omega \cdot t - k \cdot x) \tag{2.3}$$

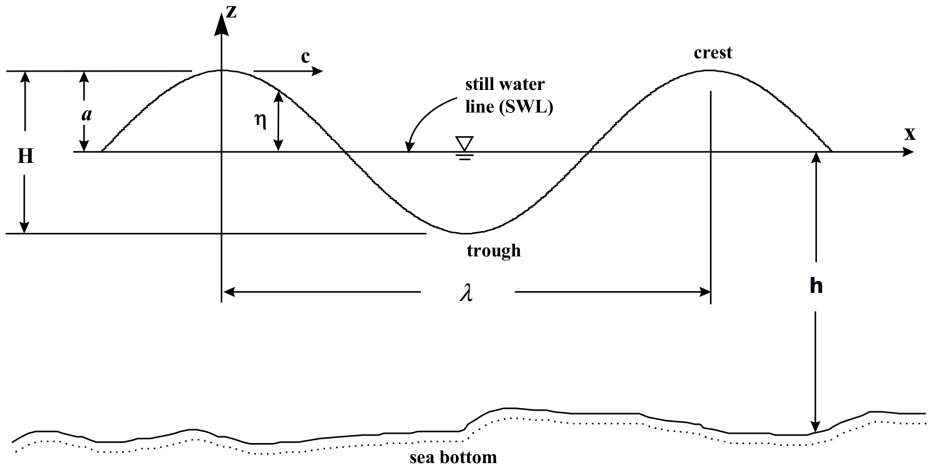

Figure 2.3: Illustration of a regular wave[20]

Equation 2.4 shows how different regular waves can be combined to create the water surface elevation of irregular seas. In this equation n stands for the wave component number. N represents the total number of regular waves that are combined in an irregular sea. The amplitude of the different regular waves is given by ζ_n. The wave frequency and wave number of wave component n are given by ω_n and k_n respectively. Lastly the phase of the different regular waves is given by ϵ_n. In figure 2.4 a representation of the summation of regular waves is given. An energy density spectrum can be used to represent irregular waves. In figure 2.4 an example of an energy density spectrum is given along the ω axis. The definition of the energy density spectrum of the surface elevation is given in equation 2.5. In this equation $S_{\eta\eta}$ is the energy density spectrum of the water surface eleviation and $\Delta\omega$ is the difference between two successive frequencies in the wave spectrum calculation or, in other words, step size in the wave spectrum calculation.

In the history of ocean wave studies different formulas for the wave energy spectra are calculated for different sea states. The most commonly used wave spectra are Bretscheider, Pierson-Moskowitz and the JONSWAP spectra. These different wave spectra are more accurate for different sea states. The JONSWAP spectrum is fairly accurate for sea waves that occur in the North Sea. Sea waves are waves generated by local weather. The local wind will create waves and the energy density in these local sea waves can be stochastically calculated by the JONSWAP spectrum. When a storm happens somewhere in the world the storm will create large waves with a lot of energy in them. However, when the storm disappears the waves continue to exist. These waves from "far away storms" will slowly disperse. Swell waves can travel large distances before they cease to exist. The peaks of the swell waves will decrease and the period of the swell waves will increase when the waves travel further and further away from the storm that generated the waves. The Pierson-Moskowitz spectrum can describe these swell waves in a good manner and Therefore the Pierson-Moskowitz will be used to calculate the swell spectra in this study.

$$\zeta(x,t) = \sum_{n=1}^{N} \zeta_n \cdot sin(\omega_n \cdot t - k_n x + \epsilon_n) \tag{2.4}$$

$$S_{\eta\eta}(\omega_n) = \lim_{\Delta\omega \to 0} \frac{0.5 \cdot \zeta_n^2}{\Delta\omega} \tag{2.5}$$

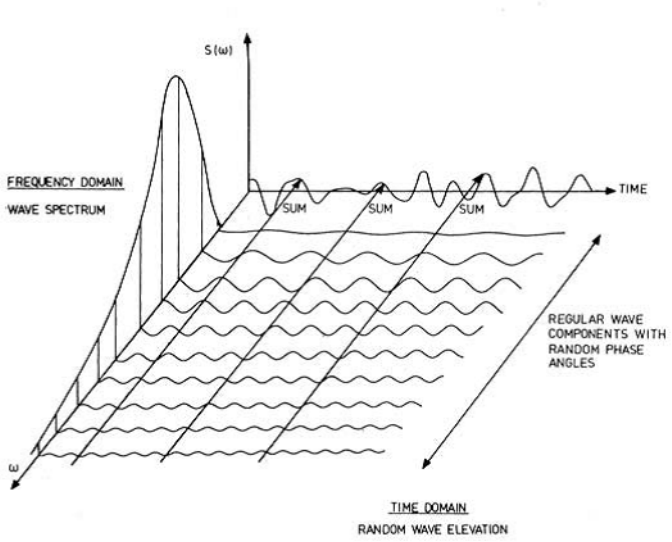

Figure 2.4: Illustration of the composition of a wave spectrum [5]

In the introduction of this research is explained that this research will be focused on the vessel and cargo behaviour and that no study will be done with regards to the waves in ports and along side quays. However the superposition principle that makes it possible to model an irregular wave as a sum of many different regular waves is very useful for the study of vessel and cargo motions. Since the wave dynamics can be split up in regular waves the responses of a vessel can be calculated for regular waves. The response of a vessel in regular waves can than be translated to the response of a vessel in irregular waves by the use of the super position principle of irregular waves. How the responses of a vessel can be calculated will be explained in the second half of this section.

In general 6 degrees of freedom are used when vessel motions are described. The degrees of freedom consist of out of three translations and three rotations. The three translations of the ship are translations acting on the rigid body of the ship. The first translation is surge in the longitudinal x-direction where the positive direction is forwards. Sway is the second translation in lateral y-direction where the positive direction is a translation to port side. The third translation is in the vertical z-direction where upwards is the positive direction. The three rotations are rotations around the axis of the translation. The first rotation is roll about the x-axis. The roll motion is expressed by ϕ. The pitch about the y-axis is the second rotation and expressed by θ. Yaw which is expressed by ψ is the third rotation which is the rotation about the z-axis. All rotations are positive in a right turning moment. Figure 2.5 shows the 6 degrees of freedom.

Besides the degrees of freedom of the vessel the degrees of freedom of the cargo are used in the multi-body calculations as described in section 3.1. In this section is also explained that the cargo degrees of freedom are given by number 7 till 12.

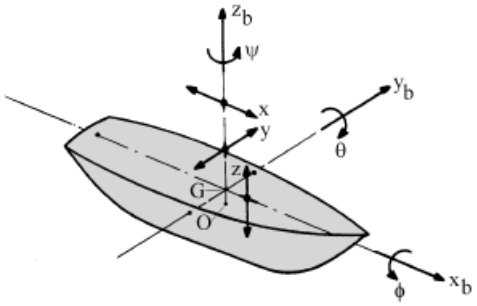

Figure 2.5: Definition of ship motions in six degrees of freedom[12]

The equation of motion that describes a mass-spring-damper system given in equation 2.2 is important because vessel motions in waves can be translated to such a system. First order ship motions are sinusoidal oscillations, which can be described by linear equations of motion. Therefore linear behaviour is assumed in most calculations. This makes it possible to apply the superposition principle. The assumed linear systems makes it possible to decompose hydrodynamic forces in mass, spring and damping coefficients. Since the motions of a vessel will move water, extra aspects must be taken into account in the equation of motion. This will be done by adding the added mass term and the potential damping term which describes the added inertia due to the acceleration of water and the damping due radiation of water, which creates waves, respectively. Since not all damping forces are linear the viscous damping has to be introduced. The viscous damping contains the linearized nonlinear damping coefficients for different wave frequencies and roll angles. The equation of motion given in equation 2.2 can also be used to write down the hydrodynamical properties of a vessel. This equation is given in equation 2.6. Matrices are given by uppercase boldface letters, vectors are given by lowercase boldface letters and scalars are given by lowercase, normal font letters. The letter i is used to describe the imaginary unit. In the equation $\mathbf{M}$ and $\mathbf{A}$ represents the mass and added mass matrices of the vessel. The linear damping matrix is represented by $\mathbf{B}$ while $\mathbf{B_v}$ represents the linearized viscous damping. $\mathbf{C}$ is the spring matrix and $\mathbf{x}$ represents the displacement vector while $\dot{\boldsymbol{x}}$ and $\ddot{\boldsymbol{x}}$ represent the first and second derivation of $\mathbf{x}$ to time. The wave excitation force vector is given by $\boldsymbol{F_{exc}}$. The force vector is given by a capital letter. This is an exception on the notations used in this report. Since $\boldsymbol{F_{exc}}$ is an harmonic force proportional to the incoming harmonic wave it can be assumed that $\boldsymbol{F_{exc}} = F_a e^{i\omega t}$. Since F_{exc} is assumed to be harmonic x can also be assumed to have a form equal to $\boldsymbol{x} = x_a e^{-i\omega t}$ since the response of the vessel is a direct response on the wave excitation force. This assumption makes it possible to write $\dot{\boldsymbol{x}}$ and $\ddot{\boldsymbol{x}}$ as a function of $\boldsymbol{x}$ as shown in equations 2.7 to 2.9.

$$(\boldsymbol{M}+\boldsymbol{A})\cdot\ddot{\boldsymbol{x}}+(\boldsymbol{B}+\boldsymbol{B_v})\cdot\dot{\boldsymbol{x}}+\boldsymbol{C}\cdot\boldsymbol{x}=\boldsymbol{F_{exc}} \tag{2.6}$$

$$x = x_a e^{-i\omega t} \tag{2.7}$$

$$\dot{x} = -i\omega\cdot x_a e^{-i\omega t} \tag{2.8}$$

$$\ddot{x} = -\omega^2\cdot x_a e^{-i\omega t} \tag{2.9}$$

Equation 2.6 can be split in three essential parts. The first part is the wave excitation force. This is the external force applied to the system by the waves. The second part is the response of the vessel given by $\boldsymbol{x}$ and its derivatives. From these vectors follow the motions of the vessel. The last major part in this equation is the combined ship system. This system is the combination of the mass matrices, damping matrices and stiffness matrix and their relation to the wave frequency. The combined ship system S is given in equation 2.10. The ship system contains all dynamical connections between the different degrees of freedom in terms of mass, damping and stiffness. Note that this equation is a part of the left hand side of equation 2.2. This part is important since most of the time the vessel responses are calculated with the help of the ship system and the excitation forces since the ship system and external excitation forces can be calculated independently as long as the hull form is known. Equation 2.11 shows how the response of a vessel due to waves can be calculated. This equation is basically equation 2.2 rewritten to solve the equation for $\boldsymbol{x}$ instead of $\boldsymbol{F}$. In

vessel hydrodynamics the response is given in $\left[\frac{m_a}{\zeta_a}\right]$ for translations and in $\left[\frac{\phi_a}{\zeta_a}\right]$ for rotations and are called Response Amplitude Operators, RAOs in short. m_a represents the response of a translation in meters and ϕ_a represents the response of a rotation in degrees. The wave height in meters is given by ζ_a. The RAOs are thus translations or rotations per meter wave height. Since the RAOs are related to the wave height the RAOs do not vary when the wave height changes. The RAOs are frequency dependent. Even though the RAOs are independent of the wave height, non linearities in the multi-body system requires different RAO calculations for different amplitudes of the responses of the multi-body system. The responses are coupled to the wave height and thus larger wave heights can cause different RAO calculations. An example is the viscous damping that is coupled to the vessels roll amplitude. Greater wave heights will increase the roll response of the vessel and thus a larger roll damping factor must be applied.

$$\boldsymbol{S} = -\omega^2 \cdot (\boldsymbol{M} + \boldsymbol{A}) - i\omega \cdot (\boldsymbol{B} + \boldsymbol{B_v}) + \boldsymbol{C} \tag{2.10}$$

$$\boldsymbol{x} = \boldsymbol{S}^{-1}\boldsymbol{F_{exc}} \tag{2.11}$$

The method for calculating the vessel responses for the six degree of freedom system can be expanded to the twelve degree of freedom system. In section 2.1 is explained that multi-body dynamics is a combination of smaller equations. One of these smaller equations is the vessel hydrodynamic equation shown in equation 2.6. Since this is one of the smaller equations that will be solved in the multi-body system the mass, added mass, damping, viscous damping and stiffness matrices that describe the vessels hydrodynamic particulars as well as the wave excitation force can be substituted in the first six degrees of freedom of the multi-body equation.

Since it is assumed that the cargo will be lifted above water no hydrodynamic influences on the cargo must be calculated. This does also mean that there is no hydrodynamic coupling between the cargo and the vessel. As a result only the top left quadrant of the multi-body matrices illustrated in figure 2.1 will be filled with hydrodynamic properties. The wave excitation force vector will have non-zero entries in the first six entries and all zero entries for the last six entries of the vector. This does not mean that the cargo will not move due to wave forces but that the waves will not exert a force to the cargo directly. The cargo can still be moved indirectly due to coupling between the vessel and cargo responses.

2.3. Pendulum Motions

The cargo in a crane can be assumed to move as a pendulum. The standard equation of motion as described in equation 2.2 can be used to implement the pendulum motions in the multi-body system. The mass of the cargo is filled in on the diagonal of the mass matrix for the translations and the radii of inertia for the rotations. Besides air friction other form of damping are present in the pendulum system. These other forms of damping are much smaller than the air friction and Therefore neglected. Examples of other forms of damping are rotational friction of the crane cable and an increase of heath in the cable due to friction. The air friction is small but it will not be neglected because it is a form of natural damping on the pendulum, and even though it is small, in comparison with other forms of natural damping it is relatively large. For an accurate model damping needs to be applied, otherwise the responses of the degrees of freedom will give extremely large excitations around the natural frequency. The spring constant follows from the offset of the cargo to the crane tip and the restoring force induced by gravity. Figure 2.6 shows the schematic forces acting on the pendulum while the pendulum is in motion. Gravity applies a constant force F_g. This constant force applies tension on the wire, shown as a T in the figure. When there is an offset between the crane tip and the cargo, an angle θ with regard to the vertical will exist and a horizontal component is introduced. This horizontal component F_{rest} can be calculated with equation 2.12. The offset Δx can be calculated with equation 2.13. Where l is the length of the crane wire. The angles of rotation are considered small since small motions are required for safe lifting operations. Small motions is also a necessity for linearization. When small motions occur it can be assumed that $sin\theta = \theta$ and $tan\theta = \theta$. These assumptions can be done for $\theta < 10°$ This is justified since the cargo motions need to be small. When the motions are not small the linearization will not give accurate solutions but the workability is also not sufficient. This assumption makes it possible to write the restoring force as a function of the offset, this is shown in equation 2.14. The pendulum spring stiffness follows from the restoring force and is given in equation 2.15.

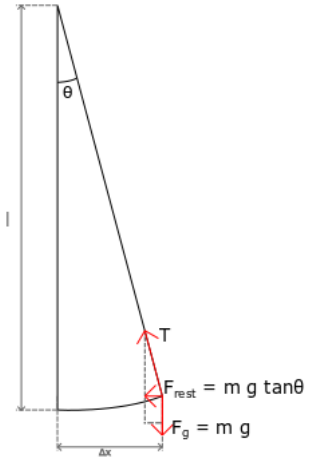

Figure 2.6: Schematic pendulum mechanics

$$F_{rest} = m \cdot g \cdot tan\theta \tag{2.12}$$

$$\Delta x = l \cdot sin\theta \tag{2.13}$$

$$F_{rest} = \frac{m \cdot g}{l} \Delta x \tag{2.14}$$

$$K_p = \frac{m \cdot g}{l} \tag{2.15}$$

For mathematical purposes Δx is explained as a function of l and θ in equation 2.13. However in the multi-body system θ will not be calculated. Δx is the result of the relative response between the crane tip and the centre of gravity of the cargo. The crane tip can move by translations of the vessel but rotations of the vessel will also cause a translation of the crane tip. When the vessel rolls the crane tip will not only rotate but also show a translation. The distance between the centre of gravity of the vessel and the crane tip will cause translations of the crane tip when the vessel rotates. The roll motion together with the vertical position of the crane tip will result in a offset in y-direction. All the different aspects of the pendulum restoring stiffness and the offset that causes a restoring force will be explained in section 3.3

Now that the horizontal restoring stiffness is known it is time to determine the vertical restoring stiffness. The vertical restoring stiffness follows from the Young's modulus and the dimensions of the crane wire. The restoring force of the crane wire is given in equation 2.16. Here the Young's modulus is given with E. A represents the cross-sectional area of the crane wire. The length of the crane wire is given with l and Δz is the offset in vertical direction. From the restoring force in vertical direction follows the vertical stiffness given in equation 2.17. The vertical offset Δz is not only dependent on the vessel and cargo heave motions. Different rotational motions will cause a vertical offset in the same way that these rotations do this in the calculations for the pendulum restoring force. The forces in vertical direction will influence the overall length of the crane cable. This will influence equation 2.13 and add some nonlinear influences to the motions. However, the stiffness value of the crane cable is high which results in small variation of the crane cable length. Since the relative change of crane cable length in comparison with the overall crane cable length, or the strain, is very small the influence of these nonlinear forces due to strain are neglected.

$$F_w = \frac{E \cdot A}{l} \Delta z \tag{2.16}$$

$$K_w = \frac{E \cdot A}{l} \tag{2.17}$$

2.4. Linearized Spring Values

Beside the hydrodynamic vessel van cargo dynamics there is a third potential dynamical aspect during lifting operations. When the vessel is moored to a quay mooring lines will influence the stiffness of the system. Mooring lines can be modelled as springs acting on the vessel. Every spring can be linearized and the corresponding stiffness values can be calculated. Due to the superposition principles these linearized values can be combined to one spring stiffness model. Described in four lines of text this sounds quite easy. However mooring lines tend to be non-linear. This is a problem since the multi-body calculations are done in the frequency domain which means that the solutions are solved in a linear environment. Therefore the mooring line stiffness must be linearized. Figure 2.7 shows the relation between the elongation of a line and the load, as percentage of the breaking strength, applied to the line. This figure shows that the applied load to elongate a polypropylene line with 1 % of its broken-in length is equal to a load of 5% of the breaking strength of mooring line. An elongation of 2% of the broken-in length requires a load of 12% of the breaking strength of the line. This proves that the elongation does not increase linearly with the load, and thus force applied to the mooring lines. Therefore the values that appear in the figure must be linearized before they are useful for the frequency domain calculations. Since lifting operations require small motions in general to be successful it is more useful to linearize the mooring lines along small elongations instead of long elongations. Therefore the mooring lines will be linearized between the 0% to 5% elongation of the broken in length. In figure 2.7 the red line shows the linearized line for polypropylene mooring lines. Equation 2.18[36] shows how the linearized mooring line stiffness can be calculated. When this equation is used to calculate the linearized stiffness of the polypropylene mooring lines it becomes clear that the stiffness depends on the total length and breaking strength of the used mooring line as shown in equation 2.19.

$$K_{line} = \frac{d(Load)}{d(Elongation)} @ Elongation \approx 0 \tag{2.18}$$

$$K_{line} = \frac{46\%\, Breaking\ strength}{10.0\%\, broken-in\ line\ length} \tag{2.19}$$

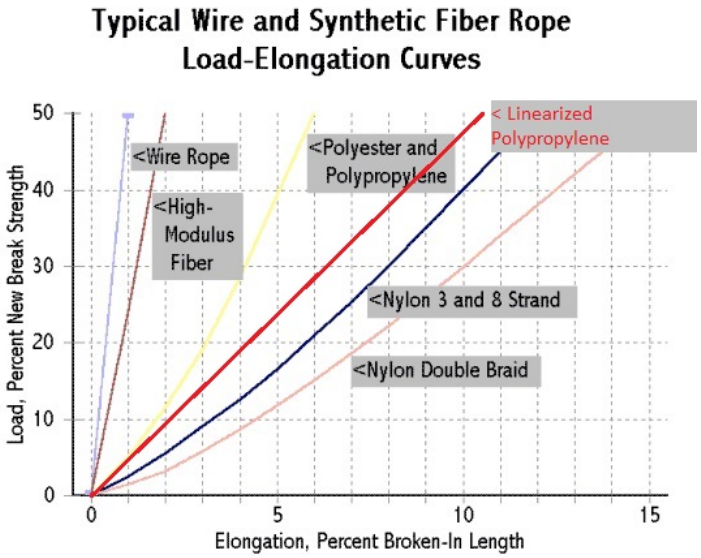

Figure 2.7: Load elongation curves of different mooring line materials[6]

2.5. Influence of Damping

Damping is a term used in the equation of motion described in equation 2.2. The principle of damping is the dissipation of energy. In physics damping restrains vibrations or motions such as mechanical oscillations. Since the mechanical system of the vessel and cargo are excited by harmonic forces damping will reduce the responses of the vessel and cargo motions. The reduced responses will create safer lifting operations and lifting operations can be fulfilled in more severe weather conditions.

A swing is a good example of a motion where damping is applied to. When a person stops pumping a swing the swing motion will die down because damping occurs. In the case of the swing damping is applied via air friction and rotation friction of the swing's ropes. Other examples of damping besides air friction are shock absorbers and viscous damping of energy dissipation via water. The last example does occur in vessel hydrodynamics. When no more external energy is added to a moving vessel the vessel will stop moving and come to a standstill. This applies for all motions from surge to yaw. It is possible to apply so much damping that a system cannot vibrate. This happens when the damping is equal to the critical damping. The critical damping can be calculated with equation 2.20. It is important to understand the critical damping value, since this is the damping value which causes the motion to be damped and return in its original state as fast as possible. When less damping is applied than the critical damping a system is under damped. An under damped system will oscillate an amount of times before coming to rest. When more damping than the critical damping is applied the system is over damped. An over damped system has no oscillations, but since there is more damping applied than necessary it takes a longer time for the body to return to its original state after excitation than it does for a critical damped body. In figure 2.8 is shown how different damping ratios influence the oscillations of a oscillating body. This figure shows how under damped, critically damped and over damped systems return to their equilibrium position and undamped systems keep oscillating after being excited by an initial force or displacement.

$$\xi_{crit} = 2\sqrt{km} \tag{2.20}$$

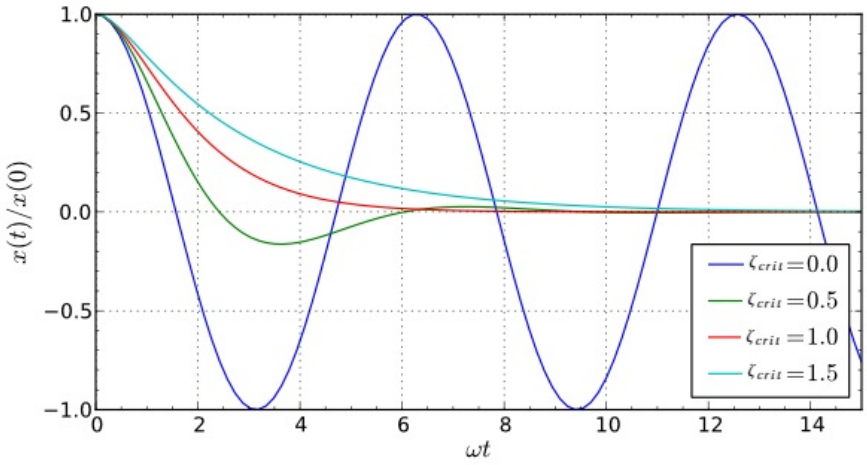

Figure 2.8: Influence of damping on the resonance and natural frequency [33]

With the physics of damping explained it is clear that damping has a positive influence on the workability of lifting operations. When damping is applied to a degree of freedom of the multi-body system of a vessel with cargo in the crane the oscillations of the degree of freedom will be reduced which results in lower responses due to excitation forces. It is fairly easy to apply damping in a mathematical model since only the damping matrix must be adjusted. However, it must be possible that the damping added to the mathematical model can also be applied in practice otherwise the mathematical model is not a good representation of the possible solutions.

2.6. Natural Frequency, Phase Difference and Resonance

The natural frequency, in other words called the eigenfrequency, is the frequency at which a harmonic motion tends to oscillate in the absence of any driving frequency or damping force. The natural frequency is thus the frequency at which a low amount of energy is required to oscillate a body. When a body is excited by an external force, e.g. ocean waves, at this natural frequency the oscillating motions of the body can become extremely large while the excitation force applies a force at the same frequency as the natural oscillation of a body which reinforces every single oscillation with a new excitation, increasing the amplitude of the new oscillation. This phenomenon is called resonance. Since the motions at the natural frequencies can become extremely large it is important to understand what the natural frequencies of a physical system is and what

can be done to influence the natural frequency or reduce the resonance motions. In figure 2.9 is shown how damping can influence the natural frequency and the motion amplitudes caused by resonance. In this figure the x axis represents the ratio between the driving frequency given by ω_A and natural frequency given by ω_n. When this ratio is 1 resonance occurs when no damping is applied to the motion. The y axis gives the result of the transfer function dependent on ω_A. The different values of ξ_{crit} in this figure represent the ratio between the damping for that curve and the critical damping.

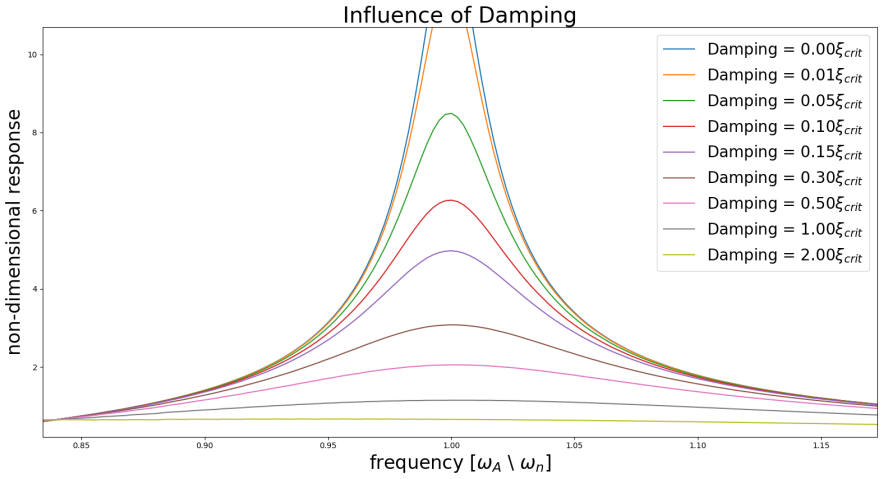

Figure 2.9: Influence of damping on the resonance and natural frequency. recreated from Katsuhiko Ogata [25]

Another important variable in the equation of motions is the phase of a motion or force. Since the excitation force and the vessel and pendulum motions are described as a harmonic motions the phase lag cannot be neglected. While all motions exist out of an real and imaginary part, as shown in equation 2.21, the phase of a motion can easily be calculated by calculating the angle between the positive real axis and the complex result of equation 2.21, as shown in equation 2.22. To be lucid this phase is not the phase difference between the wave and the vessel or pendulum motion but the phase of the motion itself. The phase difference between the different motions themselves or wave excitation forces can be calculated by calculating the difference between the different motions or wave excitation forces.

$$e^{-i\omega t} = cos(\omega t) - i \cdot sin(\omega t) \tag{2.21}$$

$$\epsilon = \begin{cases} arctan\left(\frac{ImaginaryValue}{RealValue}\right) & \text{if} \quad Re > 0 \\ arctan\left(\frac{ImaginaryValue}{RealValue}\right) + \pi & \text{if} \quad Re < 0 \\ +\frac{\pi}{2} & \text{if} \quad Re = 0, \quad \text{and} \quad Im > 0 \\ -\frac{\pi}{2} & \text{if} \quad Re = 0, \quad \text{and} \quad Im < 0 \end{cases} \tag{2.22}$$

When equation 2.22 is used for equations 2.7 till 2.9 it is clear that the phase difference between the displacement and velocity is 90 degrees and the phase difference between velocity and acceleration is 90 degrees thus the phase difference between displacement and acceleration is 180 degrees. Equation 2.6 can be written as equation 2.23. Here ω_a represents the driving frequency and the natural frequency is given by ω_n. When a harmonic motion is excitated with a small driving frequency the following statement can be made; $\frac{b}{m} \ll \omega \ll \omega_n$. The relative large natural frequency results in a relative large restoring term. Now the inertia, damping and restoring terms can placed in an Argand diagram, as shown in figure 2.10a. An Argand diagram is a diagram where complex numbers are plotted. The real numbers are plotted along the x-axis and the imaginary numbers are plotted along the y-axis. In this diagram it becomes clear that the large restoring term results in almost no phase difference between the excitation force and the motion is small. When the driving frequency approaches the natural frequency resonance will occur. At resonance the restoring and inertal terms cancel each other out perfectly. This is drawn in another Argand diagram shown in figure 2.10b. The result is a phase difference of 90 degrees. When the driving frequency is larger than the natural frequency the inertia term will dominate which results in a phase shift up to 180 degrees shown in figure 2.10c.

$$(-\omega_a^2 + i \cdot \omega_a \frac{\boldsymbol{B}}{\boldsymbol{M}} + \omega_n^2)\boldsymbol{x_a} e^{i\omega t} = \boldsymbol{F_0} e^{i\omega t} \tag{2.23}$$

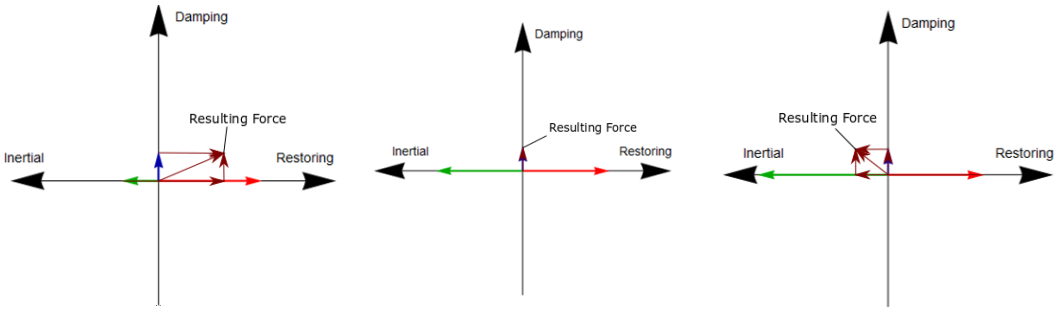

(a) Argand diagram with large restoring force [16]

(b) Argand diagram resonance frequency [16]

(c) Argand diagram with large inertia term [16]

Figure 2.10: Argand diagrams for different driving frequencies.

The phase difference between an excitation force and corresponding motion can be calculated with equation 2.24. In this formula ξ stands for the damping ratio given by $\frac{b}{b_{critical}}$. When the driving frequency ω is small the equation will give a solution close to 0. When the driving frequency and the natural frequency are equal the value within the arc-tangent function will be infinite thus the solution for ϕ_0 will be equal to 90 degrees. Finally when the driving frequency is larger than the natural frequency the phase difference will exceed the 90 degrees but will never exceed the 180 degrees. The change in phase will influence the interaction between the degree of freedom. When the swing motion of the cargo changes in phase and the roll motion does not change in phase the two motions will have another interaction and amplitude than when the two motions have the same phase.

$$\phi_0 = \begin{cases} 0 - arctan\left(\xi \frac{2\omega\omega_n}{\omega^2 - \omega_n^2}\right) & \text{if} \quad \omega \leq \omega_n, \\ \pi - arctan\left(\xi \frac{2\omega\omega_n}{\omega^2 - \omega_n^2}\right) & \text{if} \quad \omega > \omega_n \end{cases} \tag{2.24}$$

In multi-body dynamics the opposite of resonance can occur. The so called anti-resonance. Anti-resonance is a pronounced minimum in the amplitude of one oscillator at a particular frequency. When anti-resonance occurs there will also be a large shift in the oscillation phase of the body, just as it happens with resonance. It is possible for multi-body system to reduce the response to almost zero when anti-resonance occurs. However, anti-resonance only reduces the motions of one body to an extreme small response at a time. When anti-resonance occurs all the oscillations of one body are almost reduced to zero by the connection between the two different bodies. The motions of the second body will also be small, but it will not be reduced to such a low minimum as the first body. While resonance can happen at multiple degrees of freedom due to the coupling.

2.7. Natural Frequencies of Multi-Body Systems

The formula used to calculate the natural frequency of a single degree of freedom is quite simple. However in multi-body dynamics the equation is a bit harder. All the different degrees of freedom can influence all the natural frequencies. As a result the natural frequency of a body in a multi-body system can be quite different than the natural frequency of a comparable body that is not connected to a multi-body system. In single degrees of freedom the natural frequency can be calculated with equation 2.25. In this equation K stands for the stiffness value of the single degree of freedom and M represents the mass of the body. The natural frequency calculation of multi-body systems will be explained later in this section. When equation 2.15 and equation 2.25 are combined it is clear that the natural frequency of a single pendulum is equal to equation 2.26.

$$\omega_n = \sqrt{\frac{K}{M}} \tag{2.25}$$

$$\omega_{n_{pendulum}} = \sqrt{\frac{g}{L}} \tag{2.26}$$

A study from MacKay[18] shows that the natural frequencies of of a double pendulum where both pendula have the same mass and length are equal to 0.8 and 1.8 $\sqrt{\frac{g}{L}}$. This makes it clear that the natural frequency of a multi-body system can be influenced by different bodies in the multi-body system. Another study regarding small oscillations of a n-pendulum model shows that the natural frequencies of multiple degrees of freedom pendulum systems is heavily influenced by the amount of pendulums, in other words degrees of freedom. This study is done by Rubenzahl and Rajeev [29]. These studies show that the cargo cannot be seen as a simple pendulum and the cargo swing motions must be integrated in a multi-body system to study the influence of the vessel and cargo on the natural frequencies of both bodies. Different aspects such as vessel displacement, vessel metacentric height, cargo mass and crane top location do influence the natural frequency of the vessel and cargo motions. Since these values differ per loading operation the natural frequencies will also differ per loading operation. Some loading conditions can be varied to change the natural frequency in a desired way. But before the motions and the natural frequencies can be studied the method to calculate the natural frequencies must be calculated.

As explained in section 2.6 the natural frequency the frequency where the influence of the stiffness and mass is equal to each other. In one degree of freedom motions this is the natural frequency equal to $\sqrt{\frac{C}{M}}$. In multiple degree of freedom systems the stiffness and mass values are replaced by matrices. These matrices complicate the calculations of the natural frequencies but make it possible to calculate the natural frequencies of combined motions. In equations 2.27 till 2.31 an example is given for a natural frequency problem of a two degrees of freedom multi-body system. When the different mass and stiffness values of equation 2.31 are known the equation can be solved for ω_n. Since the resulting natural frequency has to be positive, real and distinct a maximum of two natural frequencies can occur for a two degrees of freedom system.

$$det\left|-\omega_n^2 \boldsymbol{M}\boldsymbol{x} + \boldsymbol{C}\boldsymbol{x}\right| = 0 \tag{2.27}$$

$$\left|-\omega_n^2 \begin{bmatrix} M_{11} & M_{17} \\ M_{71} & M_{77} \end{bmatrix} \begin{bmatrix} x_1 \\ x_7 \end{bmatrix} + \begin{bmatrix} C_{11} & C_{17} \\ C_{71} & C_{77} \end{bmatrix} \begin{bmatrix} x_1 \\ x_7 \end{bmatrix}\right| = 0 \tag{2.28}$$

$$\left|\left(\begin{bmatrix} -\omega_n^2\left(M_{hyd_{11}} + A_{hyd_{11}}\right) & 0 \\ 0 & -\omega_n^2\left(M_{cargo77}\right) \end{bmatrix} + \begin{bmatrix} C_{hyd11} + K_p & -K_p \\ -K_p & K_p \end{bmatrix}\right) \begin{bmatrix} x_1 \\ x_7 \end{bmatrix}\right| = 0 \tag{2.29}$$

$$\left|\begin{bmatrix} -\omega_n^2\left(M_{hyd_{11}} + A_{hyd_{11}}\right) + C_{hyd_{11}} + K_p & -K_p \\ -K_p & -\omega_n^2\left(M_{cargo77}\right) + K_p \end{bmatrix}\right| = 0 \tag{2.30}$$

$$\omega_n^4\left(\left(M_{hyd_{11}} + A_{hyd_{11}}\right) M_{cargo_{77}}\right) + \omega_n^2\left(\left(M_{hyd_{11}} + A_{hyd_{11}}\right) K_p + M_{cargo_{77}}\left(C_{hyd_{11}} + K_p\right)\right) + C_{hyd_{11}} K_p = 0 \tag{2.31}$$

In appendix B the mass, damping and stiffness matrices are shown for the 12 degrees of freedom system. The stiffness matrix stands out in density in regards with the mass matrix. This means that there is a lot of influence of the stiffness between different motions and these stiffness factors will influence the natural frequencies of the different degrees of freedom. The calculations for the natural frequencies of multiple degrees of freedom systems might be harder but they are not impossible. When the stiffness and mass matrices are known the natural frequencies can be calculated with the eigenvalue method. Python can be used to calculate the natural frequencies with the help of the eigenvalue method. This makes the calculation of natural frequencies fairly simple.

Thus different motions can influence each other. As explained in section 2.6 different degrees of freedom have different phases at certain driving frequencies. This means that two different degrees of freedom that are coupled at a natural frequency can have a different phase. The difference phases can influence the interaction between the two degrees of freedom. The different motions can enhance the amplitude of both bodies because both motions move with the same phase in the same direction which reinforces the amplitude or they move in counter phase of each other which can reduce the excitation amplitude of both motions.

Since the natural frequencies themselves and the calculated responses do not show how the different degrees of freedom influence the different natural frequencies the eigenvectors can be calculated. Eigenvectors show how the different different degrees of freedom act at the eigenvalues, which are directly linked to the natural frequencies. To use the properties of an eigenvector correctly first the definition of an eigenvector must be understood.

A vector is an eigenvector when the vector is a non zero vector and the vector does linear transform a matrix by a scalar factor.[9]

In other words an eigenvector of a linear transformation is a non-zero vector that, when applied to this linear transformation , does not change the direction but only scales the linear transformation by the eigenvalue. The linear transformation could take the form of an n by n matrix. The definition of an eigenvector v is given in equation 2.33 and in equation 2.34 the definition of a eigenvector of a matrix is given. Equations 2.33 and 2.34 show the definition of an eigenvector in their basic forms, however an eigenvector problem can be solved for a physical mass-spring system. Equation 2.35 shows how an eigenvalue problem can be used for a mass-spring system. When v is exchanged to x this equation is equal to the equation in the determinant function of equation 2.27.

$$\lambda = \omega_n^2 \tag{2.32}$$

$$\boldsymbol{T}(\boldsymbol{v}) = \lambda \boldsymbol{v} \tag{2.33}$$

$$\boldsymbol{A}\boldsymbol{v} = \lambda \boldsymbol{v} \tag{2.34}$$

$$\boldsymbol{C}\boldsymbol{v} = \lambda \boldsymbol{M}\boldsymbol{v} \tag{2.35}$$

When the eigenvalues, or natural frequencies, of a multi-body system are known the eigenvectors can be calculated. Every single natural frequency in a multi-body system has its own eigenvector. Equation 2.35 can be written as 2.36. When the mass and spring matrices and the natural frequencies are known this equation can be used to calculate the eigenvectors. In equations 2.37 till 2.44 an example calculation for eigenvalues and eigenvectors is given for a double pendulum. In this double pendulum the length and weight of both pendulum are equal to each other. The first pendulum is connected to the earth fixed coordinate system. The second pendulum is connected to the first weight of the first pendulum as illustrated in figure 2.11. These are the same values as used in the study done by MacKay[18]. Equations 2.27 till 2.31 showed how complicated the natural frequency calculations can become when the stiffness and mass values have complicated relations. The simpler relations from the double pendulum are used to show how the eigenvalue method works with actual results.

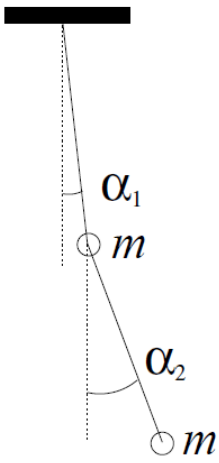

Figure 2.11: Schematic of a double pendulum used in the example calculation of the natural frequencies and eigenvectors [18]

$$(\boldsymbol{C} - \lambda \boldsymbol{M})\,\boldsymbol{v} = 0 \tag{2.36}$$

$$\boldsymbol{C} = mgl \cdot \begin{bmatrix} 2 & 0 \\ 0 & 1 \end{bmatrix}, \qquad \boldsymbol{M} = \frac{1}{2} ml^2 \begin{bmatrix} 2 & 1 \\ 1 & 1 \end{bmatrix} \tag{2.37}$$

$$\begin{bmatrix} 2-2\lambda & -\lambda \\ -\lambda & 1-\lambda \end{bmatrix} \boldsymbol{v} = 0 \tag{2.38}$$

$$\frac{g}{l} \cdot \left| \begin{bmatrix} 2-2\lambda & -\lambda \\ -\lambda & 1-1\lambda \end{bmatrix} \right| = \lambda^2 - 4\lambda + 2 = 0, \quad \text{which gives} \quad \lambda_1 = \left(2+\sqrt{2}\right)\frac{g}{l}, \quad \lambda_2 = \left(2-\sqrt{2}\right)\frac{g}{l} \tag{2.39}$$

$$\begin{bmatrix} 2-\left(2+\sqrt{2}\right) & -\left(2+\sqrt{2}\right) \\ -\left(2+\sqrt{2}\right) & 1-\left(2+\sqrt{2}\right) \end{bmatrix} \boldsymbol{v} = \begin{bmatrix} \left(-2-2\sqrt{2}\right) & -\left(2+\sqrt{2}\right) \\ -\left(2+\sqrt{2}\right) & \left(-1-\sqrt{2}\right) \end{bmatrix} \begin{bmatrix} v_{1,1} \\ v_{1,2} \end{bmatrix} = 0, \qquad \text{for } \lambda_1 \tag{2.40}$$

$$\left(-2-2\sqrt{2}\right) v_{1,1} + -\left(2+\sqrt{2}\right) v_{1,2} = 0, \quad \text{which gives} \quad v_{1,1} = -\frac{1}{2}\sqrt{2}\, v_{1,2} \tag{2.41}$$

$$\begin{bmatrix} 2-\left(2-\sqrt{2}\right) & -\left(2-\sqrt{2}\right) \\ -\left(2-\sqrt{2}\right) & 1-\left(2-\sqrt{2}\right) \end{bmatrix} \boldsymbol{v} = \begin{bmatrix} -2+2\sqrt{2} & -\left(2-\sqrt{2}\right) \\ -\left(2-\sqrt{2}\right) & -1+\sqrt{2} \end{bmatrix} = 0, \qquad \text{for } \lambda_2 \tag{2.42}$$

$$-2+2\sqrt{2} v_{2,1} + -\left(2-\sqrt{2}\right) \cdot v_{2,2} = 0, \quad \text{which gives} \quad v_{2,1} = \frac{1}{2}\sqrt{2} \cdot v_{2,2} \tag{2.43}$$

$$\boldsymbol{v_1} = \begin{bmatrix} -\frac{1}{2}\sqrt{2} \\ 1 \end{bmatrix} \quad \text{and} \quad \boldsymbol{v_2} = \begin{bmatrix} \frac{1}{2}\sqrt{2} \\ 1 \end{bmatrix} \tag{2.44}$$

The eigenvectors explain how the different bodies behave at the different natural frequencies. An eigenvector gives the relation in motion between the different degree of freedom for the corresponding natural frequency. In the case with the double pendulum the eigenvectors are given in equation 2.44. At the first natural frequency, $2+\sqrt{2}\frac{g}{l}$, the first body will move $-\frac{1}{2}\sqrt{2}$ unit length for every 1 unit length the second body moves. At the second natural frequency, $2-\sqrt{2}$, the first body will move $\frac{1}{2}\sqrt{2}$ unit length for every 1 unit length the second body moves. In figure2.12 the eigenvectors are illustrated. From the eigenvector and as seen in this figure it is clear that at the first natural frequency the two bodies have an opposing motion. When the second body moves in a positive direction the first body will move in negative direction and vice versa. At the second natural frequency the two bodies will move in the same direction. This can be seen in the eigenvector values and the illustration as well. In two degree of freedom system the responses can sometimes be described from a gut feeling or simple fast calculations. In multi-body systems with multiple degrees of freedom it is harder to predict the influence of different degree of freedom on the natural frequencies. Therefore it is important to study the eigenvectors in combination with the responses.

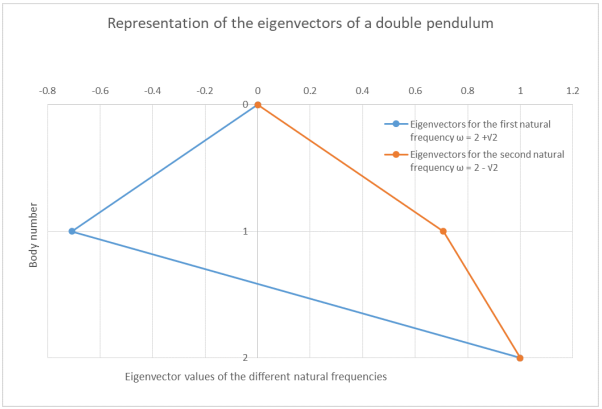

Figure 2.12: Illustration of the two eigenvectors of a double pendulum

2.8. Nonlinearities

The frequency domain solves the equations in a linear method. This means that all the forces and responses must have a linear relation with the displacement, speed and acceleration values. Most nonlinearities can be neglected while their influence is small or linearizations are present to implement the nonlinear behaviour. In section 1.6.2 is explained that sub-harmonic motions will break down before large amplitudes are generated and the Ikeda method can be used to linearize the viscous damping. Throughout this chapter is explained how different nonlinearities are linearized or neglected. However, not every nonlinearity is tackled yet.

The non-linear excitation of the pendulum is of a bigger concern for the frequency domain calculations. However, in section 2.3 is explained that for small motions the displacement can be linearized. Since large motions make it impossible to successfully execute a lifting operation it can can be assumed that lifting operations will occur with small vessel and cargo motions. An experimental study of non-linear dynamics of floating cranes by Clauss and Vannahme [2] proved that these assumptions are correct. They compared a frequency domain model of a floating crane vessel with model tests and they concluded that the frequency domain could be used for a wide range of applications. Therefore it is assumed that the non-linear behaviour of the pendulum can be neglected and the frequency domain can be used to solve the equations on motions.

Another nonlinearity is the added damping. Most forms of damping that can be used will show some form of nonlinearities. In figure 2.13 is shown how the line tension of tugger winches is linearized in Heerema's [19] tugger winch study. These linearizations will also influence the damping ratios of tugger winches.These nonlinearities are neglected in the model. However this thesis is done to calculate the influence of damping on the multi-body system. The damping values in this master study will still give insight on the required damping values. Further studies can be done to investigate the influence of the non-linearities of the damping methods.

Besides added damping the added mass and hydrodynamic damping is also non-linear. The added mass and hydrodynamic damping values are dependent on the vessel hull form, vessel motions and wave properties. In the tool created the added mass and hydrodynamic damping values are calculated for all different wave frequencies, in other words the excitation frequencies and wave directions. Even though all these different values for the added mass and hydrodynamic damping are stored and used in the tool, the changes of these values due to vessel translations or rotations are linearized. Since lifting operations are not performed when large motions occur these linearized values should be accurate enough for the tool created.

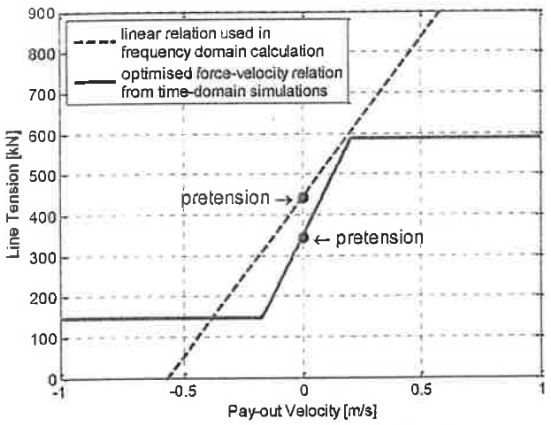

Figure 2.13: Linearized tension values of active tugger winches[19]

Second order drift forces are non-linear forces that are not taken into account. While vessel motions due to second order drift forces can result in large translations of the vessel body the frequency at which they occur is very low. These low frequencies do not match the natural frequencies a pendulum and thus the natural frequencies of the cargo motions. Therefore neglecting second order drift forces should not result in inaccurate calculations.

3
Model description

In this chapter the model is explained. In section 3.1 the layout of the model is explained. Section 3.2 describes how the vessel hydrodynamics are added to the model. Thereafter the coupling between the cargo and the vessel via the crane cable is explained in section 3.3. Next the modelling of the mooring lines is explained in section 3.4 followed by the modelling of the cargo control systems in section 3.5. The motion calculations are explained in section 3.6. In section 3.7 the significant motion calculations are explained. The verification of the model is worked out in section 3.8 followed by the validation is section 3.9. Lastly, in section 3.10, the influence of different parameters of the lifting operation are described. These can be used to alter the responses of the vessel and cargo during lifting operations.

3.1. Model Layout

First of all an overview of the model will be explained. The model is made in the mathematical programming language Python[7]. Python is a language in which multiple different programming modules can be imported. These programming modules make it possible to solve different aspects of the mathematical problem. examples are a mathematical tool for mathematical equations, a scientific computing tool for matrix calculations and a tool to plot results in to graphs. This makes Python a versatile mathematical program. Therefore Python is used to create a tool that can solve the multi-body system. In the Python tool all the different aspects of the multi-body system can be solved via the different programming modules.

In the Python tool created to calculate the responses of the multi-body system, all different mathematical systems are implemented separately. This makes the tool modular and different aspects of the lifting operation can be added to the calculation or ignored on purpose. The multi-body tool consists of different python sub-files to keep the tool structured. In these sub-files different mathematical steps are fulfilled or matrices are created. There is one main file which is used to summon all different sub files. Besides the main file there will be a file with all the settings required to solve the mathematical equations. In the settings file all different settings for the different sub files are stored. From crane tip position to mooring line configurations and from vessel hydrodynamics to cargo control system configurations.

In figure 3.1 a schematic drawing of the mathematical model is shown. The first mathematical system that is implemented in the model are the vessel hydrodynamic properties. The vessel hydrodynamics contain the properties of the vessel hull and the interaction between the hull and the water. In section 3.2 is explained how the hydrodynamics are imported. The second part that is implemented is the interaction between the cargo body and the vessel body via the crane. In section 3.3 is explained how the vessel and cargo are connected via the crane in a mathematical way. In section 3.4 is explained how the mooring lines are implemented in a mathematical way and which input variables are required to calculate the influence of mooring lines. Cargo control systems can be used to influence the cargo motions during lifting operations. The influence of cargo control systems are calculated via added stiffness and damping values. Both different influences are implemented via separate Python sub-files. In section 3.5 is explained how both the stiffness and damping values of the cargo control systems are implemented to the multi-body model. With the cargo control systems implemented all the input values required to translate the mechanical system to a mathematical model are elaborated. The next part of the model is to solve the mathematical system. In section 3.6 is explained how the responses of the mathematical model will be calculated with the help from the different input values. The responses of the multi-body system can be used to calculate statistical maximum responses of the motions. These statistical responses can be used to compare different lifting operations for different lifting configurations and different weather conditions. These statistical calculations can be done with the Python tool and are explained in section 3.7. In section 3.10 is explained how the motions are influenced by different wave spectra and how different variables of a lifting operation can influence the natural frequency of the

multi-body system. The verification of the model is explained in section 3.8. In this section different mathematical properties of the model are verified. BigLift Shipping has an inhouse lifting simulator which is used to train onboard crew. This simulator can be used to validate the Python model. The validation is explained in section 3.9.

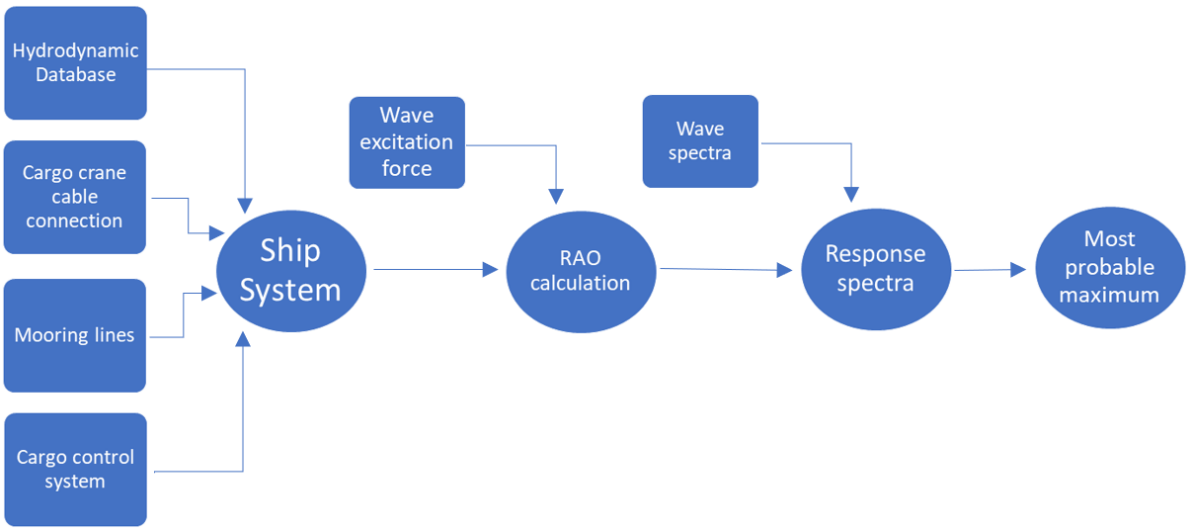

Figure 3.1: Schematic drawing off the mathematical model that is created for this study.

3.2. Vessel Input

The vessel input contains all the hydrodynamic properties of the vessel. These properties determine the relation between the hull shape, displacement, center of gravity, center of buoyancy and other properties and incoming waves from all directions. In the paragraph below will be described which hydrodynamic properties and how these properties are implemented in this model.

Response Amplitude Operators, RAOs, are transfer functions used to calculate the effect of wave spectra on vessel motions as explained in section 2.2. Many methods and different software is developed to calculate RAOs. Shipmo is such a program that calculates the motion RAOs with the help of 2D linear diffraction theory ('strip theory') [35]. Shipmo is developed by Marin. For this research Shipmo version 17.2.3 is used. In 2D strip theory methods the vessel is divided into a finite number of cross sections, or strips. For these strips the vessel hydrodynamic properties are calculated. From all these separate hydrodynamic properties the vessel's overall hydrodynamic properties can be calculated. Unfortunately these RAOs themselves are not useful for this study since they will only give the transfer function for a vessel without cargo in the crane. However Shipmo can also export the mass, added mass, damping, viscous damping and stiffness matrix as well as the corresponding excitation force vector of the six degrees of freedom of the vessel. These matrices and vector will be used to fill in the first quadrant of the 12 DoF matrices and the first 6 values of the force vector. The mass and hydrodynamic stiffness matrix are constant values for all the weather, vessel heading, vessel speed and roll amplitude input values. The vessel speed is set to zero in all calculations while lifting operations are mainly performed without forward speed. Thus for different wave frequencies, wave directions and roll amplitudes these matrices stay the same. The loading conditions, which contain the displacement and metacentric height, and hull form do have influence on the mass and hydrodynamic stiffness matrices. However, a shipmo hydrodynamic database can only be created for one specific loading condition and hullform. Therefore a new hydrodynamic database must be created for different loading conditions and hull forms. The added mass and damping are different for various weather and sailing input values. Therefore these matrices must be saved for all the different wave directions, wave frequencies roll angles. All the values that are exported from Shipmo are shown in table 3.1.

The loading conditions of the vessels are a bit tricky. Normally cargo in a crane will be translated to the crane top for simple stability calculations. However, in this model the cargo dynamics are modelled as an extra body and therefore the cargo should not be applied to the crane top as a weight. However when the cargo is neglected completely the water displacement is too low because the displacement of the vessel results from the vessel and cargo combined mass. Therefore it is assumed that the vessel displacement is the displacement of the vessel weight including the cargo but the stability values are the values of the vessel without the cargo in the crane. later on in the calculations the weight of the cargo is deducted from the vessel mass matrix. During the hydrodynamics calculation the mass of the cargo is chosen in such a way that it does not influence the loading condition of the vessel other than increasing the draught of the vessel. In practice this means that the vessel's metacentric height will not change between a loading condition without cargo in the crane and a loading condition with cargo in the crane. This property is chosen while the draught increase due to the cargo cannot be neglected and the influence of the mass on the vessel motions will be calculated via the multi-body system. On any other location the cargo will have an extra influence on the motions of the vessel.

Shipmo uses hull forms to calculate different aspects of the loading condition. The hull forms of all of BigLift Shipping's vessels are present in the database to calculate the vessel hydrodynamics with Shipmo. The combination of the vessel's hull form, draught and trim are used to calculate the mass matrix of the vessel body. The hull form is also used to calculate the influence of the hull form on all other hydrodynamic properties.

A problem with 2D linear diffraction theory is that it is not accurate at the determination of roll damping. Significant viscous effects and effects from appendages prevent the strip theory method to create accurate results. Therefore some empirical formulas and experimental data are used to predict the roll damping in the strip theory methods. Ikeda et al [13] developed a roll damping prediction method with the same accuracy as strip theory methods and this method is also based on hydrodynamic forces acting on the cross sections, or strips, of a vessel. Ikeda's method can calculate the frictional, wave, eddy and bilge keel aspects of roll damping. A side effect is that Ikeda's method is not accurate for motion calculations of vessels with a significant forward speed. However this is not a concern for this study because lifting operations are carried out without forward speed. Shipmo has a built-in Ikeda method. Therefore the extracted matrices can be used for the Python tool.

Shipmo is a validated and proven tool. Together with the easy access of Shipmo is Shipmo a useful tool for the hydrodynamic aspects of the multi-body tool created for this study. Shipmo is also used by other programs such as Safetrans. Since Safetrans is used regularly by BigLift Shipping the input files required for Shipmo are up to date and kept up to date for every update of Shipmo. The hydrodynamic coefficients calculations could also be carried out manually. However, this would require a lot of time to create a 2D strip theory or 3D panel method calculation and programming time. Another option to calculate the vessel hydrodynamics is to create a hydrodynamic database for a few different loading conditions. With these databases and interpolation all required hydrodynamic properties can be calculated. However, this is less accurate than using Shipmo to create hydrodynamic databases. Other programs such as Seaway[11] and Delfrac[3] could also be used to calculate the hydrodynamic properties of the vessel. However, the last two programs are not as easily accessible as Shipmo from BigLift Shipping. While Shipmo is easily accessible and kept up to date at all times Shipmo is chosen as program to calculate the vessel hydrodynamics in this multi-body tool.

Table 3.1: Values exported from Shipmo hydrodynamic database

Shipmo export	**Dependence and Description**
Stiffness Matrix	The stiffness matrix is dependent on the hull form and the loading conditions of the vessel. While a Shipmo hydrodynamic database is made for a specific hull form and a specific loading condition the complete matrix can be exported once for all the different wave frequencies, wave directions, vessel speeds and roll amplitudes of the vessel.
Mass Matrix	The mass matrix is dependent on the hull form and the loading conditions of the vessel. As explained for the stiffness matrix the mass matrix can be exported from the Shipmo hydrodynamic database file once and this matrix will be valid for all different wave frequencies, wave directions vessel speeds and roll amplitudes the vessel.
Added Mass Matrix	The added mass matrix contains the inertia added to the vessel motion caused by the acceleration of water due to the motions of the vessel. This is dependent on the hull form and loading condition but also dependent on the motion frequencies and motion direction induced by the wave frequencies and wave direction and roll amplitude of the vessel. Therefore the added mass must be exported for all these specific variables
Damping Matrix	The damping matrix contains the hydrodynamic damping caused by the radiation of energy due to the displacement of the water around the vessel. The damping values are dependent on the hull form and loading condition but they also depend on motion frequencies and motion direction induced by the wave frequencies and wave direction. Furthermore the damping matrix is also dependend on the roll amplitudes of the vessel. Therefore the damping values must be exported for all these specific variables. The Ikeda method[13] is used to calculate the correct roll damping values for the different appendages.
Wave Excitation Force vector	The wave excitation force vector is a vector which contains the excitation forces for the 6 motions of the vessel body caused by the incoming waves. These forces are dependent on the hull form, loading condition wave frequencies, wave directions and vessel speeds. The wave excitation force vector should be exported for all these specific variables
Hull Form, Loading condition, Wave frequencies, Wave Direction, Vessel Speed, Roll Amplitude	These variables are chosen by the user of Shipmo. The Hull form is specific for every vessel type. The loading condition contains the vessel draught, trim, GM, CoG and radii of inertia. The wave frequencies, wave directions, vessel speeds and roll angles are other variables chosen by the user of Shipmo. While all these variables are chosen by the user the variables are still exported from the hydrodynamic database so that all these values can be checked at any time and the values can be coupled to specific calculations.

All the data in the Shipmo hydrodynamic database are stored in large text files. The Python tool developed to calculate the vessel and cargo motions scans the data in these text files and exports the hydrodynamic mass, added mass, damping and stiffness matrices as well as the excitation force vector. These matrices and vector are saved for every variable necessary as explained in table 3.1. For the verification of the model the response of the six degrees of freedom of the vessel calculated by Shipmo is also exported. The verification is further elaborated in section 3.8.

Shipmo can calculate the hydrodynamic properties and wave forces for different frequencies at the once. However, Shipmo has a maximum number of 200 steps in which the wave frequency can vary. This means that that the hydrodynamic coefficients and wave excitation force can be calculated for 200 different wave frequencies. The default settings of Shipmo will calculate the hydrodynamic coefficients and wave excitation

force for a range between [redacted] rad/s and [redacted] rad/s. With 200 steps this results in a stepsize of [redacted] rad/s. To reduce this step size smaller ranges are used to calculate the hydrodynamic databases and wave excitation forces with Shipmo. Depending on the graphs that needs to be generated the range and stepsize will be adjusted. Default ranges in this report are [redacted] rad/s - [redacted] rad/s and [redacted] rad/s - [redacted] ad/s. This results in a stepsize of [redacted] rad/s and [redacted] rad/s respectively. Since the added mass and damping are frequency dependent smaller stepsizes will result in or accurate calculations of the natural frequencies. At the same time the graphs created and shown in this report will have a higher resolution.

3.3. Crane and Cargo Model

In this model the multibody system is excited by the waves. Wind forces will not applied. It is assumed that the wind force is relatively small and constant during lifting operations. Due to the relatively small forces the wind will barely influence the cargo motions. When high wind forces occur it is unsafe to execute a lifting operation hence high wind forces will not occur during actual operations. In a frequency domain calculation constant forces will not influence the amplitude of the motion. A constant force will result in a standard displacement of the equilibrium. For example a constant wind force in longitudinal direction can displace the cargo by one meter in surge direction. Since the force is constant the new location of the cargo will be the new equilibrium and the constant wind forces will not introduce any motions in the system. However, it is unlikely for a wind gust to have harmonic behaviour. Without this harmonic behaviour the superposition principle explained in section 2.2 cannot be applied. Due to the small influence on the amplitude of the motions and the non-harmonic behaviour the implementation of wind forces are neglected. This does also mean that only the body of the vessel gets directly excited by external forces and that the cargo will only move due to the connection to the vessel motions. When no tugger wires or other damping devices are used, the crane wire is the only connection between the vessel and the cargo in the crane. In section 2.3 is described how the pendulum forces result from the restoring stiffness and how the wire can be described as a, very stiff, spring for motions in the vertical direction.

Now that these stiffness components are described it is time to describe the conditions of the connection between the vessel and cargo. The vessel and the cargo are connected via the crane cable. The crane cable runs from the crane winch to the hook. However, there is a stationary sheave at the crane top. This stationary sheave prohibit motions in the cable between the cable winch and the sheave. Therefore it is assumed that the connection between the vessel and the crane cable is located at the stationary sheave at the crane top. The crane hook is connected to the cargo. This connection can be a direct connection, a connection via multiple slings or a connection via a lifting beam. When the hook is directly connected to the cargo it can be reasoned that both the body of the hook and the body of the cargo can be modelled as one bodies. The distance between the two centres of gravity is small and the weight of the cargo is often a lot higher than the weight of the crane hook. In these situations the crane hook body can be neglected. When the crane hook is connected via slings to the cargo there will be a significant distance between the cargo and the crane hook and between the crane hook and the crane tip. The hook can be seen as an extra body. Since the weight of the crane hook is relatively light in comparison with the cargo and the weight of the crane cables and slings the influence of such an extra body will be minimal. Therefore the influence of the crane hook will be neglected. The usage of a lifting beam requires the implementation of another extra body to the multibody system. A lifting beam will be relatively light which results in a small influence on the motions. At the same time not all lifting operations are done with the help of lifting beams. Therefore it is assumed that lifting beams are not used in this research. Another aspect that must be considered is the rotation of the cargo. For small and large rotations of the cargo different influences can be considered. One of the considerations is a mechanism that consists out of a rotational spring attached in the centre of gravity of the cargo. This mechanism is illustrated in figure 3.2a. In this mechanism it is assumed that the cargo rotates around the centre of gravity of the cargo and that the rotational force is compensated by the spring stiffness of the grommets or slings which connect the crane hook to the cargo. In other words the rotation of the cargo will not influence the crane cable. A second mechanism, shown in figure 3.2b, takes the influence of cargo rotations on the crane cable into account. In this mechanism the crane hook and cargo can be modelled as a double pendulum. When a double pendulum is considered the rotations of the cargo will create a horizontal translation of the crane hook. However, the radii of inertia of the cargo is much larger than the radii of inertia of the crane hook the influence of cargo rotations will be small. At the same time will large rotations create an unsafe work environment and lifting operations will not be executed in unsafe environments. Due to the small influence of the second mechanism and the requirement of a safe working environment the first mechanism will be

used. The crane cable will be modelled as a wire and not as a rigid connection. This means that the rotations of the cargo will not influence the crane cable. At the same time it simplifies the calculations since no extra body needs to be introduced to create a double pendulum model.

The stiffness values of the lifting configuration can differ per type of configuration. In equation 2.17 is explained how the stiffness values of the crane wire can be calculated. The crane cable has a modulus of elasticity equal to 110 kN/mm^2 and the diameter of the crane cable is equal to 50 mm. Depending on the required lifting capacity the amounts of revolutions of the crane cable between the crane winch and crane hook can vary. A common amount of revolutions is 16. When the distance between the crane tip and crane hook is equal to 20 meters the crane wires have a stiffness value of 173.000 kN/m. The same equation can be used to calculate the stiffness values of the grommets. Depending on the grommets used the elasticity, length of the grommet and grommet diameter and thus cross sectional area does change. Therefore the stiffness values of every type of grommet does change. According to LLoyd's Register Rules and Regulations - Rules and Regulations for the Classification of Ships par 3 Ship Structures (General) - Chapter 14 Cargo Securing Arrangements - Section 9 Strength of container securing arrangements[17] the effective modulus of elasticity for steel wire rope is equal to 90 kN/mm^2. Grommets with a working load limit of 100 $mton$ and a nominal length of 4 meters have a diameter of 84 mm. This results of a stiffness of 124.000 kN/m per grommet used in the configuration. Grommets with a working load limit of 150 $mton$ and a nominal length of 10 meters have a diameter of 102mm. This results in a stiffness of 73.500 kN/m. Since the lifting configuration will never consist out of a single grommet but multiple grommets connected to the hook the stiffness of the grommet configuration will increase. Since the stiffness of the grommets have the same magnitude as the crane cable wire the stiffness of the grommets will not be implemented in the multi-body system. For simplicity is assumed that the stiffness of the grommet configuration is equal to the stiffness of the crane cable. In the model the crane cable length will be equal to the distance between the crane tip and the centre of gravity of the cargo.

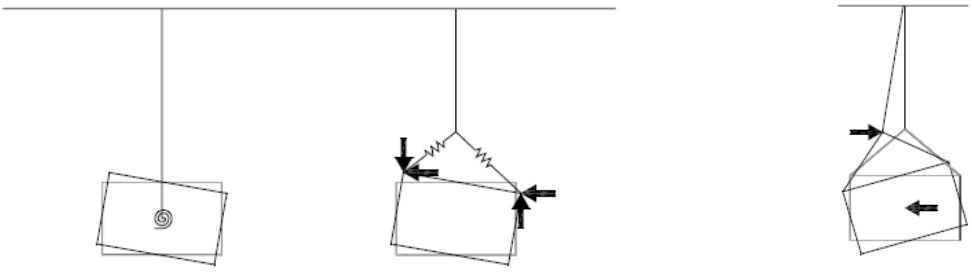

(a) Mechanism for small cargo rotations [10]

(b) Mechanism for bigger cargo rotations [10]

Figure 3.2: Representation of the influence of small and large rotations of the cargo on the crane cable configuration

The conditions set for the connection between the vessel and cargo via the crane cable make it possible to write down mathematical equations for this connection. First of all the cargo will be modelled as a pendulum connected to the vessel. The pendulum behaviour is explained in section 2.3. It is assumed that the top part of the crane cable is connected to the crane tip and the bottom part of the pendulum is connected to the centre of gravity of the cargo. When a relative translation occurs between the crane top and centre of gravity of the cargo in one of the two horizontal directions the restoring stiffness, explained in equation 2.15, together with the relative translation will cause a restoring force. A relative vertical translation between the crane tip and centre of gravity of the cargo will result in a restoring force caused by the stiffness of the crane wire, explained in equation 2.17. It is pretty clear that a translation of one of the two bodies in the multi-body system will cause a translation of the crane tip or a translation of the centre of gravity of the cargo. However, since the crane tip is a fixed point with respect to the vessel centre of gravity the rotations of the vessel will also cause a translation of the crane tip. For example, when the roll motion is multiplied with the vertical location of the crane tip a translation in the sway direction occurs. Even though the rotations might be small the long arms can cause a significant motion. Therefore the influences of the vessel rotations cannot be neglected. At the same time will the translations of the crane tip and cargo create rotation moments due to the same relation the rotations have on the translation of the crane tip. When the crane tip or cargo undergoes a translation a restoring force will occur. This restoring force multiplied by the lever arm will cause a rotational moment. In

equation 3.1 is shown how the vessel surge, pitch and yaw and the cargo surge motion influence the restoring force in the vessel surge motion. Equation 3.2 shows the influence of the different degree of freedom on the vessel roll restoring stiffness. All the different influences of the translations and rotations can be coupled in the restoring stiffness matrix. Via the superposition principle this restoring stiffness matrix can be added to the equation of motions. In table 3.2 is described which variables are used to create the restoring stiffness matrix. In appendix A the free body diagrams are shown. In these figures can be seen how the restoring forces follow from displacements in all directions. The free body diagrams of the vessel surge and vessel roll motion are also shown in figure 3.3.

In figure 3.3a can be seen that the surge motion causes a translation of the vessel. Due to this translation there is an offset between the crane tip and the centre of gravity of the cargo. When there is a offset in longitudinal direction between the crane tip and the cargo centre of gravity a restoring force in surge direction is created. 4 different degrees of freedom can cause an offset between the crane tip and the cargo centre of gravity. Which results in a restoring force in longitudinal direction. These degrees of freedom are are summarized below. In equation 3.1 the equation of the restoring force applied to the multi-body system via the crane cable is shown.

- **Vessel surge:** The vessel surge motion translates the crane tip in longitudinal direction.
- **Vessel pitch:** The vessel pitch motion multiplied with the vertical location of the crane tip causes a translation of the crane tip in the longitudinal direction.
- **Vessel yaw:** The vessel yaw motion multiplied with the transverse location of the crane tip causes a translation of the crane tip in the longitudinal direction.
- **Cargo surge:** The cargo surge motion translates the centre of gravity of the cargo in longitudinal direction.

In figure 3.3b the free body diagram of the vessel roll motion is given. A moment in the vessel roll direction is created by a force in the Y or Z direction miltiplied with an arom of theat force to the X-axis. In equation 3.2 the pendulum restoring forces acting in the vessel's roll direction are shown. In total 7 degrees of freedom have an influence on the vessel roll moment via the pendulum restoring forces. These degrees of freedom are summarized below.

- **Vessel sway:** The vessel sway motion will cause a translation of the crane tip. Together with the restoring stiffness a restoring force is created. This restoring force will cause a moment in roll direction when the force is multiplied with the vertical location of the crane tip.
- **Vessel heave:** The vessel heave motion will cause a translation of the crane tip. Together with the restoring stiffness a restoring force is created. This restoring force will cause a moment in roll direction when the force is multiplied with the transverse location of the crane tip.
- **Vessel Roll:** The vessel roll motion can cause a moment force in two ways.
  - The vessel roll motion together with the vertical location of the crane tip creates a translation of the crane tip in Y direction. This translation multiplied with the Y component of the restoring stiffness creates a force. This force creates a moment when it is multiplied with the vertical location of the crane tip.
  - The vessel roll motion together with the transverse location of the crane tip creates a translation of the winch in Z direction. This translation multiplied with the Z component of the restoring stiffness creates a force. This force creates a moment when it is multiplied with the transverse location of the crane tip.
- **Vessel pitch**: The vessel pitch motion together with the longitudinal location of the crane tip creates a translation of the crane tip in Z direction. This translation multiplied with the Z component of the restoring stiffness creates a force. This force creates a moment when it is multiplied with the transverse location of the crane tip.

- **Vessel yaw**: The vessel yaw motion together with the longitudinal location of the crane tip creates a translation of the crane tip in Y direction. This translation multiplied with the Y component of the restoring stiffness creates a force. This force creates a moment when it is multiplied with the vertical location of the crane tip.

- **Cargo sway**: The cargo sway motion will cause a translation of the centre of gravity of the cargo. Together with the restoring stiffness a restoring force is created. This restoring force will cause a moment when this force is multiplied with the vertical location of the crane tip.

- **Cargo heave**: The cargo heave motion will cause a translation of the centre of gravity of the cargo. Together with the restoring stiffness a restoring force is created. This restoring force will cause a moment when this force is multiplied with the transverse location of the crane tip.

In appendix C the complete equation of motions are given. In these equations of motions the influence of the pendulum restoring stiffness on all degrees of freedom can be found.

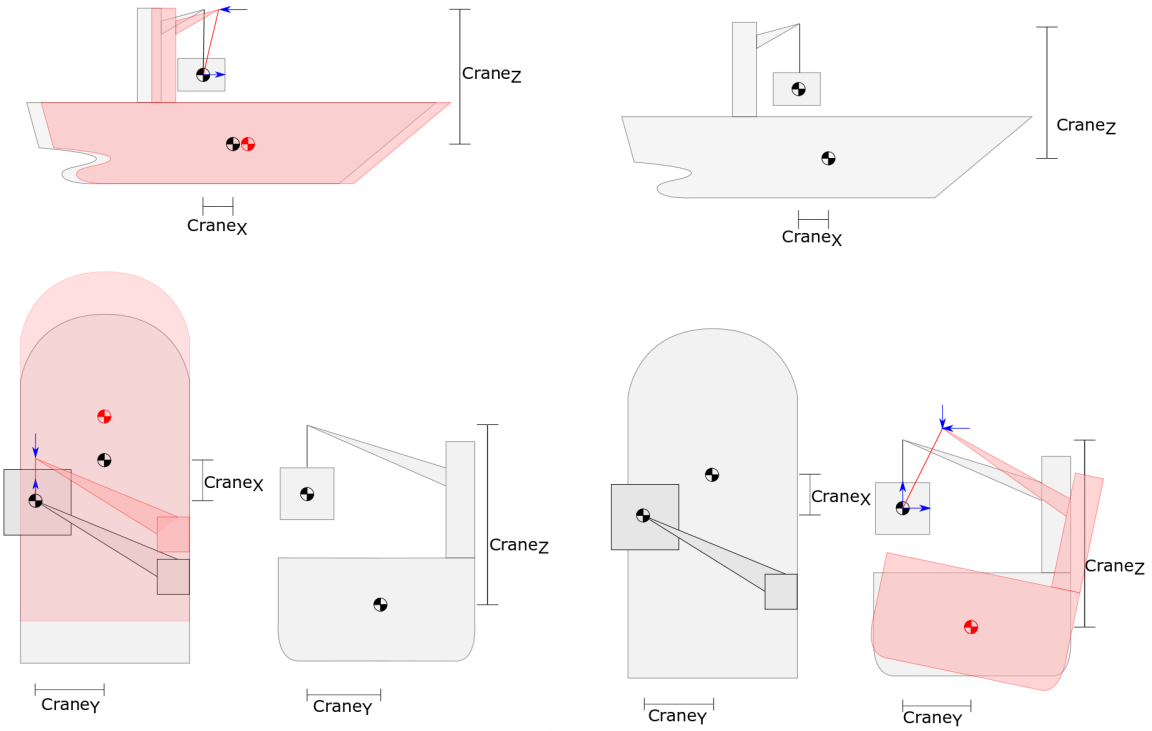

(a) Free body diagram of the interaction between the vessel and cargo via the crane cable for the surge motion of the vessel

(b) Free body diagram of the interaction between the vessel and cargo via the crane cable for the vessel roll motion

Figure 3.3: Free body diagram of the interaction between the vessel and cargo via the crane cable for the vessel surge motion and the vessel roll motion. These free body diagrams can be used to explain the influence of these degree of freedom on other degrees of freedom in the multi-body system

$$F_{res_1} = K_p \cdot x_1 + K_p \cdot Z_{Crane} \cdot x_5 - K_p \cdot Y_{Crane} \cdot x_6 - K_p \cdot x_7 \tag{3.1}$$

$$\begin{aligned} F_{res_4} = &- K_p \cdot Z_{Crane} \cdot x_2 + K_w \cdot Y_{Crane} \cdot x_3 + K_p \cdot Z_{Crane} \cdot Z_{Crane} \cdot x_4 + K_w \cdot Y_{Crane} \cdot Y_{Crane} \cdot x_4 \\ &- K_w \cdot X_{Crane} \cdot Y_{Crane} \cdot x_5 - K_p \cdot X_{Crane} \cdot Z_{Crane} \cdot x_6 + K_p \cdot Z_{Crane} \cdot x_8 - K_w \cdot Y_{Crane} \cdot x_9 \end{aligned} \tag{3.2}$$

Equations 3.1 and 3.2 show how the restoring forces of the pendulum can be calculated. However, these equations do not show how the restoring stiffness matrices are created in the Python tool. In equation 3.3 is showed how the restoring stiffness values of equation 3.1 are written in a matrix. Equation 3.4 shows how the stiffness values of equation 3.2 can be written in a matrix. When this is done for all degrees of freedom the pendulum stiffness matrix is created. In section 3.6 is explained how this matrix is implemented in the multi-body system.

$$\begin{aligned} C_{pendulum_{11}} &= K_p \\ C_{pendulum_{15}} &= K_p \cdot Z_{crane} \\ C_{pendulum_{11}} &= -K_p \cdot Y_{crane} \\ C_{pendulum_{17}} &= -K_p \end{aligned} \tag{3.3}$$

$$\begin{aligned} C_{pendulum_{42}} &= -K_p \cdot Z_{crane} \\ C_{pendulum_{43}} &= K_w \cdot Y_{crane} \\ C_{pendulum_{44}} &= K_p \cdot Z_{crane} \cdot Z_{crane} + K_w \cdot Y_{crane} \cdot Y_{crane} \\ C_{pendulum_{45}} &= -K_w \cdot X_{crane} \cdot Y_{crane} \\ C_{pendulum_{46}} &= -K_p \cdot X_{crane} \cdot Z_{crane} \\ C_{pendulum_{48}} &= K_p \cdot Z_{crane} \\ C_{pendulum_{49}} &= -K_w \cdot Y_{crane} \end{aligned} \tag{3.4}$$

The Python tool uses the input values explained in table 3.2 to calculate the pendulum restoring stiffness values. With this restoring stiffness value and the location of the crane top and the length of the crane cable the stiffness values for all 12 degrees of freedom can be calculated. A 12 by 12 matrix is created and filled with all the pendulum stiffness values. In section 3.6 is explained how this matrix is used to calculate the responses of the multi-body system.

Table 3.2: Input values needed to calculate pendulum stiffness matrix

Input	**Used for**
Cargo Mass	Used to calculate pendulum stiffness and to calculate the critical damping.
Sling length	The sling length contains the vertical distance between the crane tip and cargo CoG sed to calculate pendulum stiffness and the wire stiffness. In the model the term sling length is used but in practice it is the combined length of the crane cable, crane hook and slings. The sling length is used to calculate the influence of the vessel rotations on the pendulum motions.
Young's modulus crane wire	Used to calculate wire stiffness.
Crane wire cross sectional area	Used to calculate wire stiffness.
Difference between vessel and cargo CoG	Used to translate the rotations of the vessel in translations of the crane tip and used to translate cargo translations in rotational moments. Both are used to calculate the influence of the 12 DoF on each other.

A variable that must not be forgotten is air friction. Air friction causes damping to the pendulum motions but this is a damper that only acts on the pendulum and will not act as a damper between the two motions. While the air damping is very small it is assumed that the air damping is 0.5% of the critical damping[14]. To implement the air damping a matrix is created which contains the air damping values.

3.4. Mooring Lines Input

Mooring lines will add stiffness to the system. Since mooring lines are only connected to the vessel they will only add stiffness to the vessel. However, since it is a multi-body system the stiffness connected to the vessel body will also influence the cargo responses. Therefore the influence of mooring lines are studied. The results of this study are shown in section 5.2. The weight of the mooring lines will be neglected. Even though the size of the mooring lines can become large in both length and diameter, the weight of the lines will always be small in comparison with the vessel and cargo. The vessel could lift cargoes with less weight but this study does not focus on light weight cargo. Due to the relatively small mooring line weights the weight will not influence the mass of the vessel at all. Without weight the mooring lines will only influence the stiffness components of the multi-body system. The stiffness values will cause restoring forces when the vessel displaces from its original position. These restoring forces will counteract the inertia forces. While the inertia terms will not change a new balance between the restoring forces and inertia forces will be found when mooring lines are added to the system. The natural frequencies of the multi-body system are dependent on the stiffness and mass of the multi-body system as explained in section 2.7. The increased stiffness due to the mooring lines will increase the natural frequencies of the multi-body system.

The mooring lines will be described as springs. The spring stiffness of the mooring lines can be linearized from the elongation graph as explained in section 2.4. Besides the breaking load of a mooring line the length of the mooring line is required to calculate the spring stiffness. To calculate the overall length the X, Y and Z locations of the bollards on shore and the fairlead of the mooring winch relative to the vessel CoG are needed. With these values the difference in the X, Y and Z location of each line can be calculated. The overall line length can be calculated with equation 3.5. This line length can be used to calculate the stiffness of the mooring line.

In figure 3.4 the linearization graph shown in section 2.4 is shown for clarity. This figure can be used to calculate the stiffness values of the mooring lines. When the polypropylene mooring line is linearized for a load equal to 0 % till 10% of the minimum breaking load an elongation of 1.75% will occur. The total elongation is 1.75% of the line length calculated in equation 3.5. This stiffness can be used to calculate the X, Y and Z stiffness components of the mooring line as shown in equation 3.6. In these equations K_{moor} represents the stiffness component of the mooring lines. $X_{bollard}$, $Y_{bollard}$ and $Z_{bollard}$ represent the X,Y and Z coordinate of the coordinate on shore relative to the vessel's centre of gravity. The X,Y and Z coordinate of the winch or fairlead of the mooring line are given by X_{winch}, Y_{winch} and Z_{winch} respectively.

$$L_{line} = \sqrt{(X_{bollard} - X_{winch})^2 + (Y_{bollard} - Y_{winch})^2 + (Z_{bollard} - Z_{winch})^2} \tag{3.5}$$

$$\begin{aligned} K_{moor_x} &= K_{moor} \cdot \frac{X_{bollard} - X_{winch}}{L_{line}} \\ K_{moor_y} &= K_{moor} \cdot \frac{Y_{bollard} - Y_{winch}}{L_{line}} \\ K_{moor_z} &= K_{moor} \cdot \frac{Z_{bollard} - Z_{winch}}{L_{line}} \end{aligned} \tag{3.6}$$

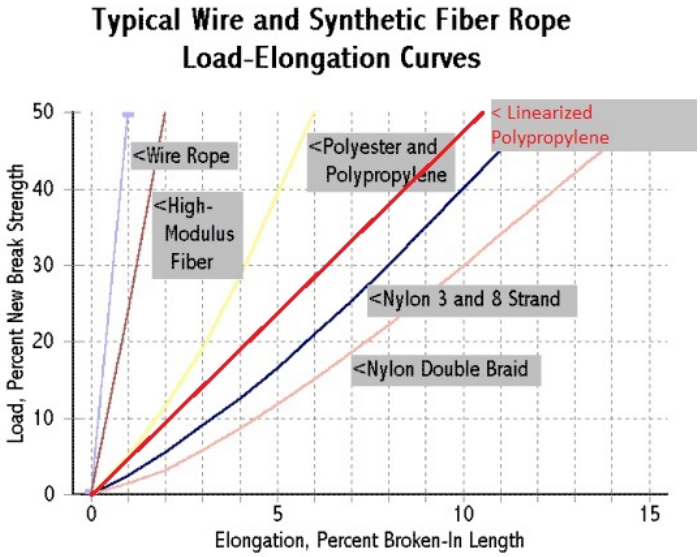

Figure 3.4: Load elongation curves of different mooring line materials[6]

Now that the stiffness components of a single mooring line are known the influence of the lines of the equation of motion can be determined. The values of K_{moor_x}, K_{moor_y} and K_{moor_z} can be multiplied with the translations to get a force. When the rotations of the vessel are multiplied with the X, Y or Z component of the fairlead location a translation of the fairlead is the result. This can be multiplied with the corresponding K_{moor_x}, K_{moor_y} or K_{moor_z} to get coupling forces between translations and rotations. At the same time, when translations are multiplied with the X, Y or Z components of the fairlead location rotational forces will be the result. Which couples the rotations and translations.

In figure 3.5a the free body diagram of the interaction between the vessel and the shore via the mooring lines for the vessel surge motion is shown. The translation of the surge motions causes an offset between the fairleads and the bollards. This offsets causes the mooring lines to stretch which results in a restoring force in the mooring lines that is applied to the vessel and the bollard. The shore itself is not part of the multi-body system and the bollards are assumed rigid. Therefore the bollards are unable to move and no new degrees of freedom are introduced. This means that the restoring forces of the mooring lines will only be applied to the vessel body. 3 different degrees of freedom can cause a translation in X direction of the vessel's fairlead. These degrees of freedom are summarized below. All these degrees of freedom cause a restoring force in the vessel's surge direction that is equal to the X component of the mooring line stiffness multiplied by the translation of the fairlead in X direction, as shown in equation 3.7.

- **Vessel surge:** The vessel surge motion translates the fairlead in longitudinal direction.
- **Vessel pitch:** The vessel pitch motion multiplied with the vertical location of the fairlead causes a translation of the fairlead in the longitudinal direction.
- **Vessel yaw:** The vessel yaw motion multiplied with the transverse location of the fairlead causes a translation of the fairlead in the longitudinal direction.

Figure 3.5b shows the free body diagram of the interaction between the vessel and the shore via the mooring lines for the vessel roll motion. When the fairleads are not located at the centre of gravity of the vessel five different degrees of freedom can apply rotational moments in the vessel's roll direction, as shown in equation 3.8. All the degrees of freedom that can influence the vessel roll motion will are summarized below.

- **Vessel sway:** The vessel sway motion will cause a translation of the fairlead. Together with the restoring stiffness a restoring force is created. This restoring force will cause a moment in roll direction when the force is multiplied with the vertical location of the fairlead.

- **Vessel heave:** The vessel heave motion will cause a translation of the fairlead. Together with the restoring stiffness a restoring force is created. This restoring force will cause a moment in roll direction when the force is multiplied with the transverse location of the fairlead.
- **Vessel Roll:** The vessel roll motion can cause a moment force in two ways.
  - The vessel roll motion together with the vertical location of the fairlead creates a translation of the fairlead in Y direction. This translation multiplied with the Y component of the restoring stiffness creates a force. This force creates a moment when it is multiplied with the vertical location of the fairlead.
  - The vessel roll motion together with the transverse location of the fairlead creates a translation of the winch in Z direction. This translation multiplied with the Z component of the restoring stiffness creates a force. This force creates a moment when it is multiplied with the transverse location of the fairlead.
- **Vessel pitch**: The vessel pitch motion together with the longitudinal location of the fairlead creates a translation of the fairlead in Z direction. This translation multiplied with the Z component of the restoring stiffness creates a force. This force creates a moment when it is multiplied with the transverse location of the fairlead.
- **Vessel yaw**: The vessel yaw motion together with the longitudinal location of the fairlead creates a translation of the fairlead in Y direction. This translation multiplied with the Y component of the restoring stiffness creates a force. This force creates a moment when it is multiplied with the vertical location of the fairlead.

Equations 3.7 and 3.8 are the restoring stiffness calculations for a single mooring line. This equation can needs to be solved for every mooring line in the multi-body system. Since linear theory is applied the superposition rule can also be used for the mooring lines. All the individual mooring line restoring forces can be added together to get the total mooring line restoring force.

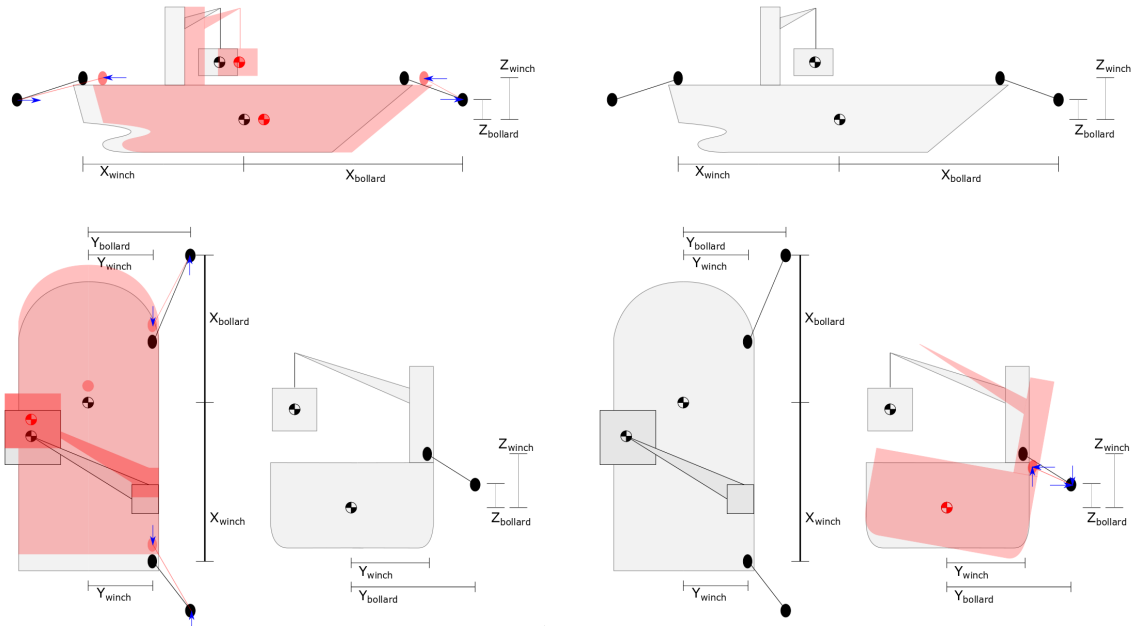

(a) Free body diagram of the interaction between the vessel and the shore via the mooring lines for the surge motion of the vessel

(b) Free body diagram of the interaction between the vessel and the shore via the mooring lines for the vessel roll motion

Figure 3.5: Free body diagram of the interaction between the vessel and the shore via the mooring lines for the vessel surge motion and the vessel roll motion. These free body diagrams can be used to explain the influence of these degree of freedom on other degrees of freedom in the multi-body system

$$F_{Moor_1} = K_{moor_x} \cdot x_1 + K_{moor_X} \cdot Z_{winch} \cdot x_5 - K_{moor_X} \cdot Y_{winch} \cdot x_6 \tag{3.7}$$

$$\begin{aligned} F_{Moor_4} = &- K_{moor_y} \cdot Z_{winch} \cdot x_2 + K_{moor_z} \cdot Y_{winch} \cdot x_3 \\ &+ K_{moor_Z} \cdot Y_{winch} \cdot Y_{winch} \cdot x_4 + K_{moor_y} \cdot Z_{winch} \cdot Z_{winch} \cdot x_4 \\ &- K_{moor_z} \cdot X_{winch} \cdot Y_{winch} \cdot x_5 - K_{moor_y} \cdot X_{winch} \cdot Z_{winch} \cdot x_6 \end{aligned} \tag{3.8}$$

Equations 3.7 and 3.8 show how the forces due to one single mooring line can be calculated. The stiffness values components of these equations can be written in a matrix. Equations 3.9 and 3.10 show how the mooring stiffness components of a single mooring line can be written in a matrix. For every single mooring line in a lifting configuration such a matrix has to be created. Since the model is a linear model the different mooring line stiffness matrices can be added together which results in a overall mooring line stiffness matrix. In section 3.6 is explained how this overall stiffness matrix is implemented in the multi-body system. All the input variables required to solve the mooring line restoring matrix are shown in table 3.3

$$\begin{aligned} C_{moor_{11}} &= K_{moor_x} \\ C_{moor_{15}} &= K_{moor_x} \cdot Z_{winch} \\ C_{moor_{16}} &= -K_{moor_x} \cdot Y_{winch} \end{aligned} \tag{3.9}$$

$$\begin{aligned} C_{moor_{12}} &= -K_{moor_y} \cdot Z_{winch} \\ C_{moor_{13}} &= K_{moor_z} \cdot Y_{winch} \\ C_{moor_{14}} &= K_{moor_z} \cdot Y_{winch} \cdot Y_{winch} + K_{moor_y} \cdot Z_{winch} \cdot Z_{winch} \\ C_{moor_{15}} &= -K_{moor_z} \cdot X_{winch} \cdot Y_{winch} \\ C_{moor_{16}} &= -K_{moor_y} \cdot X_{winch} \cdot Z_{winch} \end{aligned} \tag{3.10}$$

Fenders are neglected in the model. While the influence of the quay is neglected fenders will also be neglected. Fenders are also extremely non-linear. Implementing and linearizing fenders would cause large deviations from reality. When fenders are linearized they will also apply stiffness to the system when the vessel moves away from the quay. While fenders have a large stiffness value this would create large restoring forces due to the fenders while they do not occur in reality.

In this method a few assumptions are made. First of all the mooring line stiffness is linearized. This will give a small deviation to reality but is not really important. More important is the fact that considering mooring lines to act linear is only partly true. When elongation occurs the mooring line acts as a spring. However no suspension occurs in a mooring line system. The mooring line will simply go slack and thus no energy is stored in a spring. Assumed that a vessel is moored alongside a quay the problem of slack mooring lines can be solved by placing the mooring lines in forward as backward direction from the vessel so that K_{moor_x} is the same in positive as negative direction. In Y direction the mooring line stiffness will only be applied when the vessel motion is in the opposite direction than the location of the quay. This will give a false assumption for motions towards the quay. However fenders between the vessel and the quay will have a much higher stiffness and this fact can be neglected. Assumed that the fairlead Z position is higher than the bollard Z position the stiffness of the mooring line will only have influence on a positive heave motion. This is an inaccuracy that must be accepted for practicality when the mooring line stiffness is applied in the frequency domain. To neglect the stiffness in Z direction the fairlead and bollard position must have the same value for their Z position.

Table 3.3: Input values needed to calculate the mooring line stiffness matrix

Input	Used for
bollard X, Y and Z position	3 lists with the same length. Each input value corresponds to a single bollard on the shore. The values are used to calculate the X, Y and Z distance between the bollards on the quay and the location of the fairlead used by the corresponding mooring line.
Fairlead X, Y and Z position	3 lists with the same length. Each input value corresponds to a single fairlead on board of the vessel. The values are used to calculate the X, Y and Z distance between the fairlead and the corresponding bollard on the quay.
MBL mooring line	The minimum breaking load is used to calculate the mooring line stiffness as explained in equation 2.18.
Elongation mooring line	The elongation caused by a certain amount of load in % of the total mooring line length. This is used to calculate the the mooring line stiffness.

In the Python tool a new 12 by 12 matrix is created. The input values from table 3.3 can be used to calculate the stiffness forces of the mooring lines on all degrees of freedom. These stiffness values for all degrees of freedom will be stored in the newly created mooring stiffness matrix. This matrix can be used to calculate the influence of mooring lines on the responses of the multi-body system. In section 3.6 will be explained how the mooring line matrix can be used.

While this matrix has the same dimensions as all other matrices in the mathematical multi-body model, in reality only the upper left quadrant of the matrix will be filled and the other quadrants will only contain zero entries. While the mooring lines are only a connection between the vessel and the shore there is no coupling between the mooring lines and the cargo. This does not mean that the mooring lines will not influence the responses of the cargo. While the vessel will be influenced by the mooring lines and the cargo is coupled to the vessel the cargo will also be influenced by the mooring lines.

3.5. Cargo Control Systems

Besides influencing the motions by changing the loading conditions damping can be added to the system to reduce the responses of the vessel and cargo. In section 2.5 is explained what the influence of damping is on the dynamics of a single or multi degree of freedom system. Damping will dissipate energy from the system since the damping forces act perpendicular on the restoring forces and inertia forces, as explained in section 2.6. In the same section different methods to apply damping are explained. Passive damping can be applied via a system that is related to passive heave compensation systems. Active system can also be used. Constant tension winches and active winches will apply damping to the system.

All the different damping methods have one thing in common. There need to be a connection between the vessel and cargo other than the connection via the crane cable. This connection can be made via tugger wires. These tugger wires can be connected to the cargo via padeyes or other connection methods. The other end of the wires can be connected to winches on deck. The tugger winches can pretension the tugger wires to prevent these wires from falling slack which induces snap loads. Since snap loads can create dangerous forces they need to be prevented. At the same time snaploads are non-linear which makes it impossible to implement. The stiffness of the tugger winches varies for different materials and different pretension values. In section 2.4 is explained how lines can be linearized. Since pretension is required in the tugger lines the stiffness will not be linearized around the 0% and 10%. The pretension will induce elongation of the line. Depending on the maximum breaking load of the line, the materials, tugger wire length and the pretension the tugger wires will be linearized around an appropriate elongation percentage.

The length of the tugger wires can be calculated in an almost identical way as the length of the mooring lines explained in section 3.4. In the model the location of the tugger winches and the location of the padeyes or other connection methods to the cargo are variables that can be used. The location of the tugger winch is the location relative to the vessel centre of gravity. The location of the padeye is the location relative to the centre of gravity of the cargo. Therefore the centre of gravity of the cargo relative to the vessel centre of gravity must

be taken into account. The centre of gravity of the cargo is dependent on the crane tip location and vertical distance between crane tip and cargo centre of gravity. In equations 3.11 till 3.13 the equations for the tugger wire components are given. Equation 3.5 can be used to calculate the total tugger wire length. The stiffness components of the different directions can be calculated in the same was as the stiffness components of the mooring lines. In these equations X_{tug}, Y_{tug} and Z_{tug} represent the X, Y and Z coordinates of the tugger winches relative to the vessel's centre of gravity. The X, Y and Z coordinate of the connection of the tugger wire to the cargo relative to the cargo's centre of gravity is given by X_{pad}, Y_{pad} and Z_{pad} respectively. The distance between the crane top and the cargo's centre of gravity is given by Z_{sling}.

$$L_{tug_X} = \sqrt{\left(X_{Tug} - \left(X_{crane} + X_{pad}\right)\right)^2} \tag{3.11}$$

$$L_{tug_Y} = \sqrt{\left(Y_{Tug} - \left(Y_{crane} + Y_{pad}\right)\right)^2} \tag{3.12}$$

$$L_{tug_Z} = \sqrt{\left(Z_{Tug} - \left(\left(Z_{crane} - Z_{sling}\right) + Z_{pad}\right)\right)^2} \tag{3.13}$$

The tugger wires can be made of different materials. All the different materials will have other stiffness values. These stiffness values will influence the multi-body system. To determine the influence of the stiffness of the tugger lines different stiffness values will be compared. In section 6.1 different stiffness values are compared. In this comparison no damping is applied and only the stiffness values will influence the responses of the vessel and cargo.

One of the ways to implement damping to the system was the use of a passive system that dissipates energy via a hydraulic or pneamatic module. Dissipation forces transfer kinetic energy from the vessel and cargo into heat and kinematic energy of the fluid. Such a system can be connected between the cargo and the vessel with the help of a tugger winch. Both sides of the passive damping module will be connected to two different wires. One wire will be connected to the cargo and the other wire will be connected to the winch. The pretension of the winch can be used to apply the required force to the module and prevent the wires from falling slack. When there is a relative motion between the vessel and cargo the piston of the passive compensation will extend or contract. As explained in section 2.5 and appendix E, it is hard to determine the damping of such a system. However damping is possible. Since it is not the purpose of this thesis to develop a passive damping system the exact amount of damping that can be added to the multi-body system will not be calculated. Therefore the damping induced will be taken as a percentage of the critical damping. The critcal damping used in these calculations is depending on the stiffness of the connection between the cargo and vessel as shown in equation 3.14. In this equation M_{cargo} represents the cargo mass and C_{Tugger} represents the combined stiffness of the tugger wire and damping module.

$$\xi_{crit_{Tug}} = 2 \cdot \sqrt{M_{cargo} \cdot C_{Tugger}} \tag{3.14}$$

Another way to apply damping is via constant tension winches. Constant tension winches apply damping due to the slow activation of the system. As it was for the passive damping module it is hard to determine the damping of such a system. Therefore the same principle will be used and an percentage of the critical damping will be as damping of the system.

The damping that is applied via both ways is the total damping that will be applied. This means that it has to be dissolved in the different translation. This can be done in the same way as is done for the mooring line stiffness. For clarity the equation is rewritten in equation 3.15 because the X, Y and Z components are determined differently.

$$\begin{aligned} D_{tug_X} &= D_{tug} \cdot \frac{\left(X_{tug} - \left(X_{Crane} + X_{pad}\right)\right)}{L_{tug}} \\ D_{tug_Y} &= D_{tug} \cdot \frac{\left(Y_{tug} - \left(Y_{Crane} + Y_{pad}\right)\right)}{L_{tug}} \\ D_{tug_Z} &= D_{tug} \cdot \frac{\left(Z_{tug} - \left(\left(Z_{Crane} - Z_{Sling}\right) + Z_{pad}\right)\right)}{L_{tug}} \end{aligned} \tag{3.15}$$

Besides passive systems and constant tension winches an active system can be used to apply damping. In an active system the kinetic energy of the system is dissipated by adding energy from an external source. In section 2.5 is explained that tugger winches might be programmed to act as an active system. For an active system it is easier to determine the applied damping. The applied damping is dependent on the pay-out speed and pay-in speed of the tugger winch and the force a tugger winch can apply. Since these are two factors a tugger winch can be designed around, it is possible to calculate the vessel and cargo response for damping values instead of critcal damping percentages. However, the applicability of all different damping methods will be studied in chapter 6.

Now that the stiffness and damping components of the damping systems are explained the translation between physical forces and mathematical representation can be solved. The equation for the restoring forces and damping forces of damping systems are almost identical. While the stiffness and damping via tugger wires is applied via the same connections the influence and relations between the different degree of freedom are the same for both types of forces. In the explanation for the pendulum restoring force and mooring line restoring force is told that the vessel rotations cause a translation of the crane tip and fairleads. At the same time will translations multiplied by the location of the crane tip or fairlead result in rotational moments. This phenomenom does also occur in the forces caused by the damping systems. However, the mooring lines will only influence the degrees of freedom of the vessel and the pendulum restoring forces neglect the rotations of the cargo. The damping systems will not be connected to the centre of gravity of the cargo in most cases. Therefore, the rotations of the cargo cannot be ignored in these calculations.

In figure 3.6a the free body diagram of the vessel surge motion is shown. In this figure only the influence of the cargo control system is shown. When there is a relative displacement in surge direction between connection of the cargo control system to the vessel and the connection of the cargo control system to the cargo a restoring force is created. A relative displacement is created when the location of the connection to the vessel or the location of the connection to the cargo of the cargo control system moves is displaced further than its counter part. The restoring force of the cargo control system is applied to both the vessel and the cargo. The restoring force of the cargo control systems can be calculated by multiplying the relative displacement in surge direction between the vessel and the cargo with the X component of the restoring stiffness value. There are 6 degrees of freedom that can cause a relative displacement of the cargo control system between the vessel and cargo in surge directions. Below is summarized how these degrees of freedom cause a relative translation with regards to the vessel surge direction. In equation 3.16 is shown how the restoring force of the cargo control system applies force in the vessel surge direction.

- **Vessel surge**: The vessel surge motion itself translates the winches in the longitudinal direction.
- **Vessel pitch**: The vessel pitch motion multiplied with the vertical location of the cargo control system connection to the vessel causes a translation of the cargo control system in the surge direction.
- **Vessel yaw**: The vessel yaw motion multiplied with the transverse location of the cargo control system connection to the vessel causes a translation of the cargo control system in the surge direction.
- **Cargo surge**: The cargo surge motion causes a change in the relative distance between the cargo and the vessel itself.
- **Cargo pitch**: The cargo pitch motion multiplied with the vertical location of the cargo control system connection to the cargo causes a translation of the cargo control system in the surge direction.
- **Cargo yaw**: The cargo yaw motion multiplied with the transverse location of the cargo control system connection to the cargo causes a translation of the cargo control system in the surge direction.

In figure 3.6b the free body diagram of the vessel roll motion is shown. In this figure only the influence of the cargo control system is shown. A moment in the roll direction is created by a force in the Y or Z direction multiplied with an arm of that force to the X-axis. In equation 3.17 is shown how the restoring force in the vessel roll direction is created. There are ten different degrees of freedom that can create a restoring force in the vessel roll direction via the cargo control system. These ten degrees of freedom are summarized below. The connection of the cargo control system to the vessel will be called winch and the connection of the cargo control system to the vessel will be called padeye. In appendix A the free body diagrams for all degrees of freedom are shown.

- **Vessel sway**: The vessel sway motion will cause a translation of the winch. Together with the restoring stiffness a restoring force is created. This restoring force will cause a moment in roll direction when this force is multiplied with the vertical location of the winch.

- **Vessel heave**: The vessel heave motion will cause a translation of the winch. Together with the restoring stiffness a restoring force is created. This restoring force will cause a moment in roll direction when this force is multiplied with the transverse location of the winch.

- **Vessel Roll**: The vessel roll motion can cause a moment force in two ways.

    * The vessel roll motion together with the vertical location of the winch creates a translation of the winch in Y direction. This translation multiplied with the Y component of the restoring stiffness creates a force. This force creates a moment when it is multiplied with the vertical location of the winch.

    * The vessel roll motion together with the transverse location of the winch creates a translation of the winch in Z direction. This translation multiplied with the Z component of the restoring stiffness creates a force. This force creates a moment when it is multiplied with the transverse location of the winch.

- **Vessel pitch**: The vessel pitch motion together with the longitudinal location of the winch creates a translation of the winch in Z direction. This translation multiplied with the Z component of the restoring stiffness creates a force. This force creates a moment when it is multiplied with the transverse location of the winch.

- **Vessel yaw**: The vessel yaw motion together with the longitudinal location of the winch creates a translation of the winch in Y direction. This translation multiplied with the Y component of the restoring stiffness creates a force. This force creates a moment when it is multiplied with the vertical location of the winch.

- **Cargo sway**: The cargo sway motion will cause a translation of the padeye. Together with the restoring stiffness a restoring force is created. This restoring force will cause a moment in roll direction when this force is multiplied with the vertical location of the winch.

- **Cargo heave**: The cargo heave motion will cause a translation of the padeye. Together with the restoring stiffness a restoring force is created. This restoring force will cause a moment in roll direction when this force is multiplied with the transverse location of the winch.

- **Cargo Roll**: The cargo roll motion can cause a moment force in two ways.

    * The cargo roll motion together with the vertical location of the padeye creates a translation of the padeye in Y direction. This translation multiplied with the Y component of the restoring stiffness creates a force. This force creates a moment when it is multiplied with the vertical location of the winch.

    * The cargo roll motion together with the transverse location of the padeye creates a translation of the padeye in Z direction. This translation multiplied with the Z component of the restoring stiffness creates a force. This force creates a moment when it is multiplied with the transverse location of the winch.

- **Cargo pitch**: The cargo pitch motion together with the longitudinal location of the padeye creates a translation of the padeye in Z direction. This translation multiplied with the Z component of the restoring stiffness creates a force. This force creates a moment when it is multiplied with the transverse location of the winch.

- **Cargo yaw**: The cargo yaw motion together with the longitudinal location of the padeye creates a translation of the padeye in Y direction. This translation multiplied with the Y component of the restoring stiffness creates a force. This force creates a moment when it is multiplied with the vertical location of the winch.

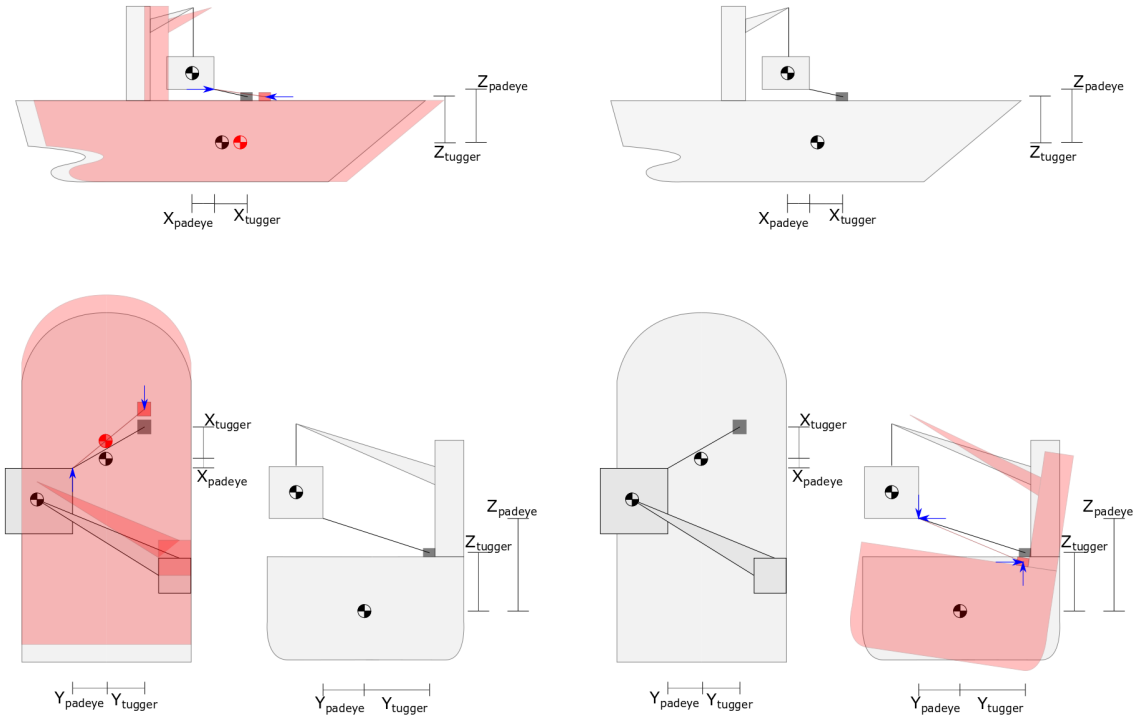

(a) Free body diagram of the interaction between the vessel and the cargo via the cargo control systems for the surge motion of the vessel

(b) Free body diagram of the interaction between the vessel and the cargo via the cargo control systems for the vessel roll motion

Figure 3.6: Free body diagram of the interaction between the vessel and the cargo via the cargo control systems for the vessel surge motion and the vessel roll motion. These free body diagrams can be used to explain the influence of these degree of freedom on other degrees of freedom in the multi-body system

In equation 3.16 is shown how the restoring force due to the cargo control system in vessel surge direction is formed. Equation 3.17 shows how the restoring force in the vessel roll direction due to the damping system is calculated. In this equations K_{T_x}, K_{T_y} and K_{T_z} represents the stiffness of the damping system in X, Y an Z direction. X, Y, and Z_{Tug} represent the X, Y and Z location of the winch. The X, Y and Z components of the location where the damping system is connected to the cargo is given by X, Y, and Z_{Pad}. The responses are given by x_1 to x_{12}. These equations can be translated to damping forces when the stiffness values K_T are changed for the damping values D_T and the response values x_n are changed in the velocities $\dot{x_n}$.

$$\begin{aligned} F_{Tugger_1} =& K_{Tug_x} \cdot x_1 + K_{Tug_x} \cdot Z_{Winch} \cdot x_5 - K_{Tug_x} \cdot Y_{Winch} \cdot x_6 \\ & - K_{Tug_x} \cdot x_7 - K_{Tug_x} \cdot Z_{Pad} \cdot x_{11} + K_{Tug_x} \cdot Y_{Pad} \cdot x_{12} \end{aligned} \tag{3.16}$$

$$\begin{aligned} F_{Tugger_4} =& - K_{Tug_y} \cdot Z_{Winch} \cdot x_2 + K_{Tug_z} \cdot Y_{Winch} \cdot x_3 + K_{Tug_y} \cdot Z_{Winch} \cdot Z_{Winch} \cdot x_4 + K_{Tug_z} \cdot Y_{Winch} \cdot Y_{Winch} \cdot x_4 \\ & - K_{Tug_z} \cdot X_{Winch} \cdot Y_{Winch} \cdot x_5 - K_{Tug_y} \cdot X_{Winch} \cdot Z_{Winch} \cdot x_6 + K_{Tug_y} \cdot Z_{Winch} \cdot x_8 - K_{Tug_z} \cdot Y_{Winch} \cdot x_9 \\ & - K_{Tug_y} \cdot Z_{pad} \cdot Z_{Winch} \cdot x_{10} - K_{Tug_z} \cdot Y_{pad} \cdot Y_{Winch} \cdot x_{10} \\ & + K_{Tug_z} \cdot X_{pad} \cdot Y_{Winch} \cdot x_{11} + K_{Tug_y} \cdot X_{pad} \cdot Z_{Winch} \cdot x_{12} \end{aligned} \tag{3.17}$$

Equations 3.16 and 3.17 represent the forces due to one single system. However, the superposition principle that is used before can also be applied for the tugger wires stiffness and the damping applied via the tugger wires. This means that the influence of multiple tugger wire systems can be calculated independently and the combined stiffness or damping factors can be added together. All the input values required to solve the matrices are given in table 3.4

Equations 3.16 and 3.17 show how the restoring forces of the tugger lines can be calculated. However, these equations have to be implemented in the python tool. In the Python tool the restoring forces are split per degree of freedom. The stiffness values of these different degree of freedom are stored in a matrix. In equations 3.18 and 3.19 is shown how the tugger line stiffness values corresponding to the vessel surge and vessel sway motion are stored in a matrix. For every single tugger line such a matrix can be made for both the stiffness values and damping values. All the stiffness and damping matrices can be combined to one overall tugger line stiffness matrix and one overall tugger line damping matrix. In section 3.6 is explained how these matrices can be used in the equation of motioon to solve the multi-body system.

$$\begin{aligned}
C_{tugger_{11}} &= K_{Tug_x} \\
C_{tugger_{15}} &= K_{Tug_x} \cdot Z_{Winch} \\
C_{tugger_{16}} &= -K_{Tug_x} \cdot Y_{Winch} \\
C_{tugger_{17}} &= -K_{Tug_x} \\
C_{tugger_{111}} &= -K_{Tug_x} \cdot Z_{Pad} \\
C_{tugger_{112}} &= K_{Tug_x} \cdot Y_{Pad}
\end{aligned} \tag{3.18}$$

$$\begin{aligned}
C_{tugger_{42}} &= -K_{Tug_y} \cdot Z_{Winch} \\
C_{tugger_{43}} &= K_{Tug_z} \cdot Y_{Winch} \\
C_{tugger_{44}} &= K_{Tug_y} \cdot Z_{Winch} \cdot Z_{Winch} + K_{Tug_Y} \cdot Y_{Winch} \cdot Y_{Winch} \\
C_{tugger_{45}} &= -K_{Tug_z} \cdot X_{Winch} \cdot Y_{Winch} \\
C_{tugger_{46}} &= K_{Tug_Z} \cdot X_{Winch} \cdot Z_{Winch} \\
C_{tugger_{48}} &= K_{Tug_y} \cdot Z_{Winch} \\
C_{tugger_{49}} &= -K_{Tug_z} \cdot Y_{Winch} \\
C_{tugger_{410}} &= K_{Tug_y} \cdot Z_{Pad} \cdot Z_{Winch} + K_{Tug_Y} \cdot Y_{Pad} \cdot Y_{Winch} \\
C_{tugger_{411}} &= -K_{Tug_z} \cdot X_{Pad} \cdot Y_{Winch} \\
C_{tugger_{412}} &= K_{Tug_Z} \cdot X_{Pad} \cdot Z_{Winch}
\end{aligned} \tag{3.19}$$

Table 3.4: Input values needed to calculate the damping and stiffness matrices for damping systems

Input	Used for
Cargo Mass	Used to calculate the critical damping. The critical damping can be used to determine the damping coefficient
Winch X, Y and Z position	The winch X, Y and Z positions are used to calculate the wire length of the wire that connects the vessel to the cargo. The positions are also used to calculate the rotational moments from vessel and cargo translations as well as the translations due to vessel and cargo rotations
Padeye X, Y and Z position	The Padeye X, Y and Z positions are used to calculate the wire length of the wire that connects the vessel to the cargo. The positions are also used to calculate the rotational moments from vessel and cargo translations as well as the translations due to vessel and cargo rotations
Crane tip location and sling length	Used to locate the centre of gravity of the cargo in comparison with the centre of gravity of the vessel. This is required to calculate the length of the wire of the damping system
Young's modulus crane wire	The Young's modulus can be used to calculate the wire stiffness when no stiffness is specified.
Tugger wire cross sectional area	The cross sectional area can be used to calculate the wire stiffness when no stiffness is specified.
Damping and stiffness values.	The damping and stiffness values can be filled in by the user of the program. These values are used to calcualte the damping and stiffness components in x, y and z direction.

For the implementation of the cargo control system two different 12 by 12 matrices will be created. One matrix will contain all the stiffness values of the cargo control mechanism for all degrees of freedom. The second matrix will contain all the damping values of the cargo control mechanism for all degrees of freedom. The stiffness and damping values of the cargo control system for every degree of freedom will be calculated. The values will be stored in the corresponding matrices. These matrices can be used to calculate the influences of adding stiffness components and damping components to the multi-body system.

3.6. Motion Calculations

In the previous sections all different aspects for the equation of motion are elaborated. Different modules are used to calculate the variables used in the equation of motion. As described in section 2.2 the equation of motion given in equation 2.2 can be used to compile equation 2.11. In section 3.1 is explained that all different aspects of the multi-body system are calculated via seperate modules. Due to the superposition principle the different mass, damper and stiffness matrices can be combined to one mass-spring-damper system. In equation 3.20 is shown how the combined mass, damping and stiffness matrices form the mathematical model of the multi-body system. In this equation $\boldsymbol{M_{hyd}}$ represents the mass matrix calculated by Shipmo. This matrix contains the displacement and inertia of the vessel. $\boldsymbol{A_{hyd}}$ represent the hydrodynamic added mass determined by Shipmo. $\boldsymbol{M_{cargo}}$ contains the influence of the cargo in the crane on the mass values of the multi-body system. The mass deducted from the vessel's hydrodynamic masses and the mass of the cargo are found in this matrix. The hydrodynamic damping values determined by Shipmo, including the Ikeda roll damping values can be found in $\boldsymbol{B_{hyd}}$. The damping due to air friction is given by $\boldsymbol{B_{air}}$ and the damping applied via cargo controll systems are given by $\boldsymbol{B_{tug}}$. $\boldsymbol{C_{hyd}}$ contain the hydrodynamic stiffness properties. The stiffness due to the interaction between cargo in the crane and the vessel are given by $\boldsymbol{C_{pen}}$ and the stiffness due to the cargo control systems are given by $\boldsymbol{C_{tug}}$. Lastly the influence of the mooring lines on the stiffness of the multi-body system is given in $\boldsymbol{C_{moor}}$. The combined mass, damping and stiffness matrices are shown in appendix B and the completely written equations of motions are shown in appendix C. The motions of both bodies caused by the wave excitation can be calculated with equation 3.21.

$$\boldsymbol{S_{model}} = -\omega^2 \cdot \left(\boldsymbol{M_{hyd}} + \boldsymbol{A_{hyd}} + \boldsymbol{M_{cargo}}\right) - i \cdot \omega \cdot \left(\boldsymbol{B_{hyd}} + \boldsymbol{B_{air}} + \boldsymbol{B_{Tug}}\right) + \left(\boldsymbol{C_{hyd}} + \boldsymbol{C_{pen}} + \boldsymbol{C_{Tug}} + \boldsymbol{C_{moor}}\right) \quad (3.20)$$

$$\boldsymbol{x}_{model}(\omega) = \boldsymbol{S_{model}}(\omega)^{-1} \cdot \boldsymbol{F_{exc}}(\omega) \quad (3.21)$$

When equations 3.20 and 3.21 are solved the responses of all degrees of freedom will be calculated. Since the model is modular all different matrices can be used or neglected in the calculations to calculate the influence of different aspects of the multi-body system. However, the hydrodynamic matrices and the wave excitation forces should always be implemented. It is assumed that the driving force of the responses of the multi-body system is the wave excitation force. These wave excitation forces are initially proportionate to the hydrodynamic system of the vessel. The other modules will influence the motions but without the vessel hydrodynamic properties all results will be without any reference points.

In figure 3.7 the response amplitude operators, RAOs in short, of the degrees of freedom of the vessel body are given. For this figure the incoming wave direction is 90 degrees with a period of 12 seconds. In section 3.8 the verification of the model will be explained and the validation is explained in section 3.9. However, the figure shows us that the different modules have different effects on the responses of the vessel. As expected the same time the different modules do not change the RAOs drastically. The peaks in the different RAOs show that there are multiple natural frequencies in the system. While different degrees of freedom get excited at the same natural frequencies it shows that the there is interaction between the different degrees of freedom.

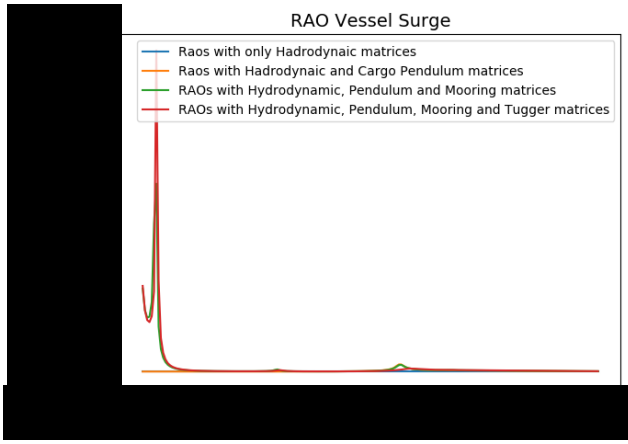

(a) Response Amplitude Operators of the vessel surge motion for different mathematical modules of the Python tool

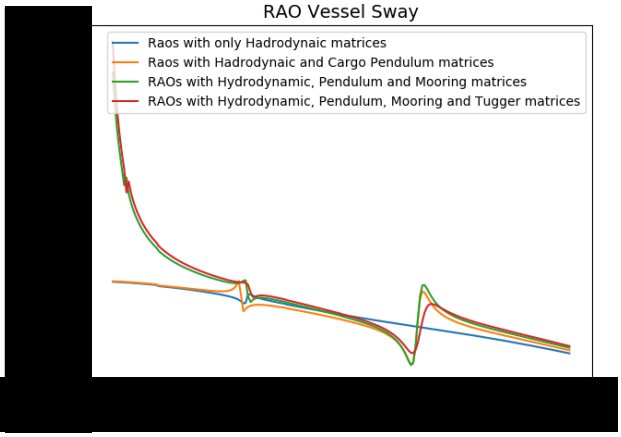

(b) Response Amplitude Operators of the vessel sway motion for different mathematical modules of the Python tool

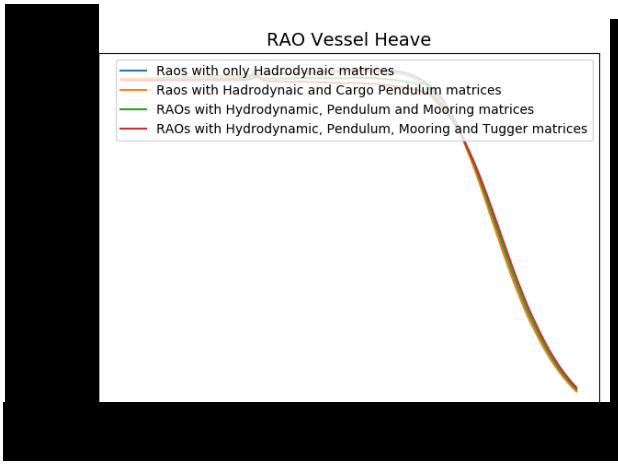

(c) Response Amplitude Operators of the vessel heave motion for different mathematical modules of the Python tool

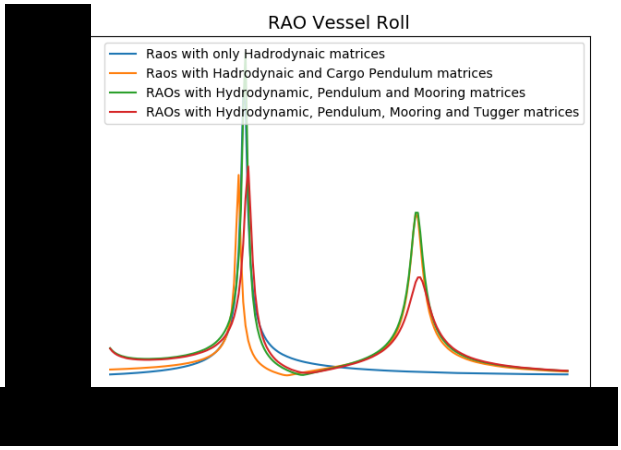

(d) Response Amplitude Operators of the vessel roll motion for different mathematical modules of the Python tool

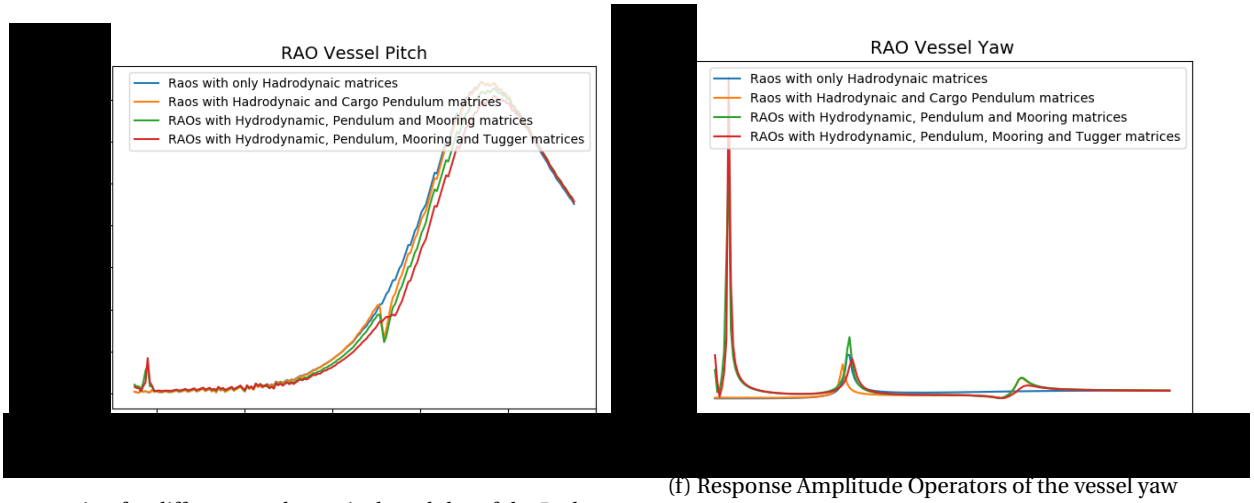

motion for different mathematical modules of the Python tool

(f) Response Amplitude Operators of the vessel yaw motion for different mathematical modules of the Python tool

Figure 3.7: Response Amplitude Operators of the vessel six degrees of freedom for different mathematical modules of the Python tool

3.7. Significant Motions

With the 12 degrees of freedom motion calculations completed the next step in motion predictions can be made. First a wave spectrum must be calculated. This wave spectrum can be used to predict the significant motion and a most probable maximum excitation and response over a certain time period.

First of all a wave spectrum must be calculated. Swell waves can often be described as a Pierson-Moskowitz spectrum and waves in the Northsea can be described as a JONSWAP spectrum. Equation 3.22 shows the equation for a Pierson-Moskowitz spectrum and the JONSWAP spectrum is given in equation 3.23. The JONSWAP spectrum is essentialy a Pierson-Moskowitz spectrum with a peak enhancement function. In the JONSWAP spectrum A is given by equation 3.24. H_s represents the significant wave height. The variable ω_p stands for the peak wave-frequency and ω stands for the wave frequency for which the energy is calculated. σ is equal to 0.07 if $\omega_p \leq \omega$ and equal to 0.09 if $\omega_p > \omega$. The variable γ is the peak enhancement factor which has a default value of 3.3. for sea waves. Swell waves don't need an peak enhancement factor thus this value is set to 1 for swell waves.

$$S_{PM}(\omega) = \frac{5}{16} \cdot H_s^2 \cdot \frac{\omega_p^4}{\omega^5} \cdot e^{\frac{-5}{4} \cdot \left(\frac{\omega_p}{\omega}\right)^4} \tag{3.22}$$

$$S_{JONSWAP}(\omega) = \left(1 - 0.287 \cdot ln(\gamma)\right) \cdot \left(\frac{5}{16} \cdot H_s^2 \cdot \frac{\omega_p^4}{\omega^5} \cdot e^{\frac{-5}{4} \cdot \left(\frac{\omega_p}{\omega}\right)^4}\right) \cdot \gamma^A \tag{3.23}$$

$$A = e^{\left(-0.5 \cdot \left(\frac{\omega - \omega_p}{\sigma \cdot \omega_p}\right)^2\right)} \tag{3.24}$$

These wave spectra can be used to determine the motion response spectra. Equation 3.25 shows how the response spectra of the motions can be calculated. These response spectra can be used to calculate the moments of the motions as shown in equation 3.26. The significant motions, in other words the mean value of the highest one-third part of the amplitudes, is calculated with the 0th moment, as shown in equation 3.27.

$$S_X = |X_{model}|^2 \cdot S_\zeta(\omega) \tag{3.25}$$

$$m_{nx} = \int_0^\infty S_X(\omega) \cdot \omega_n \cdot d\omega \qquad within = 0, 1, 2, \ldots \tag{3.26}$$

$$\overline{X}_{a_s} = 2 \cdot \sqrt{m_{0x}} \tag{3.27}$$

The moments of the motion spectra can also be used to calculate the mean period and the average zero-crossing period as shown in equation 3.28 and equation 3.29 respectively. The zero-crossing period can be used to calculate the number of zero-crossings during a certain period of time which is shown in equation 3.30. The number of zero-crossings and the 0th moment are used to calculate the most probable maximum of a motion during a certain time period. The equation for the most probable maximum is given in equation 3.31[24].

$$T_{1X} = 2\pi \cdot \frac{m_{0x}}{m_{1x}} \tag{3.28}$$

$$T_{2X} = 2\pi \cdot \frac{m_{0x}}{m_{2x}} \tag{3.29}$$

$$N = \frac{timeperiod}{T_{2X}} \tag{3.30}$$

$$MPM_X = \sqrt{m_{0x}} \cdot \sqrt{2 \cdot ln(N)} \tag{3.31}$$

In the Python model the integrals required to solve the moments of the motions from equation 3.26 are solved with the simpson's rule. In section 2.2 is explained that the frequency step size in Shipmo can be chosen by varying the range of the frequency in the calculations. For the significant motion calculations a hydrodynamic database will be generated with a frequency range that fits the response spectra in order to calculate accurate MPM values. When the range is chosen too small some parts of the response spectra will be neglected in the most probable maximum calculations. At the other hand, if the range is too large the peak values in the response spectra will be inaccurate which can also influence the most probable maximum calculations.

3.8. Verification

For the verification the model is compared to the RAO data from Shipmo. When the cargo mass is equal to 0 mton and the stiffness component of the crane wire is set to 0 the vessel RAOs of the model and the vessel RAOs of Shipmo should be exactly the same since all the hydrodynamic values are calculated with Shipmo and the influence of the pendulum is neglected. In figure 3.8 is shown that the RAOs from Shipmo and the Python tool are exactly the same.

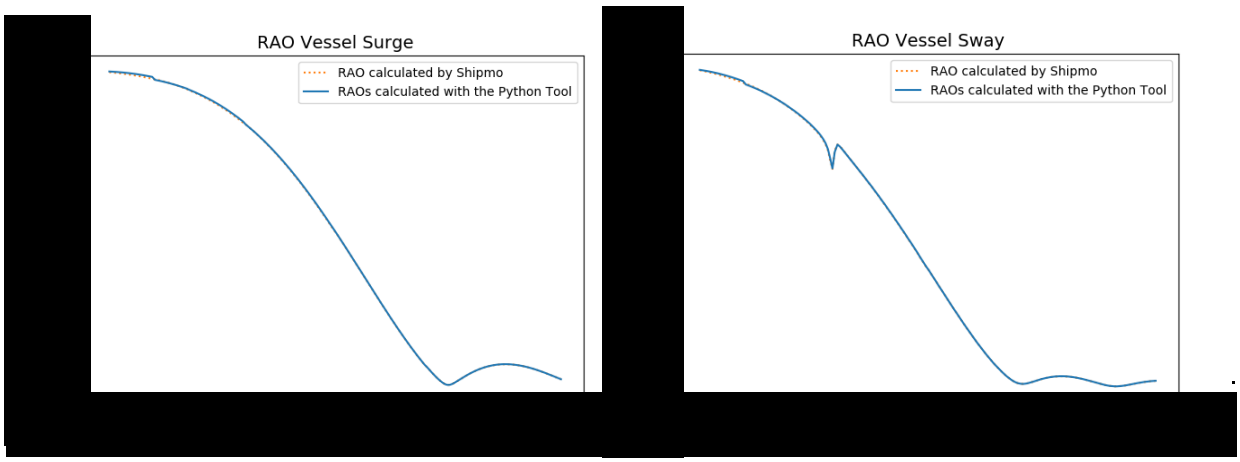

(a) Response Amplitude Operators of the vessel surge motion comparison of the calculation done by Shipmo and by the Python tool

(b) Response Amplitude Operators of the vessel sway motion comparison of the calculation done by Shipmo and by the Python tool

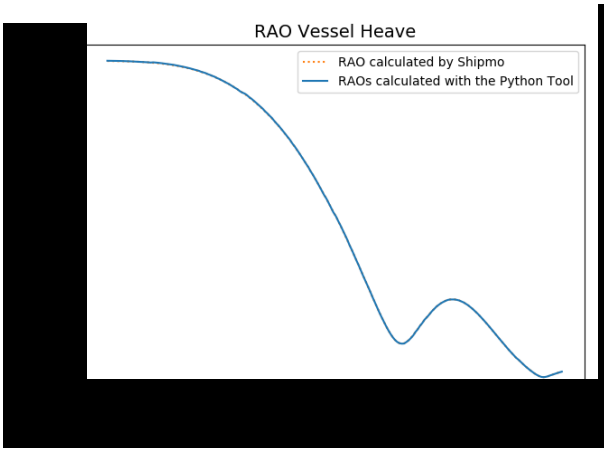

(c) Response Amplitude Operators of the vessel heave motion comparison of the calculation done by Shipmo and by the Python tool

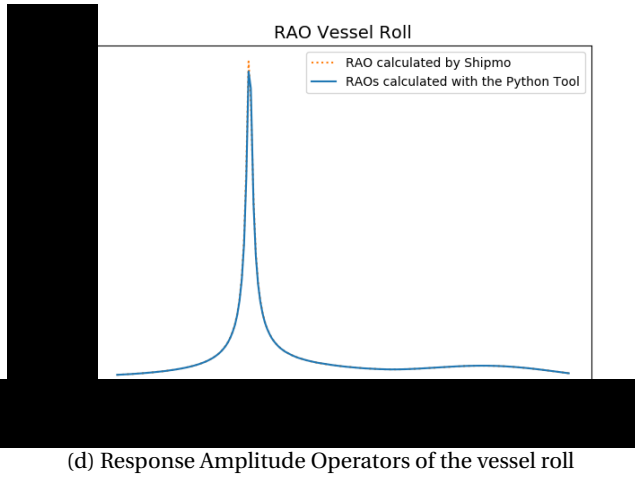

(d) Response Amplitude Operators of the vessel roll motion comparison of the calculation done by Shipmo and by the Python tool

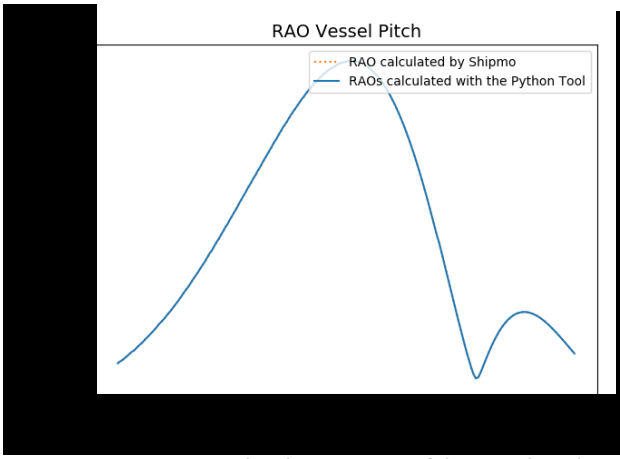

(e) Response Amplitude Operators of the vessel pitch motion comparison of the calculation done by Shipmo and by the Python tool

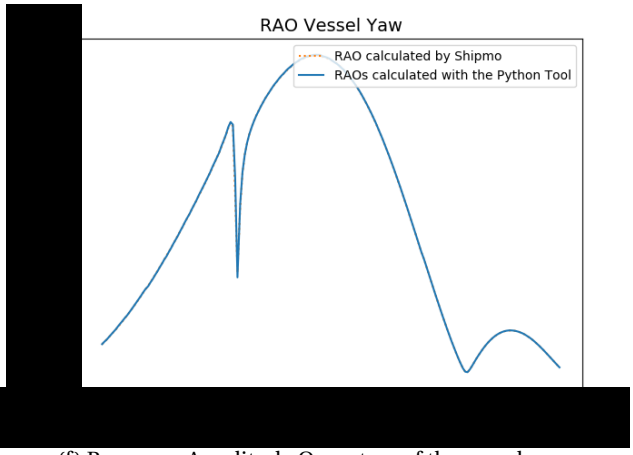

(f) Response Amplitude Operators of the vessel yaw motion comparison of the calculation done by Shipmo and by the Python tool

Figure 3.8: Response Amplitude Operators of the vessel six degrees of freedom comparison of the calculation done by Shipmo and the Python tool

Now that is established that the empty vessel calculations have the result that they are supposed to have the verification of the cargo pendulum motions can be started. With the help of stability software the hydrodynamic properties of the vessel will be calculated for the vessel in two different ways. In the hydrodynamic calculations no coupling via the crane cable occurs. In the first calculation the cargo will be attached to the crane top and in the second calculation the cargo will be placed at the CoG of the vessel. In both cases the vessel displacement will stay the same, which is important for the hydrodynamic properties of the vessel. However, there is a change in the metacentric height between the two stability calculations. The received values for draught and GM will be used in Shipmo to create two hydrodynamic database files. The hydrodynamic database file for the first case will be used to calculate the RAOs from the vessel without any pendulum motions since the influences from the cargo are applied on the GM of the vessel. In the second case the pendulum motions will be applied with the help of the Python tool created. In figure 3.10 the vessel RAOs for the first and second case are plotted. The first case has one natural frequency in the vessel roll motion which stands out. The second case has two notable natural frequencies. The first natural frequency is equal to the natural frequency of the first case. The second national frequency is initiated by the pendulum motions. The similarity in the roll natural frequency between the first and second case shows that the Python tool has a correct influence on the natural frequencies. The difference in the resonance peaks of the natural roll frequency is explained by the amount of energy in the system. In the first case all the energy from the wave excitation force is translated to the vessel. In the second case the same amount of energy is applied to the vessel but the

vessel will also transfer some of the energy to the cargo pendulum motions. Therefore there is less energy in the vessel roll motion. Hence the resonance peak is lower.

The eigenvector of the two natural frequencies that can be seen in figure 3.10d are plotted in figure 3.9. In this figure can be seen that both natural frequencies result in large excitations of the vessel roll motion and cargo sway motion. At the first natural frequency, around [redacted] both degrees of freedom move in opposite directions of each other and at the second natural frequency both degrees of freedom move in the same direction.

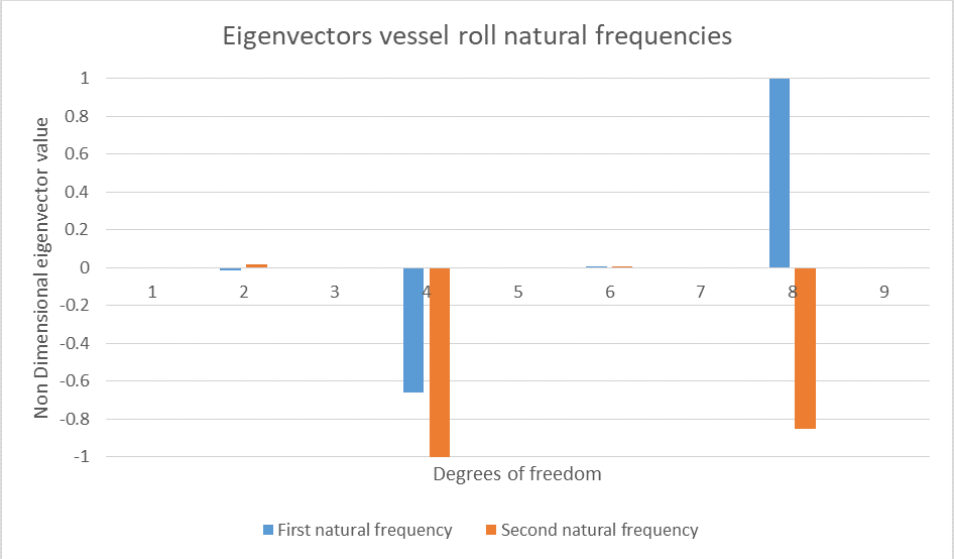

Figure 3.9: Eigenvector values of the two natural frequencies with a large influence on the vessel roll motion that occur in the multi-body model. The first natural frequency occurs around [redacted] and the second natural frequency occurs around [redacted]

In figure 3.10 can also be seen that the vessel surge, sway, pitch and yaw motion show peaks in the responses around [redacted] and [redacted] for the Python model where the cargo is modelled as a pendulum. In figure 3.11 the RAOs of the cargo surge and sway motion are given. In this figure can be seen that the cargo sway motion has strong similarities with the vessel roll motion. This will be further elaborated in chapter 4. In the figure can also be seen that the cargo surge motion has a large response around [redacted] and the cargo sway motion has a large response around [redacted] and [redacted]. All these peaks in the responses can be explained from the coupling between the vessel and cargo motions. When the cargo is modelled as a mass applied to the crane tip there are only six degrees of freedom in the multi-body system. The motions of the cargo itself and the force introduced by these motions are not part of the equation and are thus neglected. When the cargo is modelled as a pendulum the multi-body system will contain out of 12 degrees of freedom. The cargo motions are integrated in the system and new forces are introduced in the multibody system. These forces cause an interaction between the different degrees of freedom. The peak that is found in figures 3.10a and 3.10e follow from the connection between the vessel surge, vessel pitch and cargo surge motion. The peaks in the vessel sway, vessel roll, vessel yaw and cargo sway motion follows from a connection between these degrees of freedom. In appendix C the equations of motion are given. In these equations can be seen that the stiffness of the cargo pendulum introduces a restoring force that couples these degrees of freedom to each other in the multi-body system.

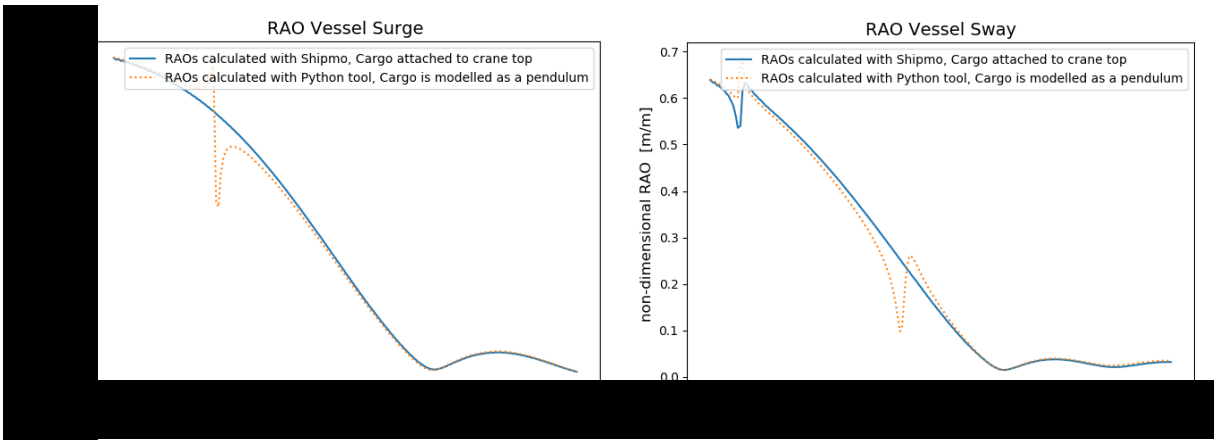

(a) Response Amplitude Operators of the vessel surge motion. A comparison is made between conventional calculations and the 12 degrees of freedom calculation.

(b) Response Amplitude Operators of the vessel sway motion. A comparison is made between conventional calculations and the 12 degrees of freedom calculation.

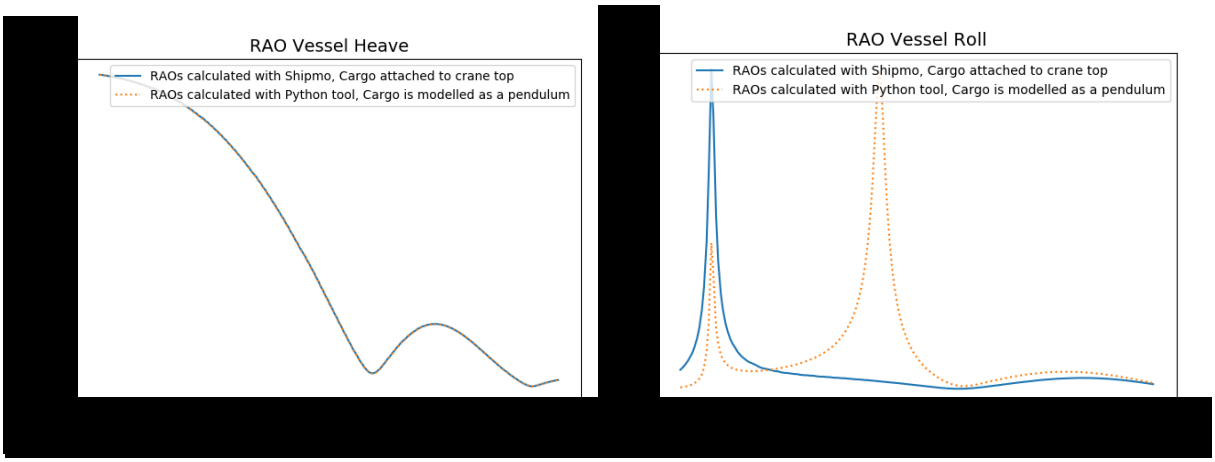

(c) Response Amplitude Operators of the vessel heave motion. A comparison is made between conventional calculations and the 12 degrees of freedom calculation.

(d) Response Amplitude Operators of the vessel roll motion. A comparison is made between conventional calculations and the 12 degrees of freedom calculation.

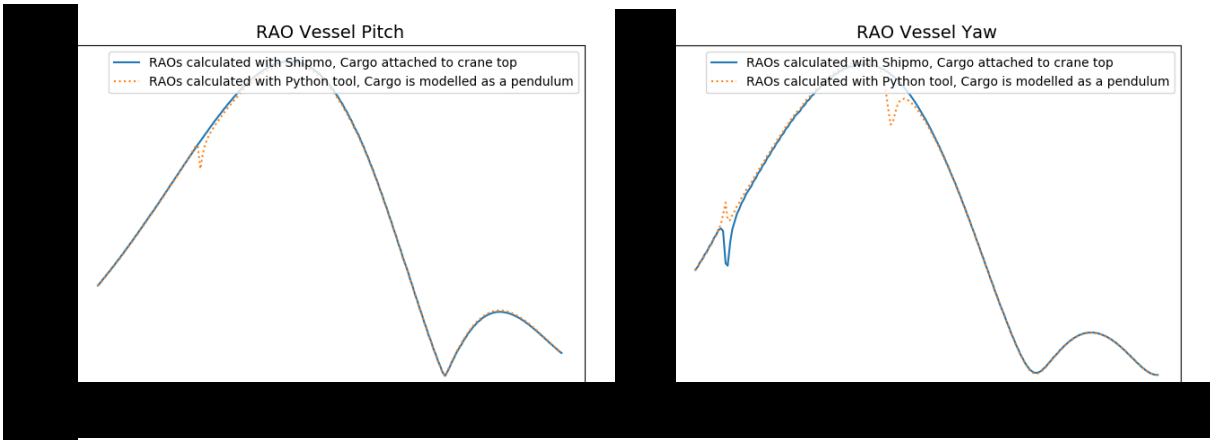

(e) Response Amplitude Operators of the vessel pitch motion. A comparison is made between conventional calculations and the 12 degrees of freedom calculation.

(f) Response Amplitude Operators of the vessel yaw motion. A comparison is made between conventional calculations and the 12 degrees of freedom calculation.

Figure 3.10: Response Amplitude Operators of the vessel six degrees of freedom for a comparison of the connection of the cargo. A comparison is made between the method where the weight of the cargo is attached to the crane top and a method where the cargo is modelled as a pendulum

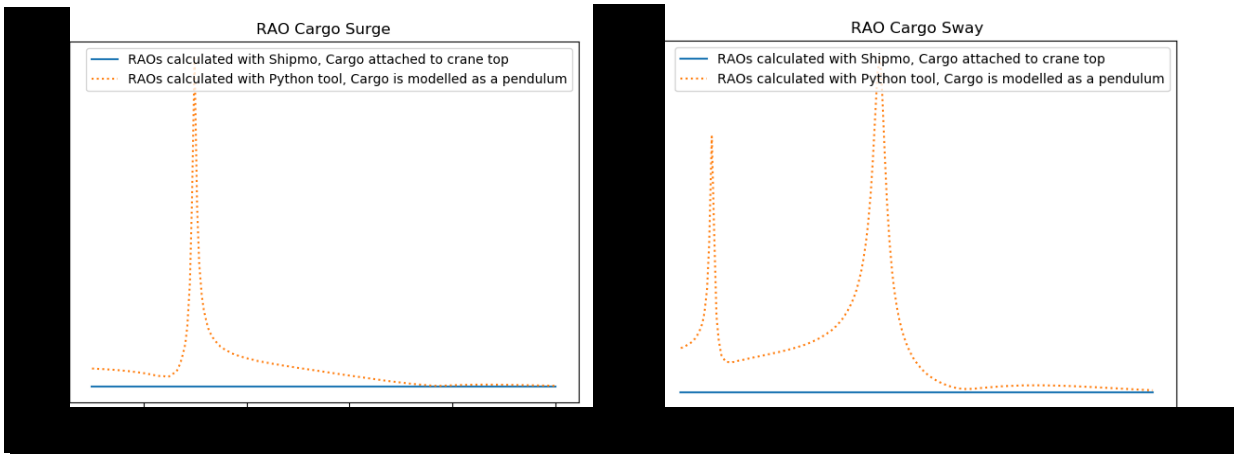

(a) Response Amplitude Operators of the cargo surge motion. A comparison is made between conventional calculations and the 12 degrees of freedom calculation.

(b) Response Amplitude Operators of the cargo sway motion. A comparison is made between conventional calculations and the 12 degrees of freedom calculation.

Figure 3.11: Response Amplitude Operators of the cargo surge and sway motion for a comparison of the connection of the cargo. A comparison is made between the method where the weight of the cargo is attached to the crane top and a method where the cargo is modelled as a pendulum

In section 3.7 is explained that the response spectrum of a motion can be calculated by multiplying the squared motion RAO with the wave spectra. In section 3.10 different wave spectra are plotted in figure 3.16. In figure 3.12 the same JONSWAP spectra are given for a frequency between [redacted] ad/s and [redacted] ad/s. For a JONSWAP spectrum with a period of 12 seconds and a peak enhancement factor of 1.0, the blue line in the figure, the waves in the spectrum have a significant density between [redacted] ad/s and [redacted] rad/s. The peak of the density is at [redacted] rad/s. For a JONSWAP spectrum with a period of 16 seconds and an peak enhancement factor of 1 the waves have a significan density between [redacted] rad/s and [redacted] rad/s. The peak of the density for this wave spectrum is at [redacted] rad/s. First the influence of the wave spectra on the vessel roll motion will be explained while the response spectra of the vessel roll motion requires the most amount of explanation. Thereafter the other response spectra will be explained.

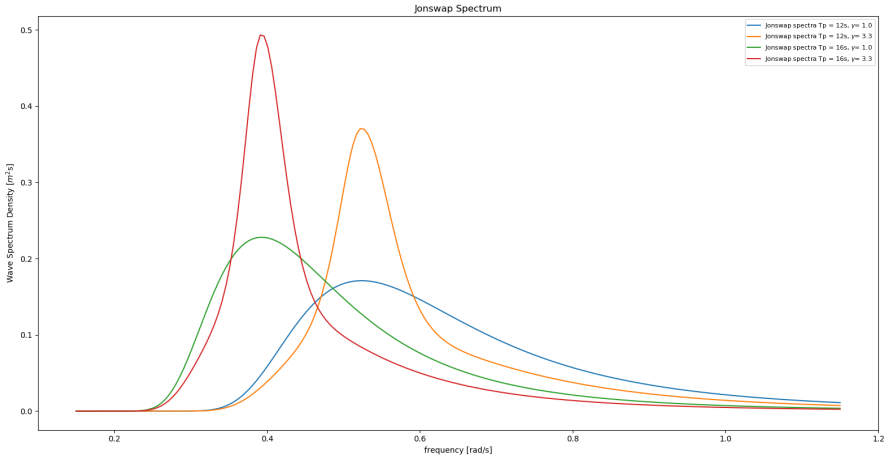

Figure 3.12: JONSWAP spectra for different wave periods and peak enhancement factors. The wave height is equal to 1 meter for all wave spectra.

The vessel roll motion RAO, given in figure 3.10d has large responses beteen [redacted] and [redacted] Both frequencies lie within the two energy density functions of the two different wave spectra. Thus when the responses of the vessel roll motion are calculated for these wave spectra two peaks should be found in the vessel roll response spectrum. The other degrees of freedom of the vessel motion also have responses within the wave spectra and should also show responses. In figure 3.13 the responses of the vessel are given for wave spectra with 12 and 16 second periods. A period of 12 seconds corresponds to a frequency of [redacted] $rrad/s$ and a period of 16 seconds corresponds to a frequency of [redacted] rad/s. The peak enhancement factor of both wave spectra is equal to 1.0. In these figures it is clear that the vessel roll motion show two peaks in its response spectra for both wave spectra. However, the first peak of the response of the vessel roll motion for a JONSWAP spectrum with a period of 12 seconds is ratter small. This is explained by small amount of energy density at the frequency of the first peak. The JONSWAP spectra with a period of 16 seconds has a higher density at the first natural frequency of the vessel roll motion than at the second natural frequency. While the RAO of the vessel roll motion show larger responses at the natural frequency the combination of the larger density of energy at the first natural frequency results in almost evenly large responses for the two peaks for responses on a wave spectra with a period of 16 seconds and a peak enhancement factor of 16 seconds.

The vessel's surge, sway and heave motion RAOs do not show any large peaks. The squared RAOs do Therefore not have extreme values. Therefore the responses of these degrees of freedom look a lot like the energy density function of the JONSWAP spectra for a period of 12 and 16 seconds respectively. The peaks that can be found in the RAOs can also be seen in the vessel response spectra, especially in the vessel surge motion. The vessel's pitch and yaw motion do also not show large values in the RAOs however, the responses of the three translations of the vessel are large for low frequencies and therefore they follow the wave spectra quite accurately. The RAO's of the vessel pitch and yaw motion are low for small frequencies and increases till a frequency of [redacted] after which the RAOs decreases again. These RAO's show larger amplitudes at the frequency at which the JONSWAP spectrum with a period of 12 seconds has the most amount of density. Therefore the Response spectra of the vessel pitch and yaw motion are larger for the JONSWAP spectrum with a period of 12 seconds than the JONSWAP spectrum with a period of 16 seconds.

Although no mathematical equations are done to verify the response spectra of the motions the response spectra behave exactly as is expected from the response spectrum. Therefore the response spectra can be used to calculate the Most Probable Maximum of the degrees of freedom in the multi-body system.

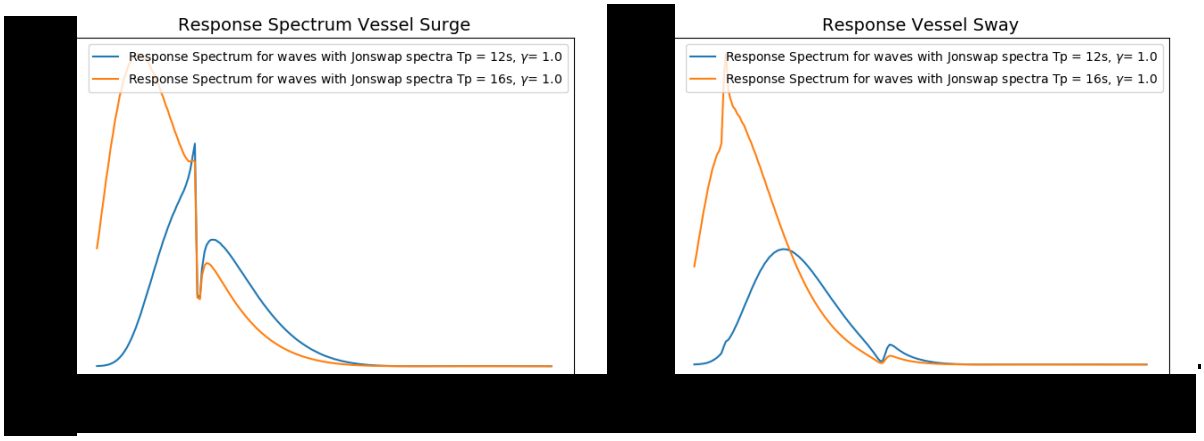

(a) Response spectrum of the vessel surge motion for waves with according to JONSWAP spectra with a period of 12 and 16 seconds and a peak enhancement factor of 1.0.

(b) Response spectrum of the vessel Sway motion for waves with according to JONSWAP spectra with a period of 12 and 16 seconds and a peak enhancement factor of 1.0.

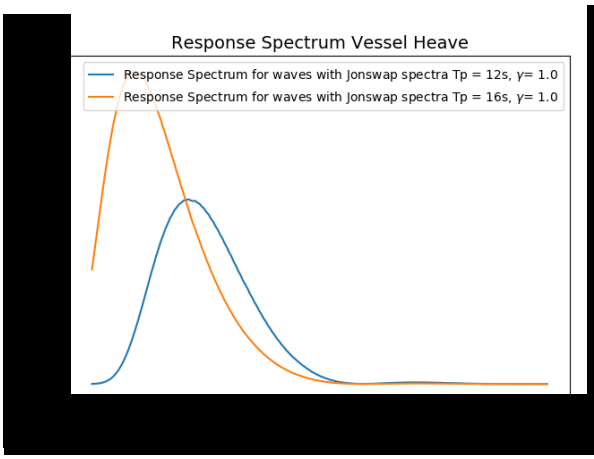

(c) Response spectrum of the vessel Heave motion for waves with according to JONSWAP spectra with a period of 12 and 16 seconds and a peak enhancement factor of 1.0.

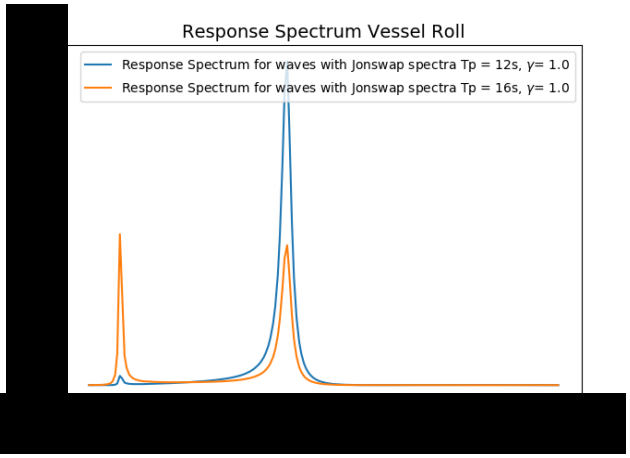

(d) Response spectrum of the vessel Roll motion for waves with according to JONSWAP spectra with a period of 12 and 16 seconds and a peak enhancement factor of 1.0.

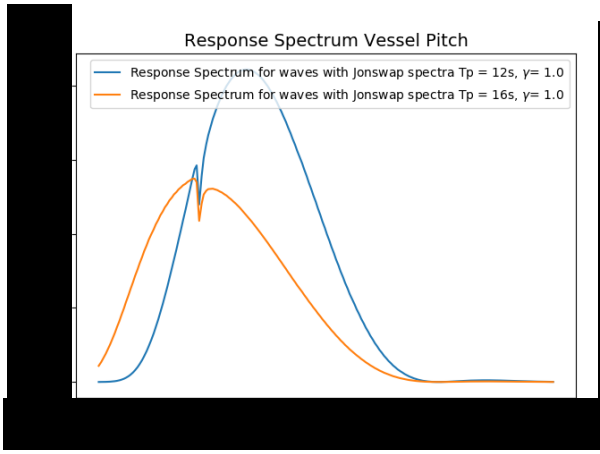

(e) Response spectrum of the vessel Pitch motion for waves with according to JONSWAP spectra with a period of 12 and 16 seconds and a peak enhancement factor of 1.0.

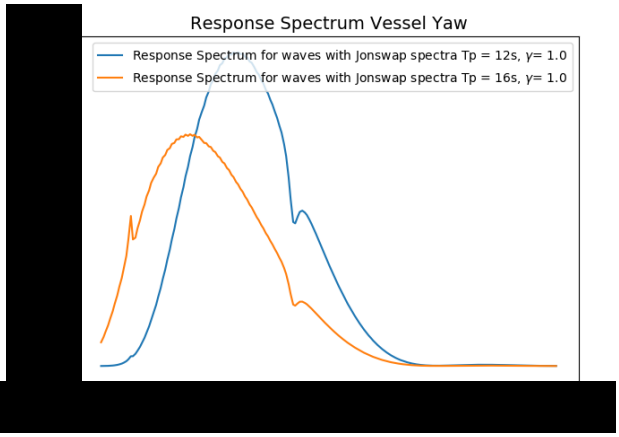

(f) Response spectrum of the vessel Yaw motion for waves with according to JONSWAP spectra with a period of 12 and 16 seconds and a peak enhancement factor of 1.0.

Figure 3.13: Response spectra of the vessel motions. The responses are calculated for waves according to JONSWAP spectra with a period of 12 and 16 seconds and a peak enhancement factor of 1.0.

The most probable maximum calculations can be verified by comparing the most probable maximum calculations for different wave heights. When the RAOs, wave period and peak enhancement factor are constant for both MPM calculations and the wave height is the only variable, the MPM should have the same ratio as the ratio between the different wave heights. When the wave height is doubled the MPM values should also be twice the original value. Table 3.5 shows that the MPM for waves with a spectra with a significant wave height of two meters is exactly twice as large as the MPM for a spectra with a significant wave height of one meter.

Table 3.5: Most probable maximum comparison where the RAOs are constant and the wave height is varied

Motion	Hs = 1 m	Hs = 2
Vessel Surge		
Vessel Sway		
Vessel Heave		
Vessel Roll		
Vessel Pitch		
Vessel Yaw		
Cargo Surge		
Cargo Sway		
Cargo Heave		
Cargo Roll		
Cargo Pitch		
Cargo Yaw		

3.9. Validation

BigLift has the availability of a crane simulator. In this simulator a vessel with its cranes and cargo can be loaded. Since it is a simulator the input variables for wave data can be selected by the user. This can make the simulator a useful tool to validate the Python tool. The simulator runs on the program Dolphin on version 4.1. The simulator itself is not validated therefore the values of the simulator must not be seen as the only truth. Every five years Marin will have the software certified. Last year this is also done by DNV-GL. However, the Dolphin version that got certified was Dolphin 5.3. Strictly speaking the software of the crane simulator is not certified. Since the version of 4.1 and 5.3 are running on the same principles the software of the crane simulator might still be of use to validate the system. Another aspect of the crane simulator that might be troubling is the validation of the vessel behaviour in the similator. The vessels of BigLift in the similator are not validated with model tests. the wave behavior of the vessel is derived from the Froude-Krylov forces in the simulator.

Second order wave motions occur in the simulator. In the python model the frequency domain is used. In this frequency domain second order forces will not be taken into account and therefore the second order motions cannot be calculated. The second order motions from the similator can be filtered with the use of a high-pass filter. Such a filter substracts all the motions with a period above 120 seconds. Manual tests showed that a filter of 120 seconds shows good results in reducing the second order motions. In figure 3.14 the unfiltered responses of the simulator of the cargo sway motion are given. Figure 3.15 the responses of the cargo sway motion that are filtered with a high-pass filter with a cutoff frequency of 120 seconds is given. These figures show that the large second order responses are filltered out and all responses oscillate around zero. The responses are definitely not linear, therefore the wave spectra are introduced in the Python model. However, the responses build-up and after a peak response decrease again. This is part of the resonance of the motions.

Figure 3.14: Unfiltered responses of the Cargo Sway motion in the crane similator. The waves have an angle of 90 degrees relative to the vessel. The significant wave height is 1 meter and the period is 12 seconds.

Figure 3.15: Filtered responses of the Cargo Sway motion in the crane similator. The second order wave forces are filtered a high pass-filter with a cutoff frequency of 120 seconds. The waves have an angle of 90 degrees relative to the vessel. The significant wave height is 1 meter and the period is 12 seconds.

The data retrieved from the simulator can be used to calculate the most probable maximum of the responses in the simulator. These most probable maximum values can be compared to the most probable maximum values of the Python model. First the timestamps of the zero-crossings must be calculated. This can by comparing the signs of the responses between two consecutive timestamps. When the sign changes from negative to positive there is a zero-crossing. The maximum response can than be calculated between all zero-crossings of the responses. The maximum responses between all different zero-crossings can be used to calculate the mean maximum as shown in equation 3.32. In this equation $\bar{x}$ represents the mean maximum value of the responses. N is the amount of zero-crossings and x_i represents the maximum between two zero-crossings. The standard deviation between the different maximums and the mean maximum response can be calculated with equation 3.33. This standard deviation can be used to calculate the most probable maximum of the motions in the simulator as shown in equation 3.34.

$$\bar{x} = \frac{1}{N-1} \cdot \sum_{i=1}^{N-1} x_i \tag{3.32}$$

$$\sigma_{max} = \sqrt{\frac{\sum_{i=1}^{N-1} (x_i - \bar{x})^2}{N-1}} \tag{3.33}$$

$$MPM_{simulator} = \sigma_{max} \cdot \sqrt{2 \cdot \ln(N-1)} \tag{3.34}$$

Table 3.6: Most probable maximum comparison between crane simulator and python tool

Motion	**MPM Simulator**	**MPM Python Tool [Roll amp = 2 deg]**	**MPM Python Tool [Roll amp = 5 deg]**	**MPM Python Tool [Roll amp = 10 deg]**
Vessel Surge				
Vessel Sway				
Vessel Heave				
Vessel Roll				
Vessel Pitch				
Vessel Yaw				
Cargo Surge				
Cargo Sway				
Cargo Heave				
Cargo Roll				
Cargo Pitch				
Cargo Yaw				

In table 3.6 the most probable maximum are given from the vessel and cargo responses in the simulator and the responses calculated by the python tool. The first thing that stands out is the vessel and cargo surge motions of the simulator. In the simulator the vessel surge motion is caused by forces that cannot be calculated by a 2D-strip theory program like Shipmo. Therefore the python tool does not show these motions. Since the cargo surge motion is coupled to the vessel surge motion the cargo surge motion is also larger in the simulator. The second part that stands out is the vessel roll motion. This motion is a lot smaller in the simulator than in the Python tool. Different users of the simulator have stated that the damping in the simulator feels exaggerated. This can explain the relative small roll motions of the vessel in the simulator. Since the vessel roll motion has a large influence on the cargo sway motion the value of this last degree of freedom is also a lot higher for the calculations done with the simulator. Since the cargo roll, pitch and yaw motions are not coupled to the pendulum motions these degrees of freedom will not be excited in the Python tool.

Since the simulator and the python tool both calculate the responses of the multi-body system with other vessel input values the answers of both methods will never equal to each other. However, besides the exceptions made in the previous paragraph, the order size of the results are equal for the two different methods.

3.10. Parameter Influence

The motions that occur due to wave excitation forces can be reduced in multiple ways. In section 2.2 is explained that the wave forces and the motions of the multi-body system have a harmonic behaviour an natural frequency will occur. In section 2.7 is described how the natural frequencies of the multi-body system can be calculated. In section 2.3 till section 3.5 is explained how different constraints are implemented in the Python tool. When the waves during a lifting operation have the same frequency as, or a frequency close to, the natural frequency of one of the motions, the system can start to resonate. Since the multi-body system has different variables, such as vessel draught, vessel metacentric height, cargo mass, crane top position and distance between crane top and cargo CoG the properties of the multi-body system can be varied. The different variables of the multi-body system can influence the different matrices in the multi-body system. When the mass and stiffness aspects of the multi-body system are changed the natural frequency of the multi-body will change.

Figure 3.16 shows the influence of the period and peak enhancement factors on the wave spectra calculated with equation 3.23. The figure shows that different wave periods and peak enhancement factors will influence the wave spectra. Although the wave spectra are calculated for a specified period the energy is distributed over a large range of frequencies. Especially the range of the Pierson-Moskowitz spectra is large. The large range of these spectra can influence the multi-body system even when the natural frequency is shifted. The combination of the vessel RAO and the wave spectrum determine how the multi-body system will respond during certain operational conditions. A different natural frequency or wave spectrum can influence the response spectra and most probable maximum which are described in equations 3.25 and 3.31 respectively.

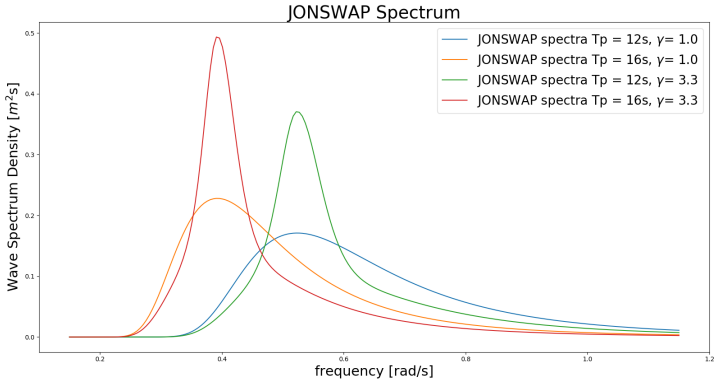

Figure 3.16: JONSWAP spectra for different periods and peak enhancement factors. Hs is equal to 1 meter for all spectra

For every lifting operation the variables in the multi-body will change, as well as the sea state during the lifting operations. Therefore it is important to calculate the natural frequencies of the multi-body system and try to adjust these natural frequencies in order to shift the natural frequencies away from the wave periods

that occur during a lifting operation. When this can be done correctly, the responses of the vessel and cargo motions will be reduced. The Python tool can be used to calculate the influence of the variables on the natural frequency of the multi-body system. In section 5.1 the influences of the variables on the natural frequencies will be calculated and explained. The mathematical and theoretical influence of these variables will be explained in this section.

In chapter 4 calculations will be done to determine the baseline behaviour of BigLift's Shipping vessel Happy Sky. Thereafter variables will be varied in chapter 5 to determine the sensitivity of these variables during lifting operations. In this section the influence of the variables will be described in a mathematical way. In chapter 5 the results of the sensitivity study will be shown.

The variables that are examined on their influence are the vessels draught, vessels metacentric height, cargo mass, crane top X,Y and Z position and the length between crane top and cargo COG. The crane top X,Y and Z positions as well as the length between the crane top and cargo COG will change without further explanation. The cargo mass will change as a percentage of the total weight in the system. This results in no displacement change of the vessel for different cargo masses. In theory the vessel will have more ballast when the cargo has a small weight than when the cargo has a heavy weight. In table 3.7 the variables and their remarks are given.

Table 3.7: Variables changed to study the influence

Variable	**Remarks**
Cargo Mass	The cargo mass will change as a percentage of the overall mass in the system. This results in a constant water displacement of the system, as long as the draught is not changed. When the cargo mass is not varied it is kept constant at 3 % of the total mass in the system.
Vessel draught	When the vessel draught changes the GM stays the same. While the waterline and center of buoyancy change, the center of gravity will change in such a way that the GM will stay the same. When the draught is not varied it is kept constant at a value of 7 meters.
Vessel GM	Changes without further explanation. When the GM is not varied it is kept constant at a value of 3 meters.
Crane top X, Y and Z position	These values will be changed independently from each other. This is done to carefully analyse the influence and interaction of the different rotations. When the crane X and Y positions are not varied they are kept constant at 0 meters. When the crane Z position is not varied it is kept constant at 30 meters.
Crane cable length	The length between the crane top and cargo COG will be varied between 10 and 30 meters. When the crane cable length is not varied it is kept constant at 20 meters.

3.10.1. Cargo Mass

In a simple pendulum the mass should not influence the natural frequency of the system, while the natural frequency is equal to $\sqrt{g/L}$. However, since this system is a coupled system other aspects besides the gravity and sling length have influence on the natural frequency of the pendulum. When the mass of the cargo increases the mass of the vessel decreases while the combined mass of the system has to stay constant. This results in a change in the mass matrix of the vessel. However the displacement has to stay the same while the mass of the cargo influences the displacement of the vessel. Therefore the hydrodynamic database is created for the total displacement of the vessel and the mass matrix is adjusted to the to the mass of the cargo. Since the roll stiffness is related to $GM \cdot \nabla$ and the GM is constant the change in vessel mass should not affect the vessel roll itself. However the coupled motions between the cargo and the vessel extent the original equation of motions as explained in sections 3.3 and 3.6. Since the decreased vessel mass and increased cargo mass should not influence on the uncoupled motions does this not mean that there is no influence at

all. While the matrix components C_{44}, M_{44}, C_{88} and M_{88} from appendix B do change with the same amount as its counterpart the whole 12 degrees of freedom stiffness matrix is more dense than the 12 degrees of freedom mass matrix. This difference in density does influence the natural frequencies of the multi-body system. An increased cargo mass will reduce the overall stiffness values of the vessel roll degree of freedom. Thus increased cargo masses will reduce the natural frequency coupled to the vessel roll motion. The overall stiffness coupled to the pendulum sway motion will increase when the cargo mass increases which results in a higher natural frequency of the natural frequency coupled to the cargo sway motion when the cargo mass is increased. In section 5.1.1 the exact influence of the cargo mass on the natural frequencies in the multi-body system are shown.

3.10.2. Crane Cable Length

The crane cable has a large influence on the restoring stiffness values of the pendulum motions as explained in section 2.3. If the crane cable length increases the restoring stiffness decreases of both the restoring pendulum stiffness and crane cable stiffness. The coupling via the crane cable has influence on almost all the vessel and cargo degrees of freedom. When the restoring pendulum stiffness and crane cable stiffness is reduced the stiffness values of all degrees of freedom will be reduced. While the stiffness values are the numerator in the natural frequency calculations the natural frequencies will reduce when the stiffness values are reduced. The reduction of the stiffness values for all degrees of freedom will result in a reduction of all natural frequencies of the multi-body system.

3.10.3. Crane Top Z Position

The crane top Z position is used in the Python model to translate the rotations of the vessel body in translations of the crane tip. When the crane top Z position is increased the vessel rotations will create larger translation of the crane tip. At the same time are moments created by forces applied to the crane top also increased when the crane top Z position is increased. This results in larger rotational restoring stiffness values due to the crane cable restoring stiffness calculations. The crane top Z position can have a large influence due to these couplings. Dependent on the coupling between the different degrees of freedom the crane top Z position will increase or decrease the natural frequencies when the crane top Z position is increased. In appendix C the complete equations of motion are given. In section 5.1.3 the influence of the crane top Z position is calculated.

3.10.4. Crane Top Y Position

The crane top Y position is, just like the crane top Z position, used in the Python model to translate the rotations of the vessel body in translations of the crane tip. When the position of the crane top is moved away from mid ship the affect of the pendulum restoring stiffness due to rotations increases. However, due to the orientations of different motions, as explained in section 2.2, the stiffness affected by the Y position of the crane top has, in opposite of the crane top Z position, a negative influence on the overall stiffness values of the equation of motion coupled to the vessel roll and cargo sway motion. The crane top Y position couples the vessel roll motion via the pendulum restoring stiffness to the vessel heave, pitch and yaw motions. Introducing new stiffness components between these degrees of freedom will also couple the motions and exitations in these directions. The complete equations of motion are given in appendix C. While the restoring pendulum stiffness is reduced when the Y position moves away from mid ship the value of the natural frequency is reduced. Since a positive and negative translation have the same affect on the stiffness components the natural frequency is reduced with the same value when the Y position of the crane top changes. Since there can be a phase difference between the vessel roll motion and pendulum sway motion the motions can reinforce each other or diminish each other. The phase difference together with the location on the crane top positions can influence the amplitude of the response. In section 5.1.4 the influences of the crane top Y position are calculated.

3.10.5. Crane Top X Position

The crane top X position has a corresponding physical influence as the crane top Y position. Only the degrees of freedom that are influenced by the crane top X position differ. While the sign of the crane top X position are cancelled in the calculation of the pendulum restoring stiffness for the vessel pitch and cargo sway motion a positive or negative sign will not influence the natural frequencies of these degrees of freedom. However,

the amplitude can be influenced by the positive or negative sign due to the phase difference between the vessel pitch and cargo surge motion. The crane top X position does also couple the vessel pitch and vessel yaw motion to the vessel roll motion via the pendulum stiffness matrix. Thus when the crane top X position is not located above the centre of gravity of the vessel an interaction between different degrees of freedoms is introduced.

The vessel hydrodynamical stiffness forces in the vessel roll direction are relatively small in comparison with the hydrodynamical stiffness forces of the vessel pitch motion. Due to these larger stiffness forces the vessel pitch motion has much smaller amplitudes than the vessel roll motions. This can also be seen in figure 3.7. The pendulum restoring stiffness values can have the same order of magnitude as the vessel hydrodynamic roll stiffness values depending on the different variables. Due to this the lifting variables can influence the vessel roll motion a lot. However due to the large hydrodynamic pitch stiffness values the loading variables have a much smaller influence on the vessel pitch motions. Due to the smaller influence the crane top X position is not supposed to create a difference in the pendulum stiffness values large enough to influence the vessel pitch motion. While the vessel pitch motion will not be influenced by the crane top X position the cargo surge motion will have no new noticeable interactions with the other degrees of freedom in terms of stiffness values. This should result in no variation of the cargo surge natural frequency when the crane top X position is varied. However, due to the difference in phases between the different degrees of freedom the crane top X position can enhance or diminish the amplitude of the cargo surge motion. In section 5.1.5 the influence of the crane top X position on the multi-body system are calculated with the Python tool.

3.10.6. Vessel Draught

The vessel draught is a variable that influences the water displacement of the vessel body. A larger displacement will result in larger mass values of the vessel body and larger added mass values of the vessel body. However, since a larger portion of the vessel hull is under water the hydrodynamic stiffness and damping values will also increase since more water has to be displaced when the vessel body is in motion. Since both the mass matrices and the hydrodynamic stiffness matrix are influenced by varying the draught and the influence of the vessel draught on these matrices has to be calculated the relation between vessel draught and vessel motions is not clear. When the mass matrices increase more than the stiffness values the natural frequency will go down. When the hydrodynamic stiffness matrix increases more than the mass matrices the natural frequency will increase.

3.10.7. Vessel Metacentric Height

The metacentric height, or GM, is a variable used to measure the stability of a vessel. In this case the vessel's transverse metacentric height will be varried. The metacenctric height is the distance between the vessel's centre of gravity and the vessel's metacentre. When the vessel undergoes a roll motion the vessel's centre of buoyancy shifts in the vessel's transverse direction. The vessel's metacentre can be determined by drawing a vertical line through the vessel's centre of buoyancy for the upright position and the heeled position. The location where both lines cross is the metacentric height as shown in figure 3.17. The metacentric height is always located directly above the vessel's centre of buoyancy.

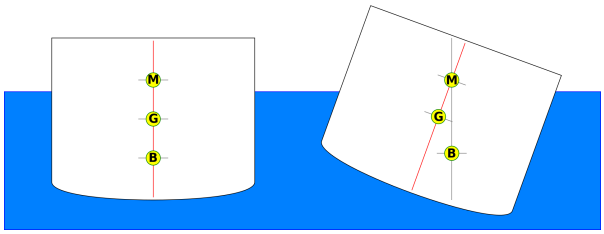

Figure 3.17: schematic of the vessel's metacentric height [39]

A large metacentric height results in a large stability of the vessel. The metacentric height has a large influence on the hydrodynamic stiffness values of the vessel's roll motion. In increased metacentric height results in larger hydrodynamical stiffness values and should Therefore increase the natural frequency of the multi-body motions.

This metacentric height is the metacentric of the vessel without cargo in the crane. Which means that when the cargo mass is applied in the crane top the GM will go down as in simple 6 degrees of freedom RAO calculations. In the Python tool the cargo is not implemented as a weight in the crane top but as a moving body. This moving body has an influence on the multi-body system. To get accurate results of the vessel and cargo motions the vessel's metacentric height without cargo must used in the calculations. Otherwise the influence of the cargo on the vessel's stability will be used twice.

4
Baseline Calculations

The model that is created for this research and explained in chapter 3 can be used to calculate the influence of different variables on the motions of both the vessel and the cargo. The model is modular and different constraints and connections can be integrated or neglected in the calculations. The basic multi-body model, which includes the vessel hydrodynamic database and cargo pendulum interaction is used to calculate the influence of different variables on the motions of the whole system. The influence of mooring lines can be added to the system to study the effect of this connection on the vessel and cargo motions. Cargo control systems can also be added to the main model which makes it possible to calculate the influence of such systems. However, before all these influences can be studied baseline values must be determined. In this chapter the baseline parameters and baseline responses will be explained and calculated. First the vessel dimensions will be explained in section 4.1. next the chosen wave direction of this study will be described in section 4.2. Thereafter the natural frequencies and eigenvectors of the baseline case are studied in section 4.3. Lastly the behaviour of the vessel with the baseline parameters will be explained with RAOs, response spectra, phases and most probable maxima values.

4.1. Baseline Case

In the study done to calculate the responses of the vessel and cargo the BigLift shipping vessel Happy Sky is used. In figure 4.1 a side view and top view drawing of the Happy Sky is shown. The Happy Sky has a length overall of 154.8 meters. The moulded breadth is equal to 26.5 meters and the summer draught is 9.5 meters. The main deck is located 13.4 meters above the keel.

Figure 4.1: Side view and top view drawing of the BigLift Shipping vessel Happy Sky

The Happy Sky is outfitted with two heavy lifting cranes. Each crane has a maximum capacity of 900 mton. The cranes have a maximum lifting height of 38.5 meters above the main deck and the radius of the crane is equal to 35.5 meters. The crane curves of the Happy Sky are shown in figure 4.2

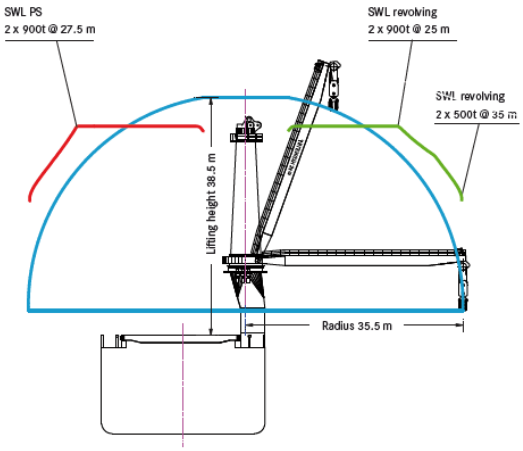

Figure 4.2: Crane curves of the BigLift Shipping vessel Happy Sky

For a clear overview the baseline variables are given in table 4.1. The variables used in the baseline calculations will now be discussed. First the origin of the coordinate system will be elaborated. The origin of the multibody system is the vessel's centre of gravity. The centre of gravity is calculated by Shipmo. While the metacentric height is an input value of Shipmo as well as the draught and hullform the CoG corresponding to the GM can be calculated. The vessel rotational degrees of freedom will rotate around the centre of gravity. The centre of gravity is the most practical location of the origin while all rotational forces are related to the distance to the centre of gravity and the location of the point of application does not require any translation calculations. Shipmo calculated the centre of gravity for the baseline calculations at 74.3 meters from the after perpendicular, 0 meters from the centre line and 9.7 meters from the keel. This means that the deck is located 3.7 meters above the centre of gravity of the vessel. Although the vessel's centre of gravity is the origin the cargo motions are relative to the cargo centre of gravity. In this way all degrees of freedom are plotted relative to earth coordinate system.

The baseline vessel draught is equal to 7 meters. This draught is a normal draught during lifting operations. Some ports do have a draught restriction but 7 meter is a draught that is accessible most of the time. The basic vessel GM in these calculations is 3 meters. This value seems to be large for default GM values but this is the GM value without any cargo attached to the crane as explained in section 3.2. When the cargo is attached in a conventional way the GM will go down drastically depending on the mass of the cargo and the location of the crane top. The crane top X an Y position will have a default value of 0 meters. This means that the cargo is lifted above the centre of gravity of the vessel. This is the most neutral place on the vessel. The crane top Z position has a baseline value of 30 meters. This height is an average height of the crane. The sling length baseline value is equal to 20 meters. While the distance between the origin and the main deck is equal to 3.7 meters the cargo centre of gravity is located 6.3 meters above the deck. 6.3 meters seems like a large distance. However, extremely large cargoes can have their centre of gravity 6.3 meters or more above the bottom of the cargo. In the baseline case it is assumed that there is enough clearance between the vessel and the cargo but in detailed operational calculations the clearance must be taken into account. A sling length of 20 meters is a length where the cargo motions have a significant influence due to the restoring stiffness of the crane. The baseline value for the cargo mass is equal to 3 % of the total weight in the system. This is not the maximum weight the vessel can lift with one crane but it still is a significant weight. The weight is depending on the vessel draught. With a draught of 7 meter the weight is approximately 650 mton. Mooring lines will not be included in the baseline behaviour and sensitivity study. In section 5.2 the influence of mooring lines is calculated and explained. With all these variables the RAO calculations as described in section 3.6 can be performed. The results of the baseline calculations will be discussed in section 4.4.

Table 4.1: Values of the variables used in the baseline case.

Variable	Value
Vessel Draught	7 meters
Vessel GMt	3 meters
Crane Top Z position	30 meters
Crane Top X position	0 meters
Crane Top Y position	0 meters
Crane cable length	20 meters
Cargo Weight	3 %

4.2. Wave Direction

As explained in section 3.6 the responses of the multi-body system are calculated from the excitation forces and the dynamical model of the multi-body system. The program Shipmo is used to calculate the vessel hydrodynamics and the wave excitation forces. These excitation forces are dependent on the wave direction, vessel speed and hull form. The hull form will stay constant in all calculations. The wave direction is the direction of the waves in comparison with the vessel heading. Since the vessel speed is assumed to be equal to zero, as explained in section 2.2, the encounter direction of the waves will be equal to the wave direction. The encounter direction is the direction from which the waves apply forces to the vessel. During lifting operations the vessel will have no speed. The relative speed to the water due to current will be neglected. Since this thesis focuses on the vessel behaviour and not on the waves behaviour the influence of current are not taken into account. Thus the hull form and vessel speed will not change in the sensitivity calculations. However, the wave direction is a variable that can change. In appendix D RAOs for all degrees of freedom for three different wave directions are given. In figure 4.3 the RAOs for the vessel roll and cargo sway motion are given. The first wave direction is equal to 90 degrees. These waves, called beam seas, travel in perpendicular direction of the vessel direction. The second RAO that is given are waves with an angle of 45 degrees. The last RAO that is given are waves with a direction of 0 degrees. These waves encounter the vessel at the stern. The vessel roll motion and cargo sway motion are the two degrees of freedom that are influenced the most due to wave excitation forces. Both degrees of freedom influence each other which explains the large responses. The complete equation of motion is given in appendix C. The equation of motion explain the full relation between vessel roll and cargo sway motions. Since these two degrees of freedom show the largest responses the RAOs are given in figure 4.3. Due to the same reason these two degree will be the focus of the sensitivity study and damping study. In the RAOs can be seen that the waves with an angle of 90 degrees create the largest responses. Especially the second natural frequency of the cargo sway motion that can be seen in the figures is extremely large for waves with an angle of 90 degrees.

In figure 4.4 the vessel pitch and cargo surge motion RAOs are given. The cargo surge motion only has one natural frequency within [redacted] ad/s and [redacted] rad/s. This natural frequency has a small frequency on the vessel's pitch motion but the interaction is not as extreme as the interaction between the vessel roll and cargo sway motion. The length of the vessel causes a large longitudinal metacentric height. Due to this long longitudinal metacentric height the vessel pitch degree of freedom generates a lot of restoring forces due to the hydrodynamic properties. Therefore the vessel pitch motion will not show large responses as the vessel roll motion. An interesting phenomenon in figure 4.4b are the larger responses at the natural frequency for waves with an incoming angle of 45 degrees than the for waves with an incoming wave angle of 90 degrees. These large responses can be explained from the larger responses of the vessel surge and pitch motion at this frequency. The vessel surge and pitch motion are coupled to the cargo surge motion. At the natural frequency the responses of these vessel motions are larger which results in a larger response on the cargo surge motion.

The largest influence on the cargo surge and cargo sway motion is the pendulum restoring forces. Due to these restoring forces a mathematical coupling between the vessel and cargo is created. While the restoring stiffness originates from the same variables for both degrees of freedom the influence of different lifting configurations and cargo control systems should be proportional. While the cargo sway motion is more complex due to the strong connection with the vessel roll motion the vessel roll and cargo sway motion will be the main focus of the sensitivity and cargo control systems study. The restoring stiffness in cargo surge direction has the same order size as the restoring stiffness in the cargo sway motion direction. However, the hydrodynamic stiffness in the vessel pitch direction is a lot larger than the hydrodynamic stiffness in the vessel roll direction. Therefore the influence of the cargo surge motion on the vessel pitch motion is a lot smaller than

the influence of the cargo sway motion on the vessel roll motion. In the RAOs shown in figure 4.3 can be seen that the waves with an angle of 90 degrees create the largest responses for the vessel roll and cargo sway motion. Therefore an wave angle of 90 degrees will be used to calculate the influence

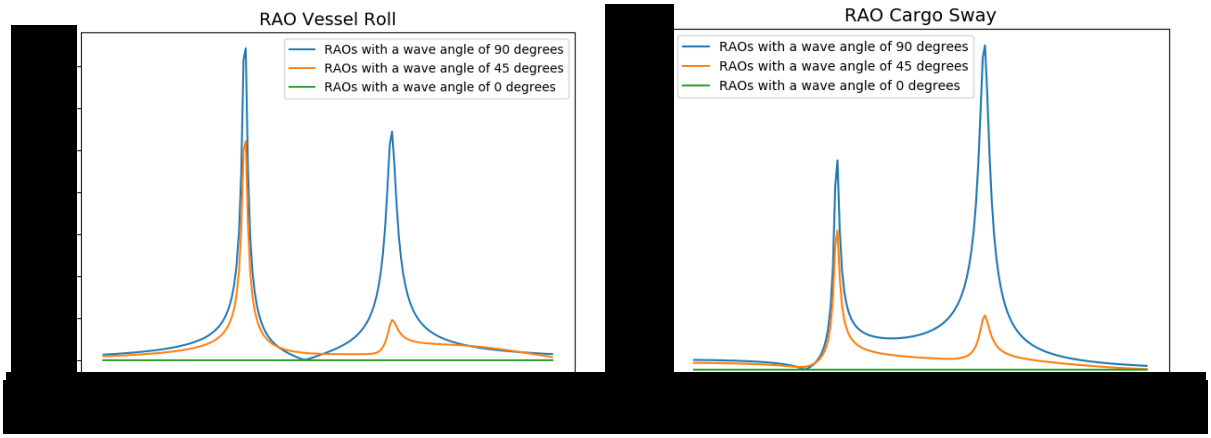

(a) Vessel roll motion RAO for different wave directions

(b) Cargo sway motion RAO for different wave directions

Figure 4.3: Influence of different wave angles on the vessel roll motion and cargo sway motion RAO

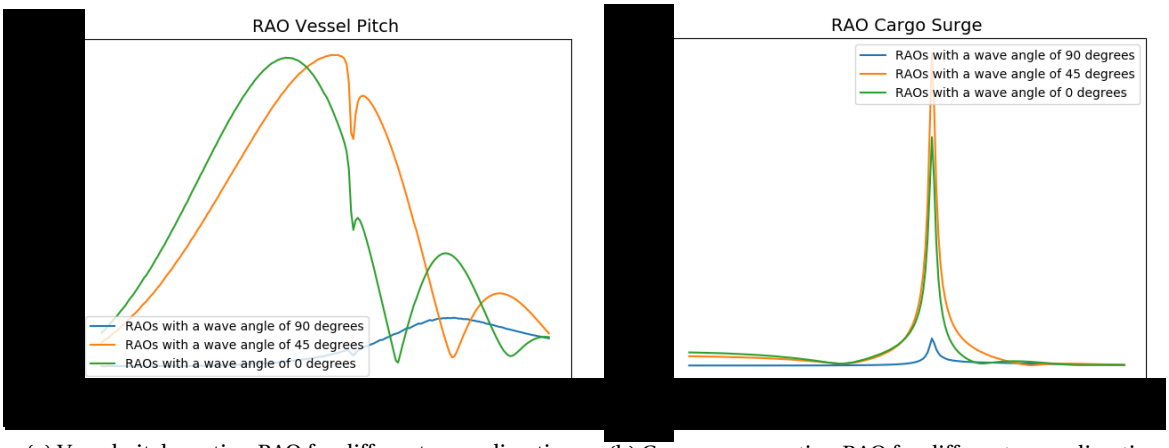

(a) Vessel pitch motion RAO for different wave directions

(b) Cargo surge motion RAO for different wave directions

Figure 4.4: Influence of different wave angles on the vessel pitch motion and cargo surge motion RAO

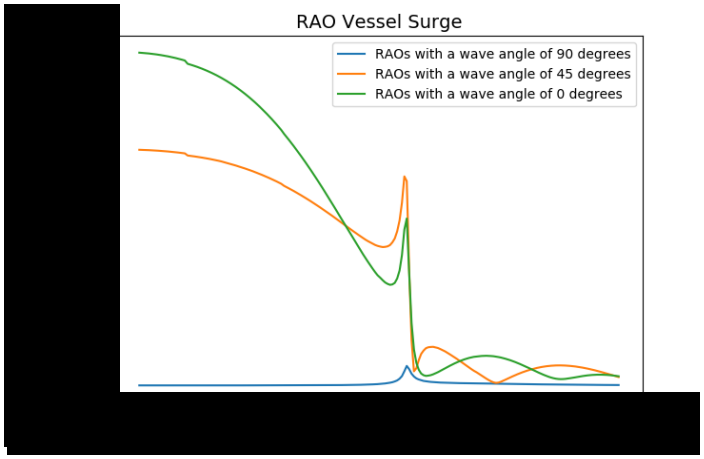

Figure 4.5: Influence of different wave angles on the vessel surge motion RAO.

4.3. Natural Frequencies and Eigenvectors

In the previous sections is explained what the baseline variables are and which wave direction will be focused on during the study. In chapter 2 is explained that the eigenvectors can be used to calculate the ratio of response between different degrees of freedom at the different natural frequencies in the system. The eigenvectors can also tell if any relation between the different degrees of freedom is missed in the previous section. Therefore the natural frequencies and eigenvectors will be calculated.

In table 4.2 the natural frequencies of the multi-body system with the baseline variables are given. The first natural frequency is fairly high and will not be excited by the waves encountered during lifting operations. Natural frequencies 7, 8 and 9 are so low that they will also not excitate the vessel during lifting operations. This leaves the second till the sixth natural frequency in a frequency range that can occur during lifting operations.

Table 4.2: Natural frequencies of the baseline multi-body system

Natural frequency	Frequency [rad/s]
1	
2	
3	
4	
5	
6	
7	-06
8	-08
9	-08

In figure 4.6 the eigenvectors of the natural frequencies 2 till 6 are plotted. The values of these eigenvectors are non-dimensional since they give a relation between the responses of different degree of freedom in the multi-body system. However, it is important to notice that there is a difference between translations and rotations. Degree of freedom 1 til 3 and 7 till 9 give the translations. Thus these values are coupled to a translation in a certain unit length. Degree of freedom 4 till 6 and 10 till 12 are angular responses. Thus these values are coupled to an angular motion. While the crane wire is assumed to be connected to the cargo centre of gravity no rotations are introduced to the cargo body in the baseline calculations. Therefore no rotations are plotted in figure 4.6. The translations and rotations are coupled in such a way that the scale on the axis for a translation of one metre is equal to a rotation of 1 degree on the same scale.

Natural frequency number 2 and 6 correspond to the large responses seen in the vessel roll and cargo sway motions in figure 4.3. The eigenvectors do also show that the other degrees of freedom have little interaction with these two natural frequencies. Natural frequency number 3 corresponds to the large responses in the cargo surge motion in figure 4.4b. This eigenvector does also show that there is little interaction between the cargo surge motion and the other degrees of freedom at this natural frequency. The two remaining natural frequencies within the operational wave frequency range are natural frequency number 4 and 5. The eigenvectors of these natural frequency show that these two natural frequencies excitate the vessel heave, vessel pitch, cargo surge and cargo heave motion. However, these natural frequencies do not have the same order of amplitudes as the other natural frequencies shown in figures 4.3 till 4.5. These two RAOs seem to correspond to the natural frequency of the vessel pitch motion. Even though the amplitude of the vessel pitch motion RAO is quite broad the amplitude of the vessel pitch motion RAO is relative small. Because of this the influence of the vessel pitch motion on the other degrees of freedom is also relatively small and no large peaks can be found at the 4th and 5th natural frequency. The eigenvectors do show that the cargo surge motion has a certain amount of coupling with the vessel pitch and vessel heave motion. However the coupling is a lot smaller for these degrees of freedom than the coupling between the vessel roll and cargo sway motion. While the responses on the 4th and 5th natural frequency are quite small in comparison with the other natural frequencies the study can be performed on the vessel roll and cargo sway motion.

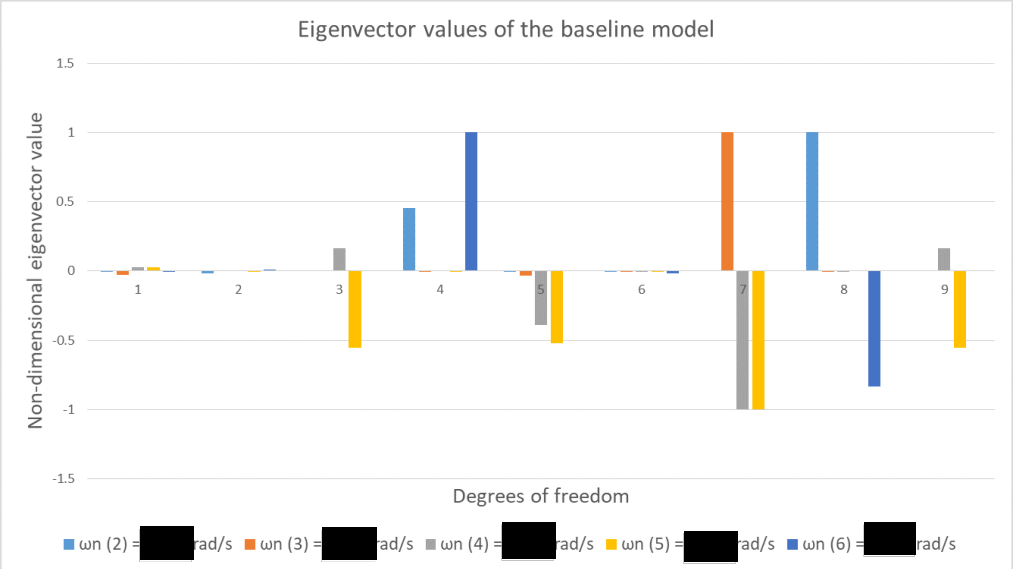

Figure 4.6: Eigenvectors of natural frequencies 2 till 6 of the baseline model

4.4. Baseline Behaviour

In this section the baseline behaviour in terms of RAOs and significant motions will be described. In figure 4.7 the RAO of the vessel roll motion is plotted. In this figure the RAO is plotted for a frequency range between [redacted] and [redacted] rad/s. As explained in section 2.2 a fairly big stepsize is the result of such a large frequency range. Therefore the RAO is plotted in figure 4.8 with a smaller frequency range. This results in a more detaild RAO graph. In figure 4.7 the peaks are angular and sharp while the peaks in figure 4.8 are more smooth. In figure 4.7 it is clear that the two dominating frequencies for the roll motion can be found around [redacted] rad/s and [redacted] rad/s. This corresponds to the natural frequencies calculated in the previous section. When a closer look is taken at the height of these resonance peaks in the different figures it becomes clear that there is also a difference in the maximum response. The RAO value at the natural frequency of [redacted] rad/s in figure 4.7 is close to [redacted] deg/m while the same RAO has a value close to [redacted] deg/m in figure 4.8a. At the second natural frequency of [redacted] rad/s the value of the RAO is equal to [redacted] deg/m in figure 4.7 while figure 4.8b shows also a value of [redacted] deg/m. The difference at the first natural frequency is caused by the stepsize of the wave frequencies. The exact value of the natural frequency lies in between two steps used to plot figure 4.7. The smaller stepsize in the detailed calculations make it possible to calculate a more exact value. The second natural frequency is close to a step of the wave frequency used in figure 4.7. As a result the value of the RAO amplitude is quite accurate. The inaccuracy at the first natural frequency shows that detailed calculations with small stepsizes are important. Therefore the responses will be calculated for a range between [redacted] and [redacted] rad/s. Detailed graphs with smaller ranges will be created to show the RAOs of multi-body system.

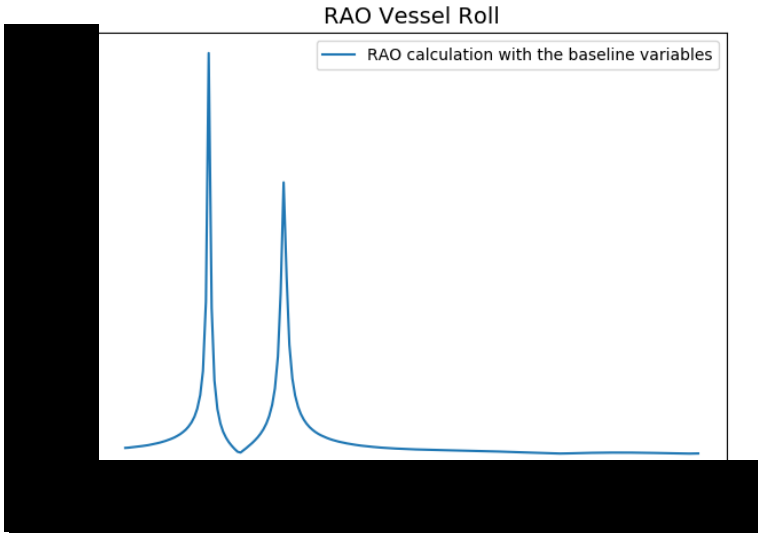

Figure 4.7: RAO of the vessel roll motion with the baseline variable values

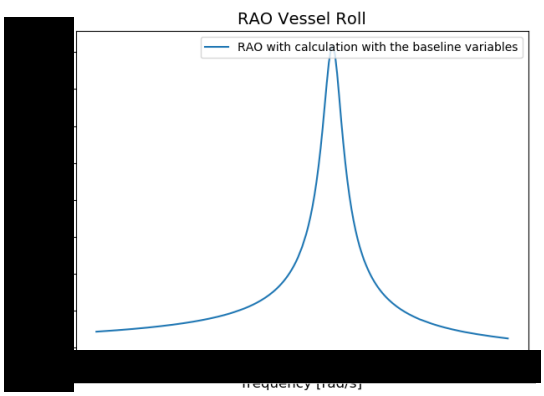

(a) Vessel roll motion RAO for a frequency between [redacted] and 0.55[redacted] /s

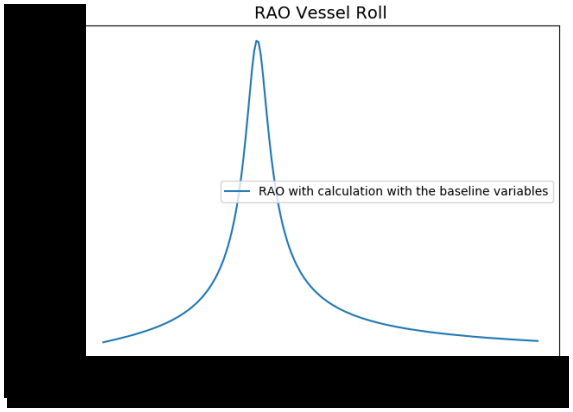

(b) Vessel roll motion RAO for a frequency between [redacted] and [redacted] rad/s

Figure 4.8: A detailed vessel roll motion RAO for frequencies between [redacted] and [redacted] rad/s and between [redacted] and [redacted] rad/s

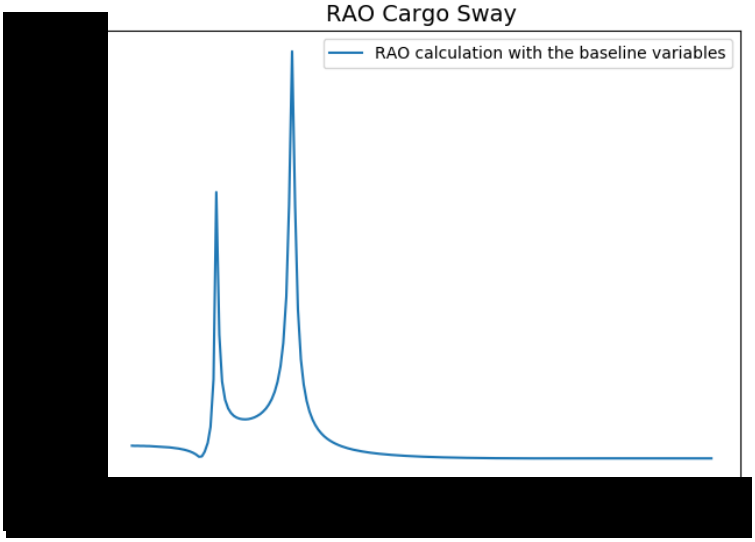

Figure 4.9: RAO of the cargo sway motion with the baseline variable values

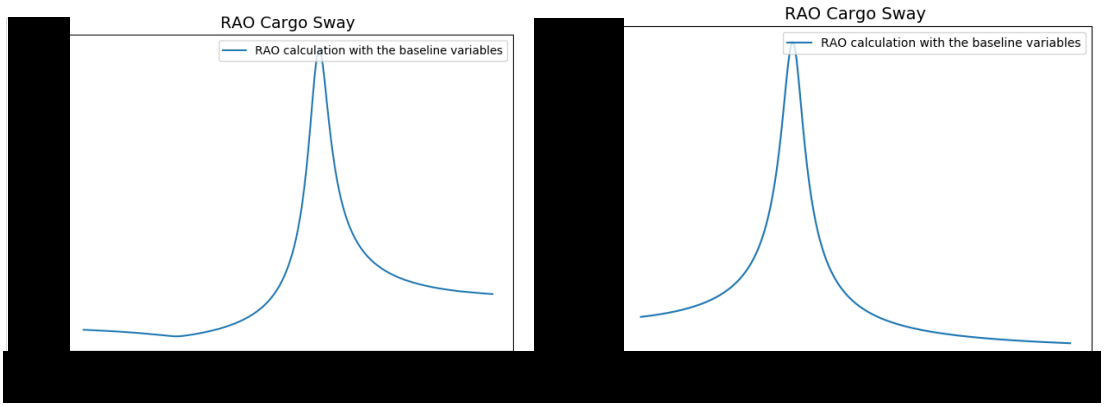

(a) Cargo sway motion RAO for a frequency between [redacted] and [redacted] rad/s

(b) Cargo sway motion RAO for a frequency between [redacted] and [redacted] rad/s

Figure 4.10: A detailed cargo sway motion RAO for frequencies between [redacted] and [redacted] rad/s and between [redacted] and [redacted] rad/s

The phases of the different degree of freedom can explain more about the natural frequencies and to which motions these natural frequencies are coupled. In section 2.6 is explained that the stiffness values, and thus the restoring force, coupled to a degree of freedom are the biggest influence on a motion when the driving frequency is smaller than the natural frequency. At the same time will the inertia forces influence the motions of a degree of freedom the most when the driving frequency is larger than the resonance frequency. The restoring forces are coupled to the displacement of a body and the inertia forces are related to the accelerations of a body. Equations 2.7 and 2.9 show that the translation and accelerations act in opposite directions in harmonic oscillations. Due to these directions of the translations and accelerations the phase of a motion will change around the natural frequencies. The phases of the vessel roll motion and cargo sway motion are given in figure 4.11. In these figures the phases the motions themselves are given. The motions, and thus their phases, are a result of the a multiplication of the squared combined ship system with the excitation force. In section 3.2 is explained that the waves exert forces on the vessel. While the waves exert forces on all six degrees of freedom the phases of the wave forces can not be deducted from the vessel and cargo responses. In figure 4.12 the phases of the wave excitation force in the vessel sway and vessel roll direction are given. These figures show that the wave forces in different directions change in a different way over a range of frequencies.

In figure 4.11 can be seen that the phases of the vessel roll motion change drastically around [redacted] rad/s, thus around the first natural frequency. The phase of the cargo sway motion does also change at the first natural frequency at [redacted] rad/s. At the second natural frequency, at [redacted] rad/s, the phase of the vessel roll motion and the cargo sway motions changes drastically again. These changes in the phase confirm that the natural frequency calculations are done correctly since the phases should change around the natural frequency as explained in section 2.6. However, big changes in the phase of a motion is not limited to the frequency. At a driving frequency of [redacted] rad/s the phase of the cargo sway motion changes while the phase of the vessel roll motion does not change. This change can be explained by the anti-resonance that occurs around this frequency for the cargo sway motion. In figure 4.9 and figure 4.10a a small dip in the response can be seen at this frequency. This indicates that anti-resonance occurs as explained in section 2.6. For driving frequencies below [redacted] rad/s the phase of the vessel roll and cargo sway motion are close to equal. This indicates that the both degree of freedom move in the same direction. The anti resonance that occurs at [redacted] rad/s causes a change in the phase of the cargo sway motion. Which results in a motion in an opposite direction of the vessel roll motion. At the first natural frequency both degree of freedom change their face with the same value. This keeps the different in direction of the motion. At [redacted] rad/s anti resonance occurs in the vessel roll motion. This can also be seen in figure 4.7. Due to this change in phase after the anti resonance the vessel roll motion and cargo sway motion have the same phase again at the second natural frequency. This causes the two degrees of freedom to move in the same direction.

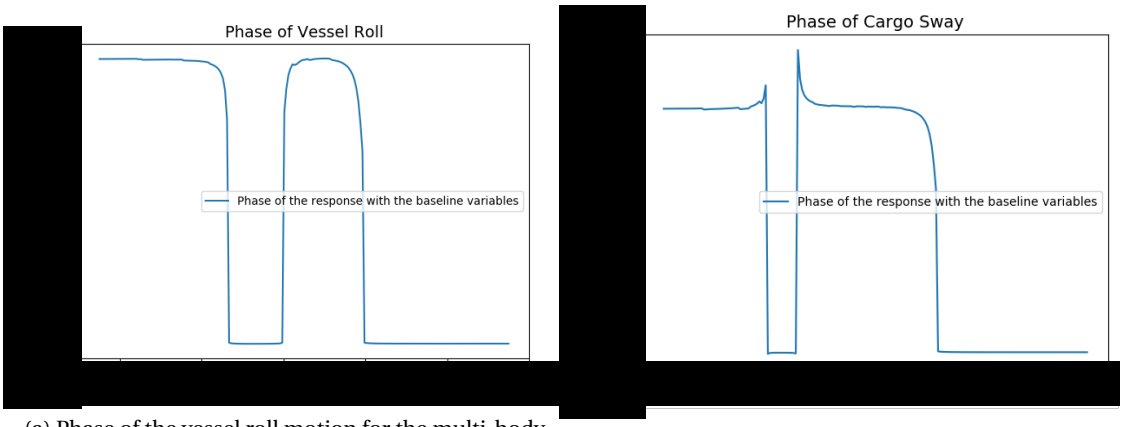

(a) Phase of the vessel roll motion for the multi-body model with baseline variables

(b) Phase of the cargo sway motion for the multi-body model with baseline variables

Figure 4.11: Phase of the vessel roll and cargo sway motion for the different frequencies within the range in which the RAOs are calculated. The Phases are calculated for the responses of the multi-body model with the baseline variables

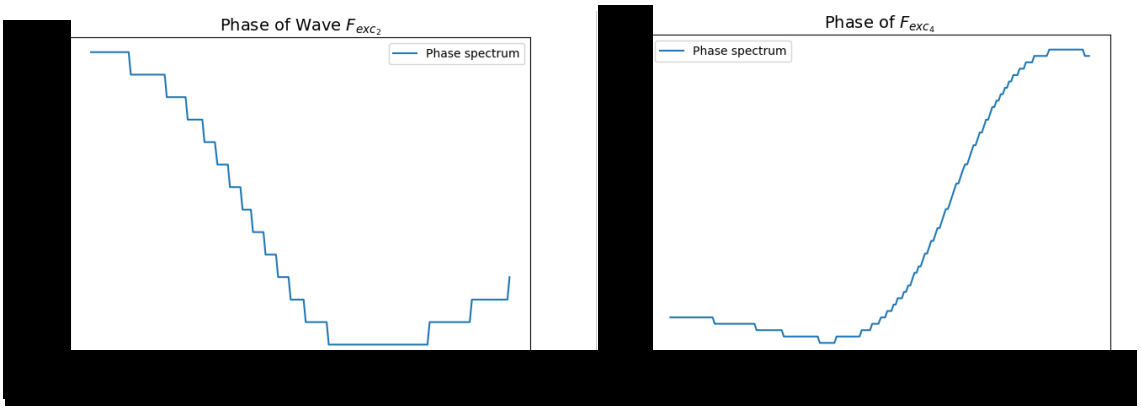

(a) Phase of the wave excitation force in vessel sway direction

(b) Phase of the wave excitation force in vessel roll direction

Figure 4.12: Phase of the wave excitation force in vessel the vessel sway and vessel roll direction.

The RAOs given in figures 4.7 till 4.10 can show great insight in the behaviour of the vessel. However, during lifting operations the waves can vary. As stated in the problem statement swell waves causes a lot of problems for BigLift Shipping. The response spectra can be used to study how the multi-body system will respond in a certain wave spectrum. Swell waves are waves with a period between the 12 and 16 seconds. In figure 4.13 The different wave spectra are plotted. A JONSWAP spectrum with a peak enhancement factor of 1 is equal to a Pierson-Moskowitz spectrum. Such a spectrum can be used to generate a approximation of a swell spectrum. In figure 4.14 the response spectra of the vessel roll and cargo sway motion are drawn for different swell periods. In these figures can be seen that the higher the wave period the less influence the natural frequency of [redacted] rad/s has. A frequency of [redacted] rad/s corresponds to a period of [redacted] seconds. Therefore it is easy to assume that the swell period of 14 seconds causes the largest response in the response spectrum. However, since the wave spectra with a period of 16 seconds has a high energy density the response spectrum related to this wave spectrum is also large. However the response around the second natural frequency is a lot smaller for the wave spectra with a higher period.

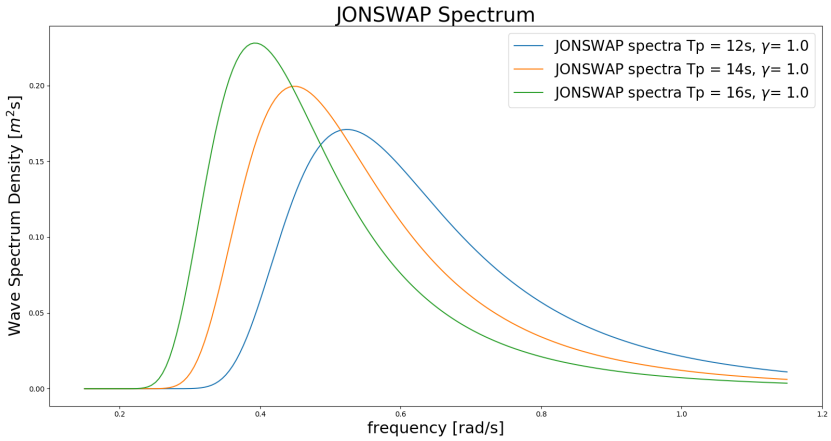

Figure 4.13: JONSWAP spectra for different wave periods. The wave periods are varied between 12 and 16 seconds. The wave height is set to 1 meter and the peak enhancement factor is equal to 1.

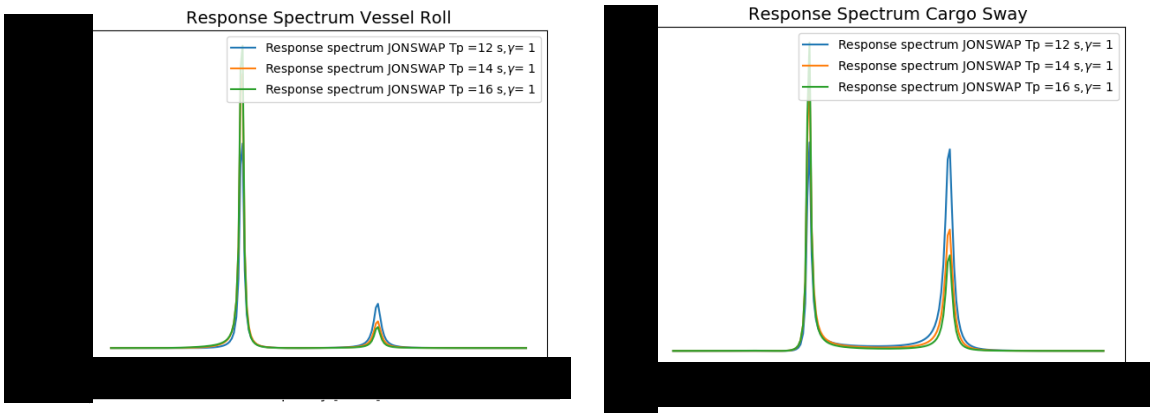

(a) Response spectrum of the vessel roll motion for the multi-body model with baseline variables

(b) Response spectrum of the cargo sway motion for the multi-body model with baseline variables

Figure 4.14: Response spectra of the vessel roll and cargo sway motion for waves with a period of 12, 14 and 16 seconds. The Phases are calculated for the responses of the multi-body model with the baseline variables

In table 4.3 the most probable maximum are given for the different swell spectra. The wave height of the swell spectra is taken equal to 1 meter. This makes the MPM values a MPM per meter wave height. The response figures showed that the response spectra for waves with a period of 14 and 16 seconds showed large responses. Due to the high responses of the vessel roll motion around the first natural frequency the MPM of the vessel roll motion is slightly larger for waves with a period of 16 seconds than for waves with a period of 14 seconds. While the cargo sway motion shows larger responses than the vessel roll motions around the natural frequency of [redacted] rad/s the response of the cargo sway motion around this frequency has a larger influence on the cargo sway motion MPM than the response of the vessel roll motion on the roll motion MPM. Due to this large influence of the response around the second natural frequency the MPM is the largest for waves with a period of 12 seconds.

Table 4.3: MPM values of the vessel roll and cargo sway motion for baseline variables. The wave height is taken equal to 1 meter.

Configuration	MPM Tp = 12		MPM Tp = 14		MPM Tp = 16	
	Vessel Roll [deg]	Cargo Sway [m]	Vessel Roll [deg]	Cargo Sway [m]	Vessel Roll [deg]	Cargo Sway [m]
Baseline variables	[redacted]	[redacted]	[redacted]	[redacted]	[redacted]	[redacted]

5
Sensitivity of lifting variables

The multi-body model is created and the baseline behaviour of the vessel and cargo is studied. The first step in reducing the responses of the multi-body model is studying the influence of the different variables during a lifting operation. In section 5.1 different variables of the multi-body system will be changed and their influence on the multi-body system will be studied. While the variables will have influence on the different mass and stiffness values in the multi-body system the variables will influence the natural frequencies in the multi-body system. The rate of change of the natural frequencies can show how much influence a variable has on the responses of the multi-body system. In section 5.2 the influences of mooring lines on the multi-body system will be worked out.

5.1. Influences of Lifting Variables

The variables that are examined on their influence are the vessels draught, vessels metacentric height, cargo mass, crane top X, Y and Z position and the length between crane top and cargo centre of gravity. For every variable a minimum of 5 different values will be used and only one variable will be changed per calculation. For every variation the natural frequency and resonance peak of vessel roll and cargo motions will written down. When the displacement is changed it is assumed that the GM will stay the same. This means that theoretically the values of KB, BM and KG will change in such a way that the GM value will be equal for different draughts. As said the GM and displacement will have 5 different values. This means that at first 5 different Shipmo hydrodynamic database files must be created for each of these two variables. With these databases the natural frequencies of the 12 degrees of freedom system be calculated. These results will be used to calculate the range of frequencies for the roll and pendulum motions. When the frequency range of interest is determined RAO databases with small frequencies steps can be made and used to create accurate natural frequency calculations. The crane top X, Y and Z positions as well as the length between the crane top and cargo COG will change without further explanation. The cargo mass will change as a percentage of the total weight in the system. This results in no displacement change of the vessel for different cargo masses. In theory the vessel will have more ballast when the cargo has a small weight than when the cargo has a heavy weight. In table 5.1 the variables and their remarks are given.

Table 5.1: Variables changed to study the influence

Variable	Remarks
Vessel draught	When the vessel draught changes the GM stays the same. While the waterline and center of buoyancy change, the center of gravity will change in such a way that the GM will stay the same. When the draught is not varied it is kept constant at a value of 7 meters.
Vessel GM	It is assumed that the vessel GM changes without influencing the other variables. In theory the vessel's KB, BM and KG will change in such a way that the GM changes but the other variables stay constant. When the GM is not varied it is kept constant at a value of 3 meters.
Crane top X, Y and Z position	These values will be changed independently from each other. This is done to carefully analyse the influence and interaction of the different rotations. When the crane X and Y positions are not varied they are kept constant at 0 meters. When the crane Z position is not varied it is kept constant at 30 meters.
Crane cable length	The length between the crane top and cargo COG will vary between 10 and 30 meters. In practice large crane cable length will cause a collision between the vessel's deck and the cargo. However, mathematically and theoretically the values can be used to study the influence of the crane cable length. When the crane cable length is not varied it is kept constant at 20 meters.
Cargo Mass	The cargo mass will change as a percentage of the overall mass in the system. This results in a constant water displacement of the system, as long as the draught is not changed. When the cargo mass is not varied it is kept constant at 3 % of the total mass in the system.

For every variable the natural frequencies are calculated in a general way. These calculations show the different ranges of the natural frequencies. While it is a multibody system with 12 degrees of freedom 12 different natural frequencies can occur. However, 2 motions are dominant in the graphs. Those motions are the roll motion and the pendulum sway motion. Both motions influence each other which causes two big excitations and two different frequencies. Since the equation of motions is solved in a range from 0.1 to 2.6 radians per second with a frequency step of 0.0125 radians per second a general frequency range can be found. In this study it became clear that the natural roll frequency occurs somewhere between the 0.35 and 0.60 radians per second and the natural pendulum frequency occurs between 0.65 and 1.05, Therefore a detailed calculation is done for these ranges with a frequency step of 0.001 radians per second.

5.1.1. Cargo Mass

The cargo mass is varied between 0% and 5% of the total mass of the system. In table 5.2 the values of the natural frequencies for different masses are given as well as the amplitude of the resonance peak for the vessel roll and cargo sway motion. In figure 5.1 the natural frequencies are plotted in relation with the cargo mass as % of all the mass in the system. In section 3.10.1 the influences of the cargo on the multi-body system are explained in detail. When the cargo mass is changed while all other variables are kept constant the cargo mass has an interesting effect on the multi-body system. While the draught of the vessel is kept constant the increased cargo mass will change the mass components that influence the natural frequencies coupled to the vessel roll motion and cargo sway motion in two different ways. While an increased cargo mass reduces the stiffness of the components coupled to the vessel roll motion the natural frequency coupled to this motion will decrease when the cargo mass increases. At the other hand an increased cargo mass increases the stiffness components coupled to the cargo sway motion which increases the natural frequency introduced due to the equation of motion of the cargo sway motion. The natural frequencies shown in table 5.2 and figure 5.1 show that this occurs for these two natural frequencies.

While both the vessel roll motion and cargo sway motion have a strong connection to each other, as explained in section 4.3, the natural frequencies coupled to both degree of freedom will also influence the other degree of freedom.

In table 5.2 can be seen that the responses show large amplitudes. While these responses are large it does not mean that these responses occur. Due to linearization the peak values can occur in a frequency domain calculation but in reality other forces prohibit the large amplitudes from existence. At the same time do environmental waves exist out of multiple linear waves, as explained in section 2.2. Due to the nature of the wave spectra the multi-body system will not be excited at the pure natural frequency. Besides these soothing aspects of the high amplitudes the change in amplitudes the effect of the cargo mass on the responses of the vessel roll and cargo sway motion. A heavier cargo reduces the amplitude of both the vessel roll and cargo sway motion for the first natural frequency. In figure 4.6 is shwon that at this natural frequency the two degrees of freedom move in opposite direction of each other. Due to the heavier weight the wave forces will excitate the two bodies to a smaller amplitude before an equilibrium is met. At the second natural frequency the two degrees of freedom move in the same direction as shown in figure 4.6. While the cargo is heavier the influence of the cargo motions will influence the vessel roll motion in a more significant way. At the other hand a heavier cargo results in a lower amplitude of the cargo sway motion at the second natural frequency. Due to the heavier cargo a smaller amplitude is a result of the wave excitation force.

Table 5.2: Influence of cargo mass on the roll and pendulum natural frequencies and amplitude of the resonance peaks.

Cargo Mass [% total mass]	First natural frequency [rad/s]	Amplitude Vessel Roll [deg]	Amplitude Cargo Sway [m]	Second natural frequency [rad/s]	Amplitude Vessel Roll [deg]	Amplitude Cargo Sway [m]
0			-	-	-	
0.5						
1						
2						
3						
4						
5						

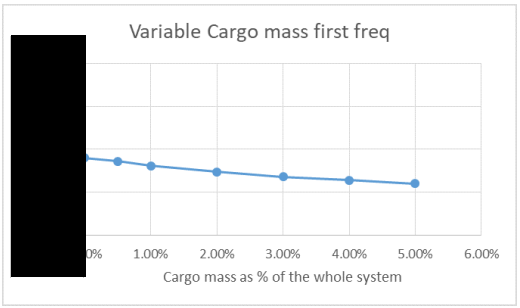

(a) Relation between the cargo mass and the natural roll frequency

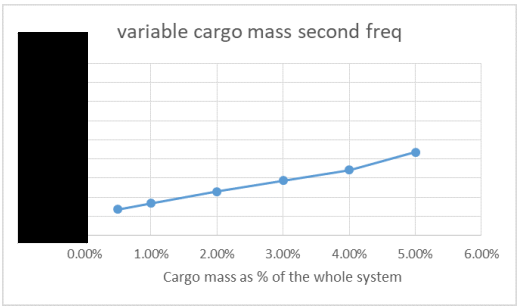

(b) Relation between the cargo mass and the natural pendulum frequency

Figure 5.1: Relation between cargo mass and the natural frequencies of the roll and pendulum motions

5.1.2. Crane Cable Length

The crane cable length is varied between 10 and 30 meters. The natural frequencies and peak values of the resonance for the different crane cable lengths can be found in table 5.3. In figure 5.2 the natural frequencies of the roll and pendulum motions are plotted. As explained in section 3.10.2 the crane cable length has a significant influence on the restoring stiffness values of the crane cable connection. The crane cable length influences the natural frequency of both the roll and pendulum motions. As shown in the figures below is the influence on the second natural frequency larger than on the first natural frequency. While the first natural frequency is mainly excited due to the vessel roll motions the change in restoring stiffness has a relatively small influence. The hydrodynamic stiffness of the vessel roll motion is larger than the restoring stiffness of

the crane cable connection. On the second natural frequency the restoring stiffness has the largest influence on the natural frequency. Hence, the influence of the crane cable length on the second natural frequency is a lot larger.

The first natural frequency is mainly excited due to the vessel roll motion. While a short crane cable length creates a large angle between the crane tip and cargo centre of gravity a lot of restoring forces are generated. When the crane cable length increases the angle between the crane top and centre of gravity decreases with the same relative horizontal distance between crane tip and cargo centre of gravity. The large angle and relative large restoring force explains the large amplitude for the small crane cable lengths and the small amplitude for the large crane cable lengths. The second natural frequency is mainly excited due to the natural frequency of the cargo sway motion. Due to the longer crane cable length the restoring stiffness is reduced and a larger roll motion is required to reach an equilibrium in stiffness values. At the same time the amplitude of the cargo sway motion RAO is reduced at the second natural frequency for longer crane cables.

Table 5.3: Influence of crane cable length on the roll and pendulum natural frequencies and amplitude of the resonance peaks.

Crane cable length [m]	First natural frequency [rad/s]	Amplitude Vessel Roll [deg]	Amplitude Cargo Sway [m]	Second natural frequency [rad/s]	Amplitude Vessel Roll [deg]	Amplitude Cargo Sway [m]
10						
15						
20						
25						
30						

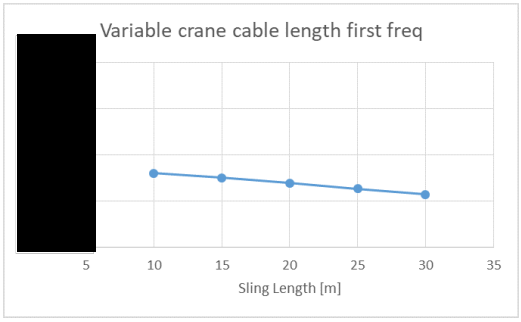

(a) Relation between the crane cable length and the natural roll frequency

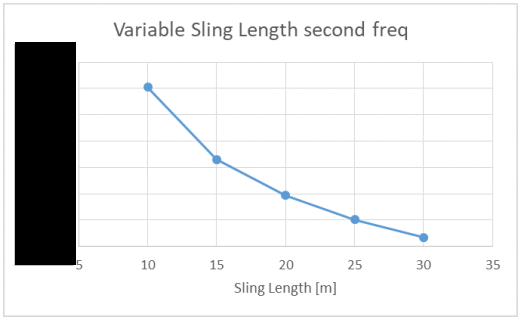

(b) Relation between the crane cable length and the natural pendulum frequency

Figure 5.2: Relation between crane cable length and the natural frequencies of the roll and pendulum motions

5.1.3. Crane Top Z Position

The position of the crane top in Z direction is varied between 20 and 60 meters. In table 5.4 the values of the natural frequencies for the different Z positions as well as the amplitude of the resonance peaks are given. The natural frequencies for the different Z positions of the crane top are plotted in figure 5.3. In section 3.10.3 is explained that the crane top Z position has a lot of influence on different coupling terms in the equation of motion. An increase of the crane top Z position increases the moments created by the restoring stiffness of the crane cable connection. However, the crane top Z position does also determine how far the crane top is translated due to the vessel roll motion. On the first natural frequency the coupling has a negative effect. When the crane top Z position is increased the natural frequency is decreased. While the first natural frequency is mainly dependent on the vessel roll motion the larger translations of the crane top result in larger influence of the cargo on the stability of the vessel. In conventional calculations the metacentric height of the vessel is adjusted relatively to the crane tip height. In this dynamical model the same influence occurs. The second natural frequency is mainly dependent on the restoring stiffness of the crane cable coupling. While the crane top Z position is increased the restoring moment that couple the vessel roll motion to the cargo sway motion is increased. Therefor the natural frequency is increased when the crane top Z position is increased.

The larger values of the crane top Z position will increase the translations of the crane top due to the vessel roll motion. These larger translations will cause a larger relative distance between the crane top and the centre of gravity of the cargo. While the first natural frequency is mostly generated due to the vessel roll motion the amplitude of the cargo sway motion increases when the crane top Z position is increased. The second natural frequency is mainly generated by the cargo sway motion. A larger crane top Z position will result in larger moment arms. With larger moment arms a smaller restoring force, or excitation is required to generate the same moment. This results in smaller amplitudes around the second natural frequency for larger crane top Z positions.

Table 5.4: Influence of the crane top Z position on the roll and pendulum natural frequencies and amplitude of the resonance peaks.

Crane top Z position [m]	First natural frequency [rad/s]	Amplitude Vessel Roll [deg]	Amplitude Cargo Sway [m]	Second natural frequency [rad/s]	Amplitude Vessel Roll [deg]	Amplitude Cargo Sway [m]
20	[redacted]	[redacted]	[redacted]	[redacted]	[redacted]	[redacted]
30	[redacted]	[redacted]	[redacted]	[redacted]	[redacted]	[redacted]
40	[redacted]	[redacted]	[redacted]	[redacted]	[redacted]	[redacted]
50	[redacted]	[redacted]	[redacted]	[redacted]	[redacted]	[redacted]
60	[redacted]	[redacted]	[redacted]	[redacted]	[redacted]	[redacted]

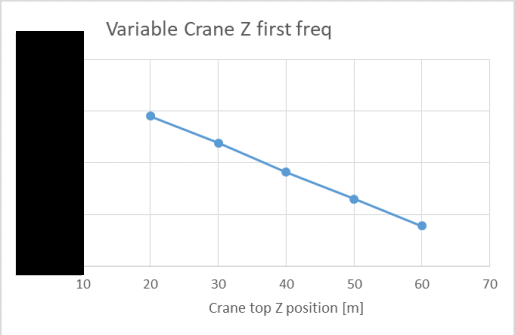

(a) Relation between the crane top Z position and the natural roll frequency

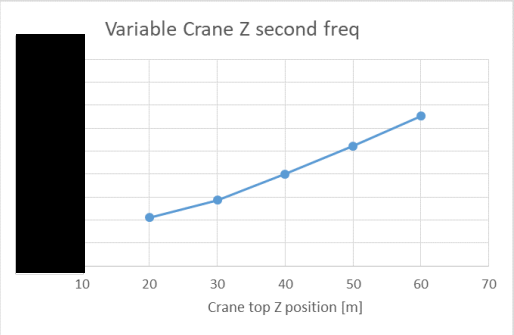

(b) Relation between the crane top Z position and the natural pendulum frequency

Figure 5.3: Relation between crane top Z position and the natural frequencies of the roll and pendulum motions

5.1.4. Crane Top Y Position

The position of the crane top in Y direction is varied between -50 and 50 meters. The outreach of the crane is 35 meter. While the cranes are located at the starboard side of the vessel the maximum outreach to port side is approximately 23 meters and the outreach to starboard side is approximately 47 meters. Thus not all Y positions studied are physically possible. However the larger crane top Y positions are used to create more mathematical data. The natural frequencies and peak values of the resonance for the different Y positions of the crane top can be found in n table 5.5. In figure 5.4 the natural frequencies of the roll and pendulum motions are plotted. As explained in section 3.10.4 the crane top Y position has a negative effect on the vessel roll and cargo sway motion stiffness components. Due to this negative effect the natural frequencies of the vessel roll and cargo sway motion will decrease.

While the positive or negative sign of the crane top Y position does not influence the natural frequencies of the multi-body system the amplitude is influenced by the different signs. In section 3.10.4 is explained that the phases of both motions in combination with the crane top Y position can cause an enhancement of the amplitude or a reduction of the amplitude. In this case the negative crane top Y positions have a smaller amplitude than the positive crane top Y positions.

Table 5.5: Influence of the crane top Y position on the roll and pendulum natural frequencies and amplitude of the resonance peaks.

Crane top Y position [m]	First natural frequency [rad/s]	Amplitude Vessel Roll [deg]	Amplitude Cargo Sway [m]	Second natural frequency [rad/s]	Amplitude Vessel Roll [deg]	Amplitude Cargo Sway [m]
-50						
-40						
-30						
-20						
-10						
0						
10						
20						
30						
40						
50						

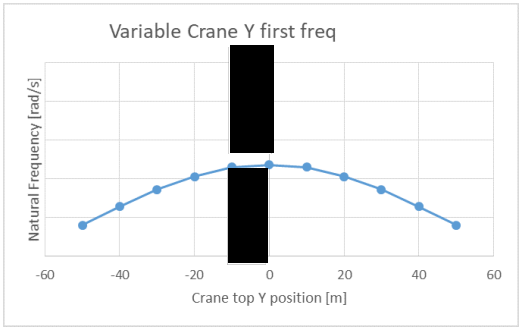

(a) Relation between the crane top Y position and the natural roll frequency

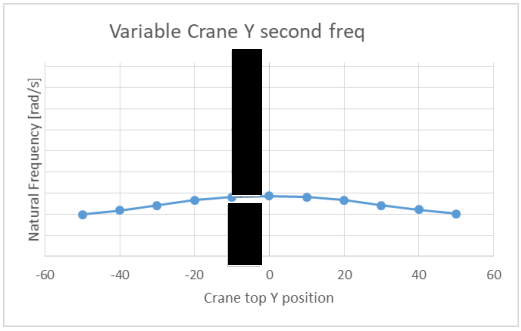

(b) Relation between the crane top Y position and the natural pendulum frequency

Figure 5.4: Relation between crane top Y position and the natural frequencies of the roll and pendulum motions

5.1.5. Crane Top X Position

The position of the crane top in X direction is varied between -50 and 50 meters. While none of the cranes can reach both the -50 and +50 meters outreach the forward crane can reach the +50 meter outreach and the aft crane can reach -50 meter outreach. In table 5.6 the natural frequencies and amplitudes of these natural frequencies the vessel roll and cargo sway motions are shown. Figure 5.5 show the natural frequencies of the vessel roll and cargo sway motions for different X positions of the crane top. The influence of the X position of the crane top on the roll and pendulum is very small. However, due to the coupling of the multiple degrees of freedom to each other, as explained in section 3.10.5, the crane top X position, although very small, has an influence on the natural frequency of the vessel roll and cargo sway motion.

Since the difference in the natural roll frequency is really small, 0.005 radians per second over a difference of 100 meter crane top translations it is safe to say that the influence of the crane position in X direction is minimal. The influence on the pendulum natural frequency is also small. However the lowest natural frequency lies around the 0 meter offset of the crane tip in X direction and it increases when the crane top moves away in both the positive and negative direction. However the influence of a negative direction is smaller than the influence of a positive direction in the calculations. This can be explained by the summation of influences. There are some parts in the equation that will influence the stiffness matrix in the same way for positive as negative directions while other parts are sign dependent. An example for a term without any direction influence is the pendulum restoring stiffness component of the yaw motion on the yaw force. Here the location of the crane top in X direction is squared which negates the direction of the crane top position. On the other hand will the pendulum restoring system component of the yaw motion on the sway force be influenced by the direction of the crane top. Resulting in a combination of these influences.

Table 5.6: Influence of the crane top X position on the roll and pendulum natural frequencies and amplitude of the resonance peaks.

Crane top X position [m]	First natural frequency [rad/s]	Amplitude Vessel Roll [deg]	Amplitude Cargo Sway [m]	Second natural frequency [rad/s]	Amplitude Vessel Roll [deg]	Amplitude Cargo Sway [m]
-50						
-40						
-30						
-20						
-10						
0						
10						
20						
30						
40						
50						

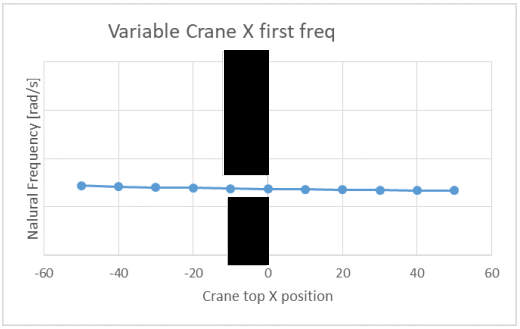

(a) Relation between the crane top X position and the natural roll frequency

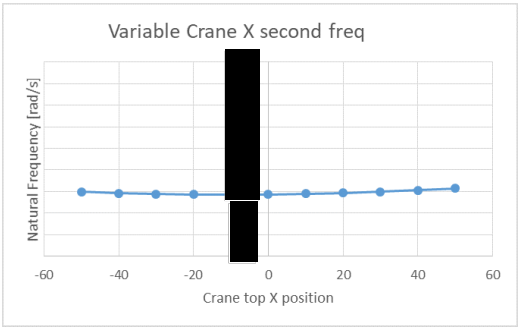

(b) Relation between the crane top X position and the natural pendulum frequency

Figure 5.5: Relation between crane top X position and the natural frequencies of the roll and pendulum motions

The vessel roll motion is a rotation around the X-axis of the vessel. Therefore the crane top X position is supposed to have a small influence. However, the crane top X position can have a larger influence on the coupling between the vessel pitch motion and cargo surge motion. Although it is explained in section 4.2 that the main focus of the study will be the interaction between the vessel roll and cargo sway motion the influence of the crane top X position on the vessel pitch and cargo surge motion will also be studied. in table 5.7 the natural frequencies and amplitudes of the vessel pitch and cargo surge motion are given. For these calculations waves with an angle of 0 degrees relative to the vessel are used.

In section 3.10.5 is explained that the pendulum restoring stiffness is a lot smaller than the hydrodynamic restoring stiffness of the vessel pitch motion. Therefore it is expected that the crane top X position will not influence the cargo surge natural frequencies. However the crane top X position can cause a very small enhanced amplitude due to the interaction between the vessel pitch and cargo surge motion.

Table 5.7: Influence of the crane top X position on the cargo surge natural frequency and amplitude of the resonance peak.

Crane top X position [m]	Vessel pitch natural frequency [rad/s]	Amplitude Vessel pitch [deg]	Amplitude Cargo Surge [m]	Cargo surge natural frequency [rad/s]	Amplitude Vessel Pitch [deg]	Amplitude Cargo Surge [m]
-50	[redacted]	[redacted]	[redacted]	[redacted]	[redacted]	[redacted]
-40	[redacted]	[redacted]	[redacted]	[redacted]	[redacted]	[redacted]
-30	[redacted]	[redacted]	[redacted]	[redacted]	[redacted]	[redacted]
-20	[redacted]	[redacted]	[redacted]	[redacted]	[redacted]	[redacted]
-10	[redacted]	[redacted]	[redacted]	[redacted]	[redacted]	[redacted]
0	[redacted]	[redacted]	[redacted]	[redacted]	[redacted]	[redacted]
10	[redacted]	[redacted]	[redacted]	[redacted]	[redacted]	[redacted]
20	[redacted]	[redacted]	[redacted]	[redacted]	[redacted]	[redacted]
30	[redacted]	[redacted]	[redacted]	[redacted]	[redacted]	[redacted]
40	[redacted]	[redacted]	[redacted]	[redacted]	[redacted]	[redacted]
50	[redacted]	[redacted]	[redacted]	[redacted]	[redacted]	[redacted]

5.1.6. Vessel Draught

For the vessel draught two comparisons are made. In the first case a comparison the cargo mass is kept at a percentage of the displacement of the vessel. Thus the cargo mass is dependent on the draught of the vessel. In the second case a comparison the cargo mass is held equal to 3% of the total mass in the multi-body system for a vessel draught of 7 meter. In this way the influence of draught and cargo mass can be studied more accurately.

In table 5.8 the comparison of the roll and pendulum natural frequencies with a relative cargo mass is given for the first case. In figure 5.6 the natural frequencies of the roll and pendulum motions of the different draughts with a relative cargo mass are plotted. In section 3.10.6 is explained that the draught of the vessel influences the displacement of the vessel. Via the displacement the mass, added mass and hydrodynamical stiffness values of the multi-body system are changed. While the hydrodynamic mass matrices are increased the cargo weight is also increased since the mass has to stay equal to 3% of the total mass in the system. When the cargo mass stays relative equal to the different displacements there is no change in the natural frequencies. This implies that the pendulum restoring stiffness, hydrodynamic stiffness values, hydrodynamic damping values, added mass values and vessel mass values increase with the same ratio when the draught is increased.

In table 5.9 the natural frequencies and resonance amplitudes of the vessels roll and pendulum swing motions are given for different draughts with a constant cargo mass. In figure 5.7 these different natural frequencies are plotted. Since the weight of the cargo does not change the pendulum restoring stiffness values will also not change. Thus only the vessel mass, added mass and hydrodynamical stiffness values change due to the increased draught. In the table and figure can be seen that the natural frequency changes a little. The increased natural frequency for larger draughts shows that the hydrodynamical stiffness values increase more than the mass and added mass values around the first natural frequencies. Since the cargo mass is relative lighter for larger draughts the influence of the pendulum restoring stiffness values is smaller. This explains the reduced natural frequency around the second natural frequency. This is the opposite phenomenon that occurs when the cargo mass is increased in section 5.1.1.

Table 5.8: Influence of the vessel draught with relative cargo mass on the roll and pendulum natural frequencies and amplitude of the resonance peaks.

Vessel draught [m]	First natural frequency [rad/s]	Amplitude Vessel Roll [deg]	Amplitude Cargo Sway [m]	Second natural frequency [rad/s]	Amplitude Vessel Roll [deg]	Amplitude Cargo Sway [m]
6.5	[redacted]	[redacted]	[redacted]	[redacted]	[redacted]	[redacted]
7	[redacted]	[redacted]	[redacted]	[redacted]	[redacted]	[redacted]
7.5	[redacted]	[redacted]	[redacted]	[redacted]	[redacted]	[redacted]
8	[redacted]	[redacted]	[redacted]	[redacted]	[redacted]	[redacted]
8.5	[redacted]	[redacted]	[redacted]	[redacted]	[redacted]	[redacted]

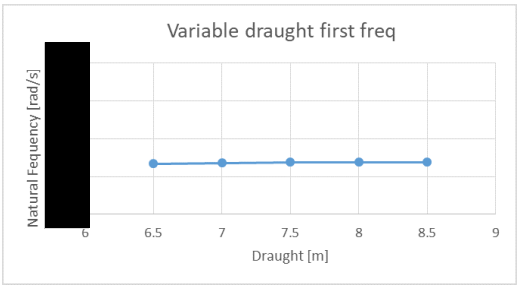

(a) Relation between the vessel draught with a relative cargo mass and the natural roll frequency

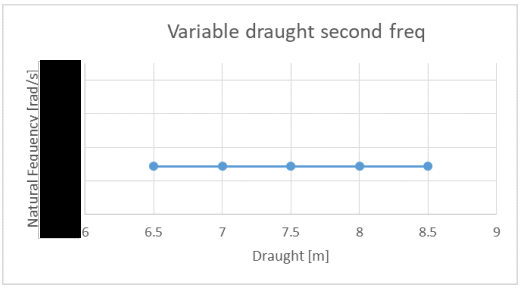

(b) Relation between the crane top Y position and the natural pendulum frequency

Figure 5.6: Relation between the vessel draught with a relative cargo mass and the natural frequencies of the roll and pendulum motions

Table 5.9: Influence of the vessel draught with a constant cargo mass on the roll and pendulum natural frequencies and amplitude of the resonance peaks.

Vessel draught [m]	First natural frequency [rad/s]	Amplitude Vessel Roll [deg]	Amplitude Cargo Sway [m]	Second natural frequency [rad/s]	Amplitude Vessel Roll [deg]	Amplitude Cargo Sway [m]
6.5	[redacted]	[redacted]	[redacted]	[redacted]	[redacted]	[redacted]
7	[redacted]	[redacted]	[redacted]	[redacted]	[redacted]	[redacted]
7.5	[redacted]	[redacted]	[redacted]	[redacted]	[redacted]	[redacted]
8	[redacted]	[redacted]	[redacted]	[redacted]	[redacted]	[redacted]
8.5	[redacted]	[redacted]	[redacted]	[redacted]	[redacted]	[redacted]

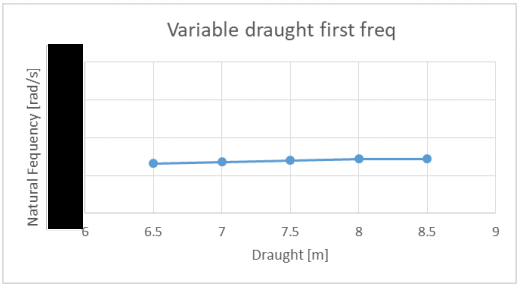

(a) Relation between vessel draught with a constant cargo mass and the natural roll frequency

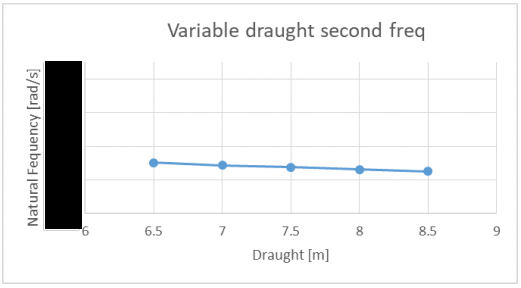

(b) Relation between vessel draught with a constant cargo mass and the natural pendulum frequency

Figure 5.7: Relation between vessel draught with a constant cargo mass and the natural frequencies of the roll and pendulum motions

5.1.7. Metacentric Height

The metacentric height is varied between 2.5 and 4.5 meters. As explained in section 3.10.7 the metacentric height has an influence on the stability of the vessel and an increased metacentric height should increase the natural frequency of the multi-body system. In this section is also explained that the metacentric height used in the calculations is the metacentric height of the vessel without any cargo in the cranes. A metacentric height of 2.5 till 4.5 meters might look large but since the cargo is not integrated in the GM values the GM values are normal for lifting operations. BigLift shipping uses stability software to calculate the stability of different loading conditions. The software used for most vessels, including the baseline and case vessel Happy Sky is called Seasafe. Seasafe shows that a weight of 450 mton will reduce the vessel's GM from 3.1 meter to 1.7 meter. This is a reduction of 1.4 meter due to the weight of the cargo. Larger cargoes will reduce the GM even further. The GM values used in the calculations might look large in comparison with normal GM values during lifting operations but the GM values are normal when the cargo mass is not used in the GM calculations.

In table 5.10 the vessel roll and cargo sway natural frequencies are given as well as the height of the resonance peaks. In figure 5.8 the vessel roll and cargo sway natural frequencies are plotted with regards to the GM values of the vessel. The GM value has a big influence on the roll motions and a smaller influence on the pendulum motions. When the metacentric height is increased the hydrodynamic stiffness matrix will increase which results in a higher natural frequency. Since the vessel motions have a higher stiffness and the pendulum is coupled to the vessel the pendulum natural frequency will also increase. Although to a lesser extent.

Table 5.10: Influence of the vessel's metacentric height on the vessel roll and cargo sway natural frequency and amplitude of the resonance peak.

GM [m]	First natural frequency [rad/s]	Amplitude Vessel Roll [deg]	Amplitude Cargo Sway [m]	Second natural frequency [rad/s]	Amplitude Vessel Roll [deg]	Amplitude Cargo Sway [m]
2.5	[redacted]	[redacted]	[redacted]	[redacted]	[redacted]	[redacted]
3	[redacted]	[redacted]	[redacted]	[redacted]	[redacted]	[redacted]
3.5	[redacted]	[redacted]	[redacted]	[redacted]	[redacted]	[redacted]
4	[redacted]	[redacted]	[redacted]	[redacted]	[redacted]	[redacted]
4.5	[redacted]	[redacted]	[redacted]	[redacted]	[redacted]	[redacted]

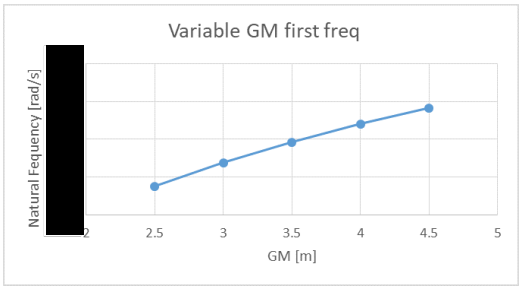

(a) Relation between vessel GM and the natural roll frequency

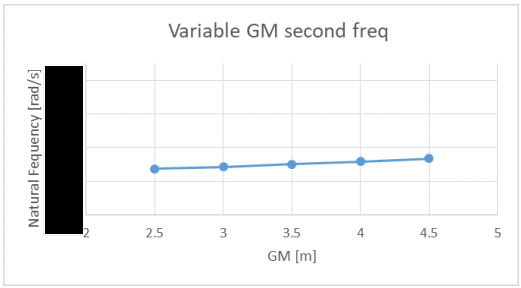

(b) Relation between vessel GM and the natural pendulum frequency

Figure 5.8: Relation between vessel GM and the natural frequencies of the roll and pendulum motions

5.1.8. Results of Lifting Variable Influence Study

The different variables have a different influence. In table 5.11 the results are summarized. The variable with the biggest influence is the crane top Z position and crane cable length. This is interesting while the crane top Z position and crane cable length will vary during lifting operations. When a certain crane top crane cable length is critical for a loading operation one can try to avoid this crane cable length by lowering the crane tip which reduces the required crane cable length for the same lifting height or reduce the lifting height itself to avoid a certain crane cable length. At the same time a critical crane top Z position could be worked around by changing the crane cable length. Depending on the required lifting height. Therefore it is recommended to do detailed calculations when the crane top Z position or crane cable length is changed to make sure that

the interaction of both lengths result in a desired natural frequency. The sign of the crane top Y position does not change the natural frequency for positive or negative signs, but the peak of the maximum excitation does change, which can make port or starboard side lifting more desired. The crane top in X position does not seem to have a significant influence on the different motions. Therefore it is recommended to change other variables first when the natural frequency of the system must be changed. The displacement of the vessel has almost no influence on the motions themselves. However the cargo mass will be constant in practice. Therefore a change in draught might reduce the influence of the cargo mass. The exact influence of the draught and cargo mass together is case sensitive. The metacentric height has a big influence on the vessel roll motions. Therefore it is recommended to do accurate stability studies before critical lifting operations are performed. The most notable variable is the cargo mass. Since it reduces the first natural frequency and increases the second natural frequency by a considerable amount. In practice the weight of the cargo cannot be changed, however the cargo mass varies for every different lifting operation. This shows that it can be useful to study the multi-body behaviour for all different lifting operations.

The different variables have different influences. Some variables can be changed more easily than other variables during practice. Therefore it is import to calculate different aspects of a loading operation such as pretension, free hanging and transit of the cargo. With a change of the vessel draught and metacentric height the natural frequencies can be changed most safely. The calculations with different Y and X positions of the crane top can help in the decision of whether the front or aft crane should be used, if the crane should rotate clockwise or counter clockwise to reach it destination and if the lifting operation should be performed from the port or starboard side of the vessel when these options are available. The cargo mass can not be changed which make the big influence of the cargo weight an interesting value but not useful for the modification of the natural frequency.

Table 5.11: Variables changed to study the influence

Variable	Influence
Vessel Draught	When the vessel draught is changed and the cargo mass is taken as a percentage of the total mass in the system the change of draught has no influence on the behaviour of he multi-body system. When the draught is increased but the cargo mass is kept equal to 577 mton an increased draught results in a higher first natural frequency and a lower second natural frequency. A larger draught will increase almost all amplitudes of of the vessel roll and cargo sway motion RAOs.
Vessel GM	When the metacentric height of the vessel is increased the natural frequencies of the vessel roll and cargo sway motion are increased. The amplitude is increased for both the vessel roll motion and cargo sway motion RAOs at the first natural frequency. The amplitude of the vessel roll motion RAO is increased and the amplitude of the cargo sway motion RAO is decreased at the second natural frequency
Crane top Z position	When the crane top Z position is increased the first natural frequency is decreased and the second natural frequency is increased. A larger crane top Z position increases the amplitude of the cargo sway motion RAO around the first natural frequency while the amplitude of the vessel roll motion RAO is reduced slightly for all crane top Z positions larger than the crane cable length. The amplitudes of the RAOs of both degrees of freedom are reduced for larger crane top Z positions at the second natural frequencies.
Crane top Y position	An increased crane top Y position in both positive and negative direction decreases the natural frequency for both natural frequencies. The sign of the crane top Y position has no influence on the amount that the natural frequencies are reduced. The sign has an influence on the amplitude of RAOs of both degrees of freedom.
Crane top X position	The crane top X position has a small influence on the vessel roll and cargo sway motion while it couples the vessel pitch and yaw motion to these degrees of freedom. The crane top X position has no influence on the natural frequencies of the vessel pitch and cargo surge motion while the change of the stiffness values is too small.
Crane cable length	An increased crane cable length reduces both of the natural frequencies that influence the vessel roll and cargo surge motion. The largest influence is found around the second natural frequency. The amplitude of the RAOs of both degrees of freedom at the first natural frequency is decreased with a longer crane cable. However, a longer crane cable increases the amplitude of the vessel roll motion RAO and the amplitude of the cargo sway motion RAO is reduced slightly.
Cargo Mass	When the cargo mass is increased the first natural frequency around [redacted] rad/s is decreased. The second natural frequency is increased when the cargo mass increases. A heavier cargo mass increases the amplitude of the vessel roll motion RAO for both frequencies while the amplitude of the cargo sway motion RAO is decreased.

5.2. Influence of Mooring Lines

In section 3.4 is explained that the stiffness of the mooring lines is dependent on the length of the mooring lines. Shorter mooring lines have a higher stiffness value than longer mooring lines. The location of the connection of the mooring line on shore and on the vessel do determine how the mooring line stiffness is divided over the X, Y and Z components. In this section multiple mooring line configurations are used to study the influence of the mooring lines on the multi-body system.

Multiple mooring configurations are studied. The effects of these configurations will be compared with the baseline configuration explained in section 4.4. The variables of the lifting configuration are also equal to the baseline configuration. The first mooring configuration that will be compared is a configuration with two mooring lines. Both mooring lines are connected to the stern of the vessel. Since the mooring lines are located at the same side of the vessel the rotational restoring moments will not cancel each other out. The locations of the bollards onshore and fairleads of the vessel can be found in table 5.12. In this table the resulting stiffness components of the mooring lines are also given. Figure 5.9 shows a sketch of the different mooring lines given in the table. The first configuration consists out of mooring line 1 and mooring line 2 in this table. The second configuration consists of the first 4 mooring lines from the table. Besides the first two mooring lines two lines at the bow of the vessel will be connected. The stiffness from these mooring lines will add stiffness in the translations of the vessel. However, the stiffness will have an opposite sign in the vessel pitch and yaw motion in comparison to mooring line 1 and mooring line 2. In the third and last configuration all mooring lines in table 5.12 are used. In this configuration shorter mooring lines are added. In the first configuration only mooring lines at the stern are connected. With this configuration mooring lines will add a small amount of stiffness in the vessel surge and sway motion. At the same time are rotational restoring forces introduced while there is only a negative moment arm in X direction. While this configuration will never be used in practice the configuration can be used mathematically to study the influence of mooring lines at one side of the vessel. At the second configuration the mooring line stiffness is doubled while 2 more mooring lines with the same length and stiffness values are connected. While these mooring line are connected to the bow of the vessel the rotational forces added in the first configuration are cancelled out by the two new lines. In the third configuration a lot more stiffness than in the first and second configuration are added. While mooring lines tend to introduce low amounts of stiffness the influence of stiffer mooring lines are studied with the third configuration. This last configuration will not be used in practice but the more extreme values will influence the responses of the vessel and cargo in more than the normal configurations.

Table 5.12: Different mooring line configurations used to calculate the influence of mooring lines on the vessel and cargo respones.

	Mooring line 1	**Mooring line 2**	**Mooring line 3**	**Mooring line 4**	**Mooring line 5**	**Mooring line 6**	**Mooring line 7**	**Mooring line 8**
Bollard X [m]	-120	-120	120	120	-60	-50	50	60
Bollard Y [m]	30	30	30	30	30	30	30	30
Bollard Z [m]	5	5	5	5	5	5	5	5
Fairlead X [m]	-70	-65	65	70	-50	-40	40	50
Fairlead Y [m]	10	12	12	10	14	14	14	14
Fairlead Z [m]	8	8	8	8	8	8	8	8
X stiffness [kN/m]	39.8	38.0	38.0	39.8	63.5	63.5	63.5	63.5
Y stiffness [kN/m]	15.9	12.4	12.4	15.9	101.6	101.6	101.6	101.6
Z stiffness [kN/m]	2.4	2.1	2.1	2.4	19.1	19.1	19.1	19.1

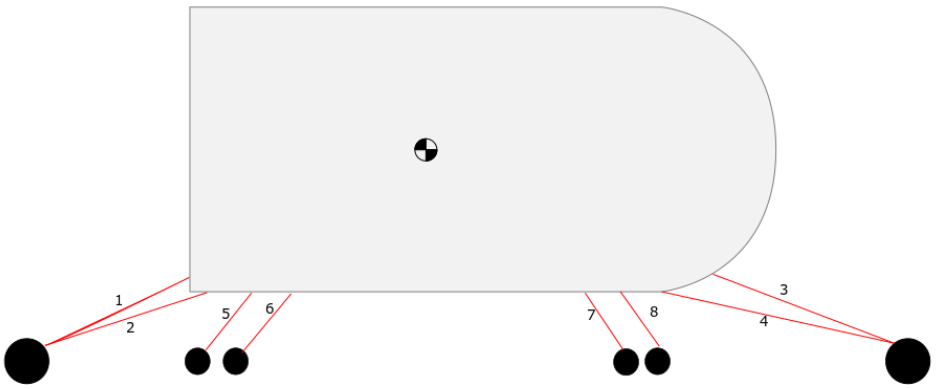

Figure 5.9: Sketch of the mooringline configuration of table 5.12

The different mooring line configurations are used to calculate the responses of the vessel and cargo. As stated before the mooring lines will increase the stiffness of the multi body system which will increase the natural frequencies of the multi-body system. The repsonses of the vessel roll motion and cargo sway motion are shown in figures 5.10 and 5.11. In these figures can be seen that the first and second mooring configurations only have a small influence on the responses of the vessel. The responses of both the vessel roll motion and the cargo sway motion are increased due to the mooring lines. The third configuration has a larger influence on the responses of both degrees of freedom. The two natural frequencies that can be seen in these figures are increased as expected. However the responses of the vessel roll motion and cargo sway motion are increased drastically around the first natural frequency. This is also the frequency of swell waves. The changes in response around the second natural frequency are minimal. Therefore it can be stated that the influence of a stiff mooring configuration has negative influence on the operability of lifting operations.

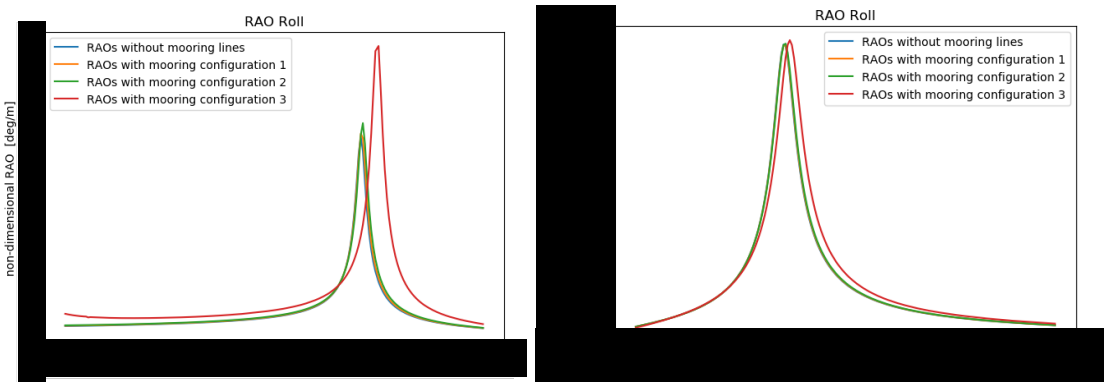

(a) Vessel roll motion RAO for different mooring line configurations

(b) Vessel roll motion RAO for different mooring line configurations.

Figure 5.10: Influence of different mooring line configurations on the vessel roll motions. The different configurations are combinations of the lines in table 5.12

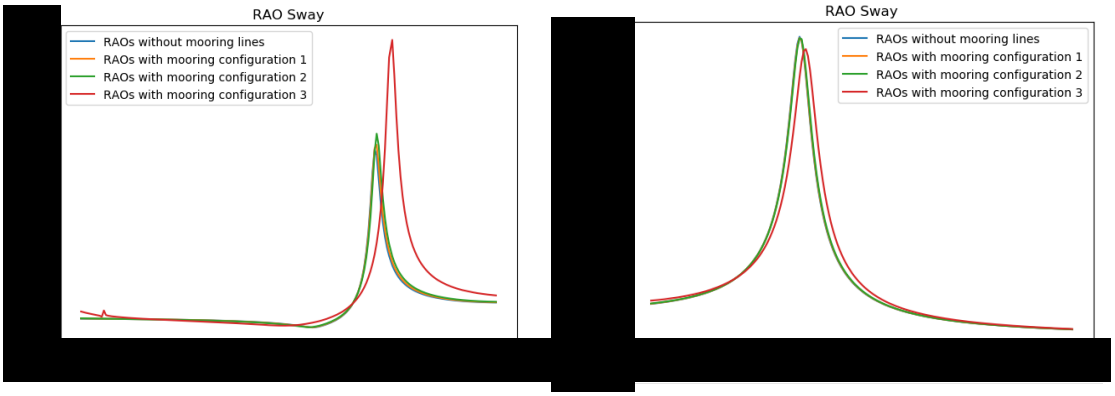

(a) Cargo Sway motion RAO for different mooring line configurations

(b) Cargo Sway motion RAO for different mooring line configurations.

Figure 5.11: Influence of different mooring line configurations on the cargo sway motions. The different configurations are combinations of the lines in table5.12

The eigenvector method is used to study the connection between the different degrees of freedom at the natural frequency around [redacted] rad/s. In figure 5.12 the eigenvector for the vessel and cargo motions without mooring lines and the eigenvector for the multi-body system with mooring line configuration 3 are given. In this eigenvector graph the vessel roll and cargo sway motion are dominant. Other degrees of freedom are also excited at this natural frequency. Therefore the eigenvector without the vessel roll and cargo sway eigenvector values is plotted in figure 5.13. In figure 5.12 can be seen that the mooring line configuration causes relative lower responses of the vessel roll motion in comparison with the other degrees of freedom. However, the vessel heave motion shows a very small increase of the excitations. Due to the stiffness introduced by the mooring lines there is extra stiffness added to the coupling of the vessel heave and roll motions. Due to these stiffness components energy from the vessel roll motion is transferred to the vessel heave motion which explains the small increase of excitation of the vessel heave motion. In figure 5.13 can also be seen that the stiffness introduced by the mooring lines in the vessel sway direction prevent the vessel from moving in this direction. Resulting in a relative smaller excitation of the vessel sway motion at this natural frequency. Other couplings to the vessel surge, cargo surge and cargo heave motion are also introduced. However the influence on these degrees of freedom is extremely small. In the equations of motion, found in appendix C, the complete mathematical coupling can be found.

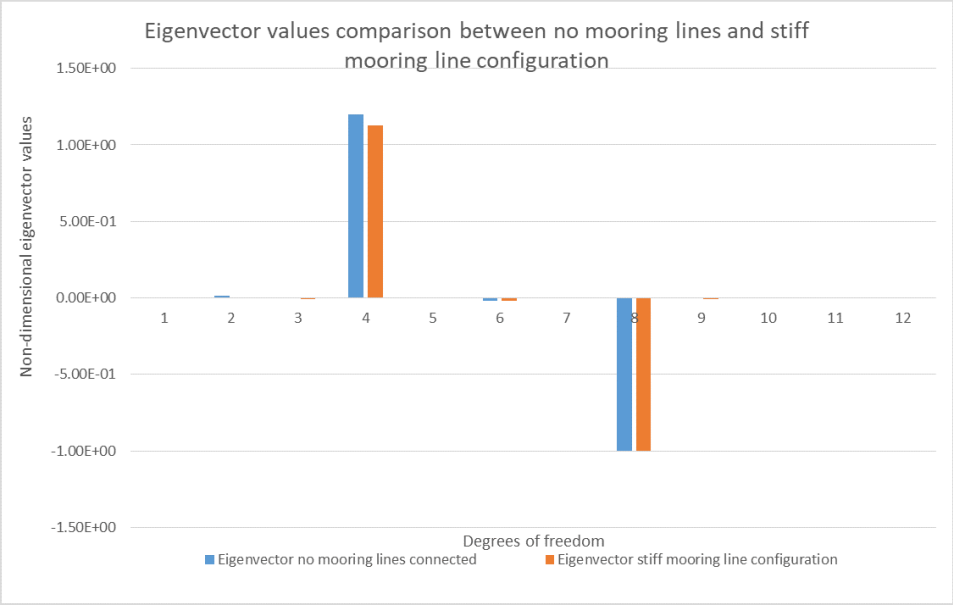

Figure 5.12: Eigenvector value comparison between the multi-body system without mooring lines and the multi-body system with a stiff mooring line configuration, configuration 3 in figures 5.10 and 5.11. The natural frequency that is compared is the natural frequency at [redacted] rad/s.

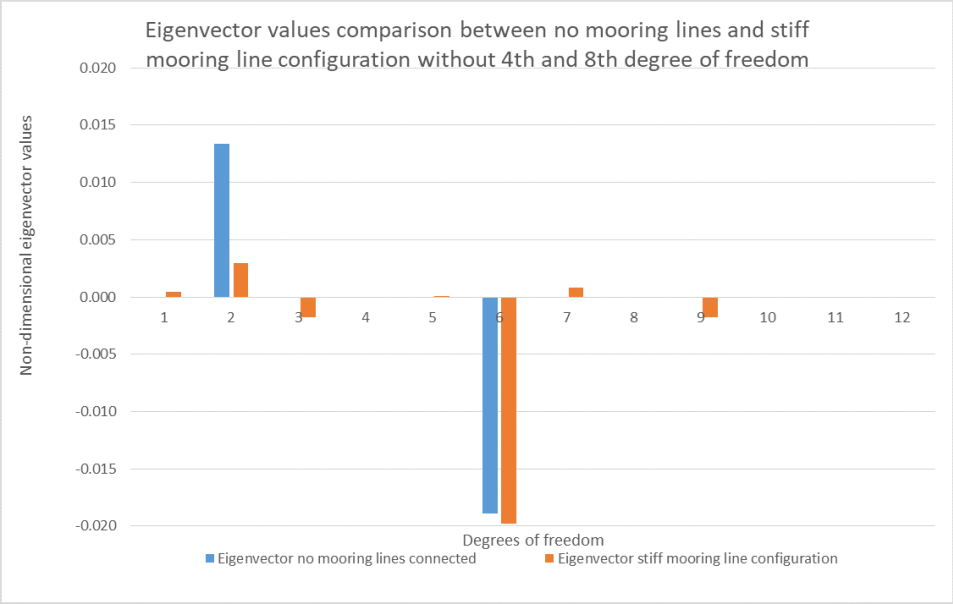

Figure 5.13: Eigenvector value comparison between the multi-body system without mooring lines and the multi-body system with a stiff mooring line configuration, configuration 3 in figures 5.10 and 5.11. . The natural frequency that is compared is the natural frequency at [redacted] rad/s. In this figure the eigenvector values of the vessel roll and cargo sway motion are neglected

Another aspect that stands out is the small response of the cargo sway motion around [redacted] rad/s which can be seen in figure 5.11. This response is the result of another natural frequency at [redacted] rad/s. This natural frequency does not influence the vessel roll motion and cargo sway motion with less stiff mooring lines. The eigenvector method is used to study this natural frequency. In figure 5.14 the eigenvector of this natural frequency is shown. This eigenvector makes it clear that the vessel heave and cargo heave motions are the two motions with the largest responses on this natural frequency. The stiff mooring line configuration causes a rotational moment due to vessel translations. Due to this phenomenom the vessel heave motion exerts a rotational force on the vessel roll and pitch motions. The vessel roll and pitch motions are connected to the

cargo sway and surge motions respectively and this relation causes the excitation of the cargo surge and cargo sway motions. A frequency of [redacted] rad/s corresponds to a period of [redacted] seconds. This is a very large period and will likely not be excited by the swell waves. However, slower waves can still excite this natural frequency and quadratic drift forces can cause larger motions. These motions are not studied in this research.

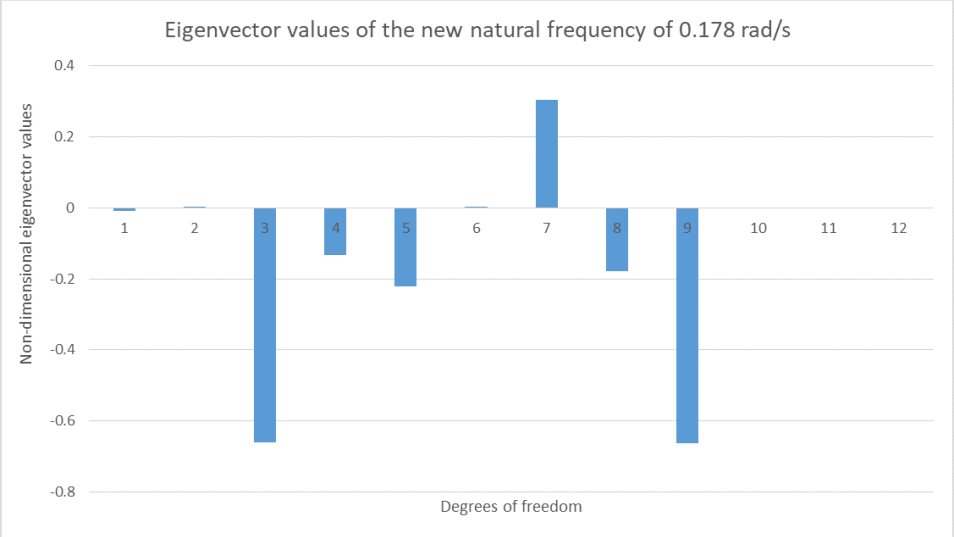

Figure 5.14: Eigenvector values of the natural frequency found at [redacted] rad/s that appears when a stiff mooring line configuration is used

6
Cargo control systems

As explained in section 2.5 damping might reduce the responses of the cargo motions. Therefore the influence of damping is modeled and used to study the behaviour of the multi-body system when damping is applied. In section 4.2 is explained that the vessel roll and cargo sway motion show the biggest responses due to wave forces. Therefore the influence of different parameters during the lifting operation was focused on these two degrees of freedom. While the vessel roll and cargo sway motion show the largest responses and are potentially the most dangerous motions during lifting operations the influence of cargo control systems on these two degrees of freedom are studied. At those two degrees of freedom the most is gained from reduced responses.

To create a good understanding of the influence of cargo control systems on the cargo motions the baseline variables used in section 4.4 will be used. In this way the influence of the different variables are not part of the comparison. This means that the crane tip will be placed above the centre of gravity. The vertical location of the crane tip will be at 30 meters and the distance between the crane tip and cargo centre of gravity will be equal to 20 meters. The mass will be equal to 3 % of the total weight in the multi-body system. The vessel will have a draught of 7 meters with a metacentric height equal to 3 meters.

In section 6.1 the influence of low stiffness tugger wires and high stiffness tugger wires will be explained. Thereafter the influence of the location of different tugger wires will be described in section 6.2. In section 6.3 the influence of passive compensation in terms of small damping percentages will be explained. Next the influence of active systems, in terms of large damping values, are explained in section 6.4. All the results are summarized in section 6.5.

In the equations used to study the influences of the tugger winches two tugger winches are used. The X, Y and Z coordinates of the two tugger winches and padeyes are given in table 6.1. Both winches are mirrored along the midship line. The X coordinates are placed far away from the cargo and crane tip. This makes it possible for the crane to move the cargo above the deck. The winches are placed as far as possible the side of the vessel. This is done to create a large Y component in the damping and spring values from the tugger wires. In section 6.2 the influence of different configurations will be examined.

Table 6.1: The coordinates of the tugger winches used in the influence calculations of the tugger winch

Coordinate	**Tugger Winch 1**$[m]$	**Tugger Winch 2**$[m]$
Winch X	-30	30
Winch Y	-15	-15
Winch Z	10	10
Padeye X	-10	10
Padeye Y	-5	-5
Padeye Z	-5	-5

6.1. Stiffness via tugger winches

In section 2.5 the influence of damping is explained. In section 3.5 is explained that a cargo control system will also introduce stiffness to the multi-body system. In appendix E different methods to control the cargo are described. The damping and mass values of the different types of wires that can be used to control the cargo are neglected in these calculations. The most simple practice to control the cargo is the application of fixed tugger winches. These tugger winches will create a connection between the vessel and the cargo with a rope or wire. When a fixed tugger system is used the connection will only consist out of a wire and no passive or active damping is applied. This means that a tugger wire can be modelled as a connection via the restoring forces. The connection can be applied via fibre ropes or steel wires. The only difference between a fibre rope or steel wire connection in this study is the stiffness of the material. All other aspects of the connection will stay the same for both types of connection. Thus the location of the tugger winch and the connection from the tugger wire to the cargo will be on the same locations for both types of lines. To compare the influence of tugger winches equipped with ropes or wires different stiffness values will be used for the tugger winch calculations.

In this section the use of polypropylene wires and steel wires connected between the vessel and cargo will be studied. These wires are connected to the vessel via a tugger winch system that can also pretension these wires. Therefore these wires are called tugger wires in practice and will be called tugger wires throughout this chapter. The stiffness values of fibre ropes and steel wires differ by 2 to 3 orders of magnitude. Both types of wires can be used to control the cargo. fibre rope, polypropylene, has stiffness values around 30 kN/m and steel wires kan have a stiffness value of 1000 to 10000 kN/m depending on the diameter of the wires. This large difference in stiffness gives reason to assume different influence on the cargo and vessel motion depending on the line material. Therefore the influence of both the polypropylene wires and steel wires are studied. In section 6.1.1 the influence of low-stiffness wires are studied and in section 6.1.2 the influence of high-stiffness tuger wires are studied.

6.1.1. Polypropylene wires

In this section the influence of low-stiffness lines are studied to determine the sensitivity of the motion responses to tugger winches. In this section 'polypropylene' wires with a stiffness value between 20 kN/m to 40 kN/m are studied. In figures 6.1 and 6.2 the RAOs of the vessel roll and cargo sway motion are given for a multi-body system including tugger wires. The lines used in this comparison have an stiffness of 20, 30 or 40 kN/m. The stiffness of the lines are low. However, when polypropylene lines are used, the same material as mooring lines, the used stiffness is achievable due to the material properties of polypropylene.

The implementation of the tugger lines will cause a higher stiffness value in the different degrees of freedom. It is assumed that the weight of the tugger lines is negligible in comparison with the weight of the cargo and the displacement of the vessel. Therefore the tugger lines will not have any influence on the weight of the multi-body system. Since the natural frequency is dependent on the mass and stiffness matrices the increased stiffness will cause a higher natural frequency. As it was for the baseline calculations and the sensitivity calculations done in chapter 4 and chapter 5 the vessel roll and cargo sway motions have two notable natural frequencies. The other natural frequencies in the system will influence the responses of these two degrees of freedom in very marginal ways or not at all. The natural frequencies for the tugger line stiffness varied between 20 and 40 kN/m are given in table 6.2. In this table the natural frequency is also converted to the corresponding natural period for easier understanding. The increased stiffness in the system increases the first natural frequency from [redacted] ad/s to [redacted] rad/s. While the frequency increases the period of one harmonic cycle decreases from [redacted] seconds to [redacted] seconds. The second natural frequency is increased from [redacted] rad/s to [redacted] rad/s. Which means that the period is decreased from [redacted] seconds to [redacted] seconds. The changes in the natural frequencies are very small while the stiffness added to the system is fairly small. For example the hydrodynamic stiffness of the vessel roll motion is equal to $5.63 \cdot 10^5 kN/m$ and the restoring stiffness of the pendulum is equal to $2.53 \cdot 10^5 kN/m$. The stiffness added to the system on this degree of freedom due to the tugger winches with a stiffness value of 40 kN/m is equal to $1.27 \cdot 10^4 kN/m$. Thus the tugger wires introduce a stiffness value almost 50 times smaller than the hydrodynamical stiffness of the vessel roll motion and 20 times smaller of the pendulum restoring stiffness of the cargo in the crane.

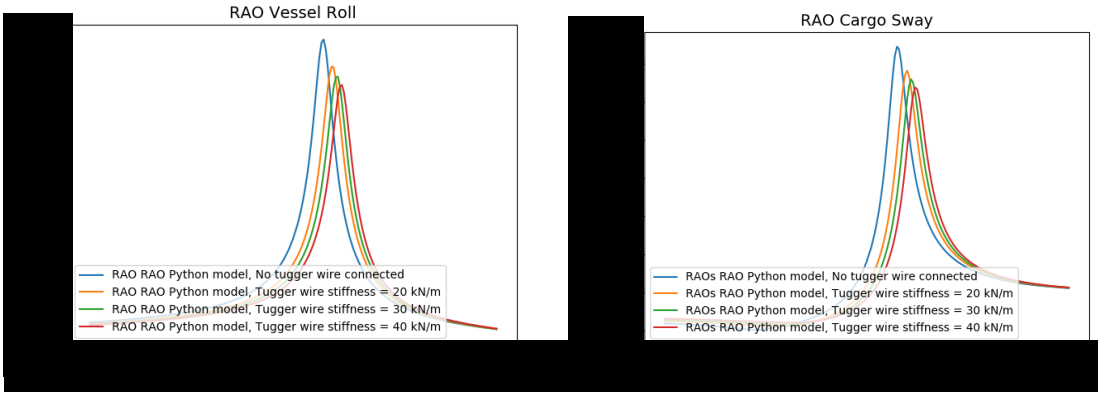

(a) Vessel roll motion RAO for a frequency between [redacted] and [redacted] rad/s for different stiffness values of the tugger winch

(b) Cargo sway motion RAO for a frequency between [redacted] and [redacted] rad/s for different stiffness values of the tugger winch

Figure 6.1: Influence of tugger winches on the vessel roll motion and cargo sway motion RAOs for a frequency between 0.35 and 0.55 rad/s. The stiffness of the tugger ropes is varried between 20 and 40 kN/m.

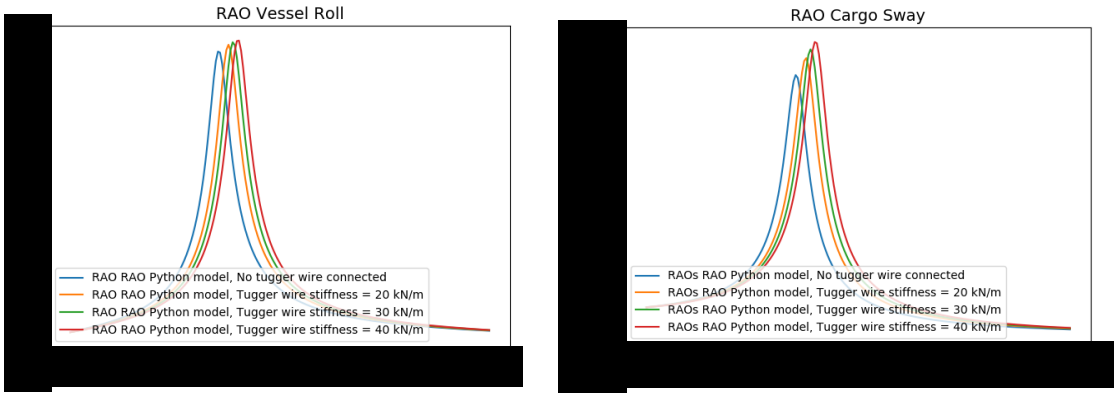

(a) Vessel roll motion RAO for a frequency between [redacted] and [redacted] rad/s for different stiffness values of the tugger winch

(b) Cargo sway motion RAO for a frequency between [redacted] and [redacted] rad/s for different stiffness values of the tugger winch

Figure 6.2: Influence of tugger winches on the vessel roll motion and cargo sway motion RAOs for a frequency between 0.65 and 1.05 rad/s. The stiffness of the tugger ropes is varried between 20 and 40 kN/m.

Table 6.2: Natural frequency comparison between different stiffness values of the tugger wire. The first and second natural frequency are given in radians per second and per second.

Tugger wire stiffess	**First natural frequency**		**Second natural frequency**	
$[kN/m]$	ω [rad/s]	Tn[s]	ω [rad/s]	Tn[s]
No tugger wires connected	[redacted]	[redacted]	[redacted]	[redacted]
20	[redacted]	[redacted]	[redacted]	[redacted]
30	[redacted]	[redacted]	[redacted]	[redacted]
40	[redacted]	[redacted]	[redacted]	[redacted]

In figures 6.1 and 6.2 can be seen that the natural frequencies of the multi-body system shift due to the added stiffness via the tugger wires. The low-stiffness tugger wires do increase the natural frequencies of the multi-body system. Besides increasing the natural frequency the amplitude peak of both the vessel roll and cargo sway motion are reduced and with this reduction the range of frequencies at which large responses occur is decreased. At the second natural frequency the amplitude is increased. This does also increase the frequency range at which large responses occur. This change in the RAOs can be explained with the interaction between the vessel and cargo motions. Since no damping is introduced no energy will dissipate from the system. The

connection between the cargo and vessel transfer energy from one body to the other body in the natural frequency. Dependent on the natural frequency, phases and excitation forces the equilibrium between cargo and vessel responses will vary for different values in the stiffness, damping and mass matrices. Since the stiffness matrix is changed the equilibrium in responses changes.

The period of the first natural frequency lies between [redacted] and [redacted] *s*. In chapter 1 is explained that the swell waves can be a problem during lifting operations. Swell waves often have a period between the 12 and 16 seconds. This means that especially the first natural frequency will be excited by swell waves. To study the influence of the different stiffness values on the motions that can occur during lifting operations the most probable maximums for the vessel roll and cargo sway motions are calculated. While swell waves are less random than wind waves the frequency and height will vary for each individual wave. At the same time the wind will not increase the wave peaks. Therefore a wave spectra with a peak enhancement factor of 1 will be used which makes the JONSWAP which is basically a Pierson-Moskowitz spectrum. The significant wave height is equal to 1 meter in these calculations and the used swell periods are 12, 14 and 16 seconds. In table 6.3 the answers of the most probable maximum calculations are given. In figure 6.3 the wave spectra for a period of 12, 14 and 16 seconds are plotted. This implies that there is less fluctuation in the wave period for a wave spectrum with a higher period than for a wave spectrum with a lower period. At the same time there is more energy in the waves with a higher period than the waves with a lower period. More energy in the waves will mean that the waves will have a larger influence on the vessel and cargo responses when a natural frequency occurs at these waves.

The MPM values calculated and showed in table 6.3 are calculated for different wave spectra with a significant wave height of 1 meter. This wave height makes scaling the MPM values extremely easy, while the MPM value can be multiplied with the actual wave height of a lifting operation to receive the MPM value of the actual lifting operation. In the tool the significant wave height can be adjusted but for this study the wave height is taken equal to 1 meter. All MPM values seem very large. However, in reality lifting operations will most likely not be performed with wave heights of 1 meter while this causes unsafe operations. For all other MPM calculations done in this study these same remarks apply.

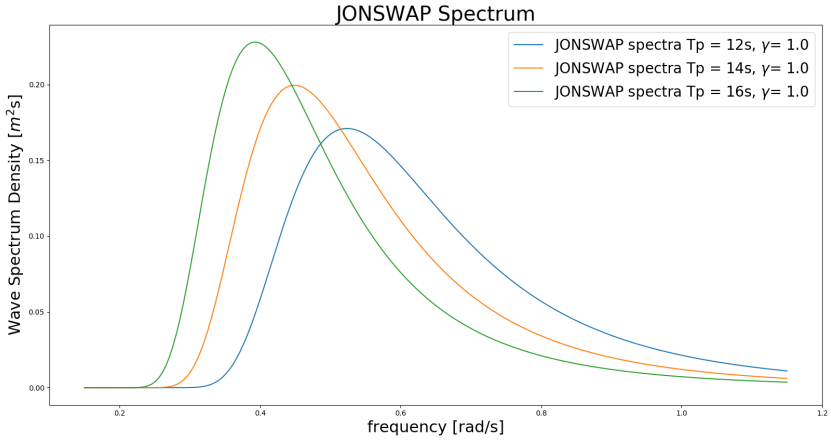

Figure 6.3: Jonswap spectra for different wave periods. The wave periods are varied between 12 and 16 seconds. The wave height is set to 1 meter and the peak enhancement factor is equal to 1.

In figures 6.4 and 6.5 the response spectra for different tugger wires with different wave spectra are given. These response spectra do explain how the multi-body system does react to specific wave spectra. The response spectra are also used to calculate the most probable maximum values of the different tugger wire configurations and different wave spectra. The figure shows that the different wave spectra can influence the height of the responses. For example, the green line in figure 6.4 shows that the wave spectra for a period of 14 seconds generate larger responses from both the vessel roll motion and the cargo sway motion than the other wave spectra do for the different stiffness values. Figure 6.5 shows that the second natural frequency has a larger influence on the response of the cargo sway motion than on the vessel roll motion.

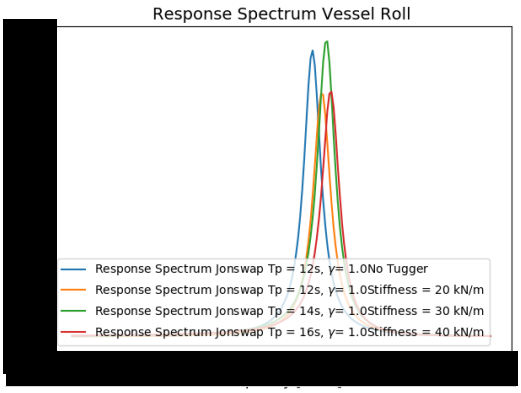

(a) Vessel roll motion RAO for a frequency between [redacted] and [redacted] rad/s for different stiffness values of the tugger winch

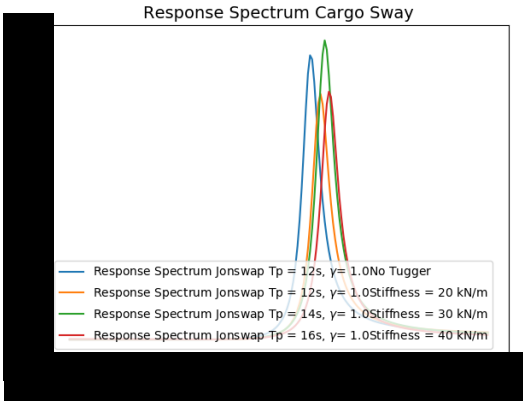

(b) Cargo sway motion RAO for a frequency between [redacted] and [redacted] rad/s for different stiffness values of the tugger winch

Figure 6.4: Influence of tugger winches on the vessel roll motion and cargo sway motion RAOs for a frequency between [redacted] and [redacted] rad/s. The stiffness of the tugger ropes is varried between 20 and 40 kN/m.

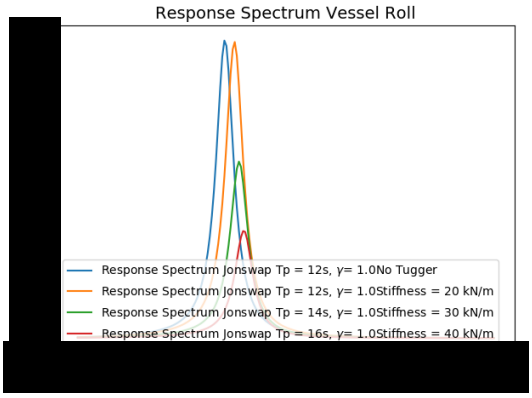

(a) Vessel roll motion RAO for a frequency between [redacted] and [redacted] rad/s for different stiffness values of the tugger winch

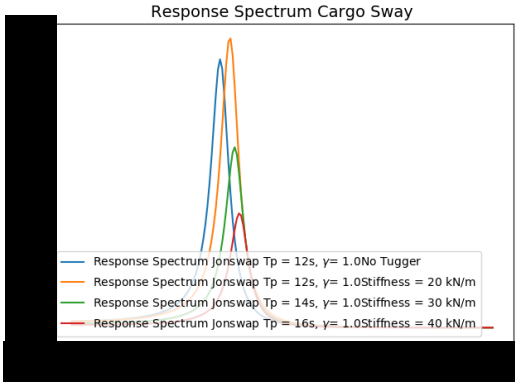

(b) Cargo sway motion RAO for a frequency between [redacted] and [redacted] rad/s for different stiffness values of the tugger winch

Figure 6.5: Influence of tugger winches on the vessel roll motion and cargo sway motion RAOs for a frequency between [redacted] and [redacted] rad/s. The stiffness of the tugger ropes is varried between 20 and 40 kN/m.

When tugger wires are connected the stiffness of the multi-body system increases. In table 6.2 is showed that tugger wires with a stiffness value of 40 kN/m reduce the natural frequency to a maximum period of [redacted] seconds. This shift of the natural period towards the 12 seconds and the decreased response of the vessel roll motion will both influence the MPM of the vessel roll motion. The MPMs for the different tugger wire stiffness values and wave spectra are given in table 6.3. The increased natural frequency will result in higher MPM values for the vessel roll motion for waves with a period of 14 seconds than waves with a higher or lower period. This can already be achieved with tugger wires with a stiffness of 20 kN/m. Since the influence of the second natural frequency was already large on the cargo sway motions, as explained in section 4.4, the increased natural frequencies will only enhance this effect which results in even higher MPM for the cargo sway motion for waves with a period of 12 seconds. The MPM of the cargo sway motions stay around equal for waves with a period of 14 seconds and is even reduced for waves with a period of 16 seconds.

Table 6.3: Most probable maximum comparison between different stiffness values of the tugger wire. The MPMs are calculated for swell waves with a period of 12, 14 and 16 seconds.

Tugger damping [kN/m]	**MPM Tp = 12**		**MPM Tp = 14 s**		**MPM Tp = 16 s**	
	Vessel Roll	Cargo Sway	Vessel Roll	Cargo Sway	Vessel Roll	Cargo Sway
No tugger wires connected	[redacted]	[redacted]	[redacted]	[redacted]	[redacted]	[redacted]
20	[redacted]	[redacted]	[redacted]	[redacted]	[redacted]	[redacted]
30	[redacted]	[redacted]	[redacted]	[redacted]	[redacted]	[redacted]
40	[redacted]	[redacted]	[redacted]	[redacted]	[redacted]	[redacted]

6.1.2. Steel wires

Beside low-stiffness fibre rope tugger wires steel tugger wires can be used to control the cargo. Steel tugger wires have a higher stiffness value for the same diameter of the wire than fibre rope wires. When steel tugger wires are used with a diameter between 0.035 and 0.055 meter stiffness values between 4000 kN/m and 10 000 kN/m can be achieved in this winch configuration. A wire with a diameter of 5.5 centimeter is extremely large for tugger wires. However the large stiffness values they introduce are intresting to study. Tugger wires with these stiffness values will almost create a rigid connection between the vessel and cargo. This increased stiffness will have a much larger influence on the multi-body stiffness than the tugger wires with a relatively low stiffness. In figure 6.7 the RAOs of the vessel roll motion are given for a multi-body system including tugger wires. The wires used in this comparison have an stiffness of 4000, 6000, 8000 or 10000 kN/m. Figure 6.8 shows the RAOs of the cargo sway motion in the same conditions.

The first thing that stands out are the small RAO values of the cargo roll motion. Especially for frequencies between [redacted] rad/s and [redacted] ad/s the responses are small. However, these RAO of the cargo sway motions become extremely large at this frequency. Especially for wire stiffness values equal to 4000 kN/m and 6000 kN/m. Instead of a small frequency range in which a larger amplitude can be seen the multi-body system show large RAO values for wave frequencies between 0.15 and 0.55 rad/s. At frequencies between [redacted] rad/s and [redacted] ad/s the complete opposite occurs. At these higher frequencies shown in figure 6.8 the vessel roll motion shows behaviour that would show that natural frequencies occur here. However these natural frequencies do not show at the responses of the cargo sway motions. Instead of resonance peaks the cargo sway motion show anti-resonance peaks. To understand the natural frequencies tot occur between [redacted] rad/s and [redacted] rad/s the natural frequencies are studied with the eigenvector method. The natural frequencies of the different tugger wire stiffness values are given in table 6.4. The eigenvector is shown in figure 6.6. In this figure can be seen that at this natural frequency the cargo roll motion has the largest response of all degrees of freedom. The stiff tugger wires connect the cargo roll motion to the vessel roll motion and cargo sway motion. However, the responses of the cargo sway motion are lower at the natural frequency than at frequencies around this natural frequency. Another aspect that can be learned from this eigenvector study is the influence of stiff tugger wires on the cargo roll motion. These stiff tugger wires forces the cargo into a rolling motion. This motion can be dangerous during lifting operations. Especially for cargoes with large sizes. Due to some of the simplifications not all moments that act on the cargo body are applied in the model. In reality the rotations of the cargo body can be smaller than the eigenvector shows in figure 6.6.

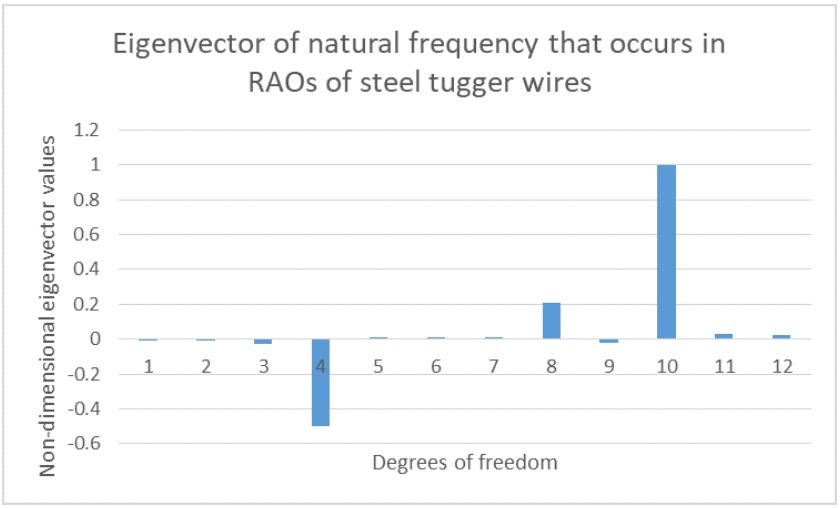

Figure 6.6: Eigenvector of the natural frequency that occurs when steeltugger wires are used. The natural frequency can be seen in figure 6.8a

Even though there are natural frequencies between [redacted] rad/s and [redacted] rad/s the responses of the two bodies might be reduced in comparison with the multibody system without tugger winches. Therefore the most probable maximum for the vessel roll and cargo sway motions are calculated. In table 6.5 the MPMs are shown for all different stiffness values and wave periods used. The wave periods are taken equal to the periods used in section 6.1.1. In this table is shown that most of the most probable maximum values for the vessel roll motion are lower when stiff tugger wires are used. Especially the tugger wire stiffness of 10000kN/m reduces the most probable maximum a lot. The cargo sway motion has a larger MPM for stiffness values between 4000 kN/m and 6000 kN/m. The MPM of the cargo sway motion is smaller for stiffness values between 8000 kN/m and 10000kN/m. However, these stiff tugger wires should not be used. The vessel roll motion and cargo sway motions might show a reduction in their most probable maximum the large response of the cargo roll motion can be dangerous.

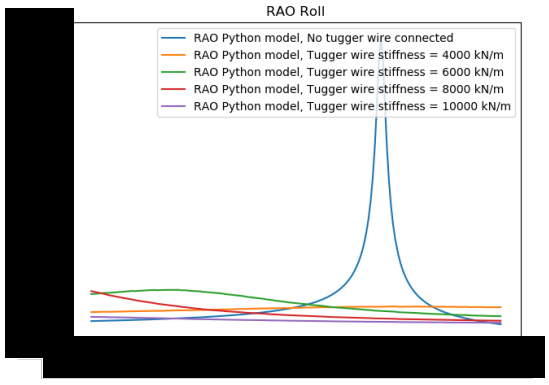

(a) Vessel roll motion RAO for a frequency between [redacted] and [redacted] rad/s for different stiffness values of the tugger winch

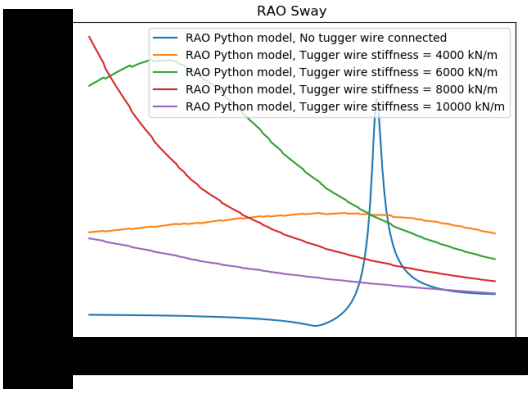

(b) Cargo sway motion RAO for a frequency between [redacted] and [redacted] rad/s for different stiffness values of the tugger winch

Figure 6.7: Influence of tugger winches on the vessel roll motion and cargo sway motion RAO for a frequency between [redacted] and [redacted] rad/s. The stiffness of the tugger ropes is varried between 4000 and 10000 kN/m.

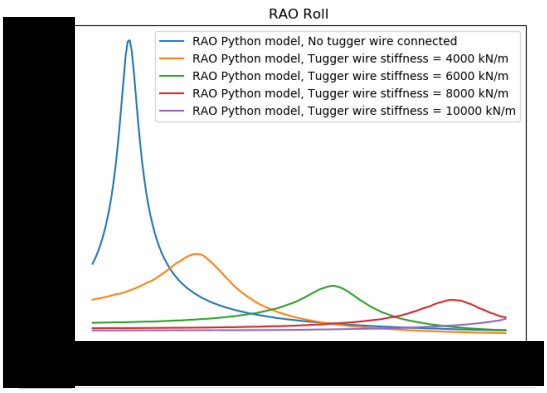

(a) Vessel roll motion RAO for a frequency between [redacted] and [redacted] rad/s for different stiffness values of the tugger winch

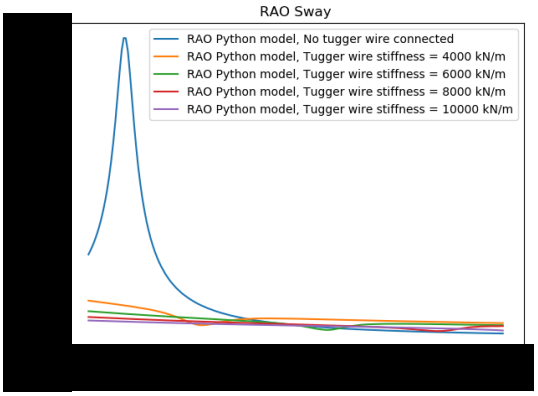

(b) Cargo sway motion RAO for a frequency between [redacted] and [redacted] rad/s for different stiffness values of the tugger winch

Figure 6.8: Influence of tugger winches on the vessel roll motion and cargo sway motion RAO for a frequency between [redacted] and [redacted] rad/s. The stiffness of the tugger ropes is varried between 4000 and 10000 kN/m.

Table 6.4: Natural frequency comparison between different stiffness values of the tugger wire.

Tugger wire stiffness $[kN/m]$	**Natural frequency** ω [rad/s]	Tp [s]
4000	[redacted]	[redacted]
6000	[redacted]	[redacted]
8000	[redacted]	[redacted]
10 000	[redacted]	[redacted]

Table 6.5: Most probable maximum comparison between different stiffness values of the tugger wire. The MPMs are calculated for swell waves with a period of 12, 14 and 16 seconds.

Tugger wire stiffess	**MPM Tp = 12 [s]**		**MPM Tp = 14 [s]**		**MPM Tp = 16 [s]**	
[kN]	Vessel Roll	Cargo Sway	Vessel Roll	Cargo Sway	Vessel Roll	Cargo Sway
No tugger wires connected	[redacted]	[redacted]	[redacted]	[redacted]	[redacted]	[redacted]
4000	[redacted]	[redacted]	[redacted]	[redacted]	[redacted]	[redacted]
6000	[redacted]	[redacted]	[redacted]	[redacted]	[redacted]	[redacted]
8000	[redacted]	[redacted]	[redacted]	[redacted]	[redacted]	[redacted]
10000	[redacted]	[redacted]	[redacted]	[redacted]	[redacted]	[redacted]

Extremely stiff connections can result in rigid connections. In figure 6.9 the RAOs of the vessel sway motion are plotted for different tugger wire stiffness values. These figures show that the cargo sway and vessel sway motion are not coupled in such a way that they influence each other. What can be seen is that the small coupling to the vessel roll and cargo sway motion does not occur when the cargo and vessel are connected with stiff tugger wires. The stiff tugger wires will reduce the amount of energy transferred from the vessel roll motion and cargo sway motion to the vessel sway motion around this natural frequency.

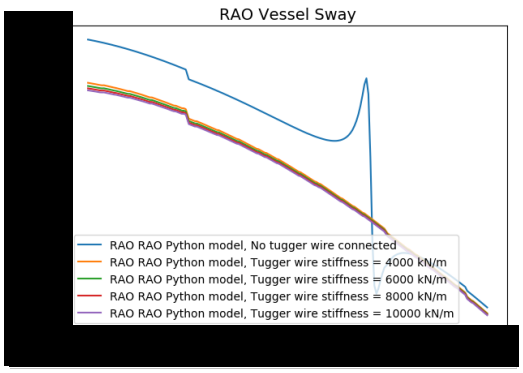

(a) Vessel sway motion RAO for a frequency between [redacted] and [redacted] rad/s for different stiffness values of the tugger winch

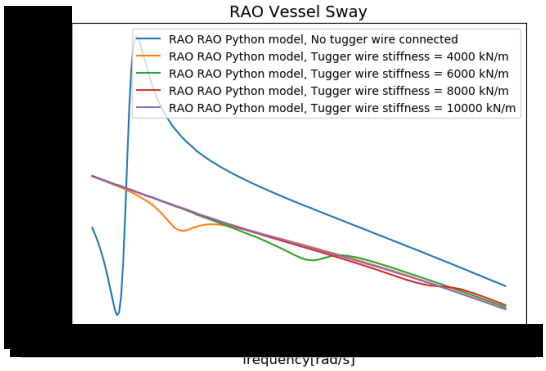

(b) Vessel sway motion RAO for a frequency between [redacted] and [redacted] rad/s for different stiffness values of the tugger winch

Figure 6.9: Influence of tugger winches on the vessel roll motion and cargo sway motion RAO for a frequency between [redacted] and [redacted] rad/s. The stiffness of the tugger ropes is varried between 4000 and 10000 kN/m.

6.2. Location of tugger winches

In section 6.1 is explained how tugger winches with a low stiffness and tugger winches with a large stiffness value influence the vessel and cargo responses. The configuration of the tugger winches are kept constant in these cases. However, a change in the configuration can show interesting changes in the responses of the vessel and cargo motions. Therefore multiple configurations are studied. In section 3.5 is explained that the stiffness and damping coefficients for every direction are dependent on the length ratio between the length of in a specific direction and total length of the tugger wire. When the configuration is changed the stiffness components of the tugger wires will change. These stiffness values will influence the responses of the vessel and cargo responses.

Three different tugger winch configurations are compared. The configurations used to study the influences are given in table 6.6. In this table the location of the connection to the cargo is given by the padeye value. All the three different configurations will consist of two tugger winches and the tugger wires will have a stiffness value of 30 kN/m. Since the same amount of tugger winches are used the total added stiffness in the multi-body system will stay the same. The first configuration is the same configuration that is used in section 6.1. In this configuration the tugger winches have a relatively large X-component. This results in relatively large stiffness values in X-direction. For this reason the second configuration has been chosen so that there is no distance in X direction between the tugger winch and the connection with the load. This increases the stiffness components in Y and Z direction. These two stiffness components will influence the vessel roll and cargo sway motions the most. In the third configuration the winches are located at opposite sides in X and Y direction. Since the two winches will apply opposite rotational moments in certain directions the influence on the rotations off both the vessel and cargo will change.

Table 6.6: Three different tugger winch configurations used to calculate the influence of the tugger winch configuration.

Coordinate	**Configuration 1**		**Configuration 2**		**Configuration 3**	
	Tugger Winch 1	Tugger Winch 2	Tugger Winch 1	Tugger Winch 2	Tugger Winch 1	Tugger Winch2
Winch X [m]	-30	30	-10	10	-30	30
Winch Y [m]	-15	-15	-15	-15	-15	15
Winch Z [m]	10	10	10	10	10	10
Padeye X [m]	-10	10	-10	10	-10	10
Padeye Y [m]	-5	-5	-5	-5	-5	5
Padeye Z [m]	-5	-5	-5	-5	-5	-5
X stiffness [kN/m]	22.2	22.2	0.0	0.0	22.2	22.2
Y stiffness [kN/m]	11.1	11.1	16.6	16.6	11.1	11.1
Z stiffness [kN/m]	16.7	16.7	25.0	25.0	16.7	16.7

In configuration 2 the X component of the stiffness value is reduced. While the stiffness of the complete tugger line stays equal to the stiffness value in configuration the stiffness components in Y and Z direction will increase. The stiffness component in X direction does not influence the vessel roll and cargo sway motion. The roll motion is influenced by both the stiffness components in Y and Z direction and the cargo sway motion is only influenced by the stiffness components in Y direction. This means that the stiffness components that are import for the natural frequency of the combined vessel roll and cargo sway motion increases. The increased stiffness values will cause higher natural frequencies. This can be seen in figures 6.10 and 6.11. The natural frequencies of all different tugger winch configurations are given in table 6.7.

In configuration 3 the X and Y locations of the two winches and connections to the cargo are mirrored. Since the X, Y and Z components of the tugger wire will have the same length as in configuration 1 the stiffness components in these directions will have the same value as in configuration 1. However, the rotational moments and restoring forces due to rotations of the two bodies are dependent on the location of the winch and location of the connection to the cargo. Since these locations are in opposite direction for both winches the rotational moments transferred via the two tugger wires will cancel each other for some degrees of freedom. However some other relations that where cancelled in the first configuration occur in configuration 3. The most notable change is the relation between the vessel roll and vessel pitch motion. In the first configuration this relation was cancelled but in the third configuration there are large stiffness values between these two degrees of freedom. The vessel pitch and vessel yaw motion are also coupled via the tugger wires in the third configuration while this connection was cancelled in the first configuration. This influence will be studied later in this section. The stiffness components between the vessel roll and cargo sway motion do also differ between the first and third configuration. The stiffness components between these two degrees of freedom are smaller in the third configuration which will reduce the stiffness in the multi-body system and reduce the natural frequency. This can be seen in figures 6.10 and 6.11. This tugger wire configuration reduces the responses of the vessel and cargo motions. This can also be seen in the figures.

As stated earlier the third tugger winch configuration introduces larger stiffness values to the vessel pitch and cargo sway motion. To study the influence of the tugger winch configuration on the vessel pitch and cargo surge motion the RAOs of these degrees of freedom are shown in figures 6.12 and 6.13. In these figures can be seen that the cargo surge motion is extremely large for frequencies between [redacted] rad/s and [redacted] rad/s. In this range of frequencies two natural frequencies are shown. one at [redacted] rad/s and one at [redacted] rad/s. The natural frequency of [redacted] rad/s is the same natural frequency that occurs in the vessel roll and cargo sway motion. This shows that the third tugger winch configuration couples these vessel roll and cargo sway motions to the vessel pitch and cargo surge motion. This can also be seen in the eigenvector given in figure 6.15. The natural frequency at [redacted] rad/s is the natural frequency of the cargo surge motion This motion is already studied in section 4.2. However due to the coupling between the vessel roll motion and cargo sway motion the cargo surge motion receives energy from waves with a direction of 90 degrees and the natural frequency of this degree of freedom gets excited. The eigenvector of the natural frequency of [redacted] rad/s is shown in figure 6.14. This figure shows that the cargo surge motion also transfers energy to the vessel roll and cargo sway motion. This explains the new natural frequency that can be seen in figures 6.10b and 6.11b. The excitations of the vessel roll motion and cargo sway motion is also proof that tugger winch configuration 3 couples the cargo surge to the cargo sway and vessel roll motions.

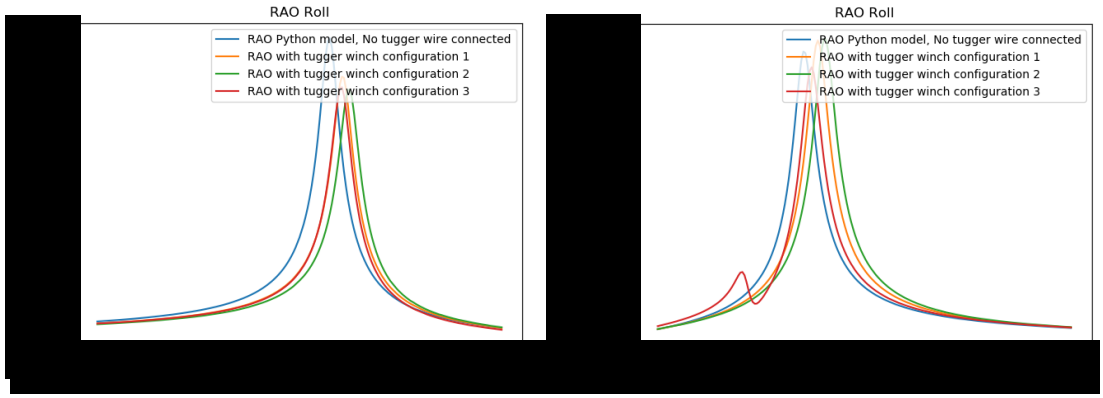

(a) Vessel roll motion RAO for a frequency between [redacted] and [redacted] rad/s for different stiffness values of the tugger winch

(b) Vessel roll motion RAO for a frequency between [redacted] and [redacted] rad/s for different stiffness values of the tugger winch

Figure 6.10: Influence of the tugger winch configuration on the vessel roll motion RAO. Configurations of the tugger winches are given in table 6.6

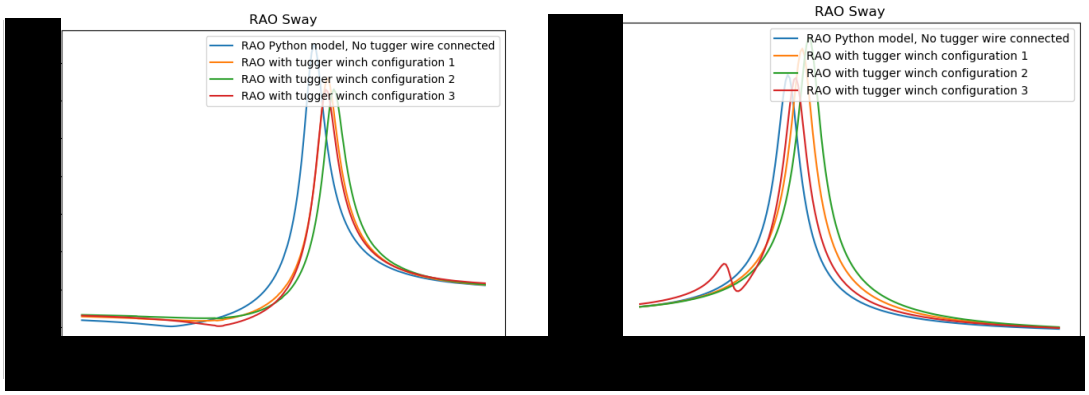

(a) Cargo sway motion RAO for a frequency between [redacted] and [redacted] rad/s for different stiffness values of the tugger winch

(b) Cargo sway motion RAO for a frequency between [redacted] and [redacted] rad/s for different stiffness values of the tugger winch

Figure 6.11: Influence of the tugger winch configuration on the cargo sway motion RAO. Configurations of the tugger winches are given in table 6.6

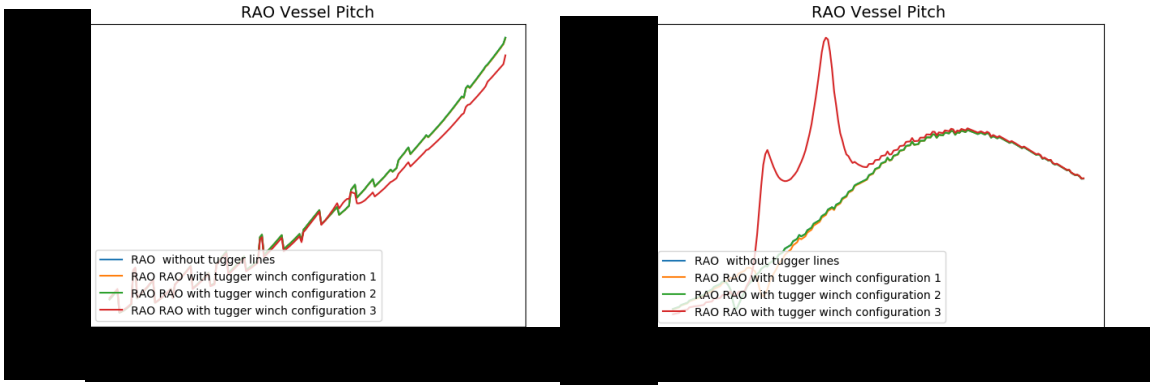

(a) Vessel pitch motion RAO for a frequency between [redacted] and [redacted] rad/s for different stiffness values of the tugger winch

(b) Vessel pitch motion RAO for a frequency between [redacted] and [redacted] rad/s for different stiffness values of the tugger winch

Figure 6.12: Influence of the tugger winch configuration on the vessel pitch motion RAO. Configurations of the tugger winches are given in table 6.6

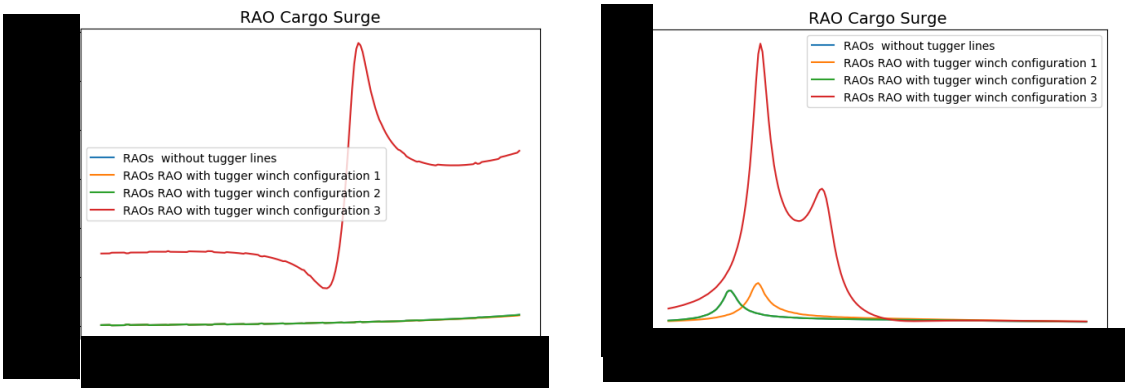

(a) Cargo surge motion RAO for a frequency between [redacted] and [redacted] rad/s for different stiffness values of the tugger winch

(b) Cargo surge motion RAO for a frequency between [redacted] and [redacted] rad/s for different stiffness values of the tugger winch

Figure 6.13: Influence of the tugger winch configuration on the cargo surge motion RAO. Configurations of the tugger winches are given in table 6.6

As explained shows the second configuration the same behaviour that tugger wires with an increased stiffness do. This can also be translated to the MPM calculations. The second tugger winch configuration reduces the roll motion MPM for all three different wave periods. However as explained in section 6.1.1 the MPM of the cargo sway motion increases for the wave spectra with small periods. In this specific case the cargo sway motion MPM is equal for winch configuration 1 and 2 for a wave spectrum with a period of 12 seconds. In configuration 3 the RAOs of the vessel roll and cargo sway motions are reduced. This results in lower MPM values for all different wave spectra. Although the third configuration adds an extra natural frequency to the two most important degrees of freedom the influence of the new natural frequency is so small that the MPMs are not increased due to this natural frequency.

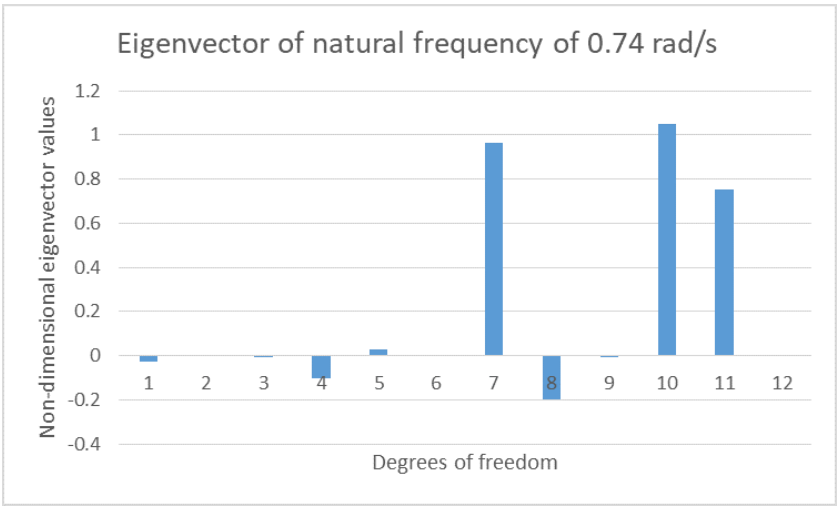

Figure 6.14: Eigenvector of the natural frequency of [redacted] rad/s for the multi-body system with the third tugger winch configuration. The tugger winch configurations are given in table 6.6

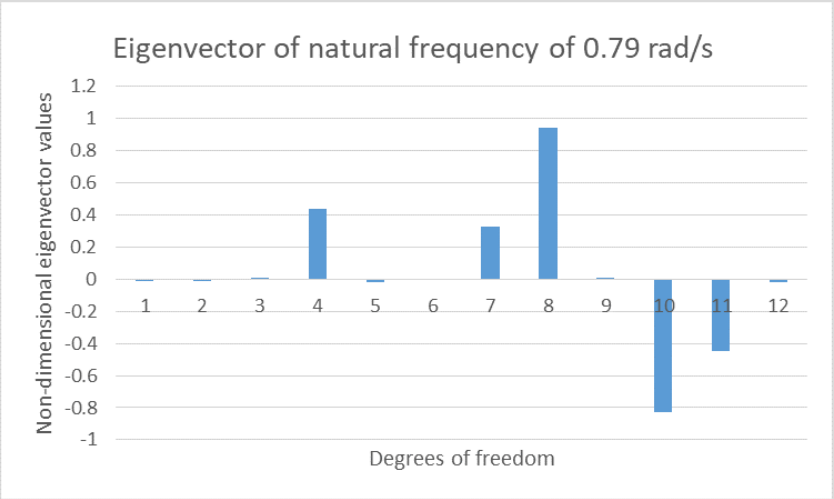

Figure 6.15: Eigenvector of the natural frequency of [redacted] rad/s for the multi-body system with the third tugger winch configuration. The tugger winch configurations are given in table 6.6

Table 6.7: Natural frequency comparison between different stiffness values of the tugger wire. The first and second natural frequency are given in radians per second and per second.

Tugger winch configuration	**First natural frequency**		**Second natural frequency**	
$[kN/m]$	ω [rad/s]	Tn[s]	ω [rad/s]	Tn[s]
No tugger wires connected	[redacted]	[redacted]	[redacted]	[redacted]
Configuration 1	[redacted]	[redacted]	[redacted]	[redacted]
Configuration 2	[redacted]	[redacted]	[redacted]	[redacted]
Configuration 3	[redacted]	[redacted]	[redacted]	[redacted]

Table 6.8: Most probable maximum comparison between different tugger winch configurations. The tugger winch configurations can be found in table 6.6. The MPMs are calculated for swell waves with a period of 12, 14 and 16 seconds.

Tugger Winch Configuration	**MPM Tp = 12**		**MPM Tp = 14 s**		**MPM Tp = 16 s**	
$[kN/m]$	Roll	Sway	Roll	Sway	Roll	Sway
No tugger wires connected	[redacted]	[redacted]	[redacted]	[redacted]	[redacted]	[redacted]
Configuration 1	[redacted]	[redacted]	[redacted]	[redacted]	[redacted]	[redacted]
Configuration 2	[redacted]	[redacted]	[redacted]	[redacted]	[redacted]	[redacted]
Configuration 3	[redacted]	[redacted]	[redacted]	[redacted]	[redacted]	[redacted]

6.3. Passive compensation

Now that the influence of tugger wires with a small and large stiffness component are known damping can be added to the system. The least complex way to implement damping is via a passive system. In section 2.5 and appendix E is explained that constant tension tugger winches are reactive to the relative motions between the cargo and the vessel. Due to the reactive behaviour the tension is adjusted after a fluctuation in the tension occurs. Over the extend of a full harmonic oscillation damping is applied to the multi-body system. However, it is difficult to impossible to determine the amount of damping that will be applied to the system via constant tension tugger winches. Another way to apply damping is via a system that is related to the passive heave compensation modules. Via hydraulics or pneumatics damping is added to the system. However, it is also impossible to determine the damping for such a system and developing a passive damping module is not part of this thesis. Reducing the motions is part of the thesis. Therefore it is assumed that damping can be added to the system in a passive way. Since there are multiple examples given to apply passive damping this is an accurate assumption.

Since the exact amount of damping can not be calculated for passive compensation systems it is assumed that the passive compensators will apply a percentage of the critical damping. The critical damping will be calculated for the stiffness applied via the tugger wires and the mass of the cargo. Since passive damping is not the most optimal form of damping it is assumed that the amount of damping will be equal to 5% to 15% of the critical damping. While the stiff tugger winches do not show any natural frequencies close to the swell wave periods the passive compensation is applied to the less stiff tugger wires used in section 6.1.1. Therefore the stiffness of the tugger wire is equal to 30 kN/m in this section. In figures 6.16 and 6.17 the RAOs are given for the vessel roll motion and cargo sway motion with damping applied. In figures 6.16a and 6.17a can be seen that the damping reduces the responses at the natural frequencies significantly. However, these figures do also show that damping also broadens the amplitude of the response around the natural frequency. However the extent to which the response spectra is broaden is negligible. Since the amount of applied damping is relatively small the natural frequency should not be influenced by the damping. This can be seen in the figures and also in table 6.9.

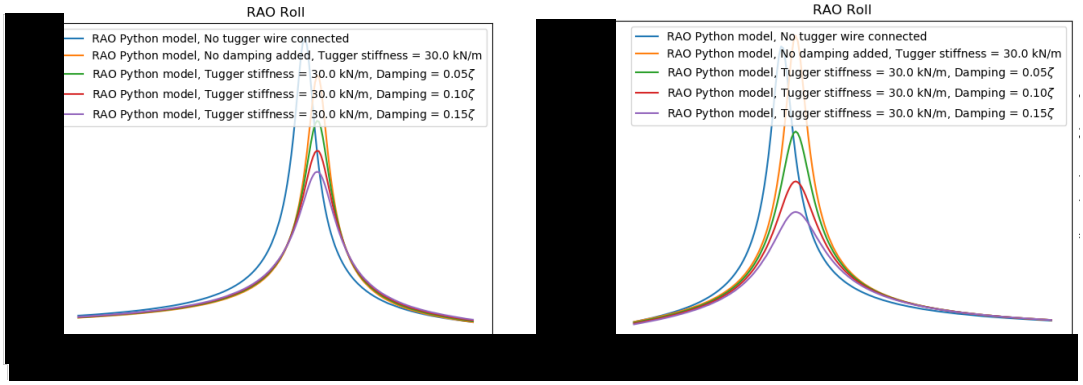

(a) Vessel roll motion RAO for a frequency between [redacted] and [redacted] rad/s for different damping values of the tugger winch

(b) Vessel roll motion RAO for a frequency between [redacted] and [redacted] rad/s for different damping values of the tugger winch

Figure 6.16: Influence of damping applied via tugger winches on the vessel roll motion RAO. The damping of the tugger ropes is varied between 5% and 15% of ξ.

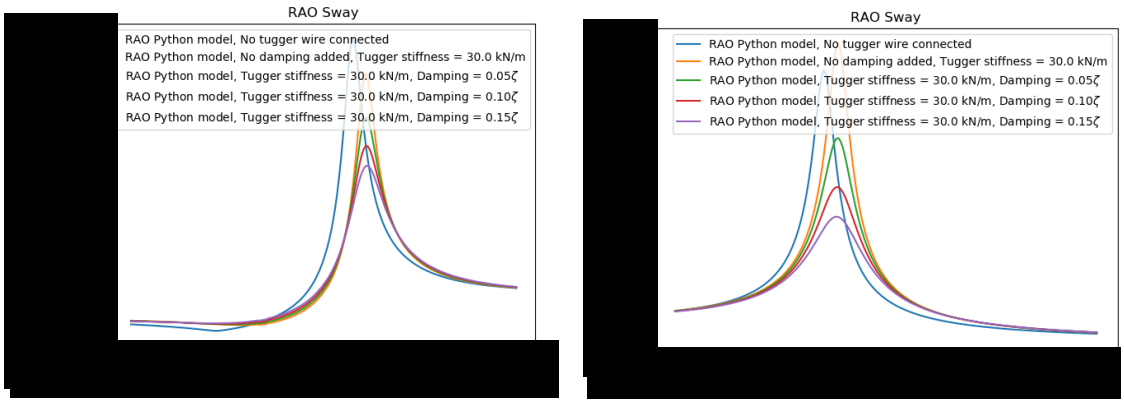

(a) Cargo sway motion RAO for a frequency between [redacted] and [redacted] rad/s for different damping values of the tugger winch

(b) Cargo sway motion RAO for a frequency between [redacted] and [redacted] rad/s for different damping values of the tugger winch

Figure 6.17: Influence of damping applied via tugger winches on the cargo sway motion RAO. The damping of the tugger ropes is varied between 5% and 15% of ξ.

Table 6.9: Natural frequency comparison between different dampin values of the tugger wire. The tugger wire stiffness used in the calculations is 30 kN. The MPMs are calculated for swell waves with a period of 12, 14 and 16 seconds.

Tugger damping	**First natural frequency**		**Second natural frequency**	
	ω [rad/s]	Tp [s]	ω [rad/s]	Tp [s]
No damping applied	[redacted]	[redacted]	[redacted]	[redacted]
0.05%	[redacted]	[redacted]	[redacted]	[redacted]
0.1%	[redacted]	[redacted]	[redacted]	[redacted]
0.15%	[redacted]	[redacted]	[redacted]	[redacted]

In tables 6.10 till 6.12 the most probable maximum can be found for the same three different wave periods as used in the previous sections and the three different damping percentages. The reduction of the responses due to damping influence the MPM calculations. The more damping is applied damping the greater the reduction of the most probable maximum for all different wave periods. In this multi-body system damping does exactly what we expect. As explained in section 6.1.1, the natural frequencies are located within the energy density distribution of the wave spectra. Since damping has the most influence on the natural frequencies the damping will reduce the vessel and cargo responses. However between the two natural frequencies of the cargo sway motion there is a fairly high response for the cargo sway motion. Between [redacted] and [redacted] rad/s the cargo sway motion has a response of [redacted] meters. Damping is not effective at influencing this response. Which explains the high MPM values of the cargo sway motion.

Tables 6.10 till 6.12 also show the reduction of the vessel roll motion MPM and cargo sway motion MPM relative to the MPM of these two degrees of freedom where no tugger wires are applied to the multi-body system. In the tables can be seen that small amounts of damping have a relatively large influence on the reduction of the MPMs. For all three different wave periods the reduction of the MPM due to damping has the same order size. However, larger amounts of damping have a relatively larger influence for MPMs for a period of 12 seconds. In figures 6.16 and 6.17 can be seen that damping has the largest influence on the natural frequency around [redacted] rad/s. While wave spectra with a period of 12 seconds have a larger influence on this natural frequency than wave spectra with a larger period the influence of damping is larger on the MPMs is larger for this period. Besides the small differences between the different wave spectra periods it can be stated that damping has a positive effect on reducing both the vessel roll and cargo sway motion.

Table 6.10: Most probable maximum comparison between different critical damping values of the tugger wire. The tugger wire has a stiffness of 30 kN. The MPMs are calculated for swell waves with a period of 12 seconds.

Tugger Damping	**MPM Tp = 12**			
	Vessel Roll		Cargo Sway	
	[deg]	reduction	[deg]	reduction
No tugger winch	[redacted]	[redacted]	[redacted]	[redacted]
Stiffness 30 kN/m, No Damping	[redacted]	[redacted]	[redacted]	[redacted]
Stiffness 30 kN/m, Damping = $0.05\xi_{crit}$	[redacted]	[redacted]	[redacted]	[redacted]
Stiffness 30 kN/m, Damping = $0.10\xi_{crit}$	[redacted]	[redacted]	[redacted]	[redacted]
Stiffness 30 kN/m, Damping = $0.15\xi_{crit}$	[redacted]	[redacted]	[redacted]	[redacted]

Table 6.11: Most probable maximum comparison between different critical damping values of the tugger wire. The tugger wire has a stiffness of 30 kN. The MPMs are calculated for swell waves with a period of 14 seconds.

Tugger Damping	**MPM Tp = 14**			
	Vessel Roll		Cargo Sway	
	[deg]	reduction	[deg]	reduction
No tugger winch	[redacted]	[redacted]	[redacted]	[redacted]
Stiffness 30 kN/m, No Damping	[redacted]	[redacted]	[redacted]	[redacted]
Stiffness 30 kN/m, Damping = $0.05\xi_{crit}$	[redacted]	[redacted]	[redacted]	[redacted]
Stiffness 30 kN/m, Damping = $0.10\xi_{crit}$	[redacted]	[redacted]	[redacted]	[redacted]
Stiffness 30 kN/m, Damping = $0.15\xi_{crit}$	[redacted]	[redacted]	[redacted]	[redacted]

Table 6.12: Most probable maximum comparison between different critical damping values of the tugger wire. The tugger wire has a stiffness of 30 kN. The MPMs are calculated for swell waves with a period of 16 seconds.

Tugger Damping	**MPM Tp = 16**			
	Vessel Roll		Cargo Sway	
	[deg]	reduction	[deg]	reduction
No tugger winch	[redacted]	[redacted]	[redacted]	[redacted]
Stiffness 30 kN/m, No Damping	[redacted]	[redacted]	[redacted]	[redacted]
Stiffness 30 kN/m, Damping = $0.05\xi_{crit}$	[redacted]	[redacted]	[redacted]	[redacted]
Stiffness 30 kN/m, Damping = $0.10\xi_{crit}$	[redacted]	[redacted]	[redacted]	[redacted]
Stiffness 30 kN/m, Damping = $0.15\xi_{crit}$	[redacted]	[redacted]	[redacted]	[redacted]

6.4. Active damping

Another way to apply damping is via an active system. In an active system damping will be applied by a winch as explained in section 2.5 and appendix E. In an active system the applied damping follows from the speed that the controller acts and the limitations of the winch. Since it is not the purpose of this research to develop active tugger winches the dimensions and limitations are unknown. However, a research from Heerema Marine Contractors [19] shows that there are tugger winches with a capacity of more than 600 $kN/m/s$. When the critcal damping equation given in equation 3.14 is used for tugger winches with a stiffness of 30 kN/m it shows that the critical damping is equal to [redacted] $kN/m/s$ when the critical damping is calculated with the tugger wire stiffness and mass of the cargo. This means that the critical damping is lower than the damping that can be applied with active tugger winches. Therefore the active winch configuration will be used to calculate the influence of high damping values.

In section 6.1 it became clear that stiff tugger winches will increase the natural frequencies by such a large value that the two important natural frequencies of the multi-body system are almost not excited by the waves with a period of 12 to 16 seconds. However, the response of the roll motion between these two natural frequencies where quite large. The response of the roll motion is not influenced by the damping. Therefore the less stiff tugger wires are used in the active tugger winch configuration. The influence of tugger wires with a stiffness of 30 kN/m in combination with a damping of 100, 200, 300 and 400 $kN/m/s$ are plotted in figures 6.18 and 6.19. The damping values of 100, 200 and 300 $kN/m/s$ are smaller than the critical damping. Therefore they should reduce the responses of the vessel and cargo motions. The damping values of 400 $kN/m/s$ is larger than the critical damping value. The over damped system causes a slower return to the equilibrium positions of the vessel and cargo bodies after an excitation. This is explained in section 2.5 and can be seen in figure 2.8. However, the stiffness of the multi-body system is not only dependent on the tugger wires. The restoring stiffness of the coupling of the cargo via the crane cables and the vessel hydrodynamic restoring stiffness are also a large part of the stiffness values. While these stiffness values are not taken into account for the critical damping calculation the damping will not be equal to the critical damping of the multi-body system.

In figures 6.18 and 6.19 can be seen that damping reduces the amplitude of the RAOs. However, damping does also increase the width of the response spectra. This phenomenom is extremely clear in figures 6.18a and 6.19a. While waves will not occur in a single frequency but in a wave spectra as explained in section 2.2 this wider response spectra might increase the most probable maximum when damping is increased. Therefore the response spectra of the vessel roll motion and cargo sway motion are given in figures 6.20 and 6.21. When the energy density function of a wave spectrum lies outside but close to the natural frequency of a degree of freedom the MPMs might increase. The response spectra show that the increased damping results in smaller response peaks but a larger response range. However, the amplitude peak is reduced so much that all the larger range of responses should not increase the MPMs. In the figures can also be seen that damping larger than the critical damping values will decrease the amplitude of the responses while the critical damping of the combined stiffness values in the degrees of freedom are not exceeded.

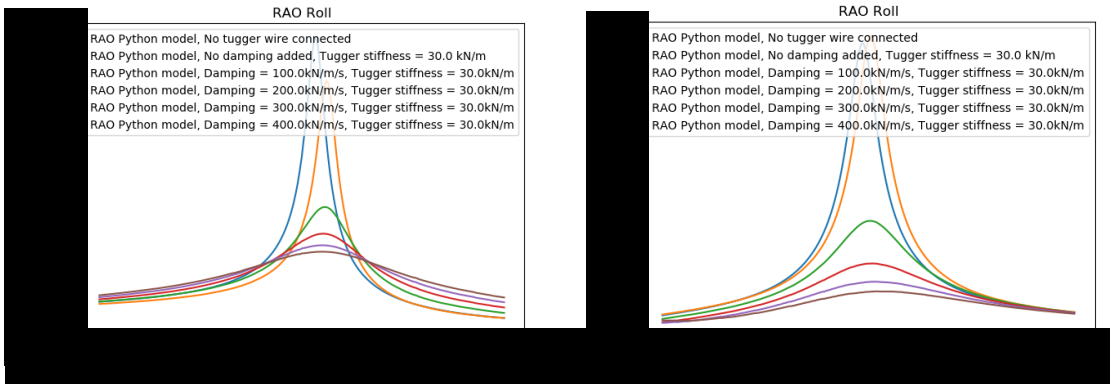

(a) Vessel roll motion RAO for a frequency between [redacted] and [redacted] rad/s for different damping values of the tugger winch

(b) Vessel roll motion RAO for a frequency between [redacted] and [redacted] rad/s for different damping values of the tugger winch

Figure 6.18: Influence of damping applied via tugger winches on the vessel roll motion RAO. The stiffness of the tugger wires is set to $30 kN/m$ and the damping is varied between 100 and 400 $kN/m/s$

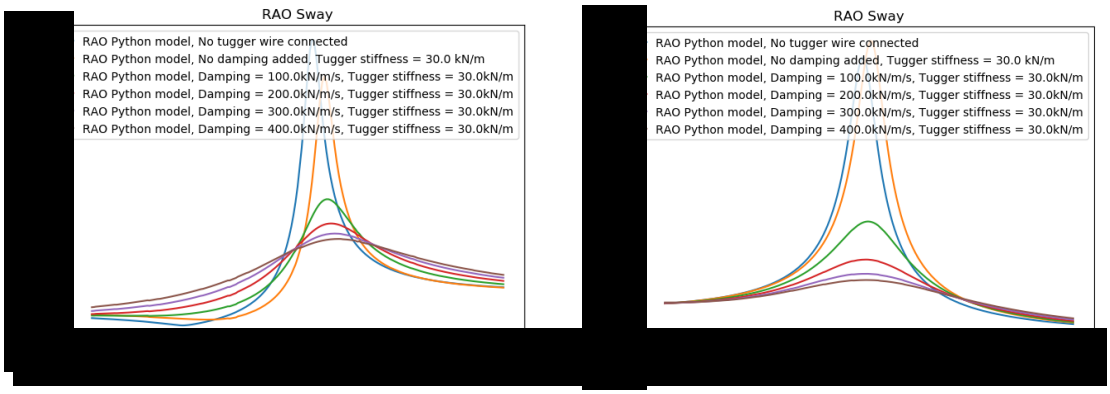

(a) Cargo sway motion RAO for a frequency between [redacted] and [redacted] rad/s for different damping values of the tugger winch

(b) Cargo sway motion RAO for a frequency between [redacted] and [redacted] rad/s for different damping values of the tugger winch

Figure 6.19: Influence of damping applied via tugger winches on the cargo sway motion RAO. The stiffness of the tugger wires is set to $30 kN/m$ and the damping is varied between 10 and 30 $kN/m/s$

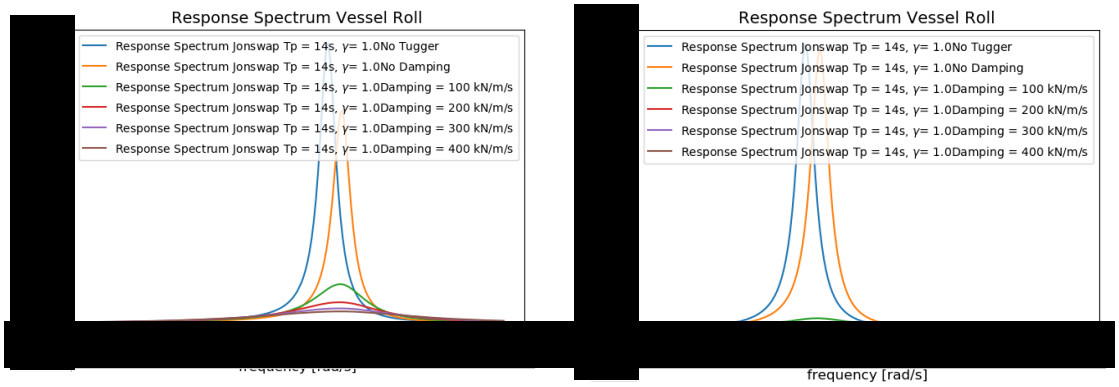

(a) Vessel roll motion response for a frequency between [redacted] and [redacted] rad/s for different damping values of the tugger winch. The wave spectra used is a Jonswap spectra with Tp = 14 s and γ = 1.0

(b) Vessel roll motion response for a frequency between [redacted] and [redacted] rad/s for different damping values of the tugger winch. The wave spectra used is a Jonswap spectra with Tp = 14 s and γ = 1.0

Figure 6.20: Influence of damping applied via tugger winches on the vessel roll motion response spectra. The stiffness of the tugger wires is set to 30kN/m and the damping is varied between 100 and 400 $kN/m/s$. The wave spectra used is a Jonswap spectra with Tp = 14 s and γ = 1.0

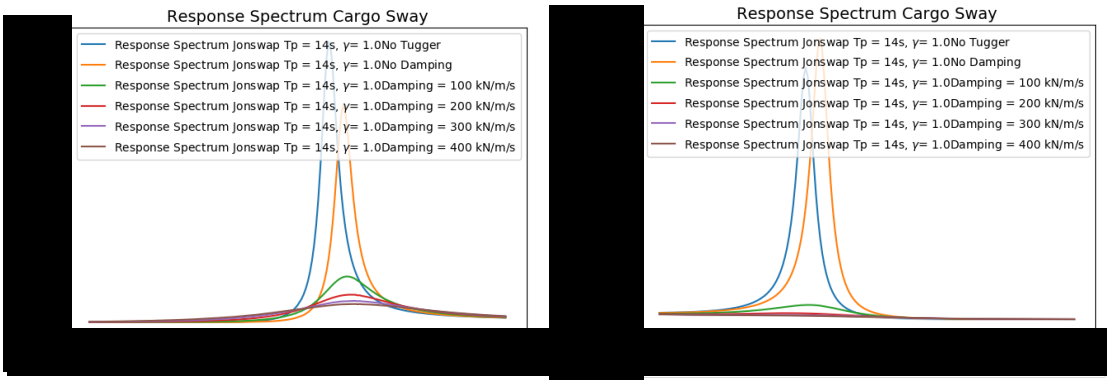

(a) Cargo sway motion response for a frequency between [redacted] and [redacted] rad/s for different damping values of the tugger winch. The wave spectra used is a Jonswap spectra with Tp = 14 s and γ = 1.0

(b) Cargo sway motion response for a frequency between [redacted] and [redacted] rad/s for different damping values of the tugger winch. The wave spectra used is a Jonswap spectra with Tp = 14 s and γ = 1.0

Figure 6.21: Influence of damping applied via tugger winches on the cargo sway motion response spectra. The stiffness of the tugger wires is set to 30kN/m and the damping is varied between 100 and 400 $kN/m/s$. The wave spectra used is a Jonswap spectra with Tp = 14 s and γ = 1.0

In tables 6.13 till 6.15 the most probable maximum values calculated with the multi-body tool with applied damping values of 100, 200, 300 and 400 $kN/m/s$. In the tables wave spectra with a period of 12, 14 and 16 seconds are used to calcualte the MPM values. The reduction relative to the MPM of the multi-body system without tugger wires is also shown. In the tables can be seen that the difference in reduction due to different damping values is relatively small. The tables show that a damping value of 400 $kN/m/s$ has a smaller influence on the most probable maximum than a damping a damping value of 300 $kN/m/s$ for all different wave spectra periods.

Tugger wires with a damping value of 300 $kN/m/s$ show the largest reduction of the MPM values for both the vessel roll and cargo sway motions. As explained in section 6.3 the natural frequency around [redacted] rad/s is reduced more than the natural frequency around [redacted] rad/s. This also applies for large amounts of damping, hence the MPMs for a wave spectra with a period closer to this natural frequency show a larger reduction.

For the wave spectra with a period of 12 seconds the difference between 100 $kN/m/s$ damping and 300 $kN/m/s$ is the influence of an increased amount of damping the largest. For all other wave spectra periods the increased reduction due to larger damping values is relatively smaller. The vessel roll motion MPM has a reduction of 41.9 % for damping values equal to 100 $kN/m/s$ and a reduction of [redacted] % for damping values equal to 300 $kN/m/s$. Thus 200 $kN/m/s$ extra damping increases the reduction of the MPM value with only [redacted] %. For the cargo sway motion and all other wave spectra periods the increased reduction is even smaller. This shows that small amounts of damping have a relatively large influence on the MPM values of the multi-body system. This was also a result given in section 6.3.

Table 6.13: Most probable maximum comparison between different damping values and a stiffness value of 30 kN/m. The damping has been varied between 100 $kN/m/s$ and 400 $kN/m/s$. The swell waves have a period of 12 seconds.

Tugger Damping	**MPM Tp = 12**			
	Vessel Roll		Cargo Sway	
	[deg]	reduction	[deg]	reduction
No tugger winch	[redacted]	[redacted]	[redacted]	[redacted]
Stiffness 30 kN/m, No Damping	[redacted]	[redacted]	[redacted]	[redacted]
Stiffness 30 kN/m, Damping = 100 kN/m/s	[redacted]	[redacted]	[redacted]	[redacted]
Stiffness 30 kN/m, Damping = 200 kN/m/s	[redacted]	[redacted]	[redacted]	[redacted]
Stiffness 30 kN/m, Damping = 300 kN/m/s	[redacted]	[redacted]	[redacted]	[redacted]
Stiffness 30 kN/m, Damping = 400 kN/m/s	[redacted]	[redacted]	[redacted]	[redacted]

Table 6.14: Most probable maximum comparison between different damping values and a stiffness value of 30 kN/m. The damping has been varied between 100 $kN/m/s$ and 400 $kN/m/s$. The swell waves have a period of 14 seconds.

Tugger Damping	**MPM Tp = 14**			
	Vessel Roll		Cargo Sway	
	[deg]	reduction	[deg]	reduction
No tugger winch	[redacted]	[redacted]	[redacted]	[redacted]
Stiffness 30 kN/m, No Damping	[redacted]	[redacted]	[redacted]	[redacted]
Stiffness 30 kN/m, Damping = 100 kN/m/s	[redacted]	[redacted]	[redacted]	[redacted]
Stiffness 30 kN/m, Damping = 200 kN/m/s	[redacted]	[redacted]	[redacted]	[redacted]
Stiffness 30 kN/m, Damping = 300 kN/m/s	[redacted]	[redacted]	[redacted]	[redacted]
Stiffness 30 kN/m, Damping = 400 kN/m/s	[redacted]	[redacted]	[redacted]	[redacted]

Table 6.15: Most probable maximum comparison between different damping values and a stiffness value of 30 kN/m. The damping has been varied between 100 $kN/m/s$ and 400 $kN/m/s$. The swell waves have a period of 16 seconds.

Tugger Damping	**MPM Tp = 16**			
	Vessel Roll		Cargo Sway	
	[deg]	reduction	[deg]	reduction
No tugger winch	[redacted]	[redacted]	[redacted]	[redacted]
Stiffness 30 kN/m, No Damping	[redacted]	[redacted]	[redacted]	[redacted]
Stiffness 30 kN/m, Damping = 100 kN/m/s	[redacted]	[redacted]	[redacted]	[redacted]
Stiffness 30 kN/m, Damping = 200 kN/m/s	[redacted]	[redacted]	[redacted]	[redacted]
Stiffness 30 kN/m, Damping = 300 kN/m/s	[redacted]	[redacted]	[redacted]	[redacted]
Stiffness 30 kN/m, Damping = 400 kN/m/s	[redacted]	[redacted]	[redacted]	[redacted]

6.5. Results

In this chapter cargo control systems are applied to the multi-body system. Tugger wires are used to get control of the cargo during lifting operations. When tugger wires are connected between the vessel and the cargo stiffness is added to the system. Besides stiffness damping can be added to the multi-body system. The influence of small critical damping percentages and high damping values are compared.

The first thing that is examined is the influence of tugger wires with a relative low stiffness. These stiffness values influence the natural frequency of the multi-body system. The increased stiffness values increase the natural frequencies of the multi-body system since the mass of the tugger wires is neglected. However, since the stiffness of the tugger wires is small the influence on the natural frequencies and responses is small.

Secondly is examined how tugger wires with large stiffness values influence the multi-body system. The tugger wires only had a small influence on the natural frequencies and responses. The stiff tugger wires reduce the responses of the vessel roll motion a lot. Especially the tugger wires with stiffness values of 8000 kN/m and 10000kN/m reduce the responses of the vessel to an absolute minimum response of [redacted] degrees for a Pierson-Moskowitz spectrum with a period of 12 seconds and a significant wave height of 1 meter. However, the tugger wires create large responses of the cargo sway motion. These responses are extremely large on frequencies between [redacted] and [redacted] rad/s. At the same time these tugger wires do create large responses for other degrees of freedom like the cargo surge and roll motions. Therefore these stiff tugger wires are not favourable over the less stiff tugger wires.

With the influence of different stiffness values of the tugger wires studied the influence of the tugger wire configurations is examined. By changing the X location of the winches in such a way that the relative distance between the winch and connection to the cargo is equal to 0 meters it became clear that the tugger wire configuration has a relative large influence on the response of the multi-body system. The location of the tugger winch and the location of the connection between the cargo and the vessel has influence on the stiffness components in X, Y and Z direction. The relative distance between the tugger winch and the connection to the cargo also has influence on the translation of forces and moments between translations and rotations of the two bodies. Due to these two relations to the tugger winch configuration the stiffness is distributed in different ways for different configurations. These different stiffness distributions influence the natural frequencies and responses of the multi-body system. When the winch configuration is chosen in a way that both winches are on opposite sides of the cargo in traverse direction a third natural frequency stand out in the RAOs. This third natural frequency is the result of newly formed relations between the vessel roll and vessel pitch motions. Therefore it is always important to verify the influence of different tugger wire configurations.

The fourth part that is examined is the influence of small amounts of damping to the system. Since the stiff tugger wires did not show any natural frequencies with large amplitudes between [redacted] rad/s and [redacted] rad/s the damping is applied to the less stiff tugger wires. Damping equal to 5%ξ and 15%ξ do reduce the amplitudes of the responses around the natural frequencies. Since the applied damping is relatively low the damping does not broaden the amplitudes around the natural frequencies. From the most probable maximum calculations followed that small amounts of damping reduce the responses a lot. An increased amount of damping results in a increased amount of reduction of the response. However, the ratio with which the motion is reduce is also reduce.

Besides calculating the responses of the multi-body system for low amounts of damping relatively large amounts of damping where applied. A side effect of the high amount of damping is that damping broadens the width of the natural frequency amplitudes. Due to this wider range of frequency in which the vessel and cargo responded the most probable maximum of the vessel roll and cargo sway motion did not show any big difference between 200 $kN/m/s$, 300 $kN/m/s$ and 400 $kN/m/s$ damping. This verifies the conclusion that small amounts of damping reduce the motions relatively more than large amounts of damping. When more damping than the critical damping is applied the responses around the natural frequencies become so wide that the MPM calculation show higher responses than smaller amounts of damping. When large amounts of damping are applied the MPM values are reduced significantly. However, There will always be motions in the system.

7
Discussion

Following the results from the sensitivity study and the tugger winch influence study there are several point to discuss about the model.

Model validity
For every model applies the fact that the quality of the output of the model is directly proportional to the quality of the model and input. *(garbage in, garbage out)*. This is also the case for this model. Since the frequency domain is used to solve the responses there are some remarks on the validity of the model. Due to the frequency domain all added parts had to be linear, all non-linear behaviour is linearizedor neglected. Higher order forces and motions are a non-linear problem. Therefore thee second order forces and motions can not be calculated with this model. One example is the stiffness values of the pendulum, mooring lines and tugger winches. All these values are linearized and dependent on the responses of the different degree of freedom. In reality these values are related to the sine/cosine function of the displacement or quadratic proportional to the elongation. Due to all these assumptions it might be useful to validate this model with a validated computational model or model tests

Due to the linearization the stiffness and damping components in the multi-body system will have an influence when there is a translation in positive or negative direction. Due to this linearization the influence of mooring lines is not calculated correctly. When a mooring line falls slack stiffness is applied in this model while this will not happen in real life. In the model tugger winches will apply stiffness throughout a whole cycle of the motions. In reality tugger winches may not be able to apply damping to the system at all times. In reality the reduction due to damping can be lower than calculated by this model. Time domain simulations or model tests can give more insight on the energy dissipation due to the systems described in this thesis. A further study regarding damping systems should be done before implementing such systems on-board of a vessel.

Intended use of results
The tool creates more insight of the interaction between the different degrees of freedom. Although the results only show the influence of certain measures on the multi-body system the different results show relations between different measures and the reaction of the multi-body system. While the vessel hydrodynamic properties are calculated by a 2D strip-theory program and all other relations are linearized the values will differ from reality. The results from this tool are meant to function as supporting information and should not function as a decision making tool. The master of the vessel is still responsible during lifting operations. The master should always consider possible risks during lifting operations. However, in the tool a lot of different aspects are taken into account. In section 3.8 is shown that the mathematical linearization of the pendulum create accurate results for the natural frequencies of the multi-body system. section 3.9 showed that the results of the Python tool and crane simulator have the same order of magnitude. This shows that the tool can be used for for supporting information and until more detailed validation is done the results should not be taken as the absolute truth.

MPM values
The MPM values in this report showed mostly responsess above the 1 degree angle or 1 meter displacement. These values might feel large however these are values are the result of wave spectra with a wave height of 1 meter. During lifting operations in ports the waves are broken. This results in lower wave heights during lifting operations. The MPM values of the responses scale proportionate with the wave height. When the wave height during lifting operations are equal to 0.5 meters, twice as small in reality as in this report, the MPM values of the responses will also be twice as small as given in this report. Since linear theory is used the allowed sea state can also be calculated from the allowable MPM of a certain motion. equation 7.1 shows how this can be done. In this equation $H_{s_{SeaState}}$ stands for the allowable wave height, $MPM_{Allowable}$ represents

the allowble MPM of the motion and $MPM_{H_{s=1}}$ represents the MPM of the corresponding motion for a sea state with the same period and a wave height of 1 meter.

$$H_{s_{SeaState}} = \frac{MPM_{Allowable}}{MPM_{H_{s=1}}} \tag{7.1}$$

Wave spectra
The tool focuses on the multi-body system and the internal reaction between the different degrees of freedom. External forces are not examined. During lifting operations the vessel will most likely operate in a port or an other, from weather protected, area. In these areas the wave spectrum will most likely differ from the JONSWAP and Pierson-Moskowitz spectra. Standing waves can also occur when waves are reflected by the quays. While the wave spectra differ from the wave spectra used in this study the results from the tool will differ from the motions in reality. This must be taken into account when the tool is used to calculate the vessel and cargo responses for accurate lifting operations. Alhough waves may differ at all different loading operations the RAOs still show how the vessel responds to different wave frequencies and wave directions. When the waves at loading cites can be described in a wavespectrum the MPM values can still be calculated.

Frequency domain
Most of the assumptions made in this tool followed by the limitations of the frequency domain. All forces and relations to forces had to be linearized. However, the frequency domain is still a good method to derive characteristic behaviours of a model. For a conceptual study and one of the fewer publicly available studies the frequency domain provides a lot of information. The non-linear components of the system are linearized and therefore their influence is not fully neglected. With the linearization of the non-linear components the influence of these components are taken into account. A validated time-domain study can be done to validate the influence of all the linearizations done in this model.

Use of the tool
This frequency domain model has shown useful results. The model did show the influence of different variables during the lifting operation. Relations between lifting operation variables and the motions of the multi-body system could be formed from these results. The model can also be used to calculate the influence of these variables on lifting operations of future projects.

This tool did also show the influence of damping on both the vessel and cargo motions. According to the tool small amounts of damping will already have a large influence on the vessel and cargo motions. These results can be used for further studies when cargo control systems are developed for heavy lifting transport vessels.

Added value with respect to similar studies
When this thesis started not much, publicly available, research was done. Although advanced, third party, multi-body dynamics computation program might be able to solve the relation between vessel and cargo degrees of freedom these programs will most-likely not consist of a solver for hydrodynamic properties. Therefor, this study created new insight in the relation between loading conditions, lifting configurations and cargo-control systems. During this thesis other studies where released from embargo or released by heavy lifting companies. Results from other studies regarding this topic are still hidden from public. Therefore it is hard to compare this research with research done by other companies. However, since it is one of the first publicly released studies regarding vessel lifting operations it will create a lot of insight for other studies.

The heavy lifting companies that already did a study regarding cargo control systems operate vessels that are only designed for lifting operations and not for the transportation of cargo. Since these vessels are designed for a different purpose these vessels will most likely respond in a different way on waves than the vessels of BigLift Shipping. This study is the first study that looked at the influence of lifting operation motions for heavy lifting transport vessels.

8
Conclusion

The purpose of this research can be split up in two parts. The first part of the research was gaining more insight on the relation between vessel motions and cargo motions during lifting operations. The second part of the research focused on reducing the motions of the two bodies during lifting operations.

The 12 degrees of freedom system
For the first part of this study a model had to be written. By writing this model the interaction of the vessel and cargo motions had to be written in mathematical equations. Multi-body dynamics is used to solve the interaction and calculate the responses of both bodies at the same time. By writing the natural behaviour it became clear that the cargo acted as a pendulum that was excited by the displacement of the crane tip. Before the influence of different lifting variables where studied baseline calculations were done in chapter 4. In conventional calculations performed for lifting operations only 6 degrees of freedom are taken into account. In the tool created for this thesis a 12 degrees of freedom multi-body system is used to calculate the responses. In conventional calculations the dynamical aspects of the cargo are not taken into account. The multi-body tool takes this influence into account. While both the conventional calculations and multi-body system calculations have the same result for the natural frequency calculations for the 6 degrees of freedom of the vessel motions the multi-body system shows that the dynamical aspects of the cargo motions also introduce natural frequencies which also interact with the 6 degrees of freedom of the vessel motions. All these natural frequencies introduced by the dynamical aspects of the cargo motions can not be calculated by the conventional tool. Thus conventional calculations fall short in calculating the natural frequencies and responses of motions during lifting operations.

During this study it became clear that the vessel roll motion, cargo surge motion and cargo sway motion have the largest amplitudes in the response amplitude operator calculations. All other degrees of freedom showed smaller amplitudes and less extreme reactions on natural frequencies.

Besides the large amplitudes in the RAOs the vessel roll and cargo sway motion showed a large amount of coupling between the two degrees of freedom. The main excitation force of the cargo sway motion follows from the restoring force that is applied via the crane cable. In the case of the vessel roll and cargo sway motion the stiffness value of this restoring force has the same order size as the hydrodynamical roll stiffness value. While both stiffness values have the same order size the influence of the coupling via the crane cable is large on both degrees of freedom. This coupling enhances the responses of both degrees of freedom.

While the cargo surge motions RAO showed large peaks there was little coupling between the cargo surge motion and other degrees of freedom. Mathematically the cargo sway motion showed identically large stiffness values for the coupling via the crane cable to the vessel pitch motion as the cargo sway motion had with the vessel roll motion. However, the hydrodynamical vessel pitch stiffness values where an order size larger than the restoring stiffness values of the coupling between the cargo surge motion via the crane cable. While the stiffness values of the vessel pitch motion is an order size larger, the influence of the cargo surge motion on the vessel pitch motion is small and both motions are only slightly enhanced by each other.

The multi-body tool created calculates more accurate responses than conventional calculations while much more aspects of a lifting operation are taken into account.

Wave directions and responses
In chapter 4 the influence of different wave angles on the multi-body system are also calculated. While the vessel roll motion and cargo sway motion have a strong coupling waves with an angle perpendicular to the vessel causes the largest responses of the vessel and cargo motions. While this wave angle is used in the rest of the thesis to calculate the influence of lifting variables and cargo control systems the study towards wave angles showed that all different wave angles can cause different degrees of freedom to show large RAOs. Therefor it is recommended to calculate the the responses of the multi-body system for different wave angles when this tool is used for lifting operations.

Influence of variables of the lifting operation
The influence of different variables of the lifting operation on the responses of the multi-body system are studied in chapter 5. This study showed that the cargo mass, crane cable lenght, crane top Z position, crane top Y position, and metacentric height of the vessel have relatively large influences on the natural frequencies of the multi-body system. Some of these variables will stay constant during the lifting operation while others will vary during the operation.

The variables that will vary during a lifting operation are the crane cable length, crane top Z position and crane top Y position. The vessels metacentric height can vary when water is pumped in to the ballast tank from outside the vessel. While these variables can change calculations with different variables should be done before a lifting operation is performed. In chapter 1 is explained that there are 5 different stages. For every stage a calculation with variables according to that stage should be done.

While some lifting variables will change in order to perform the lifting operation the tool can give valuable insight in the lifting operation. The tool can be used to calculate the influence of using the forward or aft crane or the influence or rotating the cargo clockwise or counterclockwise. When there is enough freedom during a lifting operation the crane and rotation option can be chosen in such a way that the lowest motions occur.

The cargo mass will not vary during a lifting operation. However this variable will be different for every different lifting operation. While all different lifting operations varies from each other the lifting calculations should be done for all different lifting operations. Results for previously calculated lifting operations are not sufficient for new lifting operations.

Mooring lines
The influence of mooring lines are also studied in chapter 5. While normal mooring lines do not influence the multi-body system very much very stiff mooring configurations influence the responses a lot. When mooring lines with short lengths are connected between the vessel and shore the stiffness of these lines are large. These large stiffness values increase the natural frequencies of the multi-body system. Besides these increased natural frequencies the amplitudes of the motions are also increased. The mooring lines couple the vessel sway motions to vessel roll motions. While vessel sway motions are inhibited the responses of the vessel roll motions are increased, which also increases the responses of the cargo sway motion. Therefor it can be concluded that a stiff mooring line configuration deliver no reduction of the vessel and cargo motions during lifting operations in waves.

Cargo control systems
The model used to calculate the influence between the different degrees of freedom in the vessel-cargo system is expanded with systems to control the cargo motions. Currently the most widespread practice is the use of tugger winches. These winches add additional stiffness to the vessel-cargo system. The implementation of the cargo control system showed that only adding stiffness to the multi-body system will not result in lower motions during lifting operations.

Besides the influence of conventional tugger winches the influence of damping is examined. Damping added via the tugger winches influence the responses around the natural frequencies. Especially small amounts of damping have a relative large influence on the responses of the vessel and cargo. This shows that small amounts of damping can be usefull during lifting operations.

This study showed that adding damping to the system will reduce the cargo motions. Besides the reduction of the cargo motions the vessel motions are reduced. Especially the vessel roll motion. While the vessel roll motion has a strong coupling to the cargo sway motion a reduction of the cargo sway motion results in a reduction of the vessel roll motion. This study showed that adding damping to the system can be useful to increase the safety and workabiltiy during lifting operations.

Overall conclusion
The overall conclusion form this research is that it is useful to look at the different variables of the multi-body system. The conventional 6 degrees of freedom stability calculations fall to short when the responses of the vessel are calculated during lifting operations. The dynamical aspects of the cargo hanging from the crane can have a large influence on the vessel motions, especially when the cargo has a large mass.

The study did also show that small amounts of damping can heavily influence the multi-body system of both the vessel and cargo motions. Besides the damping of the cargo motions the vessel motions are reduced when the cargo is damped. This study showed that it is useful to apply small amounts of damping to the multi-body system to increase the safety and workability during lifting operations.

Even though the model created for the calculations and used for creating the results of this research is a frequency domain model the different results showed large influences of the implementation of a multi-body system, variables of the multi-body system and damping. Because the model already showed large influences it shows that the frequency domain method can be a useful method to study the behaviour of the multi-body system.

By creating this tool and using this tool to examine the influence of the interaction of the vessel and cargo, the different variables during lifting operations and cargo-control mechanisms, it is proven that the tool is a valuable extension to BigLift's engineering methods. This tool can be used to predict vessel and cargo motions during lifting operations in waves. The creation of this tool and the results from the tool fulfilled the thesis objective.

"Determine the influence of vessel motions on cargo motions on each other during lifting operations in waves and develop a method to decrease the motions during lifting operations in waves"

While the thesis objective is fulfilled the presented tool provides insight and creates more knowledge regarding lifting operations in waves. The tool forms a bridge between used practices, mathematical knowledge and physical relations. The tool also showed how different methods can be used to decrease the responses of the multiple degrees of freedom during lifting operations.

Bibliography

[1] R.I. Cambero and Sausedo-Solorio J.M. Dynamics of the shift in resonance frequency in a triple pendulum. *Meccanica*, 2011.

[2] G.F. Claus and M Vannahme. Experimental study of the nonlinear dynamics of floating cranes. *The ninth international offshore and polar engineering conference*, 1999.

[3] Dr. I. Dmitrieva. *DELFRAC*. Tu Delft, 1994.

[4] Greenwood D.T. *Advanced Dynamics*. Cambridge University Press, 2003.

[5] O.M. Faltinesen. *Sea loads on ships and offshore structures*. Cambridge University Press, Cambridge, UK, 1990.

[6] J.F. Flory, S.P. Banfield, and Dr. A. Ractliffe. Computer mooring load analysis to improve port operations and safety, 2013. URL `https://www.tensiontech.com/papers/optimoor`.

[7] Python Software Foundation. Python^{TM}, 2019. URL `https://www.python.org/doc/`.

[8] G. González. A pendulum with a moving support point, 2006. URL `http://www.phys.lsu.edu/faculty/gonzalez/Teaching/Phys7221/PendulumWithMovingSupport.pdf`.

[9] J. Healy. Eigen what?, 2017. URL `https://www.physicssayswhat.com/2017/03/24/eigen-what/`.

[10] J.W.A.M. IJzermans. Heavy lifting during wave exposure. Master's thesis, TU Delft, 2005.

[11] J.M.J. Journee. *User manual of Seaway*. Tu Delft, 2001.

[12] J.M.J. Journée and W.W. Massie. *OFFSHORE HYDROMECHANICS*. Wiley, 2007.

[13] Y. Kawahara, K. MAEKAWA, and Y. IKEDA. A simple prediction formula of roll damping of conventional cargo ships on the basis of ikeda's method and its limitation. *Proceedings of the 10th International Conference on Stability of Ships and Ocean Vehicles*, 2010.

[14] L.A. Ladino and H.S. Rondón. Determining the damping coefficient of a simple pendulum oscillating in air. *Physics Educatoin Educ. 52*, 2007.

[15] H. Lageveen. Modelling and steering of tuggerwinches. Master's thesis, TU Delft, 2014.

[16] This Condensed Life. Phase difference after resonance, 2016. URL `https://thiscondensedlife.wordpress.com/2016/05/02/phase-difference-after-resonance/`.

[17] LLoyd's Register Group LTD. Lloyd's register rules and regulations - rules and regulations for the classification of ships, 2017.

[18] D.J.C. MacKay. Normal modes and the douple pendulum, 2001. URL `http://www.inference.org.uk/teaching/dynamics/course.html`.

[19] G. Meskers and R. van Dijk. A damping tugger system for offshore heavy lifts. *OMAE*, 2012.

[20] A. Montanari. Mechanics of sea waves, 2017. URL `https://distart119.ing.unibo.it/albertonew/?q=node/104`.

[21] A. Montanari. Ocean-wave spectra, 2017. URL `https://distart119.ing.unibo.it/albertonew/?q=node/104`.

[22] BEXCOZ N.V. *DeepRope Polyester & Dyneema mooring ropes manual 2004*. Le Lis, 2015.

[23] M.K. Ochi. On prediction of extreme values. *Journal of Ship Research*, 1973.

[24] M.K. Ochi. Principles of extreme value statistics and their application. *The society of naval architects and marine engineers*, 1981.

[25] Katsuhiko Ogata. *System Dynamics (4th ed.)*. University of Minnesota, 2005.

[26] M.J. Ormond. Depth compensated subsea passive heave compensator, 2014. URL http://www.ipaustralia.com.au/applicant/intermoor-inc/patents/AU2009233731/.

[27] Jasna. Prpić-Oršić, V. Slapničar, and A. Turk. Berth operability estimation related to ship motion, 2014. URL https://www.researchgate.net/publication/291342321_Berth_operability_estimation_related_to_ship_motion.

[28] S.S. RAO. *Mechanical Vibrations*. Prentice-Hall Inc., 2004.

[29] R Rubenzahl and S.G. Rajeev. Small oscillations of the n-pendulum and the "hanging rope" limit $n \to \infty$. http://www.pas.rochester.edu/~rrubenza/projects/RR_PHY235W_TermPaper.pdf, 2017.

[30] BigLift Shipping. Biglift compony profile, 2019. URL https://www.bigliftshipping.com/en/company/profile.

[31] D. Skandali. Identification of response amplitude operators for ships based on full scale measurements. Master's thesis, TU Delft, 2015.

[32] M. St. Denis and W.J. Pierson. On the motion of ships in confused seas. *Vol. 61*, pages 1–53, 1953.

[33] Stackexchange physics. Critical damping ratios and oscillations plotted, 2014. URL https://physics.stackexchange.com/questions/106091/faster-than-critical-damping-for-harmonic-oscillator.

[34] P.P. Urone, P. Hinrichs, K. Dirks, and M. Sharma. Adiabatic processes of an ideal gas, 2019. URL https://phys.libretexts.org/Bookshelves/University_Physics/Book%3A_University_Physics_(OpenStax)/Map%3A_University_Physics_II_-_Thermodynamics%2C_Electricity%2C_and_Magnetism_(OpenStax)/3%3A_The_First_Law_of_Thermodynamics/3.6%3A_Adiabatic_Processes_for_an_Ideal_Gas.

[35] E.F.G. van Daalen. *MARIN Shipmo User Manual*. MARIN, 2015.

[36] Y. Wang, A. van Deyzen, and B. Beimers. Less=moor: A time-efficient computational tool to assess the behavior of moored ships in waves. *Physics Educatoin Educ. 52*, 2007.

[37] F.E. Wester. Heave compensated floatover operation. Master's thesis, TU Delft, 2015.

[38] F.M. White. *Fluid Mechanics*. McGraw-Hill, New York, NY, 7 edition, 2011.

[39] Wikipedia. Metacentric height, 2019. URL https://en.wikipedia.org/wiki/Metacentric_height.

[40] D. Wood. The superposition principle & resultant waves, 2019. URL https://study.com/academy/lesson/the-superposition-principle-resultant-waves.html.

[41] J.K. Woodacre, R.J. Bauer, and R.A. Irani. A review of vertical motion heave compensation systems. *Ocean Engineering 104*, pages 140–154, 2015.

[42] Q. Yuan. Actively damped heave compensation (adhc) system. *Proceedings of the 2010 American Control Conference*, pages 1544–1549, 2010.

A

Free body diagrams

A.1. Free body diagrams crane cable connection

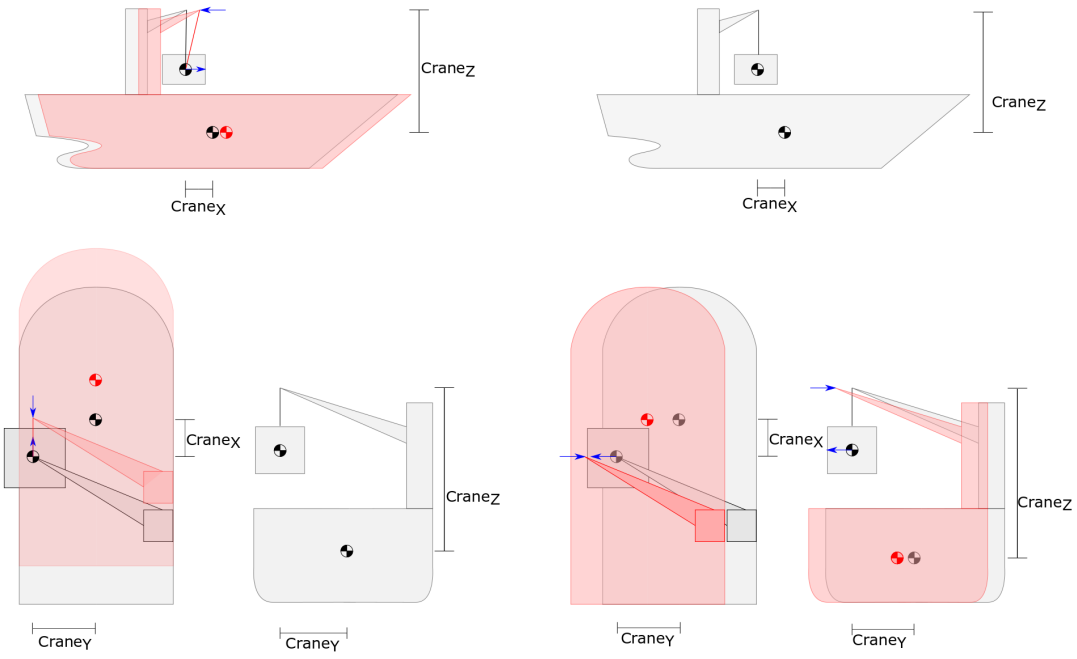

(a) Free body diagram of the interaction between the vessel and cargo via the crane cable for the surge motion of the vessel (X_1)

(b) Free body diagram of the interaction between the vessel and cargo via the crane cable for the sway motion of the vessel (X_2)

Figure A.1: The two free body diagrams of the interaction between the vessel and cargo via the crane cable or the surge motion of the vessel and the sway motion of the vessel

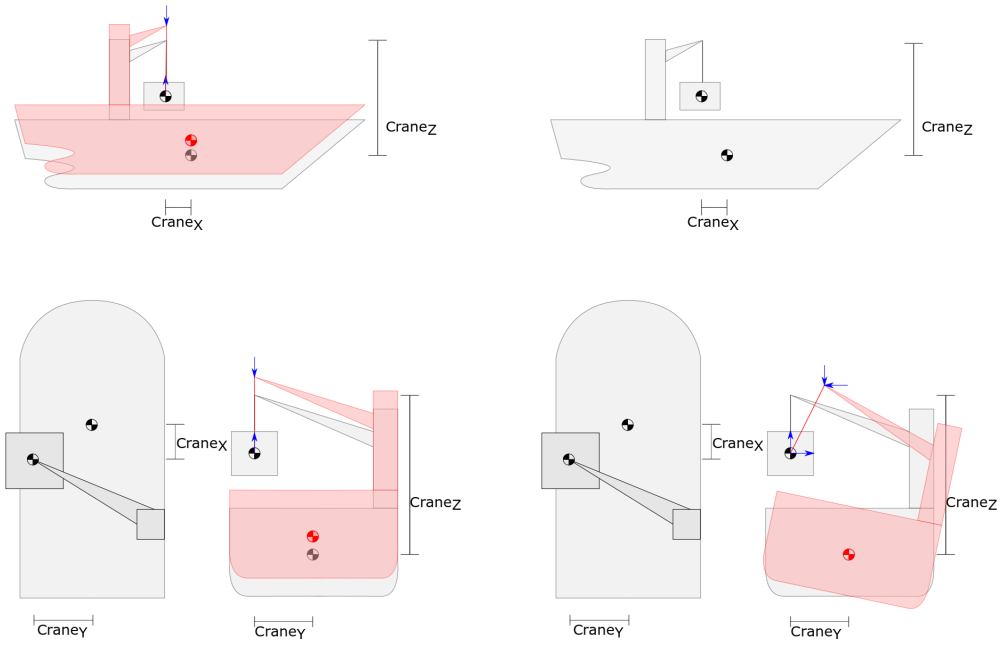

(a) Free body diagram for of the interaction between the vessel and cargo via the crane cable the heave motion of the vessel (X_3)

(b) Free body diagram for of the interaction between the vessel and cargo via the crane cable the roll motion of the vessel (X_4)

Figure A.2: The two free body diagrams of the interaction between the vessel and cargo via the crane cable for the heave motion of the vessel and the roll motion of the vessel

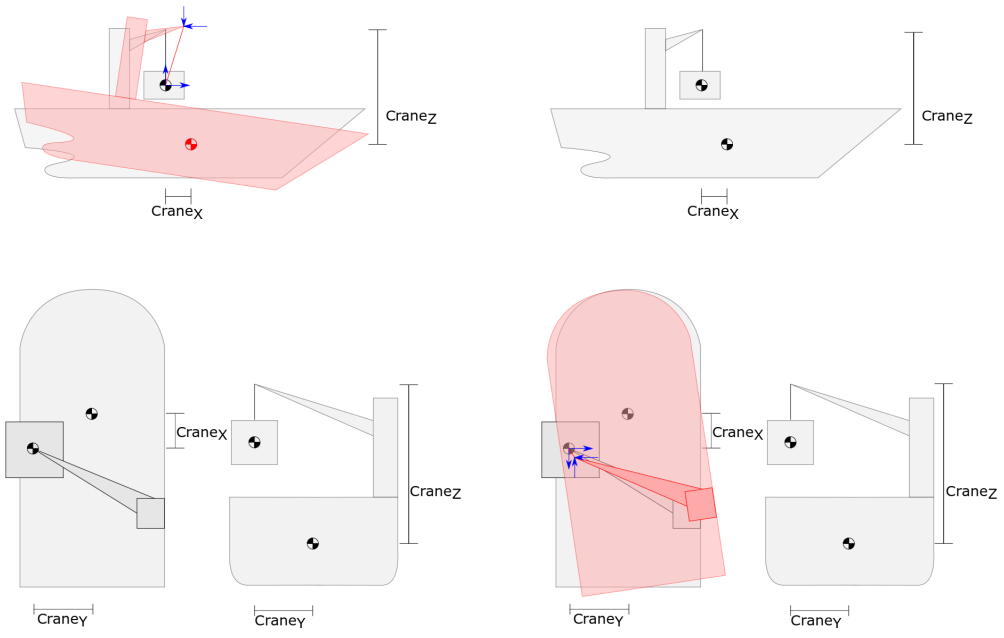

(a) Free body diagram for of the interaction between the vessel and cargo via the crane cable the pitch motion of the vessel (X_5)

(b) Free body diagram for of the interaction between the vessel and cargo via the crane cable the yaw motion of the vessel (X_6)

Figure A.3: The two free body diagrams of the interaction between the vessel and cargo via the crane cable for the pitch motion of the vessel and the yaw motion of the vessel

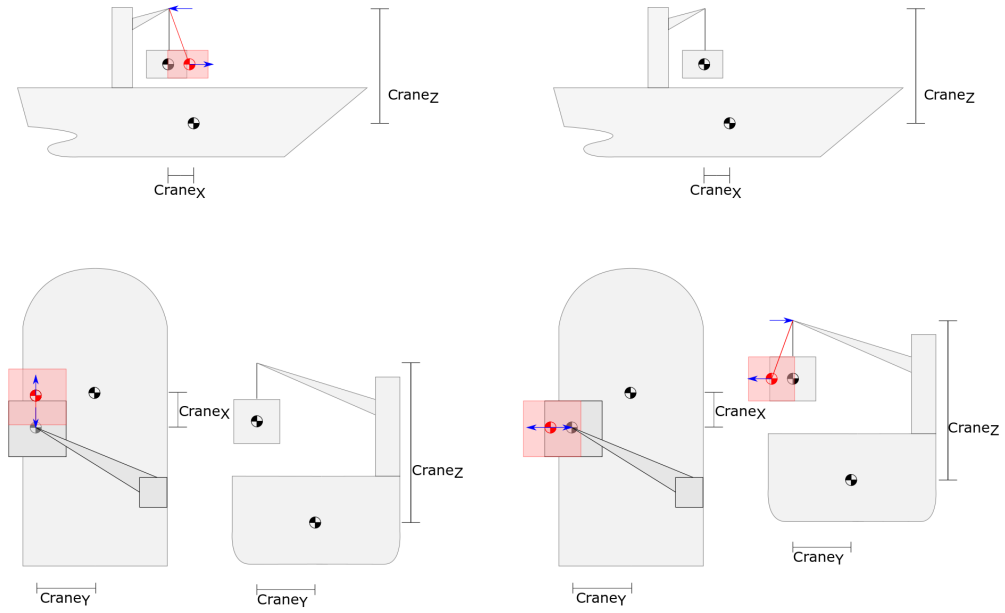

(a) Free body diagram for of the interaction between the vessel and cargo via the crane cable the surge motion of the cargo (X_7)

(b) Free body diagram for of the interaction between the vessel and cargo via the crane cable the sway motion of the cargo (X_8)

Figure A.4: The two free body diagrams of the interaction between the vessel and cargo via the crane cable for the surge motion of the cargo and the sway motion of the cargo

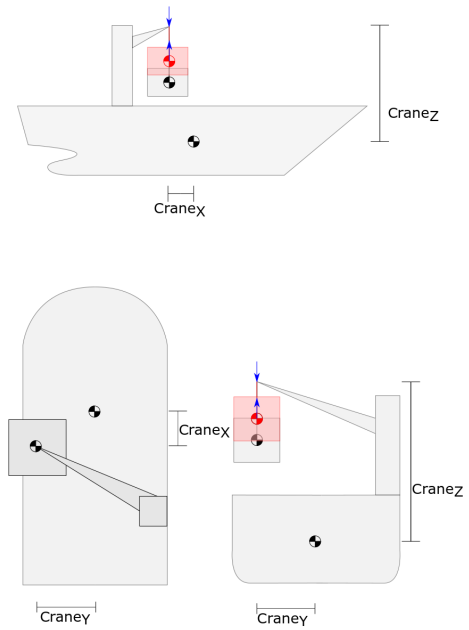

(a) Free body diagram for the heave motion of the cargo (X_9)

Figure A.5: The free body diagram of the interaction between the vessel and cargo via the crane cable for the heave motion of the vessel and the roll motion of the vessel

A.2. Free body diagrams mooring line connection

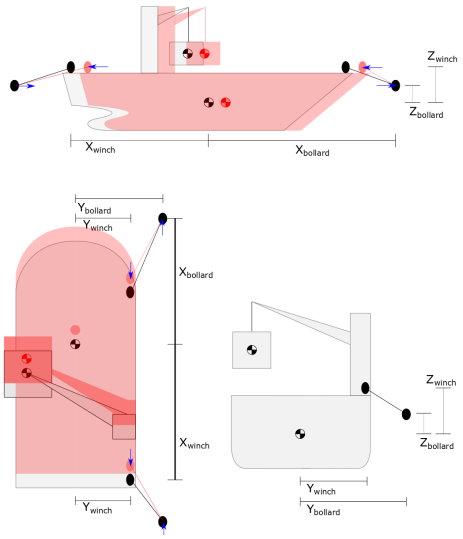

(a) Free body diagram of the interaction between the vessel and the shore via mooring lines for the surge motion of the vessel (X_1)

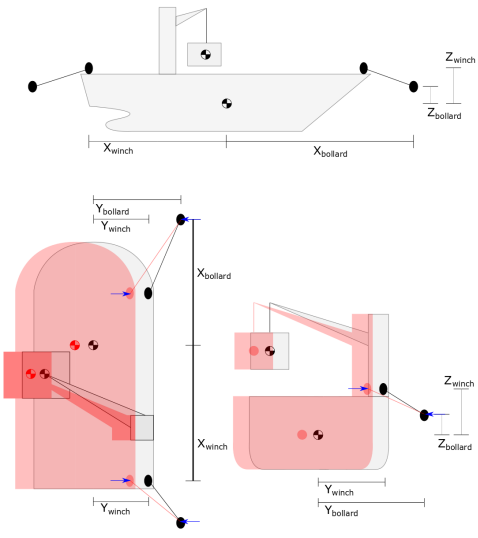

captionFree body diagram of the interaction between the vessel and the shore via mooring lines for the sway motion of the vessel (X_2)

Figure A.6: The two free body diagrams of the interaction between the vessel and the shore via mooring lines for the surge motion of the vessel and the sway motion of the vessel

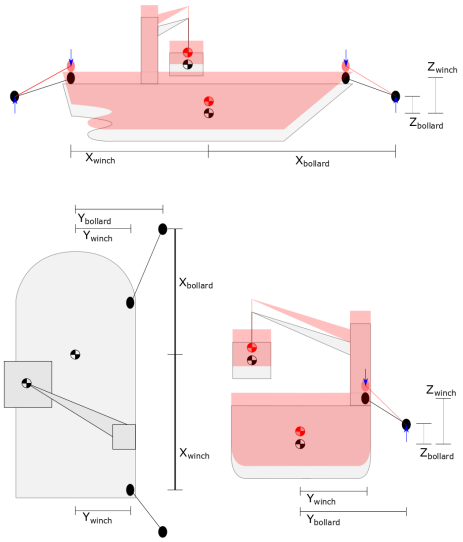

(a) Free body diagram of the interaction between the vessel and the shore via mooring lines for the heave motion of the vessel (X_3)

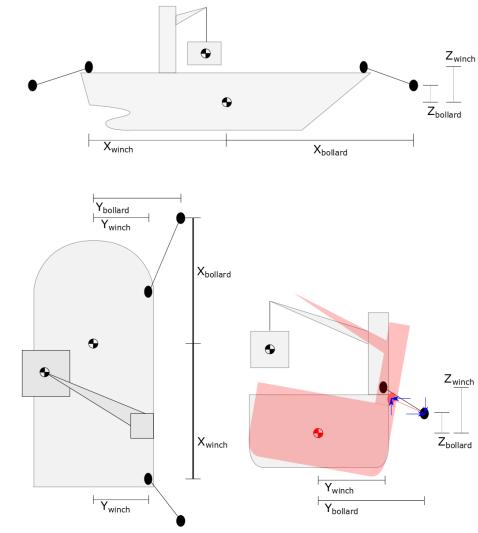

captionFree body diagram of the interaction between the vessel and the shore via mooring lines for the roll motion of the vessel (X_4)

Figure A.7: The two free body diagrams of the interaction between the vessel and the shore via mooring lines for the heave motion of the vessel and the roll motion of the vessel

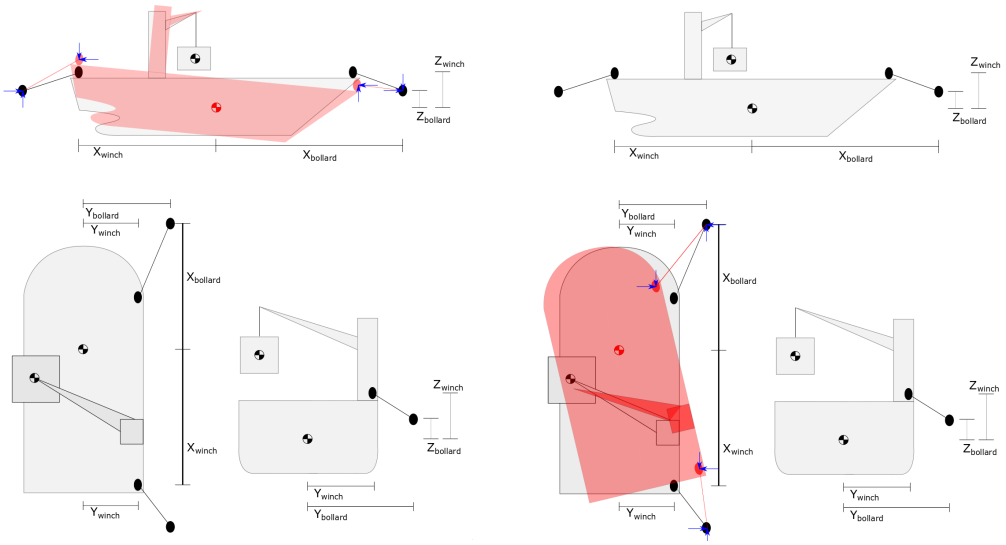

(a) Free body diagram of the interaction between the vessel and the shore via mooring lines for the pitch motion of the vessel (X_5)

captionFree body diagram of the interaction between the vessel and the shore via mooring lines for the yaw motion of the vessel (X_6)

Figure A.8: The two free body diagrams of the interaction between the vessel and the shore via mooring lines for the pitch motion of the vessel and the yaw motion of the vessel

A.3. Free body diagrams cargo control system connection

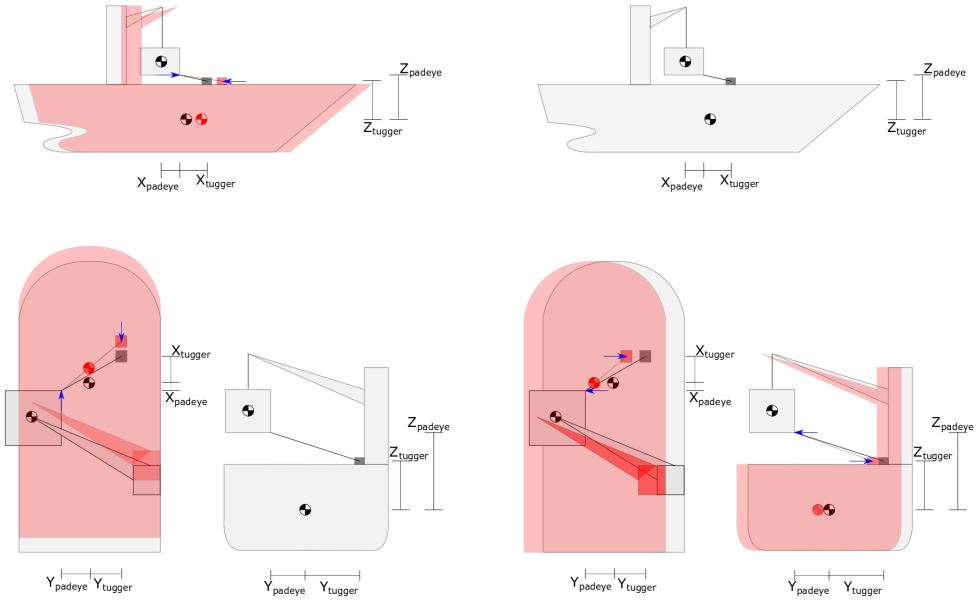

(a) Free body diagram of the interaction between the vessel and the cargo via cargo control systems for the surge motion of the vessel (X_1)

(b) Free body diagram of the interaction between the vessel and the cargo via cargo control systems for the sway motion of the vessel (X_2)

Figure A.9: The two free body diagrams of the interaction between the vessel and the cargo via cargo control systems for the surge motion of the vessel and the sway motion of the vessel

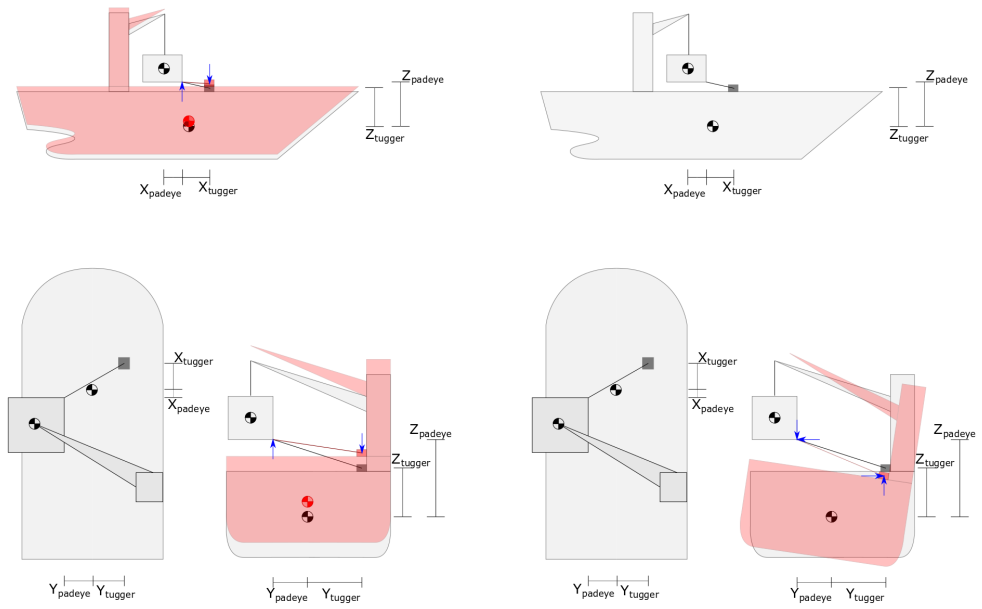

(a) Free body diagram of the interaction between the vessel and the cargo via cargo control systems for the heave motion of the vessel (X_3)

(b) Free body diagram of the interaction between the vessel and the cargo via cargo control systems for the roll motion of the vessel (X_4)

Figure A.10: The two free body diagrams of the interaction between the vessel and the cargo via cargo control systems for the heave motion of the vessel and the roll motion of the vessel

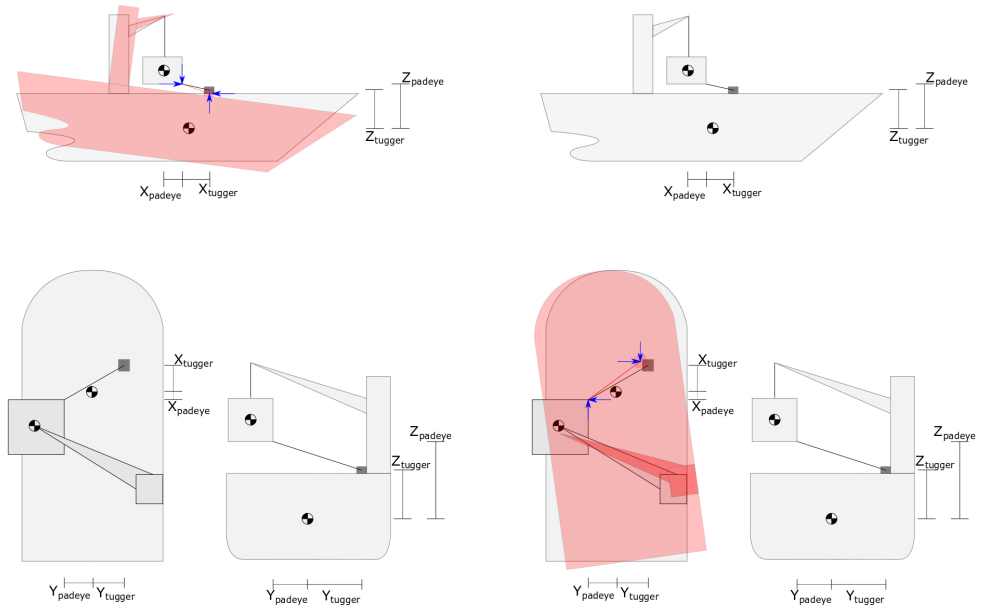

(a) Free body diagram of the interaction between the vessel and the cargo via cargo control systems for the pitch motion of the vessel (X_5)

(b) Free body diagram of the interaction between the vessel and the cargo via cargo control systems for the yaw motion of the vessel (X_6)

Figure A.11: The two free body diagrams of the interaction between the vessel and the cargo via cargo control systems for the pitch motion of the vessel and the yaw motion of the vessel

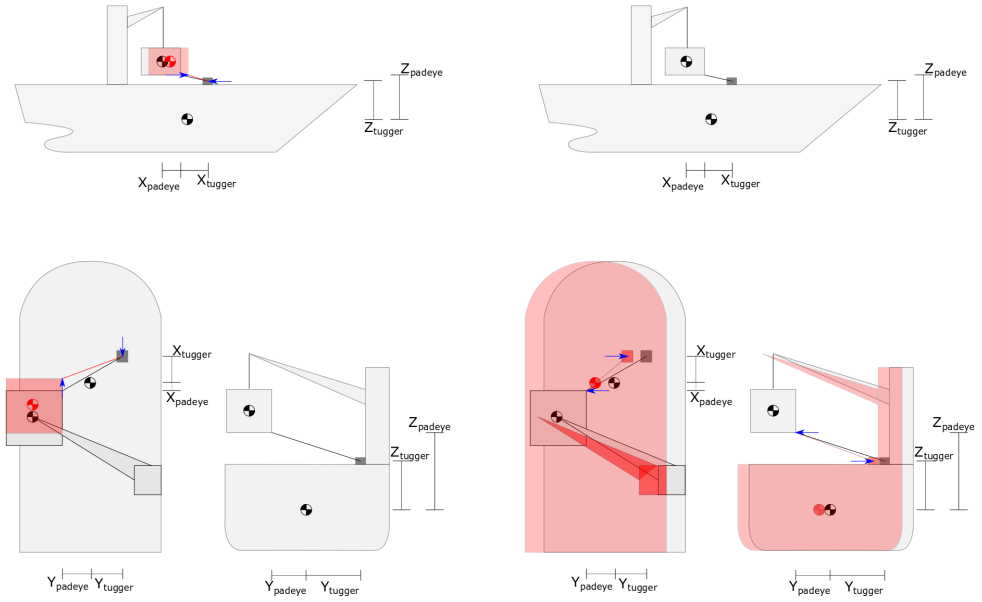

(a) Free body diagram of the interaction between the vessel and the cargo via cargo control systems for the surge motion of the cargo (X_7)

(b) Free body diagram of the interaction between the vessel and the cargo via cargo control systems for the sway motion of the cargo (X_8)

Figure A.12: The two free body diagrams of the interaction between the vessel and the cargo via cargo control systems for the surge motion of the cargo and the sway motion of the cargo

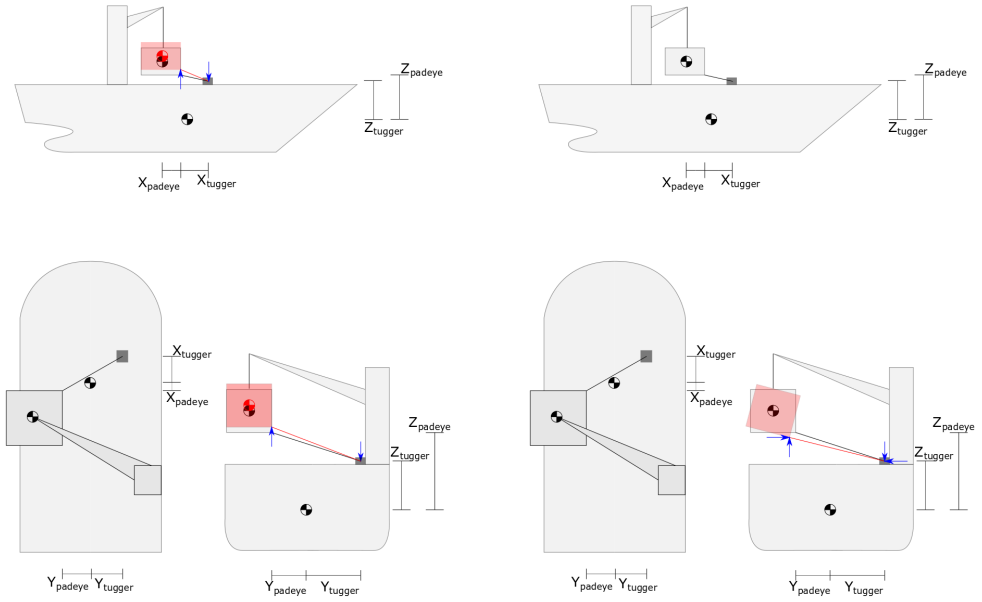

(a) Free body diagram of the interaction between the vessel and the cargo via cargo control systems for the heave motion of the cargo (X_9)

(b) Free body diagram of the interaction between the vessel and the cargo via cargo control systems for the roll motion of the cargo (X_{10})

Figure A.13: The two free body diagrams of the interaction between the vessel and the cargo via cargo control systems for the heave motion of the cargo and the roll motion of the cargo

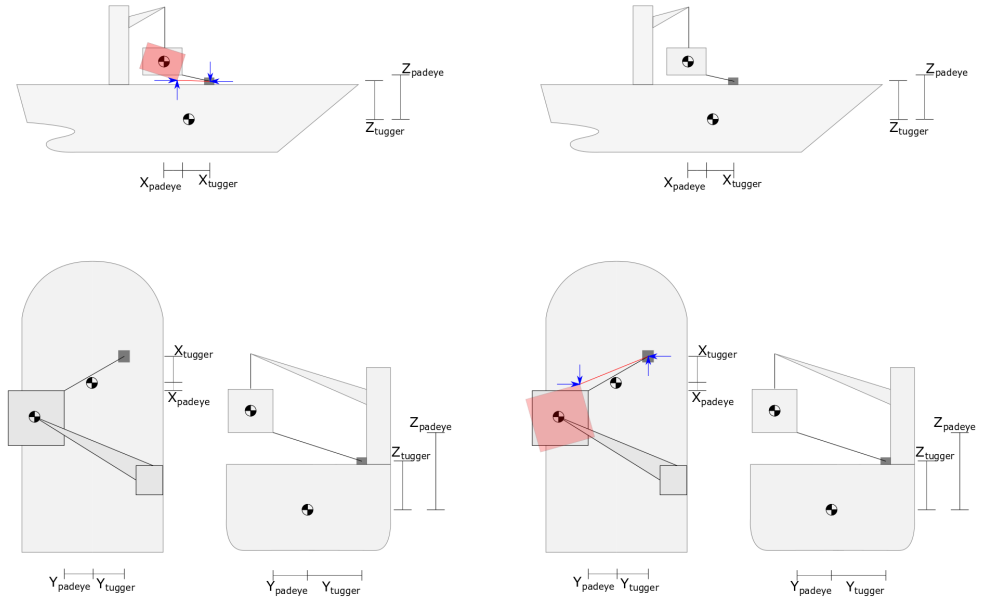

(a) Free body diagram of the interaction between the vessel and the cargo via cargo control systems for the pitch motion of the cargo (X_{11})

(b) Free body diagram of the interaction between the vessel and the cargo via cargo control systems for the yaw motion of the cargo (X_{12})

Figure A.14: The two free body diagrams of the interaction between the vessel and the cargo via cargo control systems for the pitch motion of the vessel and the yaw motion of the cargo

B
Matrices

$$\begin{bmatrix}
M_{11} & 0 & 0 & 0 & 0 & 0 & 0 & 0 & 0 & 0 & 0 & 0 \\
0 & M_{22} & 0 & M_{24} & 0 & M_{26} & 0 & 0 & 0 & 0 & 0 & 0 \\
0 & 0 & M_{33} & 0 & M_{35} & 0 & 0 & 0 & 0 & 0 & 0 & 0 \\
0 & M_{42} & 0 & M_{44} & 0 & M_{46} & 0 & 0 & 0 & 0 & 0 & 0 \\
0 & 0 & M_{53} & 0 & M_{55} & 0 & 0 & 0 & 0 & 0 & 0 & 0 \\
0 & M_{62} & 0 & M_{64} & 0 & M_{66} & 0 & 0 & 0 & 0 & 0 & 0 \\
0 & 0 & 0 & 0 & 0 & 0 & M_{77} & 0 & 0 & 0 & 0 & 0 \\
0 & 0 & 0 & 0 & 0 & 0 & 0 & M_{88} & 0 & 0 & 0 & 0 \\
0 & 0 & 0 & 0 & 0 & 0 & 0 & 0 & M_{99} & 0 & 0 & 0 \\
0 & 0 & 0 & 0 & 0 & 0 & 0 & 0 & 0 & M_{1010} & 0 & 0 \\
0 & 0 & 0 & 0 & 0 & 0 & 0 & 0 & 0 & 0 & M_{1111} & 0 \\
0 & 0 & 0 & 0 & 0 & 0 & 0 & 0 & 0 & 0 & 0 & M_{1212}
\end{bmatrix}$$

$$\begin{aligned}
M_{11} &= M_{hyd_{11}} + A_{hyd_{11}} \\
M_{22} &= M_{hyd_{22}} + A_{hyd_{22}} \\
M_{24} &= A_{hyd_{24}} \\
M_{26} &= A_{hyd_{26}} \\
M_{33} &= M_{hyd_{33}} + A_{hyd_{33}} \\
M_{35} &= A_{hyd_{35}} \\
M_{42} &= A_{hyd_{42}}
\end{aligned}$$

$$\begin{aligned}
M_{44} &= M_{hyd_{44}} + A_{hyd_{44}} \\
M_{46} &= A_{hyd_{46}} \\
M_{53} &= A_{hyd_{53}} \\
M_{55} &= M_{hyd_{55}} + A_{hyd_{55}} \\
M_{62} &= A_{hyd_{62}} \\
M_{64} &= A_{hyd_{64}} \\
M_{66} &= M_{hyd_{66}} + A_{hyd_{66}}
\end{aligned}$$

$$\begin{aligned}
M_{77} &= M_{pen} \\
M_{88} &= M_{pen} \\
M_{99} &= M_{pen} \\
M_{1010} &= I_{pen_X} \\
M_{1111} &= I_{pen_Y} \\
M_{1212} &= I_{pen_Z}
\end{aligned}$$

$$\begin{bmatrix}
B_{11} & 0 & 0 & 0 & B_{15} & B_{16} & B_{17} & 0 & 0 & 0 & B_{111} & B_{112} \\
0 & B_{22} & 0 & B_{24} & 0 & B_{26} & 0 & B_{28} & 0 & B_{210} & 0 & B_{212} \\
0 & 0 & B_{33} & B_{34} & B_{35} & 0 & 0 & 0 & B_{39} & B_{310} & B_{311} & 0 \\
0 & B_{42} & B_{43} & B_{44} & B_{45} & B_{46} & 0 & B_{48} & B_{49} & B_{410} & B_{411} & B_{412} \\
B_{51} & 0 & B_{53} & B_{54} & B_{55} & B_{56} & B_{57} & 0 & B_{59} & B_{510} & B_{511} & B_{512} \\
B_{61} & B_{62} & 0 & B_{64} & B_{65} & B_{66} & B_{67} & B_{68} & 0 & B_{610} & B_{611} & B_{612} \\
B_{71} & 0 & 0 & 0 & B_{75} & B_{76} & B_{77} & 0 & 0 & 0 & B_{711} & B_{712} \\
0 & B_{82} & 0 & B_{84} & 0 & B_{86} & 0 & B_{88} & 0 & B_{810} & 0 & B_{812} \\
0 & 0 & B_{93} & B_{94} & B_{95} & 0 & 0 & 0 & B_{99} & B_{910} & B_{911} & 0 \\
0 & B_{102} & B_{103} & B_{104} & B_{105} & B_{106} & 0 & B_{108} & B_{109} & B_{1010} & B_{1011} & B_{1012} \\
B_{111} & 0 & B_{113} & B_{114} & B_{115} & B_{116} & B_{117} & 0 & B_{119} & B_{1110} & B_{1111} & B_{1112} \\
B_{121} & B_{122} & 0 & B_{124} & B_{125} & B_{126} & B_{127} & B_{128} & 0 & B_{1210} & B_{1211} & B_{1212}
\end{bmatrix}$$

$B_{11} = B_{hyd_{11}} + B_{tugger_{11}}$
$B_{15} = B_{tugger_{15}}$
$B_{16} = B_{tugger_{16}}$
$B_{17} = B_{tugger_{17}}$
$B_{111} = B_{tugger_{111}}$
$B_{112} = B_{tugger_{112}}$
$B_{22} = B_{hyd_{22}} + B_{tugger_{22}}$
$B_{24} = B_{hyd_{24}} + B_{tugger_{24}}$
$B_{26} = B_{hyd_{26}} + B_{tugger_{26}}$
$B_{28} = B_{tugger_{28}}$
$B_{210} = B_{tugger_{210}}$
$B_{212} = B_{tugger_{212}}$
$B_{33} = B_{hyd_{33}} + B_{tugger_{33}}$
$B_{34} = B_{tugger_{34}}$
$B_{35} = B_{hyd_{35}} + B_{tugger_{35}}$
$B_{39} = B_{tugger_{39}}$
$B_{310} = B_{tugger_{310}}$
$B_{311} = B_{tugger_{311}}$
$B_{42} = B_{hyd_{42}} + B_{tugger_{42}}$
$B_{43} = B_{tugger_{43}}$
$B_{44} = B_{hyd_{44}} + B_{tugger_{44}}$
$B_{45} = B_{tugger_{45}}$
$B_{46} = B_{hyd_{46}} + B_{tugger_{46}}$
$B_{48} = B_{tugger_{48}}$
$B_{49} = B_{tugger_{49}}$
$B_{410} = B_{tugger_{410}}$
$B_{411} = B_{tugger_{411}}$
$B_{412} = B_{tugger_{412}}$
$B_{51} = B_{tugger_{51}}$
$B_{53} = B_{hyd_{53}} + B_{tugger_{53}}$
$B_{54} = B_{tugger_{54}}$
$B_{55} = B_{hyd_{55}} + B_{tugger_{55}}$
$B_{56} = B_{tugger_{56}}$
$B_{57} = B_{tugger_{57}}$
$B_{59} = B_{tugger_{59}}$
$B_{510} = B_{tugger_{510}}$
$B_{511} = B_{tugger_{511}}$
$B_{512} = B_{tugger_{512}}$
$B_{61} = B_{tugger_{61}}$
$B_{62} = B_{hyd_{62}} + B_{tugger_{62}}$
$B_{64} = B_{hyd_{64}} + B_{tugger_{64}}$
$B_{65} = B_{tugger_{65}}$
$B_{66} = B_{hyd_{66}} + B_{tugger_{66}}$
$B_{67} = B_{tugger_{67}}$
$B_{68} = B_{tugger_{68}}$
$B_{610} = B_{tugger_{610}}$
$B_{611} = B_{tugger_{611}}$
$B_{612} = B_{tugger_{612}}$
$B_{71} = B_{tugger_{71}}$
$B_{75} = B_{tugger_{75}}$
$B_{76} = B_{tugger_{76}}$
$B_{77} = B_{air_{77}} + B_{tugger_{77}}$
$B_{711} = B_{tugger_{711}}$
$B_{712} = B_{tugger_{712}}$
$B_{82} = B_{tugger_{82}}$
$B_{84} = B_{tugger_{84}}$
$B_{86} = B_{tugger_{86}}$
$B_{88} = B_{air_{88}} + B_{tugger_{88}}$
$B_{810} = B_{tugger_{810}}$
$B_{812} = B_{tugger_{812}}$
$B_{93} = B_{tugger_{93}}$
$B_{94} = B_{tugger_{94}}$
$B_{95} = B_{tugger_{95}}$
$B_{99} = B_{air_{99}} + B_{tugger_{99}}$
$B_{910} = B_{tugger_{910}}$
$B_{911} = B_{tugger_{911}}$
$B_{102} = B_{tugger_{102}}$
$B_{103} = B_{tugger_{103}}$
$B_{104} = B_{air_{1010}} + B_{tugger_{104}}$
$B_{105} = B_{tugger_{105}}$
$B_{106} = B_{tugger_{106}}$
$B_{108} = B_{tugger_{108}}$
$B_{109} = B_{tugger_{109}}$
$B_{1010} = B_{tugger_{1010}}$
$B_{1011} = B_{tugger_{1011}}$
$B_{1012} = B_{tugger_{1012}}$
$B_{111} = B_{tugger_{111}}$
$B_{113} = B_{tugger_{113}}$
$B_{114} = B_{tugger_{114}}$
$B_{115} = B_{tugger_{115}}$
$B_{116} = B_{tugger_{116}}$
$B_{117} = B_{tugger_{117}}$
$B_{119} = B_{tugger_{119}}$
$B_{1110} = B_{tugger_{1110}}$
$B_{1111} = B_{air_{1111}} + B_{tugger_{1111}}$
$B_{1112} = B_{tugger_{1112}}$
$B_{121} = B_{tugger_{121}}$
$B_{122} = B_{tugger_{122}}$
$B_{124} = B_{tugger_{124}}$
$B_{125} = B_{tugger_{125}}$
$B_{126} = B_{tugger_{126}}$
$B_{127} = B_{tugger_{127}}$
$B_{128} = B_{tugger_{128}}$
$B_{1210} = B_{tugger_{1210}}$
$B_{1211} = B_{tugger_{1211}}$
$B_{1212} = B_{air_{1212}} + B_{tugger_{1212}}$

$$\begin{bmatrix}
C_{11} & 0 & 0 & 0 & C_{15} & C_{16} & C_{17} & 0 & 0 & 0 & 0 & 0 \\
0 & C_{22} & C_{23} & C_{24} & C_{25} & C_{26} & 0 & C_{28} & 0 & 0 & 0 & 0 \\
0 & 0 & C_{33} & C_{34} & C_{35} & 0 & 0 & 0 & C_{39} & 0 & 0 & 0 \\
0 & C_{42} & C_{43} & C_{44} & C_{45} & C_{46} & 0 & C_{48} & C_{49} & 0 & 0 & 0 \\
C_{51} & 0 & C_{53} & C_{54} & C_{55} & C_{56} & C_{57} & 0 & C_{59} & 0 & 0 & 0 \\
C_{61} & C_{62} & C_{63} & C_{64} & C_{65} & C_{66} & C_{67} & C_{68} & 0 & 0 & 0 & 0 \\
C_{71} & 0 & 0 & 0 & C_{75} & C_{76} & C_{77} & 0 & 0 & 0 & 0 & 0 \\
0 & C_{82} & 0 & C_{84} & 0 & C_{86} & 0 & C_{88} & 0 & 0 & 0 & 0 \\
0 & 0 & C_{93} & C_{94} & C_{95} & 0 & 0 & 0 & C_{99} & 0 & 0 & 0 \\
0 & 0 & 0 & 0 & 0 & 0 & 0 & 0 & 0 & 0 & 0 & 0 \\
0 & 0 & 0 & 0 & 0 & 0 & 0 & 0 & 0 & 0 & 0 & 0 \\
0 & 0 & 0 & 0 & 0 & 0 & 0 & 0 & 0 & 0 & 0 & 0
\end{bmatrix}$$

$C_{11} = C_{pen} + C_{moor} + C_{tugger_{11}}$
$C_{15} = C_{pen} + C_{moor} + C_{tugger_{11}}$
$C_{16} = C_{pen} + C_{moor} + C_{tugger_{11}}$
$C_{17} = C_{pen} + C_{tugger_{17}}$
$C_{111} = C_{tugger_{111}}$
$C_{112} = C_{tugger_{112}}$
$C_{22} = C_{pen} + C_{moor} + C_{tugger_{22}}$
$C_{23} = C_{hyd}$
$C_{24} = C_{hyd} + C_{pen} + C_{moor} + C_{tugger_{24}}$
$C_{25} = C_{hyd}$
$C_{26} = C_{pen} + C_{moor} + C_{tugger_{26}}$
$C_{28} = C_{pen} + C_{tugger_{28}}$
$C_{210} = C_{tugger_{210}}$
$C_{211} = C_{tugger_{211}}$
$C_{33} = C_{hyd} + C_{pen} + C_{moor} + C_{tugger_{33}}$
$C_{34} = C_{hyd} + C_{pen} + C_{moor} + C_{tugger_{34}}$
$C_{35} = C_{hyd} + C_{pen} + C_{moor} + C_{tugger_{35}}$
$C_{39} = C_{pen} + C_{tugger_{39}}$
$C_{310}\ C_{tugger_{310}}$
$C_{311}\ C_{tugger_{311}}$
$C_{42} = C_{pen} + C_{moor} + C_{tugger_{42}}$
$C_{43} = C_{hyd} + C_{pen} + C_{moor} + C_{tugger_{43}}$
$C_{44} = C_{hyd} + C_{pen} + C_{moor} + C_{tugger_{44}}$
$C_{45} = C_{hyd} + C_{pen} + C_{moor} + C_{tugger_{45}}$
$C_{46} = C_{pen} + C_{moor} + C_{tugger_{46}}$
$C_{48} = C_{pen} + C_{tugger_{48}}$
$C_{49} = C_{pen} + C_{tugger_{49}}$
$C_{410} = C_{tugger_{410}}$
$C_{411} = C_{tugger_{411}}$
$C_{412} = C_{tugger_{412}}$
$C_{51} = C_{pen} + C_{moor} + C_{tugger_{51}}$
$C_{53} = C_{hyd} + C_{pen} + C_{moor} + C_{tugger_{53}}$
$C_{54} = C_{hyd} + C_{pen} + C_{moor} + C_{tugger_{54}}$
$C_{55} = C_{hyd} + C_{pen} + C_{moor} + C_{tugger_{55}}$
$C_{56} = C_{pen} + C_{moor} + C_{tugger_{56}}$
$C_{57} = C_{pen} + C_{tugger_{57}}$
$C_{59} = C_{pen} + C_{tugger_{59}}$
$C_{510} = C_{tugger_{510}}$
$C_{511} = C_{tugger_{511}}$
$C_{512} = C_{tugger_{512}}$
$C_{61} = C_{pen} + C_{moor} + C_{tugger_{61}}$
$C_{62} = C_{pen} + C_{moor} + C_{tugger_{62}}$
$C_{63} = C_{hyd}$
$C_{64} = C_{hyd} + C_{pen} + C_{moor} + C_{tugger_{64}}$
$C_{65} = C_{hyd} + C_{pen} + C_{moor} + C_{tugger_{65}}$
$C_{66} = C_{hyd} + C_{pen} + C_{moor} + C_{tugger_{66}}$
$C_{67} = C_{pen} + C_{tugger_{67}}$
$C_{68} = C_{pen} + C_{tugger_{68}}$
$C_{610} = C_{tugger_{610}}$
$C_{611} = C_{tugger_{611}}$
$C_{612} = C_{tugger_{612}}$
$C_{71} = C_{pen} + C_{tugger_{71}}$
$C_{75} = C_{pen} + C_{tugger_{75}}$
$C_{76} = C_{pen} + C_{tugger_{76}}$
$C_{77} = C_{pen} + C_{tugger_{77}}$
$C_{711} = C_{tugger_{711}}$
$C_{712} = C_{tugger_{712}}$
$C_{82} = C_{pen} + C_{tugger_{82}}$
$C_{84} = C_{pen} + C_{tugger_{84}}$
$C_{86} = C_{pen} + C_{tugger_{86}}$
$C_{88} = C_{pen} + C_{tugger_{88}}$
$C_{810} = C_{tugger_{810}}$
$C_{812} = C_{tugger_{812}}$
$C_{93} = C_{pen} + C_{tugger_{93}}$
$C_{94} = C_{pen} + C_{tugger_{94}}$
$C_{95} = C_{pen} + C_{tugger_{95}}$
$C_{99} = C_{pen} + C_{tugger_{99}}$
$C_{910} = C_{tugger_{910}}$
$C_{911} = C_{tugger_{911}}$
$C_{102} = C_{tugger_{102}}$
$C_{103} = C_{tugger_{103}}$
$C_{104} = C_{tugger_{104}}$
$C_{105} = C_{tugger_{105}}$
$C_{106} = C_{tugger_{106}}$
$C_{108} = C_{tugger_{108}}$
$C_{109} = C_{tugger_{109}}$
$C_{1010} = C_{tugger_{1010}}$
$C_{1011} = C_{tugger_{1011}}$
$C_{1012} = C_{tugger_{1012}}$
$C_{111} = C_{tugger_{111}}$
$C_{113} = C_{tugger_{113}}$
$C_{114} = C_{tugger_{114}}$
$C_{115} = C_{tugger_{115}}$
$C_{116} = C_{tugger_{116}}$
$C_{117} = C_{tugger_{117}}$
$C_{119} = C_{tugger_{119}}$
$C_{1110} = C_{tugger_{1110}}$
$C_{1111} = C_{tugger_{1111}}$
$C_{1112} = C_{tugger_{1112}}$
$C_{121} = C_{tugger_{121}}$
$C_{122} = C_{tugger_{122}}$
$C_{124} = C_{tugger_{124}}$
$C_{125} = C_{tugger_{125}}$
$C_{126} = C_{tugger_{126}}$
$C_{127} = C_{tugger_{127}}$
$C_{128} = C_{tugger_{128}}$
$C_{1210} = C_{tugger_{1210}}$
$C_{1211} = C_{tugger_{1211}}$
$C_{1212} = C_{tugger_{1212}}$

C

Equations of Motion

Table C.1: Definition of abbreviations used in the equations of motion

Abbreviation	**Meaning / Definition**
F_{exc_n}	Excitation forces of the n-th degree of freedom
x_n	Response of the n-th degree of freedom.
$M_{hyd_{nm}}$	Hydrodynamic mass values. Influence of m-th degree of freedom on the n-th degree of freedom
$A_{hyd_{nm}}$	Hydrodynamic added mass values. Influence of m-th degree of freedom on the n-th degree of freedom
$B_{hyd_{nm}}$	Hydrodynamic damping values. Influence of m-th degree of freedom on the n-th degree of freedom
$B_{air_{nm}}$	Air damping of the pendulum motions.
$B_{tug_{xyz}}$	Damping values of the damping applied via the tugger winch system in x,y, and z direction respectively
$C_{hyd_{nm}}$	Hydrodynamic restoring stiffness values. Influence of m-th degree of freedom on the n-th degree of freedom
K_{pen}	Restoring stiffness value of the cargo pendulum motion
K_{wire}	Wire stiffness of the crane cable
$K_{moor_{xyz}}$	Restoring stiffness value of a mooring line in x, y, and z direction respectively
$K_{tug_{xyz}}$	Restoring stiffness value of the tugger wires in x, y, and z direction respectively
X_{cr}, Y_{cr}, Z_{cr}	X, Y, and Z position of the crane tip
$X_{winch}, Y_{winch}, Z_{winch}$	X, Y, and Z position of the fairlead of the mooring line respectively to the centre of gravity of the vessel.
$X_{tug}, Y_{tug}, Z_{tug}$	X, Y, and Z position of the tugger winch respectively to the centre of gravity of the vessel
$X_{pad}, Y_{pad}, Z_{pad}$	X, Y, and Z position of the connection of the tugger wire to the cargo

Surge vessel

$$
\begin{aligned}
F_{exc_1} = &-\omega^2 \cdot \left(M_{hyd_{11}} + A_{hyd_{11}}\right) \cdot x_1 \\
&- i\omega \cdot \left(\left(B_{hyd_{11}} + \sum\left(B_{tug_x}\right)\right) \cdot x_1 + \left(\sum\left(B_{tug_x} \cdot Z_{tug}\right)\right) \cdot x_5 - \left(\sum\left(B_{tug_x} \cdot Y_{tug}\right)\right) \cdot x_6\right. \\
&\left. - \left(\sum\left(B_{tug_x}\right)\right) \cdot x_7 - \left(\sum\left(B_{tug_x} \cdot Z_{pad}\right)\right) \cdot x_{11} + \left(\sum\left(B_{tug_x} \cdot Y_{pad}\right)\right) \cdot x_{12}\right) \\
&+ \left(K_{pen} + \sum K_{moor_x} + \sum K_{tug_x}\right) \cdot x_1 + \left(K_{pen} \cdot Z_{Cr} + \sum\left(K_{moor_x} \cdot Z_{Winch}\right) + \sum\left(K_{tug_x} \cdot Z_{tug}\right)\right) \cdot x_5 \\
&- \left(K_{pen} \cdot Crane_Y + \sum\left(K_{moor_x} \cdot Y_{Winch}\right) + \sum\left(K_{tug_x} \cdot Y_{tug}\right)\right) \cdot x_6 - \left(K_{pen} + \sum K_{pen_x}\right) \cdot x_7 \\
&- \left(\sum\left(\left(K_{tug_x} \cdot Z_{pad}\right)\right) x_{11} + \left(\sum\left(\left(K_{tug_x} \cdot Y_{pad}\right)\right) \cdot x_{12}\right.\right.
\end{aligned}
\tag{C.1}
$$

Sway vessel

$$
\begin{aligned}
F_{exc_2} = &-\omega^2 \cdot \left(\left(M_{hyd_{22}} + A_{hyd_{22}}\right) \cdot x_2 + A_{hyd_{24}} \cdot x_4 + A_{hyd_{26}} \cdot x_6\right) \\
&- i\omega \cdot \left(\left(B_{hyd_{22}} + \sum B_{tug_y}\right) \cdot x_2 + \left(B_{hyd_{24}} - \sum\left(B_{tug_y} \cdot Z_{tug}\right)\right) \cdot x_4 + \left(B_{hyd_{26}} + \sum\left(B_{tug_y} \cdot X_{tug}\right)\right) \cdot x_6\right. \\
&\left. - \sum B_{tug_y} \cdot x_8 + \sum\left(B_{tug_y} \cdot Z_{pad}\right) \cdot x_{10} - \sum\left(B_{tug_y} \cdot X_{pad}\right) \cdot x_{12}\right) \\
&+ \left(K_{pen} + \sum K_{moor_Y} + \sum K_{tug_Y}\right) \cdot x_2 - \left(K_{pen} \cdot Z_{Cr} + \sum\left(K_{moor_Y} \cdot Z_{winch}\right) + \sum\left(K_{tug_Y} \cdot Z_{tug}\right)\right) \cdot x_4 + \\
&\left(K_{pen} \cdot X_{Cr} + \sum\left(K_{moor_Y} \cdot X_{Winch}\right) + \sum\left(K_{tug_y} \cdot X_{tug}\right)\right) \cdot x_6 - \left(K_{pen} + K_{tug_y}\right) \cdot x_8 \\
&+ \left(\sum\left(K_{tug_y} \cdot Z_{pad}\right)\right) \cdot x_{10} - \left(\sum\left(K_{tug_y} \cdot X_{pad}\right)\right) \cdot x_{12}
\end{aligned}
\tag{C.2}
$$

Heave vessel

$$
\begin{aligned}
F_{exc_3} = &-\omega^2 \cdot \left(\left(\left(M_{hyd_{33}} + A_{hyd_{33}}\right) \cdot x_3 + A_{hyd_{35}} \cdot x_5\right)\right. \\
&- i\omega \left(\left(B_{hyd_{33}} + \sum\left(B_{tug_z}\right)\right) \cdot x_3 + \left(\sum\left(B_{tug_z} \cdot Y_{tug}\right)\right) \cdot x_4 + \left(B_{hyd_{35}} - \sum\left(B_{tug_z} \cdot X_{tug}\right)\right) \cdot x_5\right. \\
&\left. - \left(\sum\left(K_{tug_z}\right)\right) \cdot x_9 - \left(\sum\left(K_{tug_z} \cdot Y_{pad}\right)\right) \cdot x_{10} + \left(\sum\left(K_{tug_z} \cdot X_{pad}\right)\right) \cdot x_{11}\right) \\
&+ \left(K_{wire} + \sum K_{moor_Z} + \sum K_{tug_z}\right) \cdot x_3 + \left(K_{wire} \cdot Y_{Cr} + \sum\left(K_{moor_Z} \cdot Y_{Winch}\right) + \sum\left(K_{tug_z} \cdot Y_{tug}\right)\right) \cdot x_4 \\
&- \left(K_{wire} \cdot X_{cr} + \sum\left(K_{moor_Z} \cdot X_{winch}\right) + \sum\left(K_{tug_z} \cdot X_{tug}\right)\right) \cdot x_5 - \left(K_{wire} + K_{tug_z}\right) \cdot x_9 \\
&- \left(\sum\left(K_{tug_z} \cdot Y_{pad}\right)\right) \cdot x_{10} + \left(\sum\left(K_{tug_z} \cdot X_{pad}\right)\right) \cdot x_{11}
\end{aligned}
\tag{C.3}
$$

Roll vessel

$$
\begin{aligned}
F_{exc_4} = &-\omega^2 \cdot (A_{42} \cdot x_2 + (M_{44} + A_{44}) \cdot x_4 + A_{46} \cdot x_6) - \\
&- i\omega \left(\left(B_{hyd_{42}} - \sum \left(B_{tug_y} \cdot Y_{tug} \right) \right) \cdot x_2 + \left(\sum \left(B_{tug_z} \cdot Y_{tug} \right) \right) \cdot x_3 \right. \\
&+ \left(B_{hyd_{44}} + \left(\sum \left(B_{tug_y} \cdot Z_{tug}^2 \right) \right) \left(\sum \left(B_{tug_z} \cdot Y_{tug}^2 \right) \right) \right) \cdot x_4 \\
&- \left(\sum \left(B_{tug_z} \cdot X_{tug} \cdot Y_{tug} \right) \right) \cdot x_5 + \left(B_{46} - \left(\sum \left(B_{Tug_y} \cdot X_{tug} \cdot Z_{tug} \right) \right) \right) \cdot x_6 \\
&+ \left(\sum \left(B_{tug_y} \cdot Z_{winch} \right) \right) x_8 - \left(\sum \left(B_{tug_z} \cdot Y_{winch} \right) \right) x_9 \\
&+ \left(\sum \left(B_{tug_y} \cdot Z_{pad} \cdot Z_{tug} \right) + \sum \left(B_{tug_z} \cdot Y_{pad} \cdot Y_{tug} \right) \right) \cdot x_{10} \\
&+ \left(\sum \left(B_{tug_z} \cdot X_{pad} \cdot Y_{tug} \right) \right) \cdot x_{11} - \left(\sum \left(B_{tug_y} \cdot X_{pad} \cdot Z_{tug} \right) \right) \cdot x_{12} \Big) \\
&- \left(K_{pen} \cdot Z_{cr_Z} + \sum \left(K_{moor_Y} \cdot Z_{winch} \right) + \left(\sum \left(K_t ug_y Z_{tug} \right) \right) \right) \cdot x_2 + \\
&\left(C_{hyd_{43}} + K_{wire} \cdot Y_{cr} + \left(\sum \left(K_{moor_Z} \cdot Winch_Y \right) \right) + \left(\sum \left(K_{tug_z} \cdot Y_{tug} \right) \right) \right) \cdot x_3 \\
&+ \left(C_{hyd_{44}} + K_{pen} \cdot Z_{cr}^2 + K_{wire} \cdot Y_{cr}^2 + \left(\sum \left(K_{moor_Z} \cdot Y_{winch}^2 \right) \right) + \left(\sum \left(K_{moor_Y} \cdot Z_{winch}^2 \right) \right) \right. \\
&+ \left(\sum \left(K_{tug_y} \cdot Z_{tug}^2 \right) \right) + \left(\sum \left(K_{tug_z} Y_{tug}^2 \right) \right) \Big) \cdot x_4 \\
&- \left(C_{hyd_{45}} + K_{wire} \cdot X_{cr} \cdot Y_{cr} + \sum \left(K_{moor_Z} \cdot X_{winch} \cdot Y_{winch} \right) + \left(\sum \left(K_{tug_z} \cdot X_{tug} \cdot Y_{tug} \right) \right) \right) \cdot x_5 \\
&- \left(K_{pen} \cdot X_{cr} \cdot Z_{cr} + \sum \left(K_{line_Z} \cdot X_{winch} \cdot Z_{winch} \right) + \left(\sum \left(K_{tug_y} \cdot X_{tug} \cdot Z_{tug} \right) \right) \right) \cdot x_6 \\
&+ \left(\left(K_{pen} \cdot Z_{cr} \right) + \left(\sum \left(K_{tug_y} \cdot Z_{winch} \right) \right) \right) \cdot x_8 - \left(\left(K_{wire} \cdot X_{cr} \right) + \left(\sum \left(K_{tug_z} \cdot Y_{winch} \right) \right) \right) \cdot x_9 \\
&- \left(\left(\sum \left(K_{tug_y} \cdot Z_{pad} \cdot Z_{tug} \right) \right) + \left(\sum \left(K_{tug_z} \cdot Y_{pad} \cdot Y_{tug} \right) \right) \right) \cdot x_{10} \\
&+ \left(\sum \left(K_{tug_z} \cdot X_{pad} \cdot Y_{tug} \right) \right) \cdot x_{11} - \left(\sum \left(K_{tug_y} \cdot X_{pad} \cdot Z_{tug} \right) \right) \cdot x_{12}
\end{aligned}
\tag{C.4}
$$

Pitch vessel

$$
\begin{aligned}
F_{exc_5} = &-\omega^2 \cdot (A_{53} \cdot x_3 + (M_{55} + A_{55}) \cdot x_5) \\
&- i\omega \left(\sum \left(B_{tug_x} \cdot Z_{tug} \right) \cdot x_1 + \left(B_{53} - \sum \left(B_{tug_z} \cdot X_{tug} \right) \right) \cdot x_3 - \sum \left(B_{tug_z} \cdot Y_{tug} \cdot X_{tug} \right) \cdot x_4 \right. \\
&+ \left(B_{55} + \sum \left(B_{tug_x} \cdot Z_{tug}^2 \right) + \sum \left(B_{tug_z} \cdot X_{tug}^2 \right) \right) \cdot x_5 - \sum \left(B_{tug_x} \cdot Y_{tug} \cdot Z_{tug} \right) \cdot x_6 \\
&- \sum \left(B_{tug_x} \cdot Z_{winch} \right) \cdot x_7 + \sum \left(B_{tug_z} \cdot Z_{winch} \right) \cdot x_9 + \sum \left(B_{tug_z} \cdot Y_{pad} \cdot X_{tug} \right) \cdot x_{10} \\
&- \left(\sum \left(B_{Tug_x} \cdot Z_{pad} \cdot Z_{tug} \right) + \sum \left(B_{tug_z} \cdot X_{pad} \cdot X_{tug} \right) \right) \cdot x_{11} + \sum \left(B_{tug_x} \cdot Y_{pad} \cdot Z_{pad} \right) \cdot x_{12} \Big) \\
&\left(K_{pen} \cdot Crane_Z + \sum \left(K_{moor_x} \cdot Z_{winch} \right) + \sum \left(K_{tug_x} \cdot Z_{tug} \right) \right) \cdot x_1 + \\
&\left(C_{hyd_{53}} - K_{wire} \cdot X_{cr} - \sum \left(K_{moor_Z} \cdot X_{winch} \right) - \sum \left(K_{tug_z} \cdot X_{tug} \right) \right) \cdot x_3 \\
&+ \left(C_{hyd_{54}} - K_{wire} \cdot Y_{cr} \cdot X_{cr} - \sum \left(K_{moor_Y} \cdot Y_{winch} \cdot X_{winch} \right) - \sum \left(K_{tug_z} \cdot Y_{tug} \cdot X_{tug} \right) \right) \cdot x_4 \\
&+ \left(C_{hyd_{55}} + K_{pen} \cdot Z_{cr}^2 + K_{wire} \cdot X_{cr}^2 \right. \\
&+ \sum \left(K_{moor_X} \cdot Z_{winch}^2 \right) + \sum \left(K_{moor_Z} \cdot X_{winch}^2 \right) + \sum \left(K_{tug_x} \cdot Z_{tug}^2 \right) + \sum \left(K_{tug_z} \cdot X_{tug}^2 \right) \Big) \cdot x_5 \\
&- \left(K_{pen} \cdot Y_{cr} \cdot Z_{cr} + \sum \left(K_{moor_X} \cdot Y_{winch} \cdot Z_{winch} \right) + \sum \left(K_{tug_x} \cdot Y_{tug} \cdot Z_{tug} \right) \right) \cdot x_6 \\
&- \left(K_{pen} \cdot Z_{cr} + \sum \left(K_{tug_x} \cdot Z_{winch} \right) \right) \cdot x_7 + \left(K_{pen} \cdot X_{cr} + \sum \left(K_{tug_z} \cdot X_{winch} \right) \right) \cdot x_9 \\
&+ \sum \left(K_{tug_z} \cdot Y_{pad} \cdot X_{pad} \right) \cdot x_{10} - \left(\sum \left(K_{tug_x} \cdot Z_{pad} \cdot Z_{tug} \right) + \sum \left(K_{tug_Z} \cdot X_{pad} \cdot X_{tug} \right) \right) \cdot x_{11} \\
&+ \sum \left(K_{tug_x} \cdot Y_{pad} \cdot Z_{tug} \right) \cdot x_{12}
\end{aligned}
\tag{C.5}
$$

Yaw vessel

$$
\begin{aligned}
F_{exc_6} = &-\omega^2 \cdot (A_{62} \cdot x_2 + A_{54} \cdot x_4 + (M_{66} + A_{66}) \cdot x_6) \\
&- i\omega \cdot \left(-\sum \left(B_{tug_x} \cdot Y_{tug}\right) \cdot x_1 + \left(B_{62} + \sum \left(B_{tug_y} \cdot X_{tug}\right)\right) \cdot x_2 + \left(B_{64} - \sum \left(B_{tug_y} \cdot Z_{tug} \cdot X_{tug}\right)\right) \cdot x_4 \right. \\
&+ \sum \left(B_{tug_x} \cdot Z_{tug} \cdot Y_{tug}\right) \cdot x_5 + \left(B_{66} + \sum \left(B_{tug_y} \cdot X_{tug}^2\right) + \sum \left(B_{tug_X} \cdot Y_{tug}^2\right)\right) \cdot x_6 \\
&+ \sum \left(B_{tug_x} \cdot Y_{winch}\right) \cdot x_7 - \sum \left(B_{tug_y} \cdot X_{winch}\right) \cdot x_8 + \sum \left(B_{tug_y} \cdot Z_{pad} \cdot X_{tug}\right) \cdot x_{10} \\
&- \sum \left(B_{tug_x} \cdot Z_{pad} \cdot Y_{tug}\right) \cdot x_{11} - \left(\sum \left(B_{tug_y} \cdot X_{pad} \cdot X_{tug}\right) + \sum \left(B_{tug_x} \cdot Y_{pad} \cdot Y_{tug}\right)\right) \cdot x_{12} \Big) \\
&+ \left(K_{pen} \cdot Y_{cr} - \sum \left(K_{moor_X} \cdot Y_{winch}\right) - \sum \left(K_{tug_x} \cdot Z_{tug}\right)\right) \cdot x_1 \\
&+ \left(K_{pen} \cdot X_{cr} + \sum \left(K_{moor_Y} \cdot X_{winch}\right) + \sum \left(K_{tug_y} \cdot X_{tug}\right)\right) \cdot x_2 + C_{hyd_{63}} \cdot x_3 \\
&+ \left(C_{hyd_{64}} - K_{pen} \cdot Z_{cr} \cdot X_{cr} - \sum \left(K_{moor_Y} \cdot Z_{winch} \cdot X_{winch}\right) - \sum \left(K_{tug_y} \cdot Z_{tug} \cdot X_{tug}\right)\right) \cdot x_4 \\
&+ \left(C_{hyd_{65}} - K_{pen} \cdot Z_{cr} \cdot Y_{cr} - \sum \left(K_{moor_X} \cdot Z_{winch} \cdot Y_{winch}\right) - \sum \left(K_{tug_X} \cdot Z_{tug} \cdot Y_{tug}\right)\right) \cdot x_5 \\
&+ \left(K_{pen} \cdot X_{cr}^2 + K_{pen} \cdot Y_{cr}^2 + \sum \left(K_{moor_X} \cdot Y_{winch}^2\right)\right. \\
&\left. + \sum \left(K_{moor_Y} \cdot Y_{winch}^2\right) + \sum \left(K_{tug_x} \cdot Y_{tug}^2\right) + \sum \left(K_{tug_y} \cdot X_{tug}^2\right)\right) \cdot x_6 + \\
&\left(K_{pen} \cdot Y_{cr} + \sum \left(K_{tug_x} \cdot Y_{winch}\right)\right) \cdot x_7 - \left(K_{pen} \cdot X_{cr} + \sum \left(K_{tug_y} \cdot X_{winch}\right)\right) \cdot x_8 \\
&+ \sum \left(K_{tug_y} \cdot Z_{pad} \cdot X_{tug}\right) \cdot x_{10} - \sum \left(K_{tug_x} \cdot Z_{pad} \cdot Y_{tug}\right) \cdot x_{11} \\
&- \left(\sum \left(K_{tug_y} \cdot X_{pad} \cdot X_{tug}\right) + \sum \left(K_{tug_x} \cdot Y_{pad} \cdot Y_{tug}\right)\right) \cdot x_{12}
\end{aligned}
\tag{C.6}
$$

Surge Cargo

$$
\begin{aligned}
F_{exc_7} = &-\omega^2 M_{77} \cdot x_7 \\
&- i\omega \left(-\sum B_{tug_x} \cdot x_1 - \sum \left(K_{tug_x} \cdot Z_{tug}\right) \cdot x_5 + \sum \left(B_{tug_x} \cdot Y_{tug}\right) \cdot x_6 \right. \\
&+ \left(B_{air_{77}} + \sum B_{tug_x}\right) \cdot x_7 + \sum \left(B_{tug_x} \cdot Z_{pad}\right) \cdot x_{11} - \sum \left(K_{tug_x} \cdot Y_{pad}\right) \cdot x_{12} \Big) \\
- &\quad \left(K_{pen} + \sum K_{tug_x}\right) \cdot x_1 - \left(K_{pen} \cdot Z_{cr} + \sum \left(K_{tug_x} \cdot Z_{tug}\right)\right) \cdot x_5 \\
&+ \left(K_{pen} \cdot Crane_Y + \sum \left(K_{tug_x} \cdot Y_{tug}\right)\right) \cdot x_6 + \left(K_p en + \sum K_{tug_x}\right) \cdot x_7 \\
&+ \sum \left(K_{tug_x} Z_{tug}\right) \cdot x_{11} - \sum \left(K_{tug_x} \cdot Y_{pad}\right) \cdot x_{12}
\end{aligned}
\tag{C.7}
$$

Sway Cargo

$$
\begin{aligned}
F_{exc_8} = &-\omega^2 M_{88} \cdot x_8 \\
&- i\omega \left(-\sum B_{tug_y} \cdot x2 + \sum \left(B_{tug_y} \cdot Z_{tug}\right) \cdot x_4 - \sum \left(K_{tug_y} \cdot X_{tug}\right) \cdot x_6 \right. \\
&+ \left(B_{air_{88}} + \sum K_{tug_y}\right) \cdot x_8 + - \sum \left(B_{tug_y} \cdot Z_{pad}\right) \cdot x_{10} - \sum \left(K_{tug_y} \cdot Y_{pad}\right) \cdot x_{12} \Big) \\
&- \left(K_{pen} + \sum K_{tug_y}\right) \cdot x_2 + \left(K_{pen} \cdot_{cr} + \sum \left(K_{tug_y} \cdot Z_{tug}\right)\right) \cdot x_4 \\
&- \left(K_{pen} \cdot X_{cr} + \sum \left(K_{tug_{Yx}} \cdot X_{tug}\right)\right) \cdot x_6 + \left(K_{pen} + \sum K_{tug_y}\right) \cdot x_8 \\
&- \sum \left(K_{tug_y} \cdot Z_{pad}\right) \cdot x_{10} + \sum \left(K_{tug_y} \cdot X_{pad}\right) \cdot x_{12}
\end{aligned}
\tag{C.8}
$$

Heave Cargo

$$
\begin{aligned}
F_{exc_9} = &-\omega^2 M_{99} \cdot x_9 \\
&- i\omega \left(-\sum B_{tug_z} \cdot x_3 - \sum \left(B_{tug_z} \cdot Y_{tug}\right) \cdot x_4 + \sum \left(B_{tug_z} \cdot X_{tug}\right) \cdot x_5 \right. \\
&+ \left(B_{air_{99}} + \sum B_{tug_z}\right) \cdot x_9 + \sum \left(B_{tug_z} \cdot Y_{pad}\right) \cdot x_{10} - \sum \left(B_{tug_z} \cdot X_{pad}\right) \cdot x_{11} \Big) \\
&- \left(K_{wire} + \sum K_{tug_z}\right) \cdot x_3 - \left(K_{wire} \cdot Y_{cr} + \sum \left(K_{tug_z} \cdot Y_{tug}\right)\right) \cdot x_4 \\
&+ \left(K_{wire} \cdot X_{cr} + \sum \left(K_{tug_z} \cdot X_{tug}\right)\right) \cdot x_5 + \left(K_{wire} + \sum K_{tug_z}\right) \cdot x_9 \\
&+ \sum \left(K_{tug_z} \cdot Y_{pad}\right) \cdot x_{10} - \sum \left(K_{tug_z} \cdot X_{pad}\right) \cdot x_{11}
\end{aligned}
\tag{C.9}
$$

Roll Cargo

$$
\begin{aligned}
F_{exc_{10}} = &-\omega^2 M_{1010}\cdot x_{10}\\
&-i\omega\left(\sum\left(B_{tug_y}\cdot Z_{pad}\right)\cdot x_2-\sum\left(B_{tug_z}\cdot Y_{pad}\right)\cdot x_3\right.\\
&-\left(\sum\left(B_{tug_y}\cdot Z_{tug}\cdot Z_{pad}\right)+\sum\left(B_{tug_z}\cdot Y_{tug}\cdot Y_{pad}\right)\right)\cdot x_4\\
&+\sum\left(B_{tug_z}\cdot X_{tug}\cdot Y_{pad}\right)\cdot x_5+\sum\left(B_{tug_y}\cdot X_{tug}\cdot Z_{pad}\right)\cdot x_6-\sum\left(B_{tug_y}\cdot Z_{pad}\right)\cdot x_8\\
&+\sum\left(B_{tug_z}\cdot Y_{pad}\right)\cdot x_9+\left(B_{air_{1010}}+\sum\left(B_{tug_y}\cdot Z_{pad}^2\right)+\sum\left(B_{tug_z}\cdot Y_{pad}^2\right)\right)\cdot x_{10}\\
&-\sum\left(B_{tug_z}\cdot X_{pad}\cdot Y_{pad}\right)\cdot x_{11}-\sum\left(B_{tug_y}\cdot X_{pad}\cdot Z_{pad}\right)\cdot x_{12}\Big)\\
&+\sum\left(K_{tug_y}\cdot Z_{pad}\right)\cdot x_2-\sum\left(K_{tug_z}\cdot Y_{pad}\right)\cdot x_3\\
&-\left(\sum\left(K_{tug_y}\cdot Z_{tug}\cdot Z_{pad}\right)+\sum\left(K_{tug_z}\cdot Y_{tug}\cdot Y_{pad}\right)\right)\cdot x_4\\
&+\sum\left(K_{tug_z}\cdot X_{tug}\cdot Y_{pad}\right)\cdot x_5+\sum\left(K_{tug_y}\cdot X_{tug}\cdot Z_{pad}\right)\cdot x_6-\sum\left(K_{tug_y}\cdot Z_{pad}\right)\cdot x_8\\
&+\sum\left(K_{tug_z}\cdot Y_{pad}\right)\cdot x_9+\left(\sum\left(K_{tug_y}\cdot Z_{pad}^2\right)+\sum\left(K_{tug_z}\cdot Y_{pad}^2\right)\right)\cdot x_{10}\\
&-\sum\left(K_{tug_z}\cdot X_{pad}\cdot Y_{pad}\right)\cdot x_{11}-\sum\left(K_{tug_y}\cdot X_{pad}\cdot Z_{pad}\right)\cdot x_{12}
\end{aligned}
\tag{C.10}
$$

Pitch Cargo

$$
\begin{aligned}
F_{exc_{11}} = &-\omega^2 M_{1111}\cdot x_{11}\\
&-i\omega\left(-\sum\left(B_{tug_x}\cdot Z_{pad}\right)\cdot x_1+\sum\left(B_{tug_z}\cdot X_{pad}\right)\cdot x_3+\sum\left(B_{tug_z}\cdot Y_{tug}\cdot X_{pad}\right)\cdot x_4\right.\\
&-\left(\sum\left(B_{tug_x}\cdot Z_{tug}\cdot Z_{pad}\right)+\sum\left(B_{tug_z}\cdot X_{tug}\cdot X_{pad}\right)\right)\cdot x_5+\sum\left(B_{tug_x}\cdot Y_{tug}\cdot Z_{pad}\right)\cdot x_6\\
&+\sum\left(B_{tug_x}\cdot Z_{pad}\right)\cdot x_7-\sum\left(B_{tug_z}\cdot X_{pad}\right)\cdot x_9-\sum\left(B_{tug_z}\cdot Y_{pad}\cdot X_{pad}\right)\cdot x_{10}\\
&+\left(B_{air_{1111}}+\sum\left(B_{tug_x}\cdot Z_{pad}^2\right)+\sum\left(B_{tug_z}\cdot X_{pad}^2\right)\right)\cdot x_{11}-\sum\left(B_{tug_x}\cdot Y_{pad}\cdot Z_{pad}\right)\cdot x_{12}\Big)\\
&-\sum\left(K_{tug_x}\cdot Z_{pad}\right)\cdot x_1+\sum\left(K_{tug_z}\cdot X_{pad}\right)\cdot x_3+\sum\left(K_{tug_z}\cdot Y_{tug}\cdot X_{pad}\right)\cdot x_4\\
&-\left(\sum\left(K_{tug_x}\cdot Z_{tug}\cdot Z_{pad}\right)+\sum\left(K_{tug_z}\cdot X_{tug}\cdot X_{pad}\right)\right)\cdot x_5+\sum\left(K_{tug_x}\cdot Y_{tug}\cdot Z_{pad}\right)\cdot x_6\\
&+\sum\left(K_{tug_x}\cdot Z_{pad}\right)\cdot x_7-\sum\left(K_{tug_z}\cdot X_{pad}\right)\cdot x_9-\sum\left(K_{tug_z}\cdot Y_{pad}\cdot X_{pad}\right)\cdot x_{10}\\
&+\left(\sum\left(K_{tug_x}\cdot Z_{pad}^2\right)+\sum\left(K_{tug_z}\cdot X_{pad}^2\right)\right)\cdot x_{11}-\sum\left(K_{tug_x}\cdot Y_{pad}\cdot Z_{pad}\right)\cdot x_{12}
\end{aligned}
\tag{C.11}
$$

Yaw Cargo

$$
\begin{aligned}
F_{exc_{12}} = &-\omega^2 M_{1212}\cdot x_{12}\\
&-i\omega\left(\sum\left(B_{tug_x}\cdot Y_{pad}\right)\cdot x_1-\sum\left(B_{tug_y}\cdot X_{pad}\right)\cdot x_2+\sum\left(B_{tug_y}\cdot Z_{tug}\cdot X_{pad}\right)\cdot x_4\right.\\
&-\sum\left(B_{tug_x}\cdot Z_{tug}\cdot Y_{pad}\right)\cdot x_5-\left(\sum\left(B_{tug_y}\cdot X_{tug}\cdot X_{pad}\right)+\sum\left(B_{tug_x}\cdot Y_{tug}\cdot Y_{pad}\right)\right)\cdot x_6\\
&-\sum\left(B_{tug_x}\cdot Y_{pad}\right)\cdot x_7+\sum\left(B_{tug_y}\cdot X_{pad}\right)\cdot x_8-\sum\left(B_{tug_y}\cdot Z_{pad}\cdot X_{pad}\right)\cdot x_{10}\\
&+\sum\left(B_{tug_x}\cdot Z_{pad}\cdot Y_{pad}\right)\cdot x_{11}+\left(B_{air_{1212}}+\sum\left(B_{tug_y}\cdot X_{pad}^2\right)+\sum\left(B_{tug_x}\cdot Y_{pad}^2\right)\right)\cdot x_{12}\Big)\\
&\sum\left(K_{tug_x}\cdot Y_{pad}\right)\cdot x_1-\sum\left(K_{tug_y}\cdot X_{pad}\right)\cdot x_2+\sum\left(K_{tug_y}\cdot Z_{tug}\cdot X_{pad}\right)\cdot x_4\\
&-\sum\left(K_{tug_x}\cdot Z_{tug}\cdot Y_{pad}\right)\cdot x_5-\left(\sum\left(K_{tug_y}\cdot X_{tug}\cdot X_{pad}\right)+\sum\left(K_{tug_x}\cdot Y_{tug}\cdot Y_{pad}\right)\right)\cdot x_6\\
&-\sum\left(K_{tug_x}\cdot Y_{pad}\right)\cdot x_7+\sum\left(K_{tug_y}\cdot X_{pad}\right)\cdot x_8-\sum\left(K_{tug_y}\cdot Z_{pad}\cdot X_{pad}\right)\cdot x_{10}\\
&+\sum\left(K_{tug_x}\cdot Z_{pad}\cdot Y_{pad}\right)\cdot x_{11}+\left(\sum\left(K_{tug_y}\cdot X_{pad}^2\right)+\sum\left(K_{tug_x}\cdot Y_{pad}^2\right)\right)\cdot x_{12}
\end{aligned}
\tag{C.12}
$$

D

RAOs

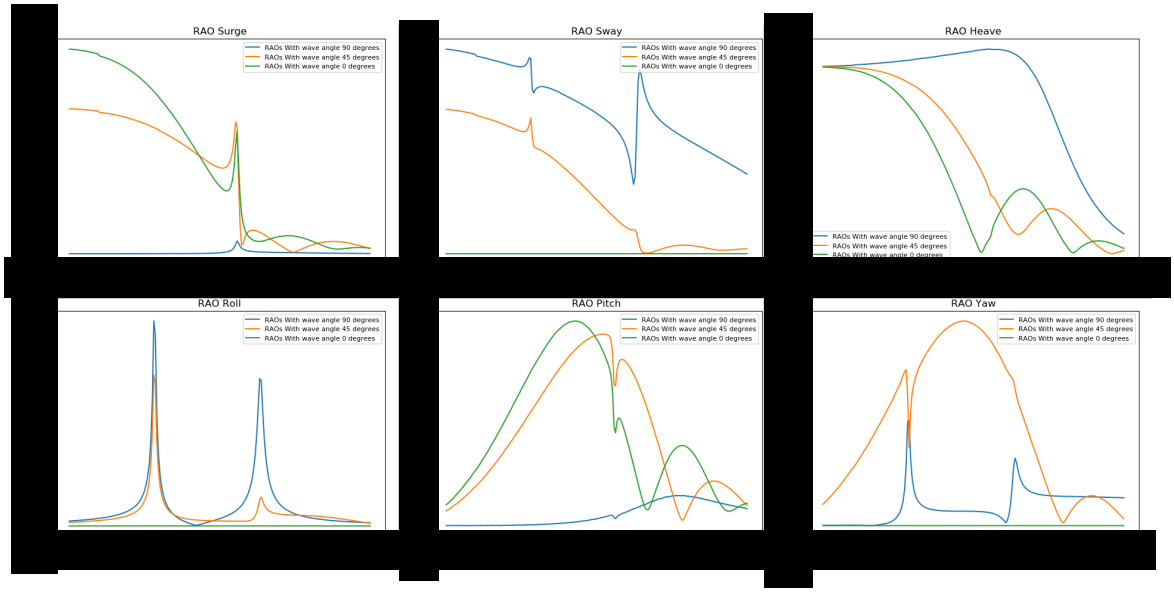

Figure D.1: Comparison between the influence of different wave angles on the vessel RAOs

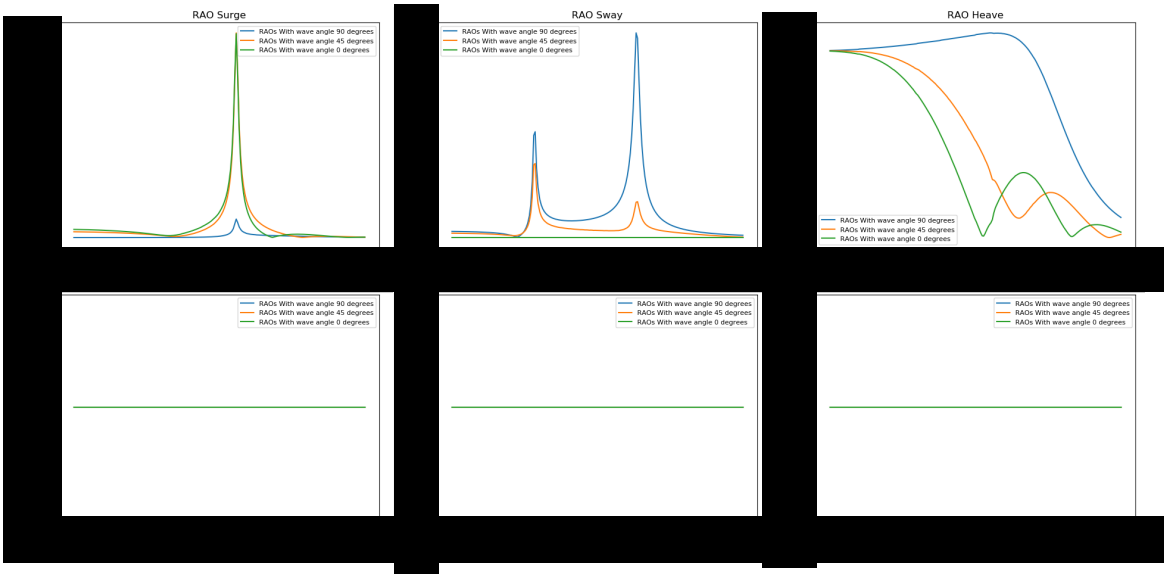

Figure D.2: Comparison between the influence of different wave angles on the cargo RAOs

E

Working principle passive heave compensation

In chapter 2 is explained that damping can be applied to reduce the responses of the cargo. One of the possible methods to reduce the cargo is a variant of a passive heave compensator. Since it is not the goal of this thesis to develop such a system the working principle of passive heave compensators is not explained in chapter 2. The working principle of a passive heave compensator is explained in this chapter.

E.1. Passive Compensation

For vertical motions heave compensation systems are used to reduce the vertical motions of the cargo. There are two main categories of heave compensation. The passive heave compensation and the active heave compensation. Both systems are proven concepts for vertical motions and the same concepts can be studied for damping in horizontal motions when the compensation methods are rotated from the vertical direction to a horizontal direction. A passive heave compensation uses passive actuation, hence its name. Passive actuation implies that stored energy in the system is used and no energy is added via external sources to apply the damping. Passive heave compensation uses pneumatic energy stored in pressure vessels to control the behaviour of the load. In figure E.1 a schematic drawing of a passive heave compensator is given. The passive heave compensation is actuated by a vertical response of the vessel or cargo. When the vessel and cargo are not moving the piston will find it's equilibrium where the force from the pressure applied to the piston is equal to the gravity force applied to the piston. Ideally this is halfway of the middle pressure vessel. This is shown in the second image in figure E.1. The weight of the cargo applies the same force on the piston as the high pressure substance in the accumulator pressure vessel. When the vessel has a positive heave motion the topside of the pressure vessel will move upwards while the piston is not directly moved in the same direction which is shown in the last image in figure E.1. This causes a compression of the the gas in the accumulator vessel which results in a higher pressure of the gas in this vessel. The increased pressure increase the force applied to the piston which will push the piston back towards the equilibrium position. The same physics apply when the cargo has a negative heave motion but instead of the pressure vessel moving upwards the piston will move downwards. When the vessel has a negative heave motion the pressure vessel will move down while the piston stays in place as shown in the first image of figure E.1. This causes the volume of the accumulator to increase which reduces the pressure which reduces the pressure force on the piston.

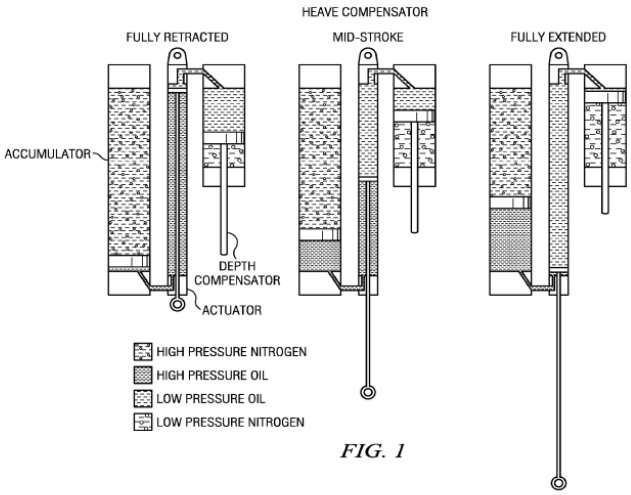

Figure E.1: Schematic drawing of a passive heave compensator

Since passive actuation takes place in passive heave compensation systems the influence of this actuation must be taken into account. The actuation can be modelled as a spring. The properties of this spring depend on the air volume and pressure in the accumulator. When a large volume of air with high pressure is present in the accumulator the stiffness of the heave compensator is low. Due to the relative small compression from the accumulator stroke the change in force of the pressure will be small. When this is the case the accelerations towards the equilibrium are small when the rod is displaced. On the other side, when the volume of air and the pressure in the accumulator is small the stiffness will be relative high. Due to the relative large compression from the accumulator the stroke from the piston will be large. This causes a large acceleration of the piston or casing towards the equilibrium position.

As explained are the pressure and the volume of the accumulator important for the stiffness of passive compensators. The pneumatic forces are approximated using the adiabatic compression law. Which implies that there will not be any pressure losses in the system, the gas acts as an ideal gas and the process is reversible. When these assumptions are done the polytropic process equation becomes usable[34]. The polytropic process equation is given in equationE.1. In this equation p represents the pressure. The volume is given by V and κ stands for the heat capacity ratio. This heat capacity ratio is depending on the temperature, pressure and the type of gas. This polytropic process makes it possible to compare the state of compression for different stages as shown in equation E.2. The force applied to the piston due to pressure in the cylinder can be calculated with equation E.3. In this equation F_p represents the force applied to the piston by the pressure in the accumulator. p represents the pressure in the accumulator and the area of the piston head is given by A.

$$p \cdot V^{\kappa} = constant \tag{E.1}$$

$$p_0 \cdot V_0^{\kappa} = p_1 \cdot V_1^{\kappa} \tag{E.2}$$

$$F_p = p \cdot A \tag{E.3}$$

These equations can be used to linearize the stiffness of the passive heave compensator cylinders. In equation E.4 is shown how the stiffness can be linearized by taking the derivative of the force in the cylinder exerted on the pistion with respect to the response x. The force on the piston due to the pressure in the cylinder can be calculated with equation E.5. In this equation p_0 and V_0 are the pressure when the piston is in it's equilibrium position. The pressure acting on the piston is taken equally over the whole pneumatic part of the system. The volume is the combined volumo f pressured air on all vessels and tubes on the passive side of the accumulator. k_{cyl} is the stiffness of the complete passive heave compensator cylinder. In equations E.6 ad E.7 the stiffness value of the passive heave compensator has been further elaborated.

$$k_{cyl} = \frac{\delta F_{cyl}}{\delta x} \tag{E.4}$$

$$F_{cyl} = \frac{p_0 \cdot A \cdot V_0^{\kappa}}{(V_0 - A \cdot x)^{\kappa}} \tag{E.5}$$

$$k_{cyl} = \frac{\kappa \cdot p_0 \cdot A^2}{V_0} \tag{E.6}$$

$$k_{cyl} = \frac{\kappa \cdot m_c^2 \cdot g^2}{16 \cdot p_0 \cdot V_0} \tag{E.7}$$

In equation E.6 κ is a function of p and A is related to p_0. While the mass of the cargo and the acceleration due to gravity is known all over the world, equation E.6 can be derived to E.7. In these equations m_c is the mass of the cargo. g represents the gravitational acceleration. p_0 and V_0 can be varied without influencing the other variables in a significant way. When p_0 and V_0 are increased the stiffness factor of a passive heave compensator will be reduced. If p_0 is increased κ will also increase. However, this increment is smaller than the increment of $p0$ and thus this does not change the influence of p_0 on the stiffness of a passive compensator.

While heave compensation systems work in the vertical direction the gravitational acceleration and mass of the cargo needs to be used to determine the force of the weight in equilibrium position. When a passive compensation system is used in horizontal directions the force due to the pretension needs to be used to determine the stiffness of the passive compensator system.

Besides the stiffness forces caused by the displacement of the piston in the accumulator viscous friction of the fluid and the friction of the piston seals cause viscous forces. These viscous and friction forces can be modeled as damping forces. The damping forces are non-linear but in this study the forces are assumed to be linear to use them in the mathematical model. The first type of friction that will be discussed is the viscous friction of the fluid in the passive heave compensator. The friction caused by the piston is discussed last.

The working concept of the passive heave compensation is the viscous friction from the fluid flow in the passive heave compensator. Viscous friction takes place in all elements of the passive heave compensator where fluids move, are compressed or decompressed. In other words the viscous friction is present in the accumulator, cylinders where fluids are stored and all the parts in between these vessels. The viscous friction has the largest impact in the pipes connecting the cylinder where the piston is located with the accumulator. Due to the relative small cross section in the pipes the fluid has the highest velocity[37]. Therefore the forces in these pipes will be explained first.

The regime of the fluid flow is important for the calculation of viscous friction. The regimes indicate if a flow behaves laminar or turbulent. The Reynolds number can indicate in what regime the flow is present. The Darcy-Weisbach[38] equation can be used to calculate the viscous friction in pipes. This equation is given in equation E.8. Here Δp indicates the pressure difference in the accumulator. The Darcy friction factor, f_D is related to the flow regime which is based on the Reynolds number. L and D represent the length and diameter of the pipe respectively. The density of the fluid is given by ρ and v represents the flow velocity of the fluid. This equation shows that the friction is dependent on the velocity squared which makes it a non-linear equation. Another effect that can be found in this equation is the the ratio between L and D influences the friction. Since the purpose of this thesis is a study to the motions and responses of vessel with cargo in the crane and not a study to design a damper this equation will not be used. Therefore the exact value for viscous friction cannot be determined.

$$\Delta p = f_D \cdot \frac{L}{D} \cdot \frac{\rho v^2}{2} \tag{E.8}$$

The second friction force that was talked about is the friction between the piston and the cylinder. The friction can be calculated with the Coulomb model of friction given by equations E.9 and E.10. Here F stands for the force caused by the friction. The velocity of the piston is given by v. F_c represents the coulomb friction. The friction factor is given by μ and F_n is the normal force of the wall.

$$F = F_c \cdot \text{sign}(v) \tag{E.9}$$

$$F_c = \mu \cdot F_n \tag{E.10}$$

The friction factor and normal force are dependent on the design of the passive heave compensator. The design of the piston, materials of the seal and cylinder wall are all examples of factors that influence the coulomb friction. There are more effects that influence the coulomb friction but since the goal of this thesis is to develop a mathematical model to create insight in the responses of a vessel and the cargo in the crane a passive damping system will not be developed. Therefore the piston friction force cannot be used for this mathematical model.

Lastly the piston friction in the passive heave compensator can cause stick-slip effects. This is the spontaneous jerking motion that can occur when the force difference does not exceed the friction force. Since this is a non-linear effect it will not be approached in the damping model.

The friction caused by a passive compensator is thus non-linear. However without the design of a passive compensator the friction that will be applied in the multi-body dynamics cannot be determined. However, the ratio of L and D can influence the viscous friction. Since the viscous friction can be tuned damping will be added to the system. Friction in passive compensation works as a damper because friction transforms energy from the motions to energy in heat. Since this effect always occurs it is possible to assume that damping will be applied even though the various friction methods do not give a clear damping value. The damping that will be applied in this model is the a percentage of the critical damping calculated with equation 2.20. The damping applied in the model by passive compensaters is given by equation E.11. In this equation ζ_{PC} represents the damping applied by passive compensators. $\zeta_{\%}$ represents the percentage of critical damping that the passive compensator should damp. The mass of the cargo is given by m_c and the stiffness of the passive compensator is given by k_{cyl}.

$$\zeta_{PC} = \zeta_{\%} \cdot 2 \cdot \sqrt{m_c \cdot k_{cyl}} \tag{E.11}$$

This theory regarding the passive heave compensators can tell us how damping and stiffness are added to the system. However the actual amount of stiffness and damping applied to the system is unknown until a passive compensation system is designed. This part of the appendix was added to illustrate how passive heave compensators dissipate energy from the system and how the dissipation can be calculated. While it is proven that passive heave compensators can add damping to the system it is useful to calculate the influence of passive compensators on horizontal cargo motions.

E.2. Active compensation

Besides passive activation damping can be applied via active activation. During some lifting operations tugger winches are used. Tugger winches are winches with a cable or rope connected to the load in the crane. In figure E.2 a schematic drawing of tugger winches connected to cargo in a crane is given. In this figure the tugger wires are drawn with purple lines and the winches are represented by the red cylinders. Tugger winches are often connected to heavy loads to manipulate the motions of the load. These winches are pretensioned when connected to the load to prevent the tugger lines from falling slack. There are two conventional types of controlling the winches. The first is a fixed tugger winch. The second type is a constant tension tugger winch.

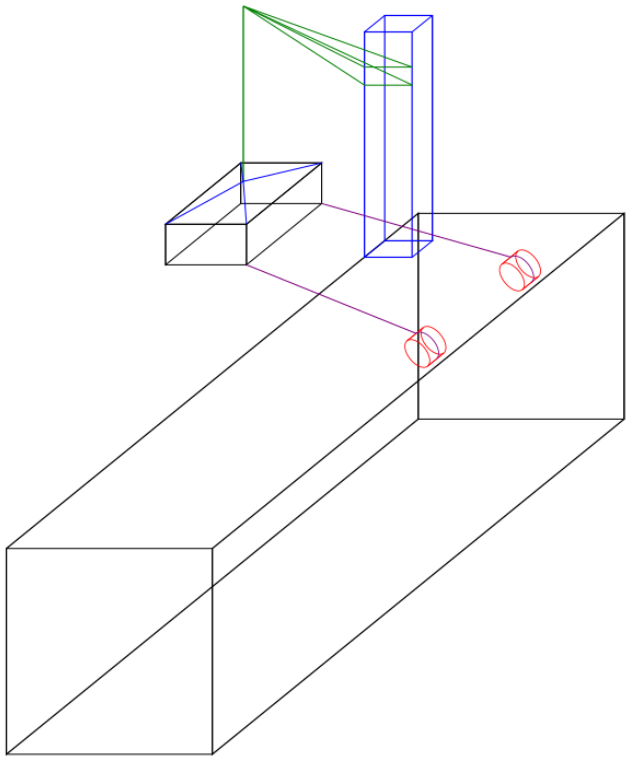

Figure E.2: Schematic drawing of tugger winches applied to cargo in a crane

When the fixed tugger method is used the winches are put on brake when the pretension is finished. The line will act as a spring in the same way as a mooring line act as a spring on the vessel. The extra stiffness in the multi-body system will influence the natural frequencies of the different degree of freedom. In section 2.6 will be explained how stiffness influences the natural frequencies of responses. Since the tugger winches are put on a break this technically is not an active system. In fact, no damping is added via the tugger winches and fixed tugger lines should be modeled as springs between the location of the winch and the connection point on the cargo. However, the stiffness effects of fixed tugger winches are part of every other system that introduces damping. Therefore the fixed tugger winches had to be mentioned and the stiffness components will be added when the influence of damping is examined in chapter 6.

A problem with fixed tugger winches is the force applied to the tugger lines. When a load of 500 mton has a response of 1 meter in horizontal direction on waves with a period of 12 seconds the horizontal dynamic load will be equal to 14 mT. While the waves forces drive the motions of the vessel and cargo system the wave period depicts the period of the motions of the multi-body system. This means that a pretension of 14 mT must be appliled to prevent a slack line. The capacity of the tugger line must be above 28 mT to prevent the line from snapping.

The second method to apply tugger winches to the cargo is a constant tension method. A big advantage of the constant tension is the reduced chance of a breaking tugger line. With the constant tension method a winch is set to deliver a constant tension to the tugger lines. When the load of the cargo is moving towards the tugger lines the tension in the line reduces and the tugger winch will reel in the tugger line to increase the tension towards the constant tension value. When the cargo is moving away from the tugger winch the tension in the tugger line increases. This causes the tugger winch to give line to reduce the tension in the line to the constant tension value. When this system is working perfectly the winch will move with the same speed and phase as the motions of the cargo and there is no tension difference in the line. When there is no tension difference there is no effect of the tugger winches on the dynamic system. Since there is no influence a perfectly working constant tension winch will not influence the responses of the cargo and vessel in a meaningful way. However, in practice the constant tension winches are not perfect. The reaction of the

winch is always delayed on the motion of the cargo. This causes the tension to fluctuate around the constant tension value. In a complete cycle of the motion a small amount of energy will dissipate from the system which can me modelled as damping. The amount of energy dissipated from the system is hard to model and therefore impossible to calculate. However small amounts of damping will occur. Therefore, the constant tension winches can be modelled in the same was as a passive compensation system, by applying damping equal to small percentages of the critical damping. The stiffness of the tugger lines can be calculated in the same way as the stiffness of the mooring lines explained in section 2.4.

Another active system that might be useful for reducing the cargo motions is an active heave compensation system. As in a passive heave compensation system the system is developed to reduce the motions of the cargo in the heave direction. Instead of pneumatics, cylinders and pistons this system uses winches to reduce the motions of the cargo. In figure E.3 a schematic of active heave compensation is given. Since this is an active system this type of system requires energy input. Instead of a reaction on the forces the motions of the vessel are monitored. The motions of the vessel are relayed to a controller. Via the controller an actuator will oppose the heave motion. Thus when the vessel has a positive heave motion the controller will force the actuator to move the load in the opposite direction[41]. In figure E.3 the motions of the vessel are opposed by the winch. Such an active system can create possibilities for damping during lifting operations. When the important motions of the vessel are monitored an active control system can be put in place. This system could actively apply damping to the multi-body system. A recently released study from H. Lageveen [15] shows that tugger winches in combination with a controller can be used for active damping. Since it is not in the interest of this study to develop an active damping mechanism no further study to such mechanism is done.

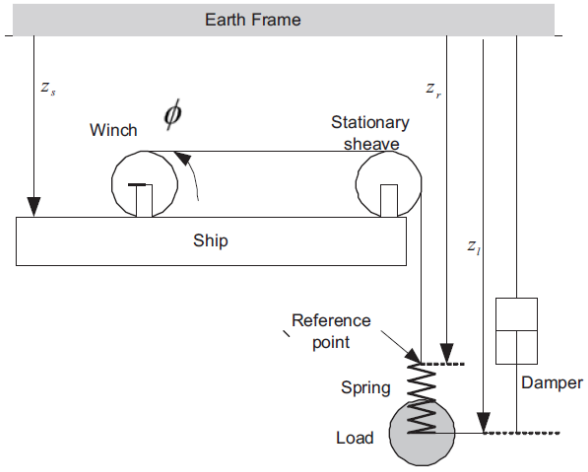

Figure E.3: Schematics of a winch based active heave compensator. For simplicity the crane dynamics is neglected. The stationary sheave represents the crane tip[[42]

As for the passive compensator systems the active compensator systems do not give actual damping values. However the existence of these systems show that damping can be applied via a system related to active heave compensation or active tugger winches. This part of the appendix was written to show that there are practical solutions to apply damping. Further studies should be done to determine how such a system should look like and what the specifications of such a system are.